Mobile Gait Analysis via instrumented Shoe Insoles - eSHOE

Detection of movement patterns and features in healthy subjects and hip fracture patients

DISSERTATION

submitted in partial fulfillment of the requirements for the degree of

Doktor der Technischen Wissenschaften

by

DI(FH) Harald Jagos

Registration Number 0526667

to the Faculty of Informatics

at the TU Wien

Advisor: a.o. Univ.-Prof. i.R. DDDr. Frank Rattay

The dissertation has been reviewed by:

_____   _____
Dietmar Rafolt   Eugen Gallasch

Vienna, 1st December, 2016

_____
Harald Jagos

Erklärung zur Verfassung der Arbeit

DI(FH) Harald Jagos
Anton-Sattler-Gasse 91/1/18, 1220 Vienna

Hiermit erkläre ich, dass ich diese Arbeit selbständig verfasst habe, dass ich die verwendeten Quellen und Hilfsmittel vollständig angegeben habe und dass ich die Stellen der Arbeit – einschließlich Tabellen, Karten und Abbildungen –, die anderen Werken oder dem Internet im Wortlaut oder dem Sinn nach entnommen sind, auf jeden Fall unter Angabe der Quelle als Entlehnung kenntlich gemacht habe.

Wien, 1. Dezember 2016

_____

Harald Jagos

Danksagung

Auf dem bedeutsamen Weg zur Fertigstellung dieser Arbeit und damit zum Abschluss meines Doktorat haben mich viele Menschen begleitet. Die Arbeit nahm ihren Anfang mit der anstoßenden Idee von **Prof. Wolfgang Zagler**. Abgesehen von der Idee zu dieser wissenschaftlichen Arbeit selbst habe ich von ihm sehr viel über die Gestaltung technischer Hilfsmittel für Menschen mit besonderen Bedürfnissen gelernt und in das eSHOE einfließen lassen können. Großer Dank gebührt meinem Dissertationsbetreuer, **Prof. Frank Rattay**, der mir oft geholfen hat meinen Fokus wieder zu finden und mit viel Geduld oft wertvolle Ratschläge gespendet hat. Schon während der technischen Entwicklung war medizinischer Input gefragt. Ich möchte an dieser Stelle meine Wertschätzung für die langjährige, informelle Begleitung des Projektes von Frau **Prim. Katharina Pils** zum Ausdruck bringen. Sie hat dazu beigetragen eSHOE zu einem praxistauglichen Prototypen zu machen und hat den Weg für die klinische Pilotstudie bereitet, die zu einem wertvollen Bestandteil dieser Arbeit wurde. Die reibungslose Abwicklung der Studie wäre natürlich nicht möglich gewesen ohne die Kooperationsbereitschaft vieler Mitarbeiter des Sophienspitals. Danke an dieser Stelle an Frau Dr. Claudia Wassermann, die ihre bereit war Patientinnen und Patienten zu rekrutieren und bei fast jeder einzelnen Messung dabei war. Danke auch an Frau OA Christa Chhatwal, die oft die GAITRite-Messungen begleitet hat und mit Rat und Tat zur Seite stand. Nicht zu vergessen sind natürlich die Patientinnen und Patienten selbst, die bereitwillig an den Messungen der Studie teilgenommen und bis zum Ende durchgehalten haben, und die freiwilligen ProbandInnen und Probanden, alle samt Mitarbeiter und Mitarbeiterinnen des Sophienspitals.

Die umfassenden technischen Tätigkeiten wären nicht ohne tatkräftige studentische Mitarbeit möglich gewesen. Im Laufe und im Rahmen des Projekts wurden eine Reihe von Bachelor- und Masterarbeiten abgewickelt, der Großteil davon von Studierenden der FH Technikum Wien. Besonders hervorheben möchte ich dabei drei Personen: Veronika David, Stefan Reich und Daniel Polasek. **Veronika David** war eine der ersten die ich für das Schreiben einer Masterarbeit im Rahmen der eSHOE Geschichte begeistern konnte. Wir haben auch nach ihrem Abschluss weiter zusammen gearbeitet und für ihre loyale und fleißge Mitarbeit über die Jahre bin ich sehr dankbar. **Stefan Reich**, er war genau zur rechten Zeit am rechten Ort. Er begann an dem Projekt in einem sehr frühen Stadium mitzuarbeiten und hat es von seiner Bachelor- bis zur Masterarbeit begleitet und bereichert. Seine unermüdliche Begeisterung, sein Einfallsreichtum und sein Fleiß, den er im Zuge der Erstellung seiner Masterarbeit bewiesen hat, haben maßgeblich dazu

beigetragen das Projekt eSHOE - und nicht zuletzt auch diese Dissertation - zu dem zu machen was es heute ist. In ihm habe ich nicht nur einen unvergleichlichen Mitarbeiter gewonnen, es ist auch eine wunderbare Freundschaft aus der Zusammenarbeit entstanden. **Daniel Polasek** hat mit seiner Masterarbeit die sprichwörtlichen Kastanien aus dem Feuer geholt, die Berechnung der Schrittlänge. Durch seine rasche Auffassungsgabe, sein mathematisches und ingenieurmäßiges Talent trug er maßgeblich zur Umsetzung dieser Aufgabe bei. Auch wenn er nur vergleichsweise kurze Zeit, im Rahmen seines Auslandssemesters, in Wien verbracht hat, verbindet mich mit ihm heute mehr als nur Kollegentum. All die studentische Zuarbeit wäre nie möglich gewesen, wäre da nicht **Dr. Martin Reichel**. Er hat das Projekt eSHOE - und damit mich - viele Jahre als enger und wichtiger Kooperationspartner begleitet. Abgesehen von seiner eignen Arbeit hat er, zu seiner Zeit als Studiengangsleiter an der FH Technikum Wien, immer kräftig die Werbetrommel gerührt hat um das Thema für Studierende interessant zu machen und dabei einige wertvolle Mitstreiter rekrutiert. In der finalen Phase der Dissertation kommt noch **Prof. Dietmar Rafolt** ins Spiel. Er gab dem spin-off des eSHOE Projekts ein zu Hause an der Medizinischen Universität Wien und gab mir dadurch die Möglichkeit am Puls der biomedizin-technischen Forschung wichtige ergänzende Erfahrungen zu sammeln. Die Zusammenarbeit mit ihm war sehr bereichernd und bot mir ein ideales Umfeld zum Abschluss der Dissertation.

Mein Dank gilt selbstverständlich auch meinem privaten Umfeld, in dem ich oft Rückhalt, Zuspruch und Ablenkung fand. Danke an meine Freunde und Bekannten, die an mich geglaubt und mich seelisch und moralisch unterstützt haben. Danke meinem Vater, **Peter Jagos**, der mich oft kulinarisch versorgt und mir - speziell im letzten Jahr - auch finanziellen Rückhalt gegeben hat. Meinen größten Dank möchte ich meiner Mutter, **Eva-Maria Jagos**, aussprechen. Sie hat mir ermöglicht, diesen Weg zu beschreiten und eine akademische Laufbahn einzuschlagen. Ihr habe ich so viel mehr als das zu verdanken. Leider war es ihr nicht mehr vergönnt, diesen krönenden Abschluss meiner Ausbildung mitzuerleben. Aus diesem Grund widme ich ihr diese Arbeit.

Kurzfassung

Die klinische Ganganalyse leistet einen wichtigen Beitrag zur Unterstützung des Rehabilitationsprozesses und zur stetigen Verbesserung der stationären Behandlung. Gleichzeitig gibt es aber immer noch ungelöste Unzulänglichkeiten in der Langzeit-Versorgung von chronischen Krankheiten, die den Bewegungsapparat betreffen. Darunter fallen z.B. die eingeschränkten bzw. kurzen Gangstrecken und die Beeinflussung der Patienten durch die künstliche Laborsituation in den Ganglabors der Rehazentrum selbst. Darüber hinaus fehlt nach der Spitalsentlassung ausreichende Dokumentation über die Durchführung der Rehabilitationsübungen. Ebenso mangelt es an Rückmeldungen über den Mobilitätsstatus der PatientInnen - von detaillierten Daten und Gangparametern ganz zu schweigen.

Um die Fortsetzung der Rehabilitation nach der stationären Betreuung zu unterstützen, wurde ein auf instrumentierten Schuheinlagen basiertes, mobiles Ganganalysesystem, namens eSHOE, entwickelt. Mit dessen Hilfe wird eine selbstständige, zu Hause durchführbare Kontrolle des Gangbildes, sowie ein individuelles Gangtraining möglich. Inertial- und Drucksensoren erfassen Bewegungsdaten direkt an den Füßen, speichern diese lokal ab und übertragen sie gleichzeitig drahtlos an einen PC. Bei eSHOE ist, im Unterschied zu gängigen stationären als auch zu portablen Ganganalyse-Systemen, die Hardware zum Erfassen und Verarbeiten der Bewegungsdaten vollständig in ein Paar orthopädischer Einlegesohlen integriert. Des Weiteren beschränkt sich die Funktion von eSHOE nicht auf die simple Aufzeichnung von Bewegungsdaten. Zu den Basis-Features gehört ebenfalls die Umrechnung dieser Bewegungsdaten in Standard-Gangparameter mittels spezieller Mustererkennungs- und feature extraction Algorithmen. Das eSHOE System ist äußerlich praktisch nicht von einem gewöhnlichen Paar Einlegesohlen zu unterscheiden und ermöglicht es daher für den Träger unauffällig und unaufdringlich Daten aufzuzeichnen. Da der Anwender selbst sich während des Messens nicht in einer Laborsituation befindet und auch keine zusätzliche unhandliche Ausrüstung tragen muss, wird er dadurch weniger stark beeinträchtigt. Zusätzlich ist das Messsystem räumlich nicht eingeschränkt und ermöglicht dadurch Messungen über beliebig langen Strecken und auf unterschiedlichen Untergründen. Zu Beginn der Validierung der Ergebnisse von eSHOE wurde die Zuverlässigkeit des automatisierten Findens von Mustern und der feature extraction geprüft. Dazu wurde die Anzahl und Art der automatisch extrahierten Muster mit den händisch in den Rohdaten identifizierten Mustern verglichen. Dieselbe Vorgehensweise kam zum Einsatz bei der Überprüfung der Extraktion von den grundlegenden features initial contact (IC) und last contact (LC). Die Genauigkeit der daraus berechneten temporalen Gangparameter

wurde mithilfe eines Vergleichs mit den Ergebnissen des stationären Referenzsystems GAITRite® ermittelt. Folgende Parameter wurden verglichen: stride time (STR), stance time (STA), swing time (SWI), step time (STE) and double support time (DST). Im Rahmen einer klinischen Pilotstudie wurden als Probanden für die Vergleichsmessungen zwei Gruppen rekrutiert: elf PatientInnen mit Hüftfraktur (Alter: 78.4 ± 7.7 *Jahre*) und zwölf gesunde Testpersonen (Alter: 40.8 ± 9.1 *Jahre*). Alle Testpersonen absolvierten jeweils drei Messungen bei gewohnter, angenehmer Gehgeschwindigkeit entlang einer acht-Meter Gangstrecke, eine sechs Meter lange GAITRite®-Matte eingeschlossen. Im Zuge dieser Messungen wurde auch erhoben, ob es möglich ist, anhand der eSHOE Daten zwischen Gesunden (CRTL) und PatientInnen (PAT) zu unterscheiden. Bei den PatientInnen wurde zusätzlich noch eine Unterscheidungsmöglichkeit zwischen gesundem und betroffenem Bein untersucht. Die Differenzen zwischen den beiden Gruppen wurden mit den folgenden, nicht-parametrischen statistischen Methoden, evaluiert: *Mediantest*, *Mann-Whitney U-Test* und *Kolmogoroff-Smirnov Test*. Messungen des gesunden und verletzten Beins wurden verglichen mithilfe von *Vorzeichentest* und *Vorzeichenrangtest*. Während der Pilotstudie wurde ebenfalls untersucht, ob mithilfe regelmäßiger eSHOE Messungen der Fortschritt der Therapie, anhand des Verlaufs der Gangparameter, dokumentiert werden kann. Zu diesem Zweck sollte jede/r Patient/in während des drei- bis fünfwöchigen Aufenthalts ein Mal pro Woche drei Wiederholungen des *10-Meter Gehtests (10MGT)*, einem standardisierten Mobilitätsassessment, durchführen und dabei die eSHOE Einlegesohlen tragen. Um Unterschiede zwischen dem betroffenen und gesunden Bein festzustellen kamen wieder nicht-parametrische statistische Tests zum Einsatz. Der Therapiefortschritt wurde mittels deskriptiver Statistik dokumentiert. Die Ergebnisse der Berechnungen von Schrittlänge und gesamter zurückgelegter Distanz beim Gehen wurden in einer nicht-klinischen Studie evaluiert. Für die Berechnung der Schrittlänge wurden verschiedene, bereits existierende Ansätze herangezogen, welche zur Abschätzung der Entfernung auf Beschleunigungssensoren setzen. Darunter befinden sich Methoden der Navigation mittels dieser Inertialsensoren und des dead reckoning. Am Ende musste jedoch eine eigene Methode entwickelt werden, die sich bestimmte Aspekte aus mehreren Ansätzen zunutze macht. Diese behandelt den zufälligen Schritt-zu-Schritt bias offset und die zufällige lineare systematische Abweichung der Accelerometer- und Gyroskopsignale in Kombination mit einem, auf das Gangbild abgestimmten, zero-velocity-update (ZUPT) Kalman-Filter. Für die Schrittlängen- und Gesamtdistanzmessung wurden drei Parameter-Sets definiert und manuell (mittels Maßband) sowie mit dem optischen motion capturing System VICON® validiert.

Sensor- und achsenspezifischen Muster konnten mit einer Genauigkeit von 91.4 bis 99.8 % erkannt und extrahiert werden. Die in den Mustern enthaltenen grundlegenden Gangparameter, IC und LC, konnten links zu 97.6 % und rechts zu 98.6 % erfolgreich detektiert werden. Die Übereinstimmung der sechs Gangparameter, extrahiert aus insgesamt 347 Gangzyklen, mit dem Referenzsystem GAITRite® wurde mittels Streudiagrammen, Histogrammen und Bland-Altman-Analyse bestimmt. In der CTRL Gruppe ergaben sich mittlere Differenzen der beiden Systeme von −0.029 bis 0.029 *s* und bei PAT reichten die Differenzen von −0.046 bis 0.045 *s*. Bei der Berechnung der Schrittlänge konnte mit

dem besten Parameter-Set eine Genauigkeit von -3.0 ± 2.2 % erzielt werden. Angewandt auf eine durchschnittliche Schrittlänge von 1.3 m ergibt das -3.9 ± 2.9 $cm/Schritt$. Für die Bestimmung der gesamten Gehstrecke ergab sich bei einer Strecke von 50 m ein Fehler von -4.5 ± 0.7 % (-2.26 ± 0.35 m) und bei der 8.7 m-Strecke -2.0 ± 2.4 % (-0.17 ± 0.21 m). Unterschiede zwischen CTRL und PAT konnten in allen Gangparametern - und bei beiden Systemen, eSHOE und GAITRite® - sowohl visuell (anhand der Box plots) ausgemacht, als auch durch statistische Tests bestätigt werden. Beim Vergleich von gesundem und verletztem Bein ergaben sich anhand der Daten von eSHOE keine Unterschiede bei for stride time, step time und terminal double support time. Bei den verbleibenden Parametern, stance time, swing time and initial double support time, wurden jedoch statisch signifikante Unterschied festgestellt. Die Auswertung der GAITRite® weichen in einem Parameter von den eSHOE Ergebnissen ab, nämlich der terminal double support time, wo die statistische Analyse in einem eindeutigen Unterschied zwischen beiden Beinen resultierte. Bei der Evaluierung der Fortschrittsdaten wurde ebenfalls auf Unterschiede zwischen beiden Beinen geprüft und das Ergebnis deckt sich mit der vorherigen Untersuchung.

Schon beim Verlauf der Referenzdaten, der Dauer der Durchführung des 10MGT, zeigt sich, dass kein einheitlicher Fortschritt bei der Gesamtheit der Testpersonen erkennbar ist. Nach dem ersten Messtag verringert sich die Zeit zwar deutlich, aber danach stagnieren die Ergebnisse. Am sechsten und letzten Messtag steigt die Zeit sogar wieder leicht an. Bei den Verläufen von Median und Mittelwert der Gangparameter zeichnet sich ein ähnliches Bild ab. Wobei dort die Veränderungen nach dem ersten Tag auch nur teilweise erkennbar sind. Allerdings konnten eindeutigen Veränderung in den Verteilungen aller Gangparameter, im Verlauf über die sechs Messtage, festgestellt werden. Von Tag eins bis Tag sechs reduzieren sich Standardabweichung (Stabw) um 82%, Interquartilabstand (IQR) um 72% und die Spannweite (TR) um 84%. Zusätzlich werden die detektierten Differenzen zwischen gesundem und betroffenem Bein bei der Dauer von Stand- und Schwungphase geringer. Am ersten Tag ist die stance time des gesunden Beins noch 0.091 s länger als die des betroffenen Beins, am letzten Tag nur mehr 0.015 s. Dies entspricht einer Reduktion um 84 %. Die mittlere Dauer der Schwungphase des gesunden Beins ist am ersten Messtag noch 0.119 s kürzer als am betroffenen Bein, am sechsten und letzten Messtag ist sie nur noch um 0.017 s kürzer, eine Reduktion der Differenz um 86 %. Im Fall der Doppelstandphase fand ebenfalls eine Verminderung der Differenz zwischen beiden Beinen statt. Sie betrug 75 %, von -0.071 s auf -0.018 s. In den Parametern, denen signifikante Differenzen nachgewiesen werden konnte, zeigte sich eine Verringerung der Differenzen von Tag eins bis Tag sechs.

In Anbetracht der Validierungsergebnisse kann geschlussfolgert werden, dass eSHOE hinreichend genaue Messergebnisse für alle temporalen Gangparameter liefert. Die Abweichung zwischen den Ergebnissen von CTRL und PAT deutet jedoch darauf hin, dass die eSHOE Algorithmen bei Patientendaten weniger zuverlässig und ungenauer arbeiten. Das rührt vermutlich daher, dass die Rohsignale der Datensätze der Patienten deutlich unregelmäßiger sind als die der gesunden Kontrollen. Daher kommt es dort zu erhöhten Ungenauigkeiten, da es für die Algorithmen schwieriger ist die wiederkehrenden Muster

zu erkennen und in der Folge die Gangparameter zu extrahieren. Dennoch sind Abweichungen von $\pm 46\ ms$ in einem durchaus akzeptablen Ausmaß. Bei der Bestimmung von Schrittlänge und gesamter Gehstrecke erscheint es als ob die gegenwärtige Kombination aus Hardware und Berechnungsmethode höhere Genauigkeiten für längere Strecken als für kurze, wie etwa einer Doppelschrittlänge, zulässt. Der systematische Fehler bei der Berechnung kann durch eine höhere Abtastrate, neue Modelle von intertialen Messeinheiten mit noch besserer Signalqualität und (mathematisch) ausgereifteren Methoden zur Kompensation noch weiter reduziert werden.

Anhand der Veränderungen über die Zeit von Median und Mittelwert der Gangparameter konnte der Therapiefortschritt nicht klar dokumentiert werden. Allerdings konnte eine fortschreitende Schmälerung der Verteilungen (Stabw, IQR, TR) aller Parameter gezeigt werden. Diese Veränderungen deuten darauf hin, dass eSHOE imstande war eine Verringerung der inter-personellen Variabilität der Gangparameter festzustellen, woraus indirekt auf einen Fortschritt in der Rehabilitation geschlossen werden kann. Möglicherweise geht die tatsächliche Information des Fortschritts in der sehr breiten Streuung der Daten unter. Bei der individuellen Analyse einzelner Testpersonen konnten nämlich tatsächlich Veränderungen, z.B. eine Reduktion der stride time, festgestellt werden. Die Ursache wird in der geringen Größe sowie der heterogenen Zusammensetzung der Stichprobe vermutet. So hat sehr wahrscheinlich der Einsatz von individuell unterschiedlichen Gehhilfsmitteln zu unterschiedlichen Zeitpunkten in der Rehabilitation starken Einfluss auf die Änderung der Gangparameter und trägt damit zu deren breiten Streuung bei. Die Untersuchung einer größeren Gruppe an Testpersonen, mit noch feinkörnigerer Gruppierung (nach genauer Frakturart und/oder Implantat), die die gleichen Gehhilfsmittel zur gleichen Zeit verwenden, könnte hier Abhilfe schaffen.

eSHOE's Genauigkeit kommt zwar nicht an die von stationären Systemen heran, ist aber dennoch imstande Unterschiede zwischen gesunden Probanden und Personen mit unilateraler Verletzung zu erkennen. Dabei ist das System mit deutlich weniger Aufwand einsetzbar und wesentlich kosteneffizienter. Es erzielt mit anderen mobilen Systemen vergleichbare Genauigkeit, ist aber im Unterschied zu allen Systemen zur Gänze in das Kleidungsstück Einlegesohlen integriert. Daher ist es sehr gut geeignet zur langzeitigen und unauffälligen Aufzeichnung von Bewegungsdaten mit minimaler Beeinflussung des Trägers.

Durch den ständig wachsenden Anteil älterer Menschen und der damit in Zusammenhang stehenden steigenden Anzahl chronischer Erkrankungen werden bald Lösungen gefordert werden, die den langfristigen Erfolg von Therapie und Rehabilitation sicherstellen. Die angedachte Weiterentwicklung von eSHOE in ein Reha@Home System, zur Unterstützung des Erfolgs von Reha-Maßnahmen, könnte dieser Notwendigkeit in die Hände spielen. Der im Moment stark boomende "quantified selfTrend eröffnet zusätzlich die Möglichkeit für die Entwicklung von lifestyle-Anwendungen, die nicht auf eine Altersgruppe beschränkt sind.

Abstract

Clinical gait analysis contributes massively to rehabilitation support and improvement of in-patient care. But there are still several unresolved shortcomings such as: the absence of medical records after hospital discharge, a lack of feedback to the subject, limited walking distances in intramural settings and affection of subjects through laboratory situation.

A self-developed pair of instrumented shoe insoles, called eSHOE, fills this gap after hospital discharge and enables individual home-based monitoring and training. Motion and pressure sensors gather movement data directly on the (user's) feet, store them locally and transmit them wirelessly to a PC. In difference to current intramural and extramural gait analysis systems, the eSHOE hardware is fully embedded into a pair of orthopedic insoles. Furthermore, instead of delivering raw movement data, a combination of pattern recognition and feature extraction algorithms makes use of the multimodal sensor input and translates the motion data into standard gait parameters. Another important distinctive feature is that the measurement system, being completely integrated into a garment, enables the acquisition of movement data in an unobtrusive way. Thereby, the user or test subject is less influenced by the measurement process, because no cumbersome equipment has to be set up or attached to the body and the subject is not in an in the spotlight sort of situation. Additionally, there are no spatial restrictions, so subjects can be analyzed on walking tracks of any length and with different underground structures.

As a first step in the investigation whether eSHOE provides useful results, the reliability of the pattern detection and feature extraction results have been compared to actual number of gait cycles , which were manually counted in the raw data. The same was done for the number of basic features, such as initial contact (IC) and last contact (LC). The accuracy of the subsequently calculated temporal gait parameters was evaluated against the reference system GAITRite® in the course of a clinical pilot study. Those parameters are stride time (STR), stance time (STA), swing time (SWI), step time (STE) and double support time (DST). Eleven hip fracture patients (78.4 $\pm$ 7.7 *years*) and twelve healthy subjects (40.8 $\pm$ 9.1 *years*) were included in these trials. All subjects performed three measurements at a comfortable walking speed over eight meters, including the six-meter-long GAITRite® mat. These validation measurements were also used to investigate, whether it is possible to distinguish between eSHOE data collected from healthy subjects (CTRL) and patients (PAT). Furthermore, a comparison between healthy and injury-affected leg, within PAT, has been carried out. For these purposes

two sets of non-parametric statistical tests have been chosen. The differences between the groups have been evaluated using the *median test*, the *Mann-Whitney U-test* and the *Kolmogoroff-Smirnov test*. Measurements of healthy and affected leg have been compared by the *sign test* and the *sign rank test*. In the course of the same pilot study it was attempted to document the course of each patient's therapy success by means of the development of his or her gait parameters that can be calculated from the eSHOE data. For that purpose each patient was asked to perform three repetitions of the *10-meter walk test (10MWT)*, a standardized mobility assessment, while wearing a pair of eSHOE insoles, once a week during their (three- to five-week) stay. Non-parametric measures were used to determine differences between healthy and affected leg. Regarding therapy progress, data were evaluated by using descriptive statistics. Stride length (STL) and total distance estimation have also been evaluated in another (non-clinical) study. Several already existing approaches for distance estimation via inertial sensor signals, based on inertial navigation and dead reckoning, have been consulted. A specially designed method, which utilizes certain aspects from those methods, has been developed. It involves modeling of the random stride-to-stride bias offset and the random linear bias drift in combination with a well-timed zero-velocity-update Kalman filter. Three different parameter sets for this method have been implemented and validation against manual means (measurement tape) and the optical motion capturing system VICON® has been performed.

The extraction of sensor- and axis-specific patterns resulted in detection accuracies from 91.4 to 99.8 %. Major gait events, like initial and last contact, could be extracted with an accuracy of 97.6 % (mean left) and 98.6 % (mean right). Six temporal gait parameters were extracted from a total of 347 gait cycles. Agreement with the reference system GAITRite® was analyzed via scatter-plots, histograms and Bland-Altman plots. In the patient group the average differences between eSHOE and GAITRite® range from -0.046 to 0.045 s and in the healthy group from -0.029 to 0.029 s. The best parameter-set for stride length estimation managed to achieve an accuracy of -3.0 ± 2.2 %, applied to an average stride length of 1.3 m this results in -3.9 ± 2.9 $cm/stride$. For the total distance estimation at 50 m this parameter-set exhibited an (average) error of -4.5 ± 0.7 % (-2.26 ± 0.35 m) and -2.0 ± 2.4 % (-0.17 ± 0.21 m) at 8.7 m. Significant differences between CTRL and PAT could be identified visually and confirmed via statistical tests in both eSHOE and GAITRite® data. The comparison of healthy and affected leg among patients, regarding eSHOE data, presented equal results for stride time, step time and terminal double support time and showed statistical significant differences in stance time, swing time and double support time. The evaluation of the patient group's gait parameters' progression during the stay in geriatric care revealed the same statistical significant differences between healthy and affected. Therefore, the evaluation of therapy progress was performed for each leg separately in those parameters showing differences. The inspection of the course of the external reference data, the 10MWT duration, already reveals that there is no consistently identifiable progress in the entirety of all test subjects. There is a clear reduction of duration's median and mean after the first measurement day, but afterwards the results stagnate. On the sixth and last day there is even a slight

increase. The gait parameters' median and mean show similar courses. Even the changes after the first day are only detectable in some parameters. However, the distributions of all parameters, standard deviation (SD), interquartile range (IQR) and total range (TR), do change. From day one to day six, standard deviation (SD) is reduced by 82%, interquartile range (IQR) by 72% and total range (TR) by 84%. The differences between the means of healthy and affected leg in both, stance and swing phase duration, are getting smaller over time. While a ground contact (stance time) on the healthy foot lasts 0.091 s longer than on the injured leg on the first day, it is only 0.015 s longer on the last day. That equals a reduction in difference of 84%. The mean swing time of the healthy foot on the first day is 0.119 s shorter and 0.017 s on the last day, reducing the difference by 86%. In case of the double support time there was also a global reduction in the gap between both legs by 75% from -0.071 s to -0.018 s.

In reference to the validation results, it can be concluded that eSHOE delivers adequately accurate results regarding all temporal gait parameters. The discrepancy between the CTRL and the PAT group indicate, that the eSHOE algorithms work less effective and accurate with motion data from patients. This may root in the fact that the raw data from patients is more erratic and, therefore, more difficult to process for the algorithms. Nevertheless, deviations in the are of ± 46 ms are still acceptable. For the stride length and total distance estimation it seems that the given combination of hardware and calculation methods work more accurate over long distances than they do on shorter tracks, such as a human stride. Higher sample rate, new inertial measurement unit models, with better signal quality, and (mathematically) more sophisticated error compensation methods my provide better results in the future.

Therapy progress could not be determined directly by the detection of clear change of any parameter's median or mean during the stationary stay. However, a narrowing of the distributions, via consistent reductions of SD, IQR and TR, was present in all extracted gait parameters. This indicates, that eSHOE was at least able to detect a decrease in inter-personal gait variability. It is possible that the information about the actual progress is lost among the very broad distributions, especially occurring in the first half of the hospital stay. The individual analyses of certain test subjects, where e.g. a reduction in stride time was detectable, supports this hypothesis. Possible causes are assumed to be the small size and the heterogeneous composition of the sample. It is very likely, that the different usage of walking aids in each individual case at different times influenced the development of the gait parameters and caused the broad distributions.

eSHOE's accuracy doesn't quite match the stationary systems', but it allows the distinction between healthy subjects and persons with unilateral injuries of their lower extremities. Measurements can be performed with less effort and the system is more cost-efficient. It is as accurate as other mobile gait analysis systems, with the difference that it is completely integrated in a pair of shoe insoles. Thus, eSHOE is well-suited for unobtrusive, long-term measurement of motion data with only minimal influence on it's wearer.

Soon, the steady growing number of older people in the population and the related increasing incidences of chronic diseases will call for solutions to ensure long-term success
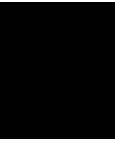
of therapy and rehabilitation success. This need could be met by the envisaged further development of eSHOE into a rehab@home system, that supports the success of therapy measures. The currently booming "quantified self" trend provides additional opportunities for lifestyle application scenarios, which are not limited to a specific age group.

Contents

Introduction

1.1 Problem statement

The quantitative analysis of human movement has reached impressive dimensions by now, concerning accuracy, versatility, and its impact on the improvement of treatment outcomes related to diseases affecting the musculoskeletal system [Andriacchi and Alexander, 2000]. The act of walking seems to be a simple task for healthy adults. However, the interaction of the central nervous system (CNS) and the peripheral neuromuscular complex is very sophisticated and is revealed if certain circumstances reduce the performance of any of the functional parts [Sudarsky, 1990]. Extensive research is available describing human locomotion in a very detailed manner [Perry, 1992, Vaughan et al., 1992, Götz-Neumann, 2003].

In spite of all the achievements and insights that clinical gait analysis has provided, there are still a few issues, especially regarding practicability, everyday relevance and costs. Most stationary and wearable motion analysis tools are expensive and often cumbersome. Furthermore, instrumented gait analysis requires medical or technical professionals. Therefore, their usage is limited to hospitals and rehabilitation clinics. Patients cannot benefit from such systems in their own homes and miss further documentation of the rehabilitation process after discharge from inpatient care. In most cases measurements are still bound to a certain room in a hospital, rehabilitation clinic or equivalent. Two major consequences are that (1) the space in which the tested person can walk is limited and (2) a laboratory setting is always an "in the spotlight" sort of situation, because the person is well aware of being measured and there are always other people in the same room, performing administrative tasks such as operating the equipment. Furthermore, walking always includes an acceleration and a deceleration phase, during which gait parameters do not reach their regular values. Therefore, walking of a rather short distance, as it is the case in many gait laboratories, often reduces the quality of the measurement results

and their everyday relevance [Oberg et al., 1993, Auvinet et al., 1999, Moe-Nilssen and Helbostad, 2004].

1.2   Aim of the work

To overcome restrictions of stationary gait analysis, a concept for a mobile, wearable measurement system has to be developed that can be worn inside a pair of ordinary shoes. This wearable measurement system is called "eSHOE". With it the untethered, extramural and long-term collection of gait parameters shall be enabled. Along with the concept a series of prototypes have to be constructed and tested under real-life conditions.

1.3   Methodological approach

In order to achieve the afore mentioned goals, circuit layout of an embedded system has to be designed. Therefore, suitable sensors for the detection of (foot) motion, a microcontroller for data processing and a radio module for data transmission have to be selected. After that printed circuit boards (PCBs) have to be manufactured, populated and tested. With two of these PCBs on-foot or better in-shoe motion analysis becomes possible. To derive standard gait parameters from this data some algorithms for the detection and recognition of patterns and features have to be developed. The combination of all these developments, sensors, technology culminates in a certain reliability and accuracy. Since eSHOE is a new and untested system, it has to be validated against a well-established and clinically accepted reference system. Finally, to evaluate the feasibility of this system for monitoring of the progress of therapy/rehabilitation (in hip fracture patients) a clinical pilot study - with proper medical supervision - has to be conducted.

1.4   Structure of the work

This thesis presents the efforts of designing, developing and constructing a wearable (foot-worn) measurement system for mobile gait analysis, called eSHOE. The research an development passed through three stages of prototypes. First two are described in brief, since the first stage was (very) experimental and the second is described in detail in [Oberzaucher, 2011]. For the third, and final, stage - from the point of view of this thesis - receives a detailed elaboration concerning hardware design and development, structure and features of firmware and PC software. These final prototypes were also put to the test concerning validity (against a clinically accepted reference system) as well as feasibility for the purpose of therapy progress monitoring. The implementation of these measures took place in the course of a clinical pilot study, which is also described in this thesis, along with all basic requirements (and documents in the appendix) for the ethics committee and the results of the investigations.

CHAPTER **2**

Medical, biomechanical and historic background

This chapter will present an excerpt of the history of the analysis of human locomotion as well as the standard procedures, technology and methodology currently in use in the field of gait analysis. As prelude to the field of gait analysis the anatomical, biomechanical and physiological basics along with terminology and concepts are described. Followed by a brief insight into the very first steps in the development of the methods for movement analysis.

2.1 Anatomical and biomechanical principles for the description of human movements

This subsection gives a short introduction to the medical terminology for body planes, body axes and movement directions. These are all relevant for the description and understanding of human locomotion. In theory there is an arbitrary number of axes and planes which can be placed along the human body. However, there are (only) three perpendicular axes and three planes of major relevance, to which body movements are referred to. Figure 2.1a depicts the planes, corresponding to the three main axes. The frontal plane with the horizontal axis, the sagittal plane with the sagittal axis and the transversal plane with the longitudinal axis. Figure 2.1b contains further specific terms, defining directions and locations on the human body. A combination of these terms ensures precise localization and descriptions of events and processes e.g. regarding human locomotion. When studying and analyzing human gait, (the movements of) a person's legs and feet are of major importance. Our lower extremities have certain degrees of freedom and ranges of motion due to the anatomy of their joints (see fig. 2.2). For one foot there are five degrees of freedom, they are composed of three translational and two rotational movements. The foot can also perform medial and lateral turning, although
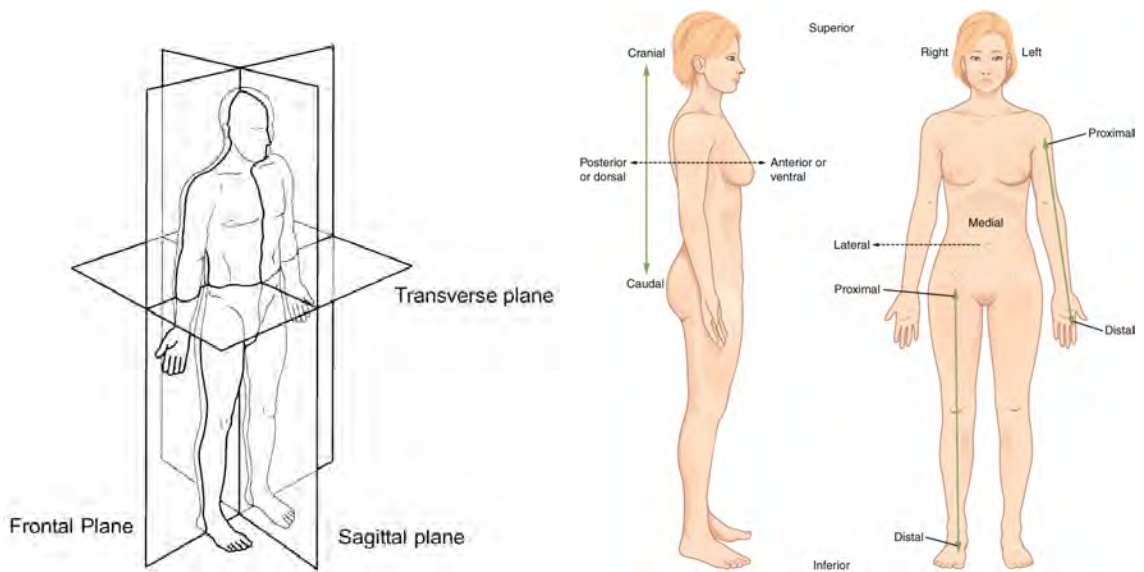
(a) Reference planes of the human body [Vaughan et al., 1992, p. 7].

(b) Directional terms applied to the human body. (Browne, Derived copy of Introduction to Anatomy Module 6: Anatomical Terminology, 2013)

Figure 2.1: Planes and axes (major) of the human body.

this movement does not originate in the foot/ankle joint but it is only possible because of the double bone structure of the Crus (Tibia and Fibula) and/or of the movement of the hip joint (depending on the leg position). Rotational movements of the foot are highly relevant for safe and balanced walking and stance. A brief overview about the foot's anatomy shall also be presented. The foot is subdivided into three regions, tarsus, metatarsus and phalanges. The tarsus consists of seven tarsal bones, the metatarsus contains five metatarsal bones and the phalanges is the region of the five toes (see fig. 2.3).
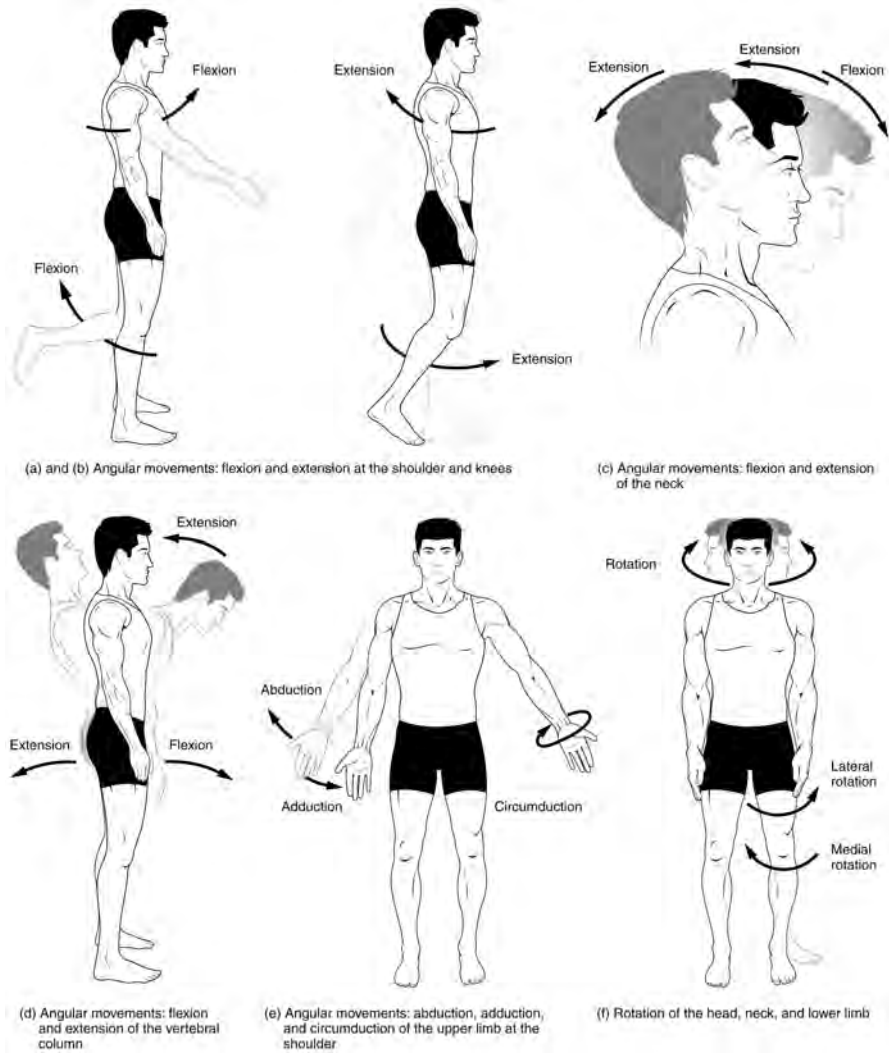
Figure 2.2: Movement directions of the human body and it's extremities.
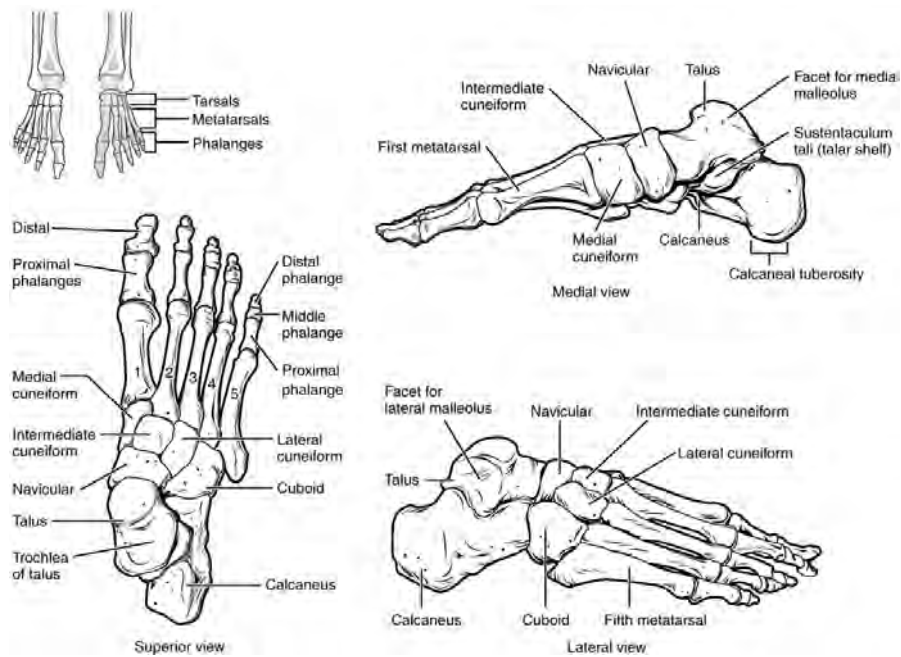
Figure 2.3: Bones of the foot (Browne, Skeletal System Module 14: Bones of the Lower Limb, 2013)

2.2 Human gait and its characteristics

Another very important basic principle for this thesis is the understanding of the fascinating dynamics, parameters and events of human gait. Apart from the efforts already mentioned in the last subsection, extensive research is available describing human locomotion and the large number of methods to analyze and quantify it. The work of the following (three) persons (in the form of books), along with a number of research papers, provided the basic information and inspiration for the now following description of instrumented gait analysis.

> "Walking is a complex interaction of joint mobility, selective muscle action and position sensibility which enables the individual to progress in the desired direction at chosen speed." (Jacquelin Perry in the preface of [Götz-Neumann, 2003].)

Jacquelin Perry, M.D. (May 31, 1918 – March 11, 2013) was an American physician who made major contributions to the field of gait analysis. In 1992 she published the book *Gait Analysis: Normal and Pathological Function*, a key text describing fundamentals of normal gait, pathological gait, current research and equipment as well as clinical considerations. Perry came into contact with observing and evaluating walking behavior and characteristics already very early in her career as physician and therapist. She dealt

with the rehabilitation of patients suffering from poliomyelitis and rheumatoid arthritis, who are often confronted with impaired ambulatory abilities. Her big achievement was a shift from a non-systematized and purely observational approach on gait analysis to a well-structured, sensor and video camera supported system. This development made it possible to catalog different pathologies and their corresponding dysfunctions. Since then she continued to broaden the field of applications of instrumented gait analysis to further pathologies, such as cerebral palsy, hemiplegia, spinal cord injuries, polio-aftercare, arthritis, joint replacement, amputations, myelodysplasia, muscular dystrophy. [Perry, 1992]

In the same year as Perry's book came out, **Christopher L. Vaughan** (born 21 April 1953), Emeritus Professor of Biomedical Engineering in the Department of Human Biology, University of Cape Town in South Africa, published *Dynamics of Human Gait* (together with Brian L. Davis and Jeremy O'Connor)[Vaughan et al., 1992] when he was an Associate Professor of Bioengineering at Clemson University (South Carolina). This book was intended to be an introduction to gait analysis and to act as a companion to the software package *GaitLab*. It is considered to be a valuable supplement to Perry's *Gait Analysis: Normal and Pathological Function*, since it provides a more technical point of view on the subject.

Kirsten Götz-Neumann is a German physiotherapist, gait analysis expert and rehabilitation consultant. In 2003 she published a book about gait analysis, *Gehen verstehen*[Götz-Neumann, 2003], which serves on the one hand as direct German rendering of Perry's *Gait Analysis: Normal and Pathological Function* and on the other hand it shines a different light on the matter, namely with emphasis on the practical aspects, important to physiotherapists. She is also running a website (`www.gehen-verstehen.com/`) offering further information and trainings concerning clinical gait analysis.

Human gait has a very clear overall structure. Due to its periodic nature it can be decomposed into gait cycles. One such gait cycle is depicted in the figure. Focusing on one leg (at a time) these cycles consist of a "stance phase", where the foot rests on the ground, and the "swing phase", during which the foot is advancing in walking direction. Gait cycles can be further segmented into eight sub-phases or events, which are also displayed in the figure: initial contact, loading response, mid stance, terminal stance, pre-swing, initial swing, mid swing, terminal swing [Perry, 1992]. Gait cycles are time normalized, so one cycle ranges from 0 to 100 percent. Starting at the first contact of the foot (in focus) with the ground ("initial contact"), initiating the stance phase, when the body weight is being transferred to this leg. With the "last contact" event the stance phase ends and the swing phase begins. One gait cycle ends (and another begins) when the foot touches the ground again at the end of the "terminal swing phase".

Human gait has a very clear overall structure. Once initiated, walking in a straight line is a periodic process. Therefore, it can be segmented into repeating portions, which are also referred to as "gait cycles". One such gait cycle is depicted in fig. 2.4. Within these cycles the characteristics of certain significant events can be determined. Most parameters focus on one leg at a time. According to [Perry, 1992] one gait cycle can be

Traditional System	Rancho Los Amigos System	Occurrance [% of gait cycle]
Heel Strike	Initial Contact	0
Foot Flat	Loading Response	0 - 12
Mid Stance	Mid Stance	12 - 31
Heel-Off	Terminal Stance	31 - 50
Toe-Off	(End of) Pre-Swing, (start) Initial Swing	50 - 62
Acceleration	(Part of) Initial and Mid Swing	62 - 75
Mid Swing	(Part of) Mid and Terminal Swing	75 - 87
Deceleration	(Part of) Terminal Swing	87 - 100

Table 2.1: Comparison between the terms of the "Traditional System" and the "Rancho Los Amigos System" for the description of gait phases and events [Götz-Neumann, 2003].

divided into two basic phases, a "stance phase" and a "swing phase". Thereby, separating the cycle into one part, where the foot touches the ground and another where it moves through the air and, therefore, does not touch the ground. These two distinct phases serve the purposes of weight acceptance, single limb support and limb advancement and they are further divided into eight sub-phases. They are commonly described using two different terminologies, the *"Traditional System"* and the *"Rancho Los Amigos System"*. Both are describing the same events and the terms can be used interchangeably. It is a personal preference really, which terms are being used. But it would seem that the Rancho Los Amigos System provides terms which are more "neutral" or less suggestive. E.g. it does not suggest that the first contact of the foot with the ground has to occur with the heel. Hence, this event is called "initial contact" instead of "heel strike". One advantage of this system is that it makes it also or better suitable for pathological gait patterns. Therefore, terms according to the Rancho Los Amigos System will be used in this thesis. Table 2.1 contains a comparison of all terms from the Traditional System and the Rancho Los Amigos Systems as well as the occurrence and duration of each event in the gait cycle. Commonly, in gait analysis mostly relative time durations are presented and discussed, expressed in percentage of the gait cycle rather than in seconds. A gait cycle begins with the first contact of the foot (heel) with the ground and it ends right before the same event, one stride later. The time elapsed between these two consecutive footfalls is called "cycle time" or "Stride Time (STR)". The event which initiates the gait cycle is called heel strike (HS) or initial contact (IC). It also commences the stance phase, which is the weight bearing fraction of the gait cycle and it usually lasts for 60 to 65 % of the gait cycle. The stance phase ends with the event of the last contact of the foot with the ground, called last contact (LC) or toe-off (TO). Time elapsing between IC and LC is also being referred to as "stance time" and it can also be expressed in seconds. The last contact or toe-off event signifies the moment, when the foot ceases to contact the ground beneath it. In case of healthy persons, this is the moment when the big toe leaves the ground, hence the name in the Traditional System. With this event the swing phase

begins, during which the foot is (1) airborne and (2) advancing in the walking direction. This phase lasts for 35 to 40 % of the gait cycle. It is concluded with the (next) initial contact of the same foot. When the duration of this phase is expressed in seconds it is called "swing time". Swing Time of the ipsilateral foot is equal to the "single support time" of the contralateral foot, which at that time is supporting the whole body weight alone.

When focussing on both legs during a gait cycle, there are a few more characteristics that can be observed. While walking at "normal" velocity there are two moments during one stride within the stance phase when both feet are touching the ground at the same time. These are called Initial Double Support Time (IDS) and Terminal Double Support Time (TDS). Double Support Time describes the time span from initial contact (heel contact) of the ipsilateral footfall to last contact (toe-off) of the contralateral footfall. Therefore, when focussing on the right leg, Initial Double Support occurs from right heel contact of left toe-off and Terminal Double Support occurs from left heel strike to right toe-off. Each double support phase lasts for 10 to 12 % of the gait cycle. Step Time is the time elapsed from initial contact of the ipsilateral foot to first contact of the contralateral foot. 2.4 contains a graphical representation of one gait cycle and all its phases and parameters.
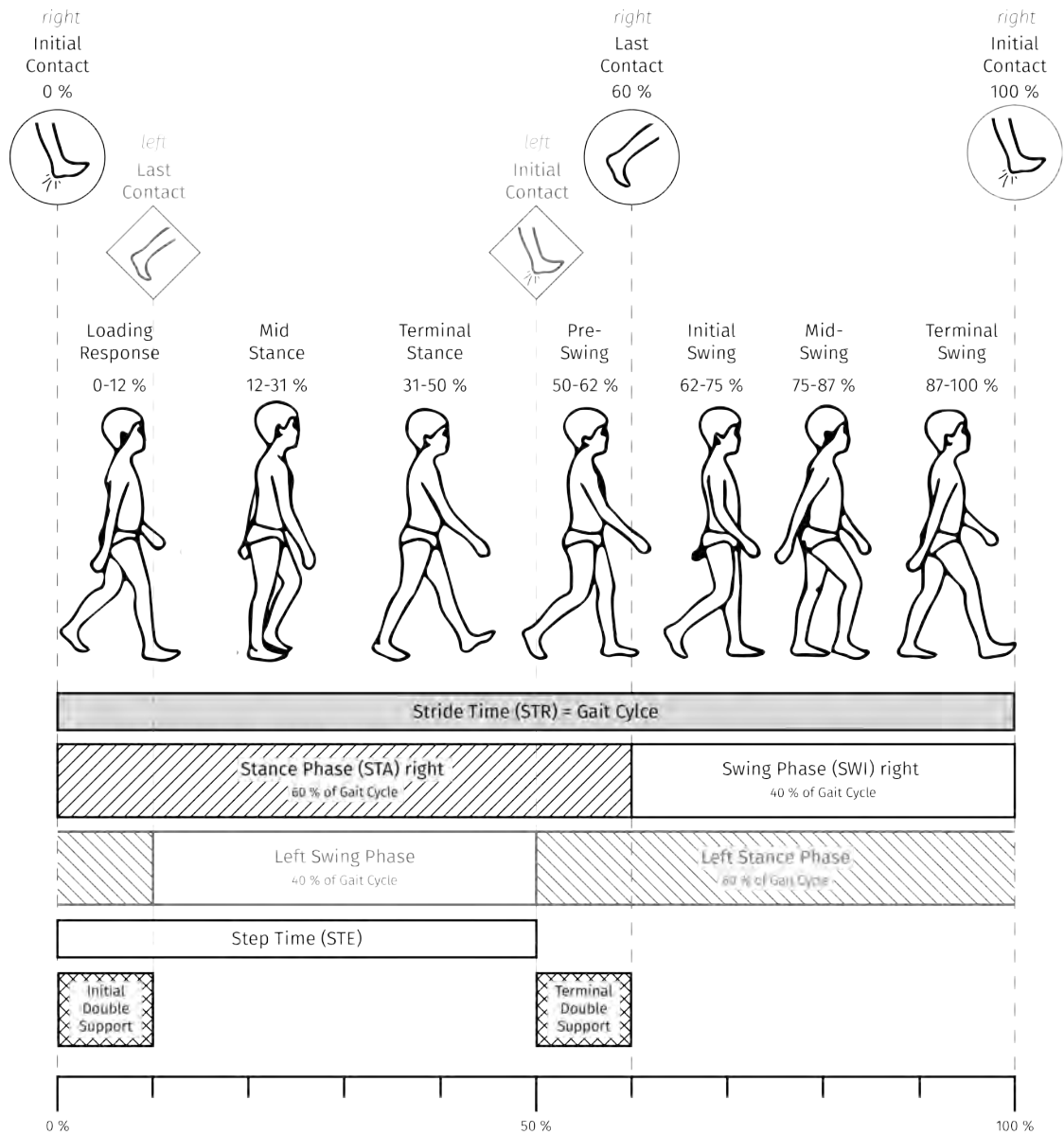
Figure 2.4: Illustration of the gait cycle of a healthy subject, segmented into its eight distinct phases. Gait cycles are time normalized, so one cycle ranges from 0 to 100 %. Starting at the first contact of the foot (in focus) with the ground ("initial contact"), initiating the stance phase, when the body weight is being transferred to this leg. With the "toe-off" event the stance phase ends and the swing phase begins. One gait cycle ends (and another begins) when the foot touches the ground again at the end of the "terminal swing phase". Image adopted from [Vaughan et al., 1992].

2.3 Hip fracture, caused by a fall, and hip replacement

Falling down is a (common) disturbance of the seemingly continuous process of walking. It happens to small children while they are learning to keep their balance and how to move independently. Usually without profound consequences, it is part of the experience. Among (young) adults it occurs during freetime activities (mostly sports), sometimes causing minor injuries. But, due to an active metabolism and intact bone structure these injuries do not pose a threat to maintain a normal lifestyle after the accident.

Reasons for falls and their consequences change profoundly, once older people (>50 years) are involved and the prevalence of osteoporosis is significantly increased. The chance of the occurance for an osteoporotic fracture has been estimated at 40–50 % for women and at 13–22 % for men [Dimai et al., 2011]. Tinetti and Campbell [Tinetti 1988, Campell 1990] reported that every third individual over the age of 65 falls down once a year. Incidence and traumatic consequences increasing with advancing age [Peel 2002]. 10 % of falls are causing injuries, 5 % are causing fractures.

The proximal fracture of the femur (also known as hip fracture) is one of the "major osteoporotic fractures". From 2001 to 2005 there occurred 757 hip fractures per 100,000 women (>50 years) and 323 fractures per 100,000 men (>50 years) every year in Austria. The regular course of the treatment and rehabilitation process after a hip fracture includes
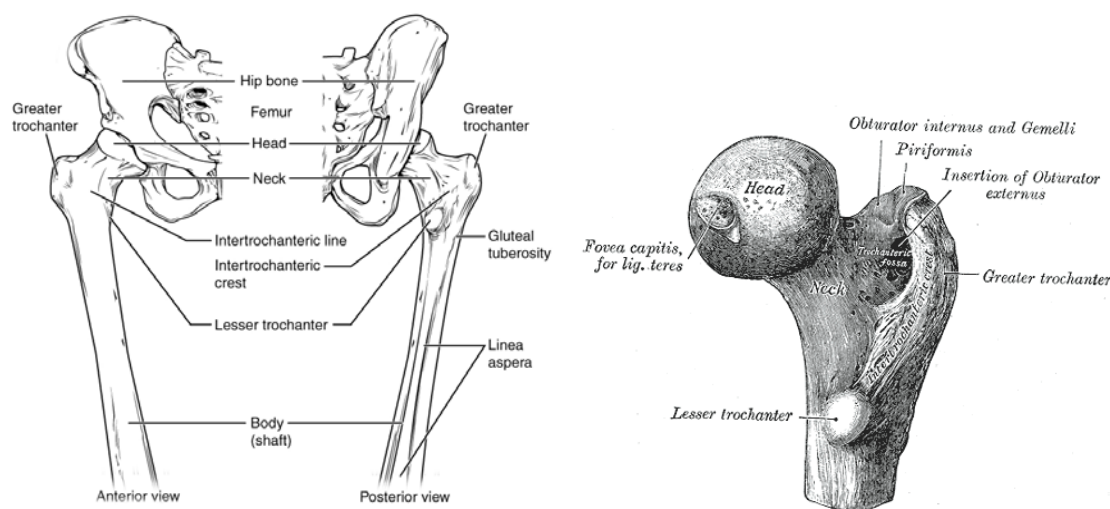
(a) Schematic illustration of the bones of the pelvis and upper leg.

(b) Femoral head.

Figure 2.5: Femur and femoral head. (a) retrieved from `http://cnx.org/resources/6e59c1693b3349bffa2c27ac7a2e29f889a08edc/810_Femur_and_Patella.jpg`, viewed 17.11.2016. (b) retrieved from `http://www.bartleby.com/107/Images/large/image243.gif`, viewed 17.11.2016.

the immediate/very fast surgical repair of the broken bone. In conjunction with the

operation is also approx. 10 days of post-operative hospital stay in (trauma-) surgical care. Thereafter starts the acute geriatric aftercare and remobilization, with an average duration of three weeks. Within this period of aftercare it is attempted to restore the patients' functionality to it's highest possible stage. However, physicians and therapist try at least to assure that a patient is able to cope in his or her familiar surroundings.

Figure 2.6: Medical care flow after hip fracture in Austria. Image adopted from [Pinter et al., 2013].

Bone fractures after fall incidents are not all similar. There are several different types of proximal femur fractures. The **medial femoral neck fracture (MFNF)** is the most common type of fracture of the femur. When a MFNF occurs, the bone fractures either near or directly at the femoral head. Contrary to the lateral femoral neck fracture it is located within the joint capsule (intracapsular). When the bone fractures in the area between greater trochanter and lesser trochanter it is called an **intertrochanteric femoral fracture (ITFF)**. A **subtrochanteric femoral fracture (STFF)** occurs when the femur is fractured below the *linea intertrochanterica*, the imaginary line running between greater trochanter and lesser trochanter. All four fracture types, along with the fracture lines, are illustrated in fig. 2.7.

The possible surgical treatments for these are dependent on the fracture type on the one hand and on the general condition of the patient (age, etc.). A replacement of the entire hip joint with artificial material, including the femoral head and the acetabulum (cotyloid cavity, where the head of the femur meets the pelvis) is called total hip replacement, total hip arthroplasty or **total endoprosthesis (TEP)**. This procedure is used when the natural hip joint is severely damaged by arthrosis. In the case of intertrochanteric fractures **dynamic hip screws (DHSs)** are often used. The fracture is stabilized by a large screw, which is inserted into the femoral head and crosses through the fracture.

Figure 2.7: Different types of hip fracture and their locations.

A plate-like part, which runs down the shaft of the femur, forms the second part of the implant. It is secured in place by a number of smaller screws. This fixation type allows controlled dynamic sliding of the femoral head along the construct. **Proximal femur nails (PFNs)**, also known as "intramedullary nail (IM nail)", are often used for static or dynamic fixation as well as compression for simple fractures of large tubular bones, such as the femur. For fractures close to the joint there are also special versions, such as the gamma-nail, available. **Bipolar femoral neck prosthesis (BFNP)** is a form hemiarthroplasty, a partially replacement of the hip joint. In this procedure (only) the femoral head is removed and replaced with a metal or composite prosthesis. This procedure is most commonly performed after a medial fracture of the neck of the femur (just below the head).

2.4 Origins of the analysis of locomotion

The analysis of human locomotion, or more precisely the optical documentation of movement, goes back to the late 19th century where the French astronomer Pierre-César Jules Janssen (1824-1907) managed to make the first photographic documentation of the transit of Venus across the sun in December of 1874. For that purpose Janssen constructed a so called "photographic revolver" (see fig. 2.8) and took a series of pictures at intervals of approximately one second that showed the planetary disk of Venus entering the solar disk of the sun [Canales, 2002]. In 1878 the English photographer Eadweard
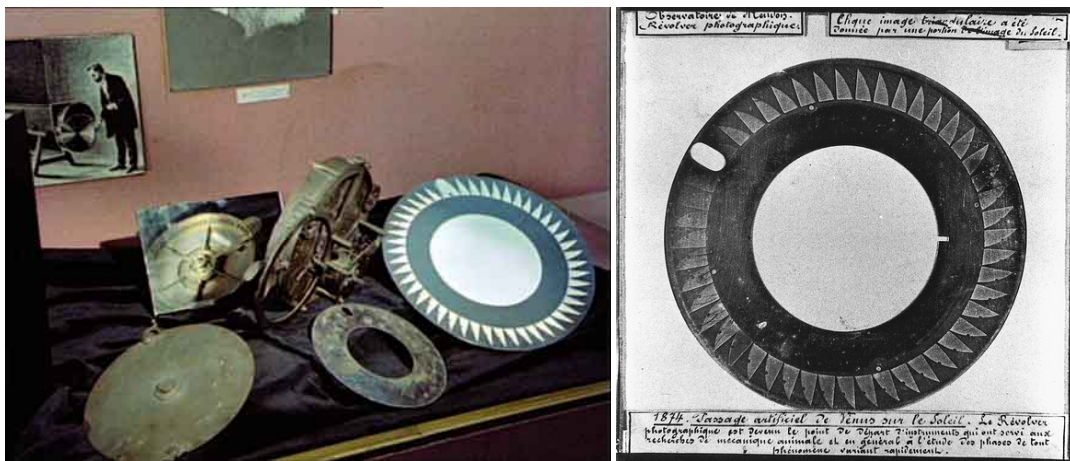
(a) Parts of Janssen's "photographic revolver".   (b) Venus transit of 1874.

Figure 2.8: Pierre-César Jules Janssen's equipment for the documentation of the Venus transit in December 1874.

Muybridge (1830-1904) was hired to conduct photographic studies on horses. There was a theory about horses' gait, that during trot all four legs of a horse are lifted off the ground. But until then there was no proof. So Muybridge designed an experiment and with its help he believed to be able to clarify that question. For this experiment he put together an array of twelve cameras, 53 *cm* (21 inches) apart, which had specially designed shutter mechanisms (double shutters). The shutters were developed for high speed motion capturing or "instantaneous photography" (with very brief exposure time < 0.5 *s*). Each of the shutters was connected to a separate trigger and could be activated automatically when the horse passed the camera. The trigger mechanism was an electrical circuit which had an open wire running across the racetrack, perpendicular to the horse's path. When the wheel of the cart the horse was pulling went across the wire, the circuit was closed, and therefore the camera triggered [Stillman et al., 1882].

Further development by Muybridge after the experiment, dealing with the display of his pictures, led to an invention he called "zoopraxiscope". What was a proof of concept of Muybridge laid the foundation of modern film making and motion pictures, which started to appear in the 1890s. Muybridge continued to study animal and human locomotion
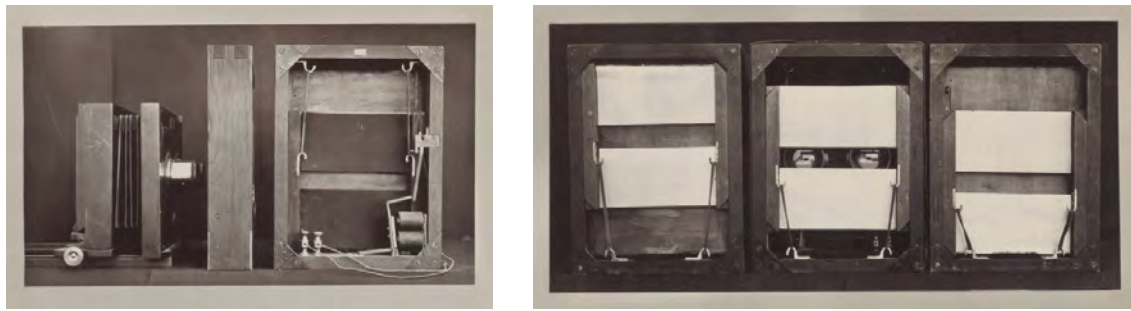
(a) Camera and back of the electronic shutter.

(b) Front of 'electro-shutters', with positions of panels before, during and after exposure.
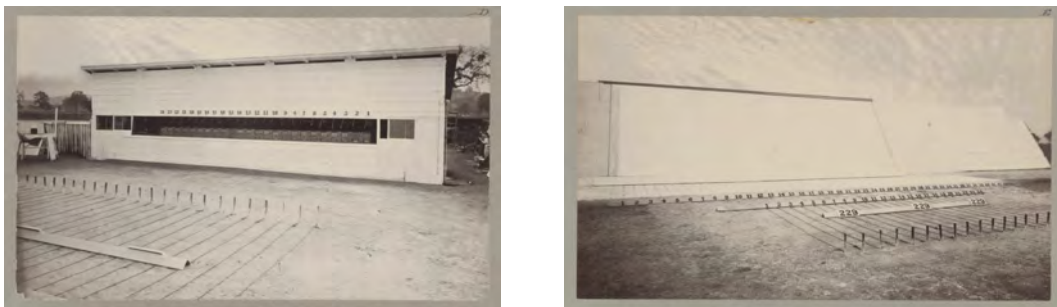
(c) 24 cameras facing the race track upon which the horses moved.

(d) The operating track upon which the horses moved in front of the cameras.

Figure 2.9: Scans from *The horse in motion* [Stillman et al., 1882].

at the University of Pennsylvania, where he conducted his Animal Locomotion Study, comprising 20,000 photographs on 781 plates of males and females performing common actions. In it he used three batteries of twelve cameras each with electronically released shutters. The pictures and discoveries were published in *The Horse in Motion* (1882) by J.D.B. Stillman [Stillman et al., 1882] and by E. Muybridge *Animals in Motion* (1899) [Muybridge, 1899]. Apart from animal locomotion Muybridge later on also used his technique to study human motions, which he published as *The Human Figure in Motion* (1907) [Muybridge, 1907]. Although Muybridge's interest was more artistic than scientific, his work influenced the developments of the science biomechanics to a large extent. Lewis S. Brown (department of art and exhibition, American museum of natural history, New York City) stated the following 1957 in the preface of a revised edition of *Animals in Motion* (1899) [Muybridge, 1957].

> "[...] Despite the moving picture and slow-motion cameras which are now available, little has been learned that Muybridge did not discover. [...] The images he captured in the sessions at Penn remain a standard reference, a dictionary of movement."

Muybridge's work influenced another photographer, who contributed further to the

Figure 2.10: Muybridge-1878 5

development of locomotion analysis, the French scientist, physiologist and chronopho-tographer Étienne-Jules Marey (1830-1904). He was familiar with Muybridge's work, but was disappointed with the lack of accuracy of Muybridge's method, since his twelve-to 36-camera system was only able to capture motion at intervals which were quite far apart. Marey's aim was to capture movements of a bird's wing while flying, which not only required a high rate of succession of pictures, at known and equidistant intervals, but also a trigger mechanism that was independent of the photographed object. For that purpose in 1882 Marey constructed a portable photographic gun ("fusil photographique", see fig. 2.11), which was able to shoot twelve sequential images at intervals of 1/720 of a second and "stored" them on a glass disk. Marey described the specifications of his development like this:

"The barrel of this gun is a tube that contains a photographic lens. Behind this, and solidly mounted on the butt, is a large cylindrical breech casing containing a clockwork mechanism. This mechanism is started by pressing the triggerand imparts the necessary movement to the different parts of the instrument. A central axis makes twelve revolutions per second and commands all the parts of the instrument. The first of this is a metal disk pierced with a narrow slot. The disk forms the shutter and lets the light penetrate only twelve times a second for the duration of 1/720 of a second each time. Behind the first disk is another turning freely on the same axis. This disk has twelve openings, and attached to it is the sensitized glass, which can be either round or octagonal. This second disk must revolve in a regular and intermittent manner so as to stop twelve times per second in front of the ray of light that

Figure 2.11: Fusil de Marey

penetrates the lens. A cam placed on the shaft produces this discontinuous rotation by effecting a mechanism that causes teeth to stop the rotating disk."

Marey's development worked in a similar way like the device that his colleague Janssen used eight years before him with the important difference that Marey's gun worked significantly faster and it was portable [Marey, 1882].

State of the art of gait analysis

This chapter contains information about the state of the art in instrumented gait analysis. It is generally subdivided into stationary or intramural systems (section 3.1) and mobile, portable or extramural systems (section 3.2). Stationary systems comprise passive and active optical motion capturing, electronic walkways and force plates. Portable systems are all about body-worn devices and measurement systems for independent and untethered mobile gait analysis.

3.1 Stationary systems

The quantitative analysis of human movement has reached impressive dimensions by now, concerning accuracy, versatility, and its impact on the improvement of treatment outcomes related to diseases affecting the musculoskeletal system [Andriacchi and Alexander, 2000].

Parameters of human gait are currently detected by stationary devices such as optical motion capture, e.g. Vicon [Kidder et al., 1996], force plates [Hansen et al., 2002] and electronic walkways, e.g. GAITRite® (CIR Systems Inc. Clifton, NJ 07012) [Menz et al., 2004].

Several technical (measurement) systems have been developed and a basic distinction is whether a measurement system is stationary (intramural) or mobile/portable (extramural). The group stationary or intramural systems is definitely there the longest and presently the most widespread technology. It incorporates optical (passive and active) motion capture (see subsections 3.1.1 and 3.1.2) and measurement of pressure or ground reaction forces (see subsections 3.1.3 and 3.1.4). Many of the stationary state of the art systems have already been evaluated concerning accuracy and validity [Menz et al., 2004, Windolf et al., 2008] and proven themselves to be relevant for clinical applications [Zijlstra et al., 2008].
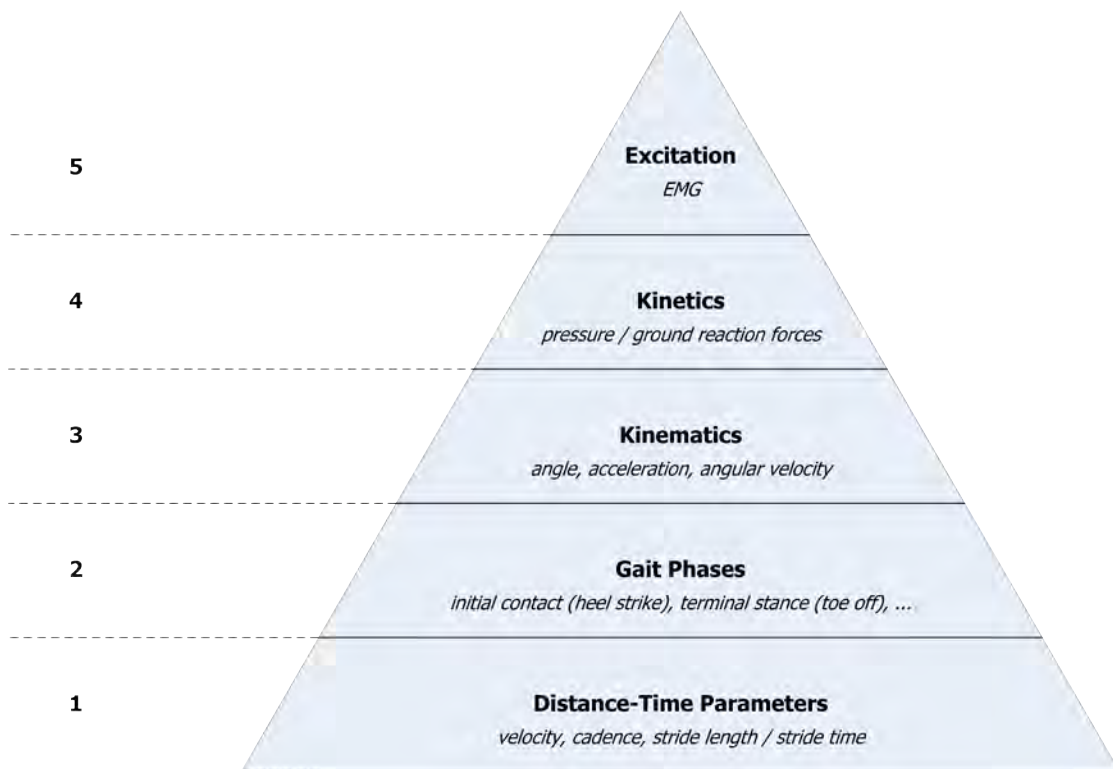
Figure 3.1: Visualization of basic gait parameters in the form of a pyramid, indicating that they are based on one another.

Mobile, portable, wearable (and therefore, extramural) measurement systems began to surface 20xx and are a constantly growing field of research, with some products already on the market. They implement pressure sensitive shoe insoles, e.g. Medilogic® and Pedar®-X [Baláš et al., 2014, Mattar et al., 2015], foot switches [Hausdorff et al., 1995], accelerometers which are attached to different parts of the human body [Aminian et al., 1999, Mariani et al., 2010, Schwesig et al., 2011, Barth et al., 2011], gyroscopes [Greene et al., 2010] and combinations of those as well as other sensor types [Paradiso et al., 1999, Pappas et al., 2001, Morris and Paradiso, 2002, Pappas et al., 2002, Benbasat et al., 2003, Paradiso et al., 2004, Pappas et al., 2004, Bamberg et al., 2008, Stirling et al., 2005, Yun et al., 2007, Mayagoitia et al., 2002]. The shoe-integrated gait sensor system (SIGS), developed by a research group of the Massachusetts Institute of Technology (MIT) [Paradiso et al., 1999, Morris and Paradiso, 2002, Benbasat et al., 2003, Paradiso et al., 2004] and the gait phase detection system (GPDS), by another group at the the Swiss Federal Institute of Technology in Zurich (ETHZ) [Pappas et al., 2001, Pappas et al., 2002, Pappas et al., 2004] both reached a certain promising point, but were not continued further. However, these two projects generated the main impact for the development of eSHOE.

The two most relevant commercially available systems are RehaGait® (Hasomed GmbH, Magdeburg, Germany) and OpenGo science® (Moticon GmbH, Munich, Germany). RehaGait® is a foot-mounted mobile inertial sensor based system [Schwesig et al., 2011] but with the difference that its application focusses on clinical or in-patient settings only. OpenGo science® is a gait analysis sensor in the form of an insole, containing capacitive pressure sensors, a 3D accelerometer and a temperature sensor with the goal of monitoring the healing process, e.g. after ankle fracture [Braun et al., 2015a]. Methods and results from these mobile gait analysis systems are described in detail in the subsections 3.2.3 and 3.2.4.

3.1.1 Optical motion capture using passive markers

Optical passive motion capture can be considered, according to Kirtley [Kirtley, 2006, p. 43], as the presently most widespread and most popular method for clinical gait analysis. This approach uses (mostly spherical) markers (with a diameter of 9.5 mm) coated with retroreflective material, which have previously been attached to a number of "anatomical landmarks" of a test subject. High speed video cameras, which have the additional capability of emitting and detecting infrared light, are used to detect these markers. One such system usually consists of two to 48 cameras. Theoretically two cameras will suffice to get a fix on the location of one marker. But each camera has a limited field of vision and the objects or subjects are moving, so one camera can very easily loose sight of a marker. Therefore, the more cameras are covering the measurement area, the better the chances are of not missing a marker, e.g. due to obscuration. A special evaluation software makes it possible to track the markers' 3D positions and trajectories via triangulation. On average these systems reach an accuracy of around 0.5 mm and 0.5°for a measuring volume of 4 × 4 × 4 m. This type of system can capture large numbers of markers at frame rates usually around 120 to 160 Hz. By lowering the resolution and tracking a smaller region of interest they can track as high as 10,000 Hz.

Well-known manufacturers of optical motion analysis systems are Vicon Motion System (Oxford, UK), Motion analysis Corp. (Santa Rosa, CA, USA), Peak Performance (Denver, CO, USA), Optotrak (Northern Digital Inc., Waterloo, ON, Canada), SIMI Reality Motion Systems GmbH (Unterschleissheim, Germany) or Ariel Dynamics, Inc. (Trabuco Canyon, CA, USA) [Hegewald, 1999, p. 32] [Kirtley, 2006, p. 42].

3.1.2 Optical motion capture using active markers

Another variation of optical motion capture works with "active" markers in the form of light sources (e.g. light-emitting diodes (LEDs)). Such systems also triangulate the position of markers. But in this case the markers themselves emit light rather than reflecting it (externally generated light) back. Possible (marker-detector) distances and volume for capture are increased, due to the Inverse-square law (¼the power at 2 times the distance). Further advantages are a high signal-to-noise ratio, very low marker jitter and

<div align="center">(a) (b)</div>
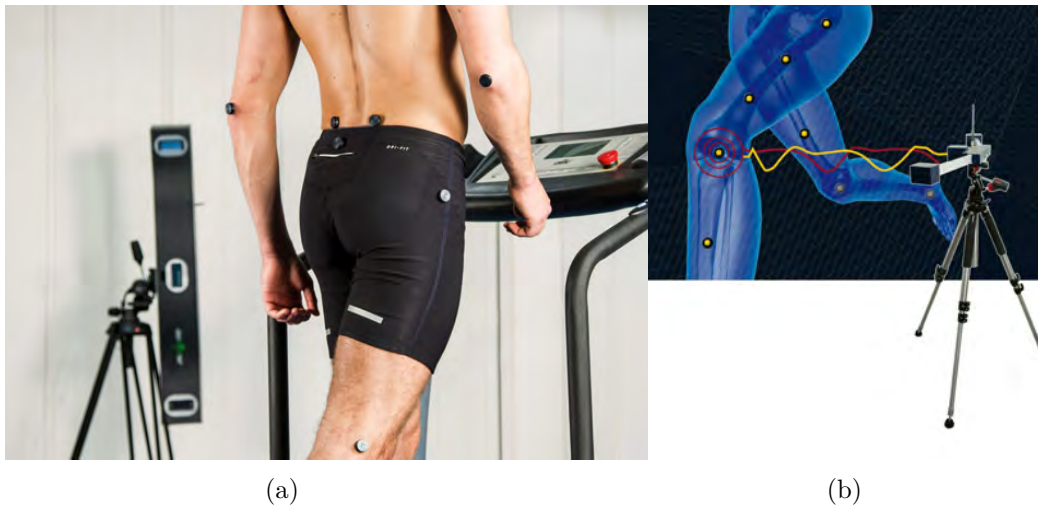
Figure 3.2: The active optical motion capture system "LUKOtronic" / "Steinbichler Motion Capturing". (a) retrieved from `http://optotechnik.zeiss.com/produkte/3d-bewegungsanalyse`, viewed 01.09.2016. (b) retrieved from `https://www.facebook.com/Lukotronic-274524062581720/`, viewed 01.09.2016.

high measurement resolution (0.1 mm within the calibrated volume). A rather popular example for optical motion capturing with active markers is the "LUKOtronic" (until 01/2012) or the "Steinbichler Motion Capturing" system, as it is now called, distributed by Zeiss Optotechnik.

3.1.3 Electronic walkway - GAITRite®

GAITRite® (CIR Systems Inc. Clifton, NJ 07012) is an electronic walkway with built-in pressure sensors, which, in combination with its application software, is capable of computing standard spatio-temporal gait parameters [Bilney et al., 2003, Menz et al., 2004]. The version used in this study is 4.6 m long with an active sensor area of 3.66 m in length and 0.61 m in width. This area contains 13,824 pressure sensors, which are arranged in a grid pattern (288 × 48) with a spatial resolution of 0.0127 m. Data from the sensors can be sampled at frequencies ranging from 60 to 240 Hz (60, 80, 100, 120, 180, 240). The walkway is connected to a PC by a serial interface cable, where the spatial and temporal characteristics of gait are processed and stored by means of the GAITRite® software. When a subject is walking across the instrumented carpet, the built-in pressure sensors are activated with each footstep. The software is able to calculate temporal and spatial gait from the steps. One of the advantages of GAITRite® is that even persons with walking aids can be analyzed without difficulty. The path of e.g. a wheeled walker can easily be identified and deleted from the data. GAITRite® proved to have good test-retest reliability [Bilney et al., 2003, Menz et al., 2004] as well as excellent agreement in comparison with the previously established standard the optical motion analysis system

(a)   (b)
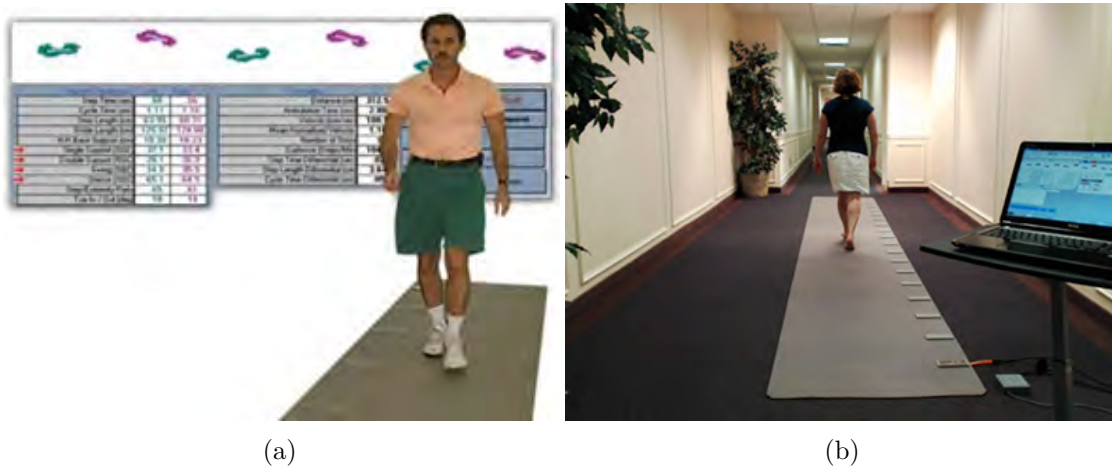
Figure 3.3: The electronic walkway GAITRite. (a) retrieved from `http://www.hopkinsmedicine.org/neurology_neurosurgery/centers_clinics/transverse_myelitis/about-tm/rehabilitation-for-tm.html`, viewed 01.09.2016. (b) retrieved from `https://spectrumnews.org/news/toolbox/folding-mat-reveals-motor-deficits-in-severe-autism/`, viewed 01.09.2016.

Vicon [Webster et al., 2005] and is therefore considered to be a valid and useful tool for the objective analysis of human locomotion.

3.1.4 Force plates

In gait analysis it is also of importance to measure *kinetic* (rather than kinematic) parameters. For this purpose different kinds of force or pressure measuring platforms are used. Strain gauges or piezoelectric sensors (e.g. Kistler), capacitance gauges, etc. inside the platforms are usually responsible for the detection of individual load and (sometimes also) the shear components of *ground-reaction-forces*. There are one-component devices, which can only measure vertical aspects of force and there are also multi-component force platforms, which measure all three components of force.

Major manufacturers of force plates are Zebris Medical GmbH (Isny im Allgäu, Germany) Biodex Medical Systems (Shirley, New York, USA), Kistler Instrumente AG (Winterthur, Switzerland), Novel GmbH (Munich, Germany).

3.2 Portable and mobile systems

3.2.1 Electromyography

Electromyography (EMG) is a diagnostic technique for capturing and evaluating of electrical activity produced by skeletal muscles. It serves the purpose of interpreting activation level, muscle (fibre) recruitment order, medical abnormalities or also to analyze the biomechanics of (human) movement. The detection of EMG signals can be achieved via two different approaches. Either via surface electrodes, attached to the subject's skin (above the muscle belly) or by needle electrodes, which are injected/inserted directly into the muscle belly percutaneously. In clinical gait analysis, electromyography (EMG) is usually always measured via surface electrodes, due to easier handling and less interference and discomfort to the test subject. [Hegewald, 1999, p. 35];[Götz-Neumann, 2003, p. 121];[Kirtley, 2006, p. 139]

Rectification and low-pass filtering (Butterworth 5th order, 3 Hz cutoff frequency) as well as intra-subject normalization are often used when dealing with EMG data acquired during gait [Burden et al., 2003, Bovi et al., 2011].

Although it allows qualitative predictions, it is not possible to differentiate between concentric, isometric and eccentric contractions of the muscles, referring (only) to EMG data [Hegewald, 1999, p. 35]. An example of an EMG-system used for gait analysis is the EMG system from Noraxon (Noraxon U.S.A. Inc., Scottsdale, Arizona).

3.2.2 Insole Pressure Measurement Systems

Alternatively to stationary force plates integrated into the floor of a gait laboratory there are also insole-based pressure measurement systems, which can be worn inside the shoes. A large number of pressure sensors (resistive or capacitive) are integrated into a very thin insole. Pressure between the foot and shoe (sole) is detected and recorded. An advantage, compared to force plates, is that it is possible to gather data from multiple steps.

Medilogic®

A popular provider of such flexible pressure measurement insoles is T&T medilogic (T&T, Schönefeld, Germany) with the medilogic® system [Kirtley, 2006, pp. 87] [Hegewald, 1999, pp. 33].It consists of a pair of pressure sensitive shoe insoles, a belt-worn "patient modem" (data logger) for data storage and wireless transmission and a "computer modem" connectable to a PC for data (pre-)processing (see fig. 3.4). Each insole contains max. 240 SSR sensors, depending on size and shape (available standard sizes: 33-34, 35-36, 37-38, 39-40, 41-42, 43-44, 45-46, 47-48, 49-50). The sensors' measurement range is 0.6 to 64 N/cm^2 (max. error of $\pm$ 0.575 N/cm^2) and the sampling rate 60 Hz (optional 50 Hz for video synchronization) or max. 300 Hz for sports version. A special analysis software provides different kinds of illustrations and analyses of the collected data, e.g. visualization of the pressure distribution, gait symmetry as well as and cyclogram and gaitlines (see fig. 3.5).

(a) Subject wearing medilogic®.

(b) Medilogic® equipment.

Figure 3.4: Medilogic insole pressure measurement system. (a) retrieved from `http://www.schuh-pongratz.de/index.php/dynamische-fussdruckmessung.html`, viewed 01.09.2016; (b) retrieved from `http://www.medilogic.com/en/products-human/footpressure-measurement/medilogic-insole/`, viewed 01.09.2016
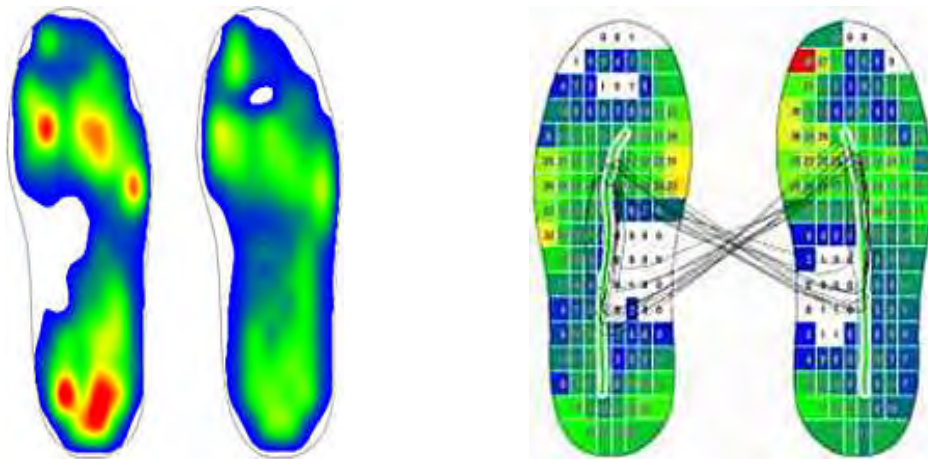
(a) Comparison of two readings of isobaric data. (b) Cyclogram, generated via medilogic insoles.

Figure 3.5: Two example displays from the medilogic® analysis software. Retrieved from `http://www.medilogic.com/en/products-human/footpressure-measurement/medilogic-insole/`, viewed 01.09.2016

Pedar®-X

The Pedar®-X (Novel GmbH, Munich, Germany) also is an insole-based measurement system for monitoring local loads between the foot and the shoe. Apart from the insoles the system also comprises the Pedar-X box, which is a data-logger, connected to the insoles via cables and attached to the subject's waist. The box gathers data at 100 Hz and is capable of wireless radio transmission via Bluetooth™ to connect to a Bluetooth-ready PC. In addition, measurement data can be stored in built-in flash memory, to be downloaded to the computer at a later stage. A special software for long-term monitoring, "pedoport®", is also available. Each insole contains 99 force sensors with a spatial resolution of ~ 10 mm (two sensors/cm²) and a pressure range of 15ˇ600 kPa. [Baláš et al., 2014, Mattar et al., 2015]

(a) Pedar®-X equipment. (b) Subject wearing Pedar®-X.

Figure 3.6: Pedar®-X insole pressure measurement system. (a) retrieved from `http://novelusa.com/index.php?fuseaction=systems.pedar`, viewed 01.09.2016; (b) retrieved from `http://novel.de/novelcontent/pedar`, viewed 01.09.2016

paroLogg

The paroLogg system from paromed GmbH & Co. KG (Neubeuern, Germany) uses slightly different technology for insole pressure measurement. Their insoles are equipped with 32 "hydrocell measurement points" each and gather data at 300 Hz, with a measurement range up to 62.5 N/cm^2. Data transmission standard is wireless LAN.
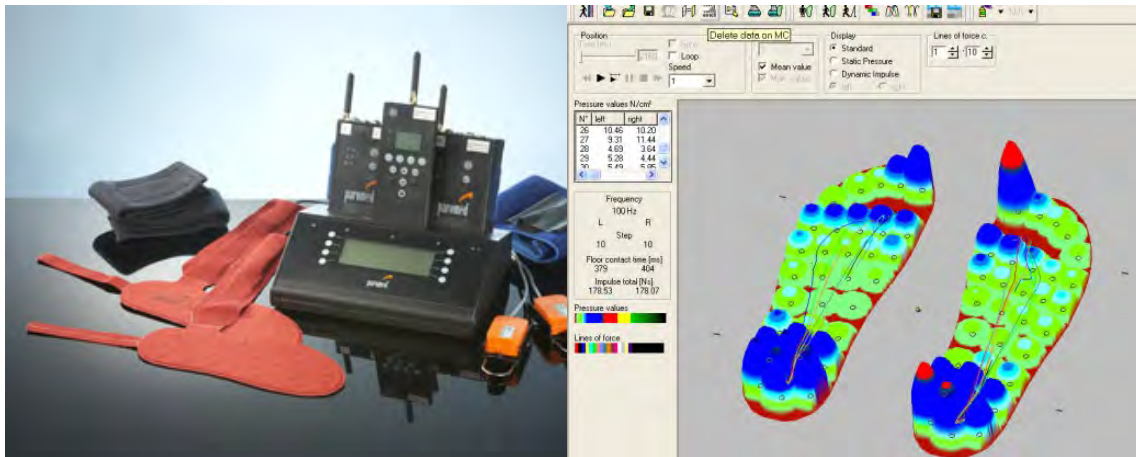
(a) ParoLogg equipment.　　　　　(b) ParoLogg user interface.

Figure 3.7: Pedar®-X insole pressure measurement system. (a) retrieved from `http://www.crispinorthotics.com/orthotics/about-us/unique-solutions/`, viewed 01.09.2016; (b) retrieved from `http://www.crispinorthotics.com/private/crispin-private/clinical-services/`, viewed 01.09.2016

3.2.3　Wearable inertial sensor systems

RehaGait® (RehaWatch®)

RehaGait® (formerly RehaWatch®) is a foot-mounted mobile inertial sensor based system by the Hasomed GmbH (Magdeburg, Germany) with clinical application areas ranging from Parkinson's disease, geriatrics, stroke and orthopedics [Schwesig et al., 2010, Schwesig et al., 2011, Donath et al., 2016b]. RehaGait®'s most recent version comprises of two inertial measurement units (IMUs), containing a 3D-accelerometer, a 3D-gyroscope and a 3D-magnetometer with a sampling rate of 500 Hz. Schwesig et al stated in [Schwesig et al., 2010] that the measurement ranges of the accelerometer and gyroscope are ± 4 g and $\pm 700 \deg/s$. In [Schwesig et al., 2011] the sensor specifications changed to ± 5 g, $\pm 600 \deg/s$ and 512 Hz. [Donath et al., 2016a] reports a new (the latest) version with the following characteristics: ± 16 g, $\pm 2000 \deg/s$ and 500 Hz. The IMUs are attached to the lateral sides of the subject's shoes via a 2006 patented mounting mechanism [Feier et al., 2006]. Figure 3.8 shows a comparison of the measurement setups of RehaWatch® in 2011 [Schwesig et al., 2011] and RehaGait® [Donath et al., 2016b]. Furthermore, it is necessary to attach a mobile processing device (data-logger) to the subject's waist. It collects data from the (shoe-mounted) sensors via cable-connection. In order to transfer the collected data to the PC, a USB-stick has to be used. Data interpretation is performed offline.

Apparently, RehaGait's offline evaluation uses the initial contact (IC) as reference event, to derive other gait events from, such as full contact, heel-off, and last contact (LC). Using these few key features as basis, more spatio-temporal gait parameters can be

(a) RehaWatch® in 2011. ©[Schwesig et al., 2011] (b) RehaGait® in 2016. ©[Donath et al., 2016b]

Figure 3.8: Photographs of the RehaWatch/RehaGait system, then (2011) and now (2016). (a) retrieved from `http://www.sciencedirect.com/science/article/pii/S0966636211000737`, viewed 12.09.2016; (b) retrieved from `http://www.ncbi.nlm.nih.gov/pmc/articles/PMC4719749/figure/Fig1/`, viewed 12.09.2016

calculated automatically, including stride length, foot height, and walking speed), gait phases and symmetry.

Reliability and validity have been assessed in [Schwesig et al., 2010], [Donath et al., 2016a] and [Donath et al., 2016b] and will be discussed in detail (in reference to eSHOE) in chapter 7. Schwesig et al tested 44 healthy subjects (13 F/31 M, age: $27, 7 \pm 4.2$ $yrs.$, weight: 71.8 ± 10.7 kg, height: 176 ± 7.3 cm), where they had to perform three trials of walking 20 m wearing RehaWatch. High reliability was reported, based on ICCs ranging from 0.691 to 0.959 and mean differences between 0.0004 and 0.912 from four selected parameters: stride time, gait speed, stance phase and minimum foot inclination. A more detailed presentation of the results for reliability, based on a comparison of measurements no. 3 and 9 from of [Schwesig et al., 2010] can be found in fig. 3.9.

Furthermore, in [Schwesig et al., 2010] an unpublished validation study is mentioned, in which ten healthy subjects (6 F/4 M, age: 27.2 ± 9.2 $yrs.$) participated. The subjects had to walk at their preferred and self-selected speed over 12 m, with ten repetitions per subject. Vicon (Oxford Metrics Ltd., Oxford, UK) served as reference system with the "Plug-In-Gait" (16-) marker setup. This study revealed high validity of cadence, stride length, stride time and walking speed with an ICC-range from 0.776 to 0.991. ICCs of less than 0.75 were found in test-retest comparisons of double support time and single support time.

Hasomed's website promotes a total of 15 publications - a mixture of journal papers, conference papers, research reports - since 2005 (`https://www.hasomed.de/de/rehagait/publikationen.html`).
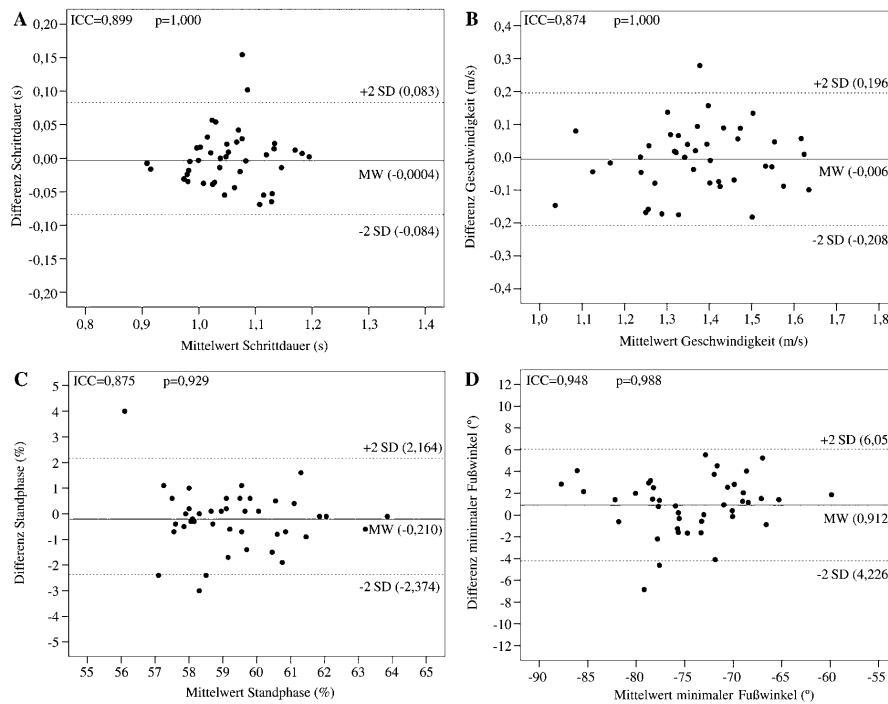
Figure 3.9: RehaGait® measurement system attached to a subject. Retrieved from `http://www.sciencedirect.com/science/article/pii/S0966636211000737`, viewed 12.09.2016. © [Schwesig et al., 2010]

Shimmer

Shimmer Research Ltd. (Dublin, Ireland) produces (among other things) wearable sensors and corresponding evaluation software. One of their products, the Shimmer3 has been used in studies, similar to the one(s) in this thesis [Klucken et al., 2011, Barth et al., 2011, Barth et al., 2012, Kugler et al., 2012]. The Shimmer3 is a portable and wearable sensor platform, containing a 10 degrees of freedom (DoF) inertial measurement unit (IMU), again comprised of accelerometer, gyroscope and magnetometer, all in 3D. Additionally, it includes internal and external connectors for electrocardiography (ECG) and EMG expansion modules. The sensor platform's version used in [Barth et al., 2011] and [Barth et al., 2015] contained a MSP430F1611 microprocessor, a three-axis accelerometer (MMA7260Q, Freescale Semiconductors, Austin, TX, USA) with adjustable range of ± 1.5 g to 6 g and a sensitivity of 0.0025 g at 4 g. The gyroscope was an InvenSense (Sunnyvale, CA, USA) 500 series, with a range of $\pm 500 \deg / s$ and a sensitivity of 2 $mV / \deg / s$. It also had a small form factor ($50 \times 25 \times 12.5$ mm) and was lightweight (15 g).

(a) Shimmer3 measurement platform.

(b) The Shimmer2R, preceding model of Shimmer3.
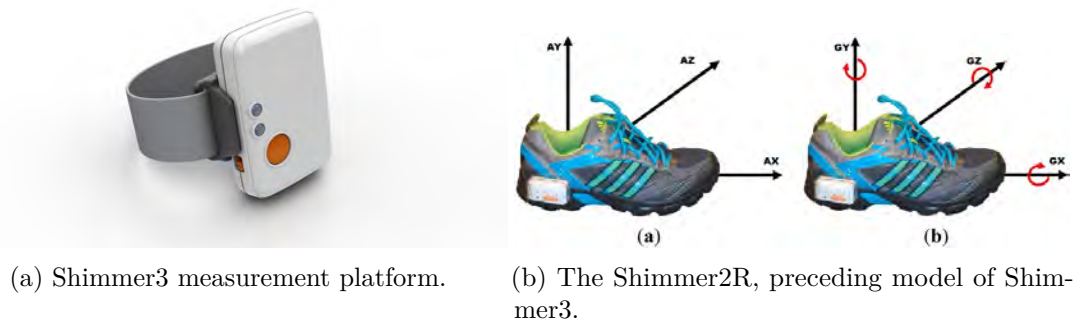
Figure 3.10: Shimmer3 measurement system. (a) retrieved from `http://www.shimmersensing.com/shop/shimmer3`, viewed 02.09.2016; (b) retrieved and adopted from `http://www.ncbi.nlm.nih.gov/pmc/articles/PMC4435165/figure/sensors-15-06419-f001/`, viewed 01.09.2016. ©[Barth et al., 2015].

3.2.4 Wearable multi-sensor systems

Gait phase detection system (GPDS)

A research group from the ETHZ developed a reliable, insole-embedded gait phase detection sensor for functional electrical stimulation (FES)-assisted walking [Pappas et al., 2001, Pappas et al., 2002, Pappas et al., 2004].

Until 2001 a wide variety of control mechanisms for FES timing control was already available. Mostly they were used to distinguish between stance and swing phase but in some cases it was also possible to detect multiple gait cycle phases or events. The dominant form of FES control, the foot-switch, proved to be a rather inefficient method, due to poor detection reliability and the lack of differentiation of foot loading and unloading. Pappas et al wanted to create a closed-loop FES timing control system via a portable gait phase detection system (GPDS) to improve the quality of leg motion.

[Pappas et al., 2001] report that they used (only) two types of (off-the-shelf) sensors for their GPDS, namely three force sensitive resistors (FSRs) and one gyroscope. A schematic of the very first version is shown in fig. 3.11. A microcontroller board (Hitachi SH7032) samples the sensors' signals at 100 Hz and with a resolution of 10 bits. They used three round FSR-152-NS (Interlink El. Inc.) with a diameter of 18.3 mm and placed them underneath the heel and underneath the first and fourth heads of the metatarsal bones. Since the FSRs are not precision sensors (part-to-part repeatability $\pm$ 25%) they were only used to indicate two states: weight applied or no weight applied. The ENC-03J gyroscope (Murata) was attached to the posterior of the shoe with its sensing axis oriented perpendicular to the sagittal plane to measure rotations of the foot in that plane (see fig. 3.11). From the gyro the bandpass-filtered (third-order, 0.25 to 25 Hz with a 20 dB gain in the passband) raw signal, delivering angular velocity, as well as the integrated signal, resulting in the inclination of the foot relative to the ground, were
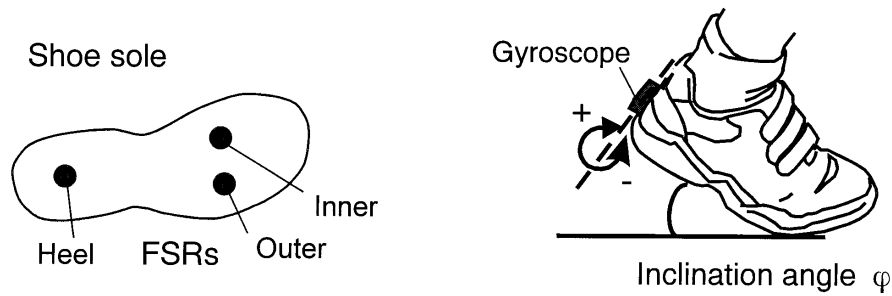
Figure 3.11: Schematic of the gait phase detection system (GPDS). Retrieved and adopted from `http://ieeexplore.ieee.org/document/928571/figures`, viewed 08.09.2016. ©[Pappas et al., 2001].
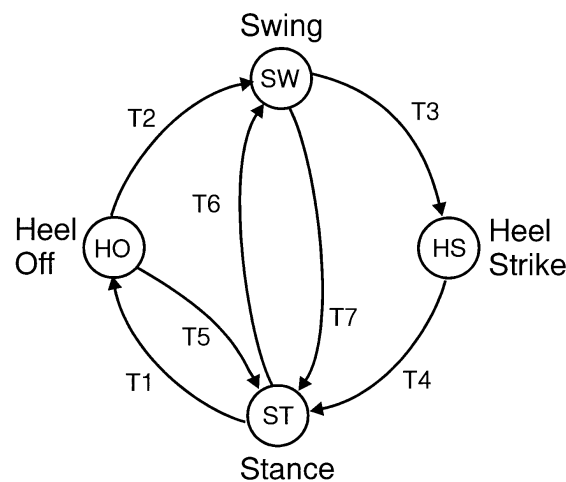
Figure 3.12: The GPDS divides the gait cycle into four phases: stance, heel-off, heel-strike, and swing. The arrows T1-T7 illustrate the possible transitions between the gait phases. Retrieved and adopted from `http://ieeexplore.ieee.org/document/928571/figures`, viewed 08.09.2016. ©[Pappas et al., 2001].

used. Due to well-known drift errors inherent to all gyros, a resetting mechanism was implemented, which set the foot inclination to zero whenever all three FSRs were loaded.

Based on the signals from the GPDS Pappas et al developed a state-machine-like algorithm for gait phase detection. They divided the gait cycle into four gait phases: stance, heel-off, swing, and heel-strike, which were modeled as four states in the state machine (see fig. 3.12). In the course of an experimental study the group covered four tasks:

1. validated their system's performance against the commercial optical motion analysis system Vicon 370 (Oxford Metrics Ltd., U.K.)
2. tested the performance of the GPDS during different walking tasks and under real environment conditions

31

3. verified that the GPDS does not falsely identify any gait phases during non-walking activities
4. determined the range of walking and running speeds for which the GPDS yields reliable results

Two groups of subjects were involved: (A) ten healthy adults (without orthopedic, metabolic, or neurological impairments or pain) and (B) six adults with various gait pathologies.

The validation measurements (1) were carried out with GPDS and Vicon collecting data simultaneously, while three able-bodied subjects were walking on a treadmill at two different speeds (3 and 5 km/h). For the motion capture analysis a three-marker setup was used, with retro-reflective markers attached to the toe, heel and knee. Three Vicon cameras were used to track the marker positions with sampling frequency 50 Hz and an accuracy of ± 1 mm. The goal was to extract a "reference" gait phase signal, which could be used to assess the accuracy of the GPDS output.

In the walking tasks part (2) all subjects of groups A and B were asked to

1. walk on level ground for 100 m;
2. walk up and down a steep road (2×50 m, inclination 15 %);
3. walk on grass, snow, earth, step over small obstacles, and step on and off the pavement (length 100 m, maximum obstacle height 10 cm);
4. ascend and descend stairs (2×50 steps).

Additionally, it was evaluated, if the system is robust to changes in ambient temperature (e.g. in transition from walking indoors to outdoors).

Part 3 of the study served the purpose of verifying that the GPDS does not falsely identify any gait phases during non-walking activities. The following non-walking activities were chosen:

1. stand up from a chair and sit down (five repetitions);
2. stand up, then bend the knees and touch the floor with the fingers (five repetitions);
3. stand upright and rotate in clockwise direction for 360° and in counter-clockwise direction for 360° around the subject's own vertical axis. Subjects were allowed to slide their feet but not to lift them.

In order to determine the range of speeds (during walking and running) for which the GPDS yields reliable results, in part 4 three able-bodied subjects were asked to walk/run on a treadmill. Speed was gradually increased from 0.5 km/h to 13 km/h in steps of 1 km/h. Ten steps at each of the speeds were recorded.

Results of the validation showed a good correlation between GPDS output and the reference gait phase signal for all trials. Synchronized Vicon measurements of the heel
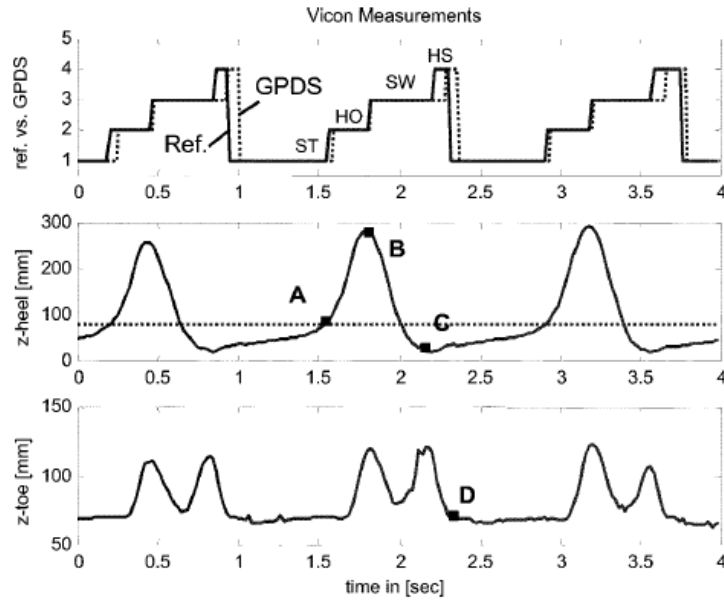
Figure 3.13: Synchronized Vicon measurements of the heel marker (middle) and toe marker (bottom) trajectories in the vertical direction. From the marker measurements (reference points A, B, C, and D) we extracted a reference gait phase signal (top, solid line), which was used to evaluate the delay time of the GPDS output signal (top, broken line). (Note: ST = stance, HO = heel-off, SW = swing, HS = heel-strike, heel-FSR = solid line, front-FSRs = broken lines). ©[Pappas et al., 2001].

and toe marker positions in the vertical direction are fig. 3.13. There was, however, a certain time delay in the detection of the heel-strike and stance phases. In 60 gait cycles (*three subjects* × 20 *steps* per subject) at 3 *km/h* walking speed the following delays (for the detection of the four gait phases relative to the reference signal) were detected: 40 *ms* for heel-off, 35 *ms* for swing, 70 *ms* for heel-strike, and 70 *ms* for stance. The reference signal itself may exhibit a certain lag, due to a (naturally) limited sample rate. In the case of Vicon the sampling frequency was 50 *Hz*, therefore, the natural inaccuracy due to quantization is 20 *ms* (or one sample period: 1/50 *Hz*). This means the gait phase detection delay was ≤ 90 *ms* in the worst case.

The authors claim that the time lag can be explained due to the fact that the reference system maps the heel-strike phase to the IC, i.e. the very first contact of the foot with the ground, whereas the FSR underneath the heel inside the GPDS is only activated in the "weight acceptance" phase (foot flat), which occurs (up to 12 %) later in the gait cycle. They also state that, all remaining time delays are to be explained in a similar fashion.

There is a trade-off between robustness and delay of the detection in the case of the GPDS. For example, the transition from stance into heel-off phase was triggered as
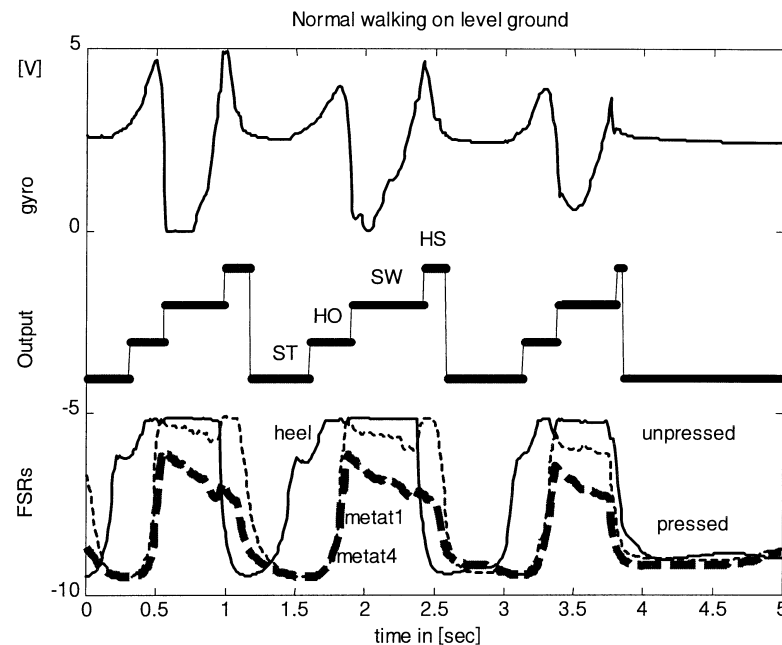
Figure 3.14: GPDS output during normal walking on level ground. ©[Pappas et al., 2001].

soon as the inclination of the foot exceeded 3°. If the system should be more robust to perturbations it is reasonable to have a higher threshold, because then less false positive detections of heel-off occur. On the other hand, a high threshold causes the heel-off event to be detected at a later point of time, hence resulting in a delay.

The results of the performance tests under different walking and environment conditions showed excellent reliability of the GPDS During the first three tasks (walking on level ground, on slopes, and irregular terrain), a total of 2857 ($= 608 + 1303 + 946$) steps was recorded for *group A* and 918 steps for *group B*. There were success rates of 100 % and 99 % for the detection of all four gait phases in group A and B, respectively. Fig. 3.14 shows an example of the GPDS output during normal walking on level ground. As would be expected, the walking characteristics of the subjects of group B exhibited much higher irregularities compared to healthy subjects' gait. These deviations from the anticipated "normal" walking style sometimes caused the GPDS to miss one of the four phases. For instance, when subjects pronounced the heel-off phase too poorly, the GPDS output switched directly from stance phase to swing phase. In another case, when the subject initiated the gait cycle with placing the foot flat on the ground, instead of heel first, the GPDS would switch from swing to stance phase.

Gait phase detection during stair climbing proved to be similarly successful. In group A 99.78 % of all 941 (asc.: 517 + desc.: 424) gait phases were correctly identified. In group B only three subjects were able climb stairs. Therefore the total of steps was lower with 122 (asc.: 64 + desc.: 58) steps. The success rate was equally high with 96 %.
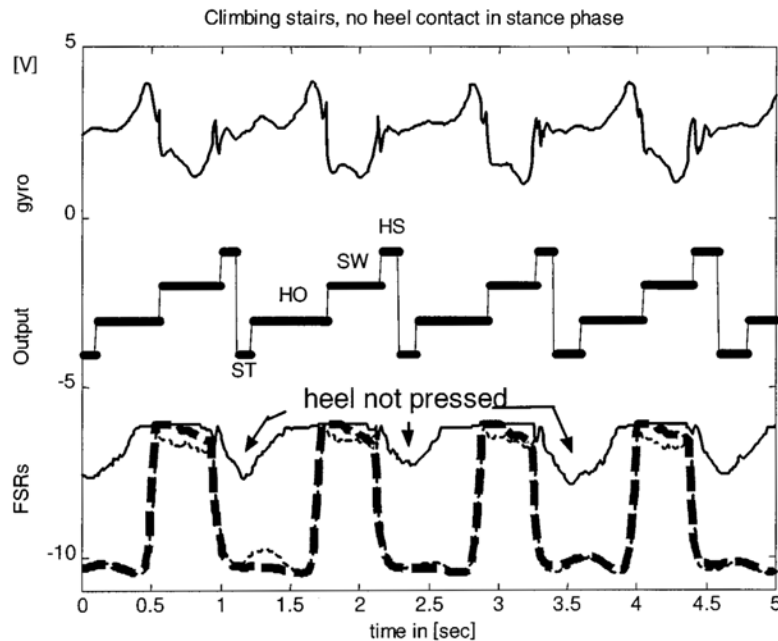
Figure 3.15: Walking up stairs. Many subjects climbed the stairs "on their toes" without placing the heel on the ground. In this case to detect the stance phase the algorithm looked for angular velocity that was equal to 0. (Note: ST = stance, HO = heel-off, SW = swing, HS = heel-strike, heel-FSR = solid line, front-FSRs = broken lines.). ©[Pappas et al., 2001].

There was one significant difference in the flow of gait phases between the stair climbing task and the normal walking. In stair climbing the first contact of the foot with the ground is established with the front part of the foot and not with the heel. Another important and interesting fact was, that some subjects didn't place the whole foot on the steps. but only the front portion while the heel remained "in the air". That was a relevant discovery, because through that the heel FSR sensor was not activated at all during stair climbing. A graphical illustration of this insight is given in fig. To compensate this special condition, in addition to the FSRs the algorithm also checked the gyro signal. It turned out, that the signal amplitude remains minimal ($\sim zero$) during the stance phase (on stairs). None of the non-walking tasks have been wrongly identified as gait phases by the GPDS.

During the running tests, it was possible to gather data at all speeds (even up to 13 km/h). But it was observed, that the gyroscope (with its ± 300 $\deg/s$ range) reached its limits, with the signal saturating during the heel-off, swing, and heel-strike gait phases (see fig. 3.16).
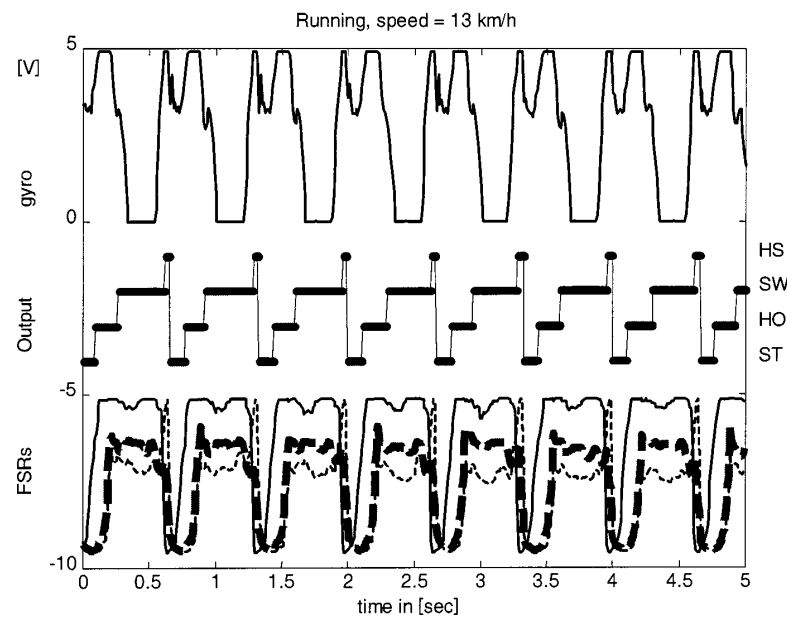
Figure 3.16: GPDS output for running at 13 km/h. Due to the high angular velocity of the foot the gyroscope signal saturated in the heel-off, swing, and heel-strike phases. However, all four gait phases were correctly identified. ©[Pappas et al., 2001].

One year later, in 2002 the research group around I.P. Pappas published another paper [Pappas et al., 2002], where they described the further development of their system and the first clinical trial with FES patients. They report, that they adapted and miniaturized their gait phase detection system (GPDS) so that all component could be embedded in a shoe insole (Bauerfeind AG. No.21270/5), shown in fig. 3.17. They changed the processing unit to a BX-24 microcontroller board (NetMedia Inc., ATMEL microcontroller) and created a small(er) pcb (dimensions: $30 \times 49 \times 7.7$ mm) that contained all components. In a clinical trial they used it in combination with the Compex-Motion FES stimulator to assist two hemiplegic patients (incomplete spinal cord injury, resulting in unilaterally dominated paraplegia $->$ one leg affected) to improve their walking performance. As reference, hip, knee and ankle joint trajectories and foot clearance were recorded vie Vicon with a five-camera- and fifteen-marker-setup. The GPDS signal was recorded synchronously to the video data. Both subjects reported increased comfort through usage of the GPDS in combination with FES, because they found it ledd tiring, more safe and they could walk faster (1.4 km/h instead of 0.6 km/h). Optical motion analysis proved that a greater similarity of ankle joint trajectories could be achieved (between non-affected and affected leg). Additionally, the subjects reported that it also freed-up mental capacity, since they didn't have to concentrate on controlling the stimulator. Through the combination no false triggers (of stimulation) occurred during non-walking activities (standing, shifting the weight from one leg to the other, standing up or sitting down). The detection delay of < 70 ms, which was observed in [Pappas et al., 2001],
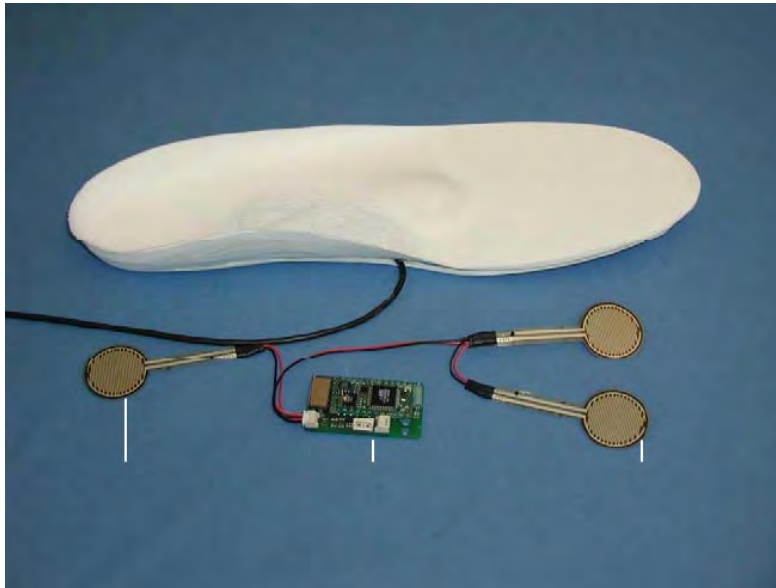
Figure 3.17: Photo of the gait phase detection system (GPDS). Retrieved from `https://www.researchgate.net/profile/Milos_Popovic3/publication/228702470/viewer/AS:102450694459392@1401437557514/background/3.png`, viewed 08.09.2016. © [Pappas et al., 2004].

proved to be insignificant.

Shoe-integrated gait sensor system (SIGS)

A research group at the Division of Health Sciences and Technology from the Massachusetts Institute of Technology (MIT) developed an on-shoe device that can be used for continuous and real-time monitoring of gait and gait parameters outside of a traditional motion laboratory. In [Morris and Paradiso, 2002] they describe the overall design concept of their so called shoe-integrated gait sensor system (SIGS) or "GaitShoe". A schematic diagram of the SIGS is shown in fig. 3.18. The system consists of an instrumented insole (fig. 3.20) and a removable instrumented universal shoe attachment (fig. 3.19) constructed from thermo-formable plastic. The insole contains the following components:

- four force sensitive resistors (FSRs)
  - two beneath the heel,
  - one beneath the first metatarsal head,
  - one beneath the fourth and fifth metatarsal head,
- two piezoelectric strips, made of polyvinlylidine fluoride (PVDF)
  - one beneath the heel,

37

       – one beneath the hallux
- two pairs of resistive bend sensors placed
  - inside the insole, aligned horizontally,
  - at the back of the shoe, aligned vertically

The shoe attachment contains several printed circuit boards (PCBs) with additional sensors (three-axes accelerometers and gyroscopes), processing electronics and a wireless data transmission module. It also houses the 9 V power supply. At that time there was another PCB in final development, which should provide capacitive sensing and sonar in order to determine distances between the shoe and the ground, between the shoes themselves and the angle between the shoes.

The concrete hardware configuration was: a 22 MIPS processor with 12-bit ADC, a 115.2 $kBps$, 916 MHz transceiver, two dual-axis accelerometers, the microelectromechanical system (MEMS)-based ADXL202E, and two types of gyroscopes: the MEMS-based ADXRS150, and the vibrating-reed-based ENC-03J (arranged orthogonally). A coarse measurement of the pressure distribution beneath the foot is possible with the four FSRs (Interlink Electronics). Underneath the heel pad two sensors with a diameter of 5 mm (FSR-402) were used, placed medially and laterally, and underneath first and fifth metatarsal heads two sensors with a diameter of 12.7 mm. The polyvinylidine fluoride (PVDF) strips (LDT0 from Measurement Specialties) provide dynamic information about heel strike (HS) / initial contact (IC) and toe-off (TO) / last contact (LC), by placing them under the heel and the great toe. The bend sensors (FLX-01 unidirectional resistive bend sensors manufactured by The Images Company) are placed back-to-back to provide information about (1) flexion at the metatarsal–phalangeal joint (the extent of "roll" off the ball of the foot) during walking and about (2) the extent of plantarflexion or dorsiflexion. Therefore, they had to be located (1) inside the insole and (2) at the back of the heel, held next to the shin. Furthermore, a capacitive sensor was developed, using a multi-electrode electric-field imaging device (Motorola MC33794DH). It was used for a more direct approach on measuring the elevation of the foot, namely via capacitive loading from the floor. Table 3.1 contains detailed information about all sensors, which were used in the GaitShoe project.

A subsequently published paper [Benbasat et al., 2003] describes the hardware in detail. The (idea for the) modular concept of the hardware, upon which the SIGS is based, existed already prior to the project itself and it was planned to use it on further (wearable electronic) solutions. The novel core about the system was the modularity and interchangeability of hardware and software (code). Each of the (above mentioned) circuit boards can be used either on its own or in any combination with the other available PCBs. Benbasat reports that five boards have been designed: main (processor/transceiver), tactile (pressure, bend, proximity sensing), inertial measurement, sonar, and power regulation (see fig. 3.21). The system consisting of IMU, tactile, main, and power boards, and insole has a total mass of 300 g. In [Benbasat et al., 2003] data was collected from one test subject, who was asked to walk in a straight line at her usual pace. The authors

Sensor	Type	Manufacturer	Range
Accelerometer	ADXL202	Analog Devices	$\pm 2\ g$
Gyro I	ADXRS150	Analog Devices	$\pm 150\ °/s$
Gyro II	ENC-03J	Murata	$\pm 300\ °/s$
FSR	FSR-400	Interlink Electronics	$0\ to\ 100\ N$
PVDF	LDT0	Measurement Specialities	
Bend sensor	FLX-01	The Images Co.	$0\ to\ 90\ °$
ELF	MC33794DH	Motorola	$10\ to\ 100\ pF$

Table 3.1: Sensors selected for the GaitShoe [Bamberg et al., 2008].
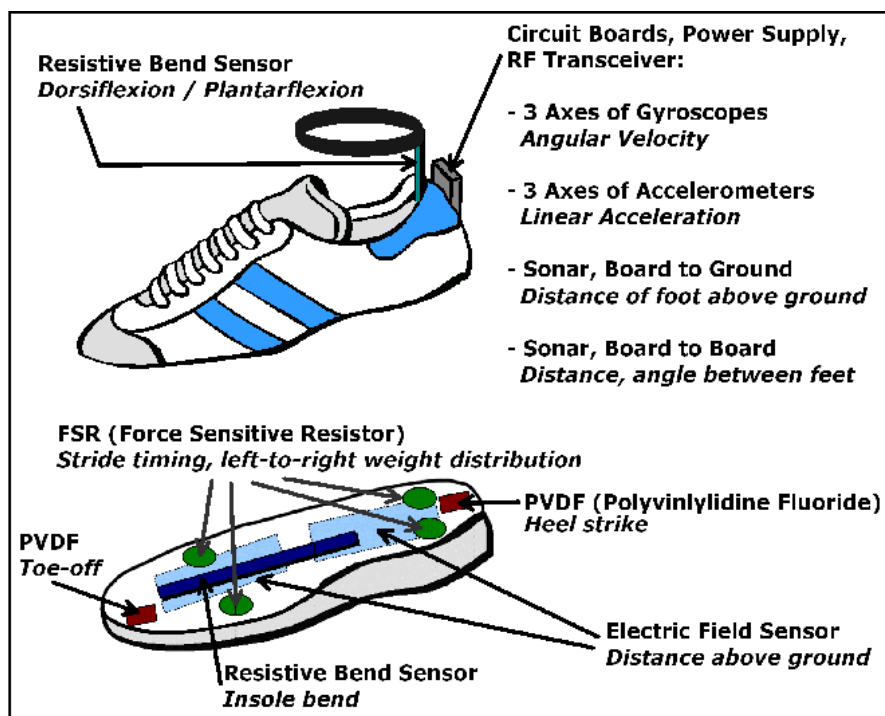
Figure 3.18: Schematic of the shoe-integrated gait sensor system (SIGS). Retrieved and adopted from `http://resenv.media.mit.edu/GaitShoe/`, viewed 05.09.2016. © [Morris and Paradiso, 2002].

(a) SIGS shoe attachment mounted onto (the back of) a shoe.

(b) SIGS shoe attachment.

Figure 3.19: Photographs of the shoe attachment part of the shoe-integrated gait sensor system (SIGS); (a) retrieved from `http://resenv.media.mit.edu/GaitShoe/shoeattachment.jpg`, viewed 06.09.2016; (b) retrieved from `http://resenv.media.mit.edu/GaitShoe/onshoe1.jpg`, viewed 06.09.2016. © [Benbasat et al., 2003].
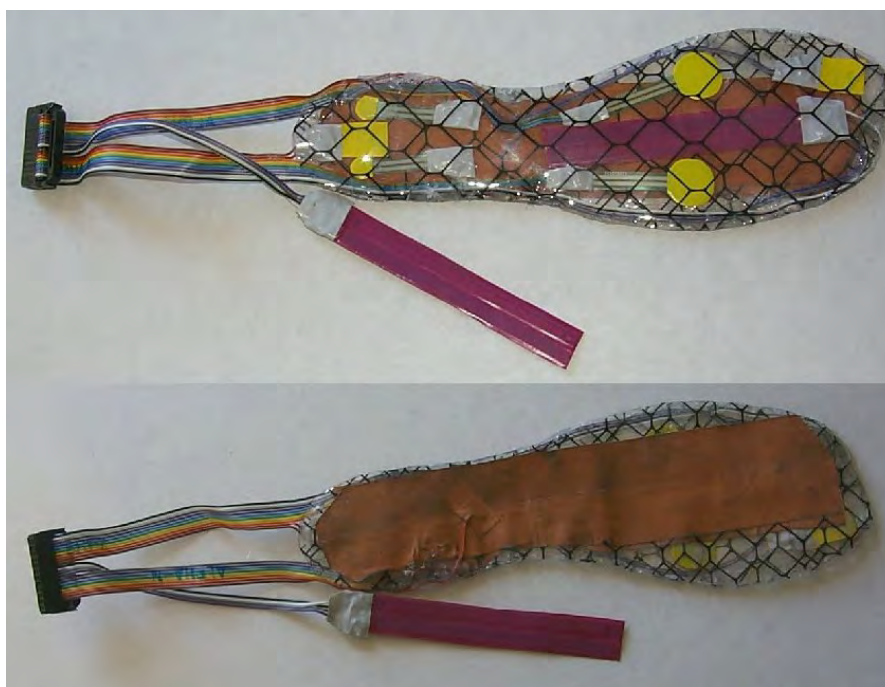
Figure 3.20: Photograph of the shoe insoles part of the shoe-integrated gait sensor system (SIGS). Retrieved from `http://resenv.media.mit.edu/GaitShoe/insoles.jpg`, viewed 06.09.2016. © [Morris and Paradiso, 2002].
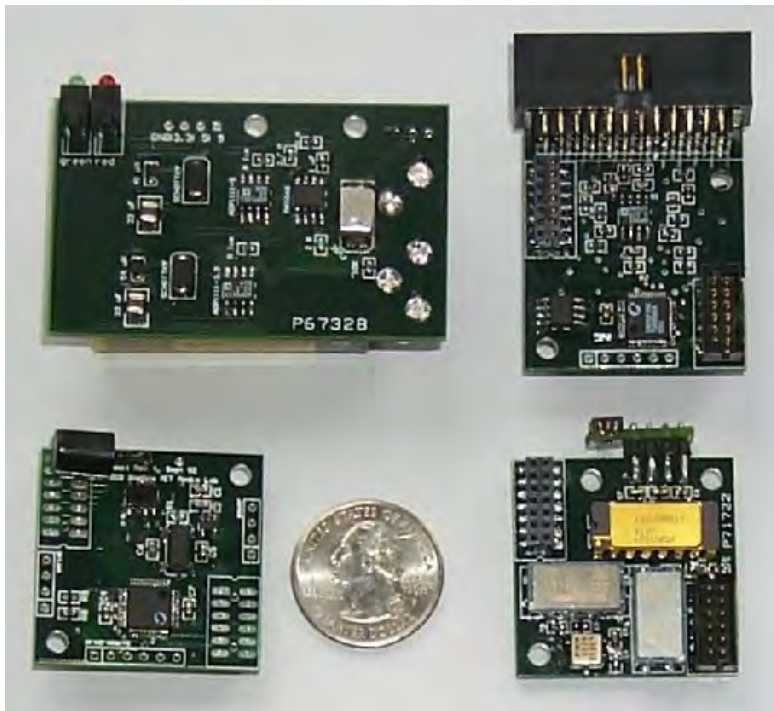
Figure 3.21: Photograph of the majority of the modular panes (PCBs) that were available at that time. Retrieved from `http://resenv.media.mit.edu/GaitShoe/proto2_stack_tops.jpg`, viewed 06.09.2016. © [Benbasat et al., 2003].

claimed that their collected data was repeatable from step to step and gave a detailed description of the most representative signal traces.

[Paradiso et al., 2004] presents an alternative application for the SIGS to clinical gait analysis. It explores the usage of SIGS in physical therapy and rehab through musical bio-feedback. Apparently pathological gait can be improved (e.g. in Parkinson patients) when they are exposed to strong rhythmic cues from a metronome or music. Paradiso then derived gait rhythm and quality by the evaluation of the load transfer between the front and back of the feet. As soon as the subject's gait became irregular the music became less melodic. At the same time the rhythm would change and become stronger, which encouraged the wearer to walk at a certain pace, and the music returned to a more quiet style. Therefore, some sort of rewarding effect has been generated, rather than letting the music disappear. Other variations of gait or load induced bio-feedback are the regulation of the maximum distributed plantar pressure by gradually modulating the key from major to minor, then progressively making it dissonant. For pressure, also more metaphorical approaches have been investigated. Such as making the music "heavier" (stronger, more aggressive voicings, etc.) when a pre-defined maximum is exceeded.

[Bamberg et al., 2008] finally presents a (more) comprehensive description of the technical details of the system. Additionally, it contains the results from a validation study which

Parameter	Healthy		Parkinson	
	Mean	StD	Mean	StD
Max. Pitch [°]	70.10	(6.60)	56.60	(10.40)
Min. Pitch [°]	-29.30	(5.30)	-21.80	(6.30)
Stride Length [m]	1.39	(0.16)	1.13	(0.26)
Stride Time [s]	1.07	(0.09)	1.22	(0.21)
Stance Time [%]	65.60	(2.50)	67.80	(3.50)

Table 3.2: Gait parameters by subject group [Bamberg et al., 2008].

included 15 subjects, comprised of ten healthy subjects and five subjects with Parkinson's disease. Each subject was asked to perform a series of locomotor tasks, while "GaitShoe" and the reference system "Selspot II" (Selective Electronics, Partille, Sweden) collected data simultaneously. The measurements were carried out inside the Massachusetts General Hospital (MGH) Biomotion Laboratory (BML). "SELSPOT II" (acronym for "Selective Light SPOT reongnition") is an active optical motion capturing system [**?**] with an accuracy of ± 1 % of full scale, which corresponds to ± 10 N of vertical force for forces and frequencies encountered during gait. The mean rms errors between the GaitShoe and Selspot were

- pitch angle: 5.2 ± 2.0 ° (calculated over 195 samples)
- displacement: 8.5 ± 5.5 cm (303 samples)

The mean differences between the GaitShoe and Selspot were

- pitch extrema: $-0.7 \pm 6.6°$; mean percentage change: 15.6 ± 18.4 % (1132 samples)
- time points of the extrema: -26.0 ± 24.2 ms
- stride length: 7.4 ± 13.6 cm; mean percent change: 6.5 ± 11.7 % (315 samples)
- heel-strike times: -6.7 ± 22.9 ms (77 samples)
- toe-off times: -2.9 ± 16.9 ms (75 samples).

The differences in certain parameters between healthy subjects and Parkinson patients has also been analysed (table 3.2). For pitch extrema, the healthy persons' gait range is much larger than that of the Parkinsonian range. The differences between the mean pitch values are 14.5° for maximum pitch, and 7.5° for minimum pitch. Correspondingly, the stride length of the healthy persons is 0.26 m longer than the Parkinsonian stride length. The stride time of the healthy subjects is shorter by 0.15 s and the percentage of the gait cycle spent in stance is nearly equivalent, with healthy subjects spending only 2.2 % less time in stance.

The article concludes that the GaitShoe has potential to provide gait analysis functionality outside laboratory settings and/or for people without access to such facilities. Compared

to traditional methods it also has the advantage that monitoring over extended time periods and in natural environments are now possible. GaitShoe was, in fact, able to distinguish between healthy gait and gait affected through Parkinson's disease, regarding mean foot pitch extrema and gait stride time. Those results were comparable to the reference system Selspot II. It was also stated that future research should focus on more extensive usage of IMU data, improvement of the wireless data transmission and that a change in the conditioning electronics for the FSRs is advised. In terms of IMU calibration and data processing, the future implementation of a Kalman filter was mentioned. Furthermore, it was suggested to continue with the utilization of the newest (state of the art) sensors. Which meant at that time e.g. the ADXL330 triaxial accelerometer from Analog Devices and dual-axis gyroscopes such as the Intelli-G chips from Invensense. Further issues were the improvement of data transmission through optimized antennae positions for reduced interference from the human body and the extension of battery life through "dynamic sensor-driven power management".

It appears that the research project never made a transition to an actual product. The latest publications found are from 2011 and 2012 and presents flexible PCBs, built-into shoe insoles

OpenGo Science

The OpenGo insole (Moticon GmbH, Munich, Germany) incorporates 13 capacitive pressure sensors, a 3D accelerometer and a temperature sensor, measuring peak pressures, pressure distribution, acceleration, motion sequences, gait patterns and temperature. A schematic illustration of the basic sensor equipment and positioning can be found in fig. 3.22. Sensor specifications (as far as available in literature [Braun et al., 2015a, Braun et al., 2015b] or on the website `http://www.moticon.de/images/pressure-sensors.jpg`) are liste in table 3.3. OpenGo operates completely wireless and data can also stored locally on a flash storage. The insole can be placed in any shoe and shoes can be changed at random during the study due to an automated zeroing system. It runs for approximately up to four weeks on a single battery charge. Data can be gathered at different sample rates, ranging from 5 to 100 Hz. The sensor insoles are available in five different double shoe sizes from EU 36/37 to EU 44/45. Two different top layers can be chosen, an easy to clean artificial leather (Ellecalf) and an anti slip Ripstop material. The top layers can be exchanged when necessary.

Four scientific publications are promoted on the website of Moticon/OpenGo (`http://www.moticon.de/products/science-research`). Braun et al carried out two clinical studies, using OpenGo, dealing with the feasibility of (partial) weight bearing after ankle fracture [Braun et al., 2015a] and validating the insoles against data from a force plate built-into a treadmill [Braun et al., 2015b].

In [Braun et al., 2015a] ten ankle fracture patients were monitored up to three months after their operation. They were ordered to follow a strict partial weight bearing routine of 20 kg on their affected leg for six weeks. After that they were allowed to increase the
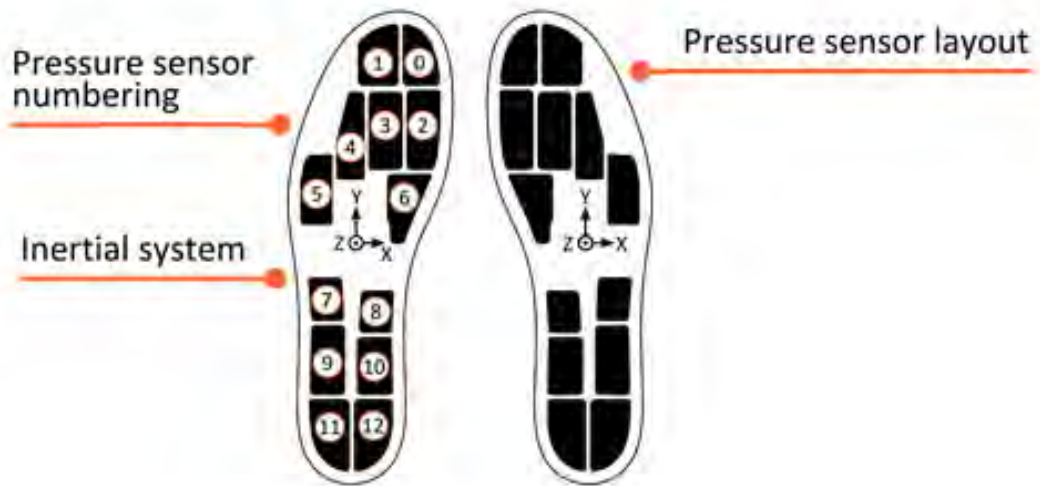
Figure 3.22: Schematic diagram of all of OpenGo's built-in sensing elements. Retrieved from `http://www.moticon.de/images/pressure-sensors.jpg`, viewed 10.09.2016. © Moticon GmbH.

(a) Top view of the OpenGo insole.

(b) Side view of the OpenGo insole.
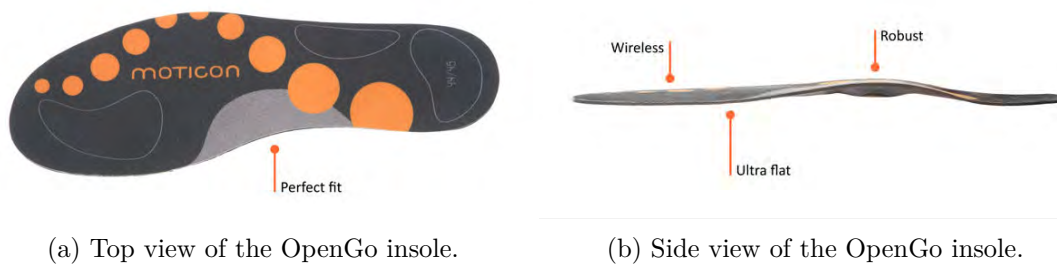
Figure 3.23: Photographs of the shoe attachment part of the shoe-integrated gait sensor system (SIGS); (a) retrieved from `http://www.moticon.de/images/sensor-insole-top.jpg`, viewed 10.09.2016; (b) retrieved from `http://www.moticon.de/images/sensor-insole-side.jpg`, viewed 10.09.2016. © Moticon GmbH.

	Inertia system	Pressure sensors
Principle	inertia mass	capacitive
Type	triaxial (MEMS)	-
Quantity	1 per insole	13 per insole
Coverage	-	$\sim 50\ \%$
Range	$\pm 2, 4, 8\ g$	$0\ to\ 40\ N/cm^2$
Sensitivity		$0.25\ N/cm^2$
Resolution	$7\ bit$	$7\ bit$
Sampling rate	$5, 10, 25, 50, 100\ Hz$	$5, 10, 25, 50, 100\ Hz$

Table 3.3: Sensors specifications for OpenGo according to information on the Moticon website `http://www.moticon.de/products/science-research`.

load up until full weight bearing under observation of a physical therapist and if they felt no pain. They distinguished between high and low performers, depending on a set of parameters that were exceeded after three weeks. The analyzed parameters were: (1) ground reaction force integral (kg/h), (2) weekly weight bearing amount, (3) overall gait activity with the injured foot, (4) ground reaction force over the 20 kg weight bearing limit in minutes (see fig. 3.24). Data was analyzed with a specialized software ("Beaker" by Moticon GmbH).

They found six patients to be high performers and four to be low performers. There were no significant differences between both groups in age, weight and height. High performers were able to apply full load to their injured foot after 3.3 ± 4.1 *days*, whereas low performers only after 13.3 ± 5.9 *days* ($p = 0.01$) (see fig. 3.25). Ultimately, all patients reached full weight bearing by week nine.

The authors state that it was possible to provide continuous fracture aftercare with an independent running time of over four weeks. Patient monitoring occurred without interference of the traditional aftercare protocol. Through the application of this novel measurement device it was possible (for the first time) to determine that there are patients who make a quicker recovery than others By the time of the usual check-up, three months after surgery, no significant difference between high and low performers in pain level and clinical scoring (Olerud–Molander Score, AOFAS) could be found. Current partial weight bearing techniques lack the ability/opportunity to track or document compliance over a long period of time.

It is concluded, that individualized aftercare protocols are necessary and that OpenGo provides the wanted functionality. Short term adjustments through real-time feedback are also conceivable and feasible. This could especially help low performers to avoid painful delays in their treatment.
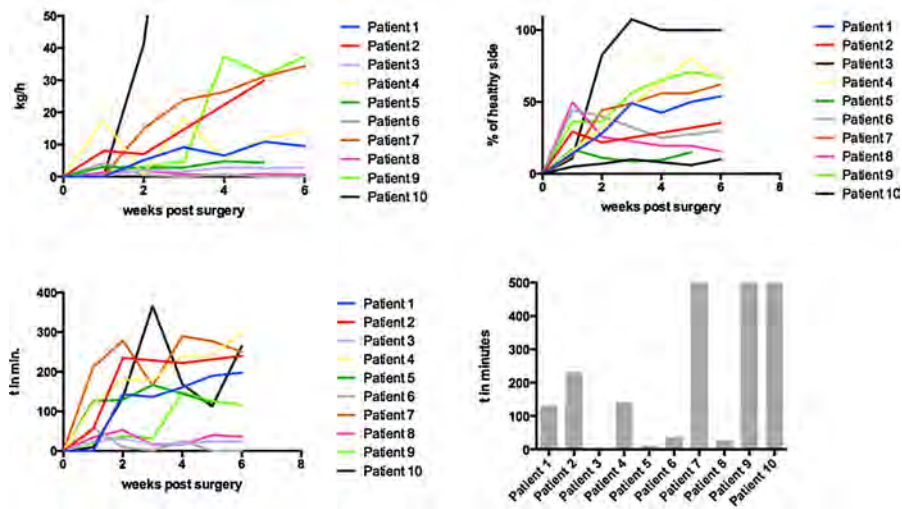
Figure 3.24: Gait analysis of each patient during the first six weeks. Top left: Average ground reaction force integral (kg/h). Top right: Highest weekly weight bearing amount for every patient in percent of the healthy contralateral side. Bottom left: Overall gait activity with the injured foot in minutes per week. Bottom right: Ground reaction force over the 20 kg weight bearing limit in minutes over six weeks. Retrieved and adopted from `http://www.sciencedirect.com/science/article/pii/S0020138315007020`, viewed 12.09.2016. © [Braun et al., 2015a].
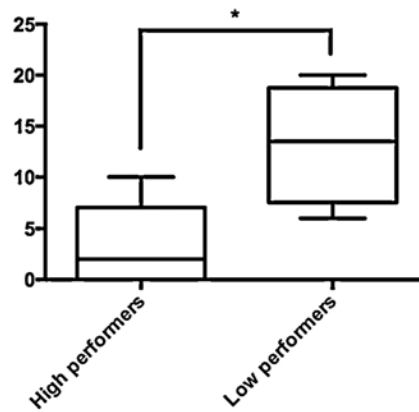
Figure 3.25: Box plots for high and low performers of their time to painless weight bearing in days (y-axis) after six weeks. Retrieved and adopted from `http://www.sciencedirect.com/science/article/pii/S0020138315007020`, viewed 12.09.2016. © [Braun et al., 2015a].

In the second publication [Braun et al., 2015b] the validity and reliability of OpenGo in a group of twelve healthy individuals (6 M/6 F, age: 25.38 ± 5.15 $yrs.$, weight: 70.4 ± 10.08 kg) has been investigated. They collected gait data in six trials of three minutes each. Subjects had to walk on a standard treadmill, equipped with a FDM-S pressure plate (Zebris Medical GmbH, Isny im Allgäu, Germany) at two different speeds (1.0 m/s and 1.7 m/s). On an area of 54×34 cm FDM-S incorporates 2560 sensors, with a 5 % accuracy. Subjects wore OpenGo inside their shoes and data was collected simultaneously to the FDM-S force plate. Both systems sampled gait data at 50 Hz.

Differences between the trials for any gait parameter within each gait speed group and differences between left and right foot proved to be not statistically significant. Differences between the two gait speeds though were significant for cycle time (0.28 ± 0.04 s; $p < 0.001$), cadence (14.29 ± 2.34 min^{-1}; $p < 0.001$), stance (left: 0.16 ± 0.31 s; $p < 0.001$; right: 0.16 ± 0.3 s; $p < 0.001$), swing (left: 0.05 ± 0.01 s; $p < 0.01$; right: 0.05 ± 0.02 s; $p = 0.02$) and double stance time (0.18 ± 0.03 s; $p < 0.001$).

Table 3.4 contains the results for the intraclass correlation (ICC 3.1/k) analysis of peak force and stance time. Corresponding Bland-Altman plots, with > 95 % of the values between the limits of agreement ($\alpha = 0.05$) for both parameters, are shown in fig 3.26. Additionally, resultant force and stance time exhibited no significant differences between both systems (36.3 ± 27.19 N; $p = 0.19$ and 0.027 ± 0.028 s; $p = 0.36$).

Parameter	ICC	95 % CI -	95 % CI +
Peak Force (single)	0.796	0.749	0.834
Peak Force (avg)	0.886	0.857	0.909
Stance Time (single)	0.837	0.357	0.956
Stance Time (avg)	0.911	0.526	0.979

Table 3.4: The intraclass correlation coefficients for single, as well as average measures. The corresponding Bland-Altman plots are shown in fig. 3.26. "95 % CI -" and "95 % CI +" are the lower and upper bounds of the 95 % confidence interval. Adopted from [Braun et al., 2015b].

Table 3.5 shows the intraclass correlation (ICC3,1/k) coefficients for the retest reliability, combined for 1.0 m/s amd 1.7 m/s.

Complete	ICC	95 % CI -	95 % CI +
single measures	0.983	0.979	0.986
average measures	0.994	0.993	0.995

Table 3.5: Retest reliability calculations for trials at both speeds combined.

(a) Peak force.

(b) Stance time.
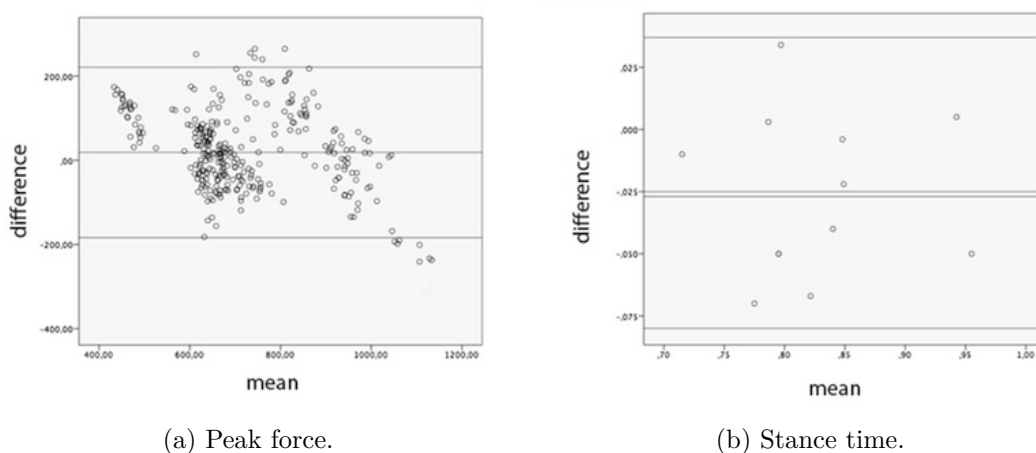
Figure 3.26: Validation results in the form of Bland-Altman plots. The three continuous lines represent the upper limit of agreement, the mean difference and the lower limit of agreement (from top to bottom). Retrieved and adopted from `http://www.ncbi.nlm.nih.gov/pmc/articles/PMC4578601/bin/13047_2015_111_Fig4_HTML.jpg`, viewed 12.09.2016; © [Braun et al., 2015b].

Multimodal biometric measurement system for mobile gait analysis and therapy monitoring – eSHOE

In this chapter the very basis for the research activities for this thesis is presented - the mobile gait analysis system "eSHOE". Starting from the creation of a concept for an (in the beginning) in-shoe and later insole biometric measurement system for mobile, unobtrusive gait analysis (section 4.1). Including basic ideas for functionality, design and the name.

The technical development underwent three major stages. Each stage contained design, manufacture and assembly of hardware, programming of firmware for a microcontroller, incorporation of the electronic components into a pair of shoe insoles and programming of a software tool for interaction with the measurement system.

In a nationally funded research project "vitaliSHOE" (by the Austrian research promotion agency FFG) such a wearable measurement system, in the form of a pair of instrumented orthopedic shoe insoles, was implemented. The main objective of vitaliSHOE was to create a monitoring and training system for senior citizens, which offered the assessment and long-term monitoring of the risk of falling and the physical activity level. In the project eSHOE also served as a new control method for a specially designed simple serious games for balance training. From the beginning of the project, the work followed a participatory approach and, therefore, involved potential primary and secondary end-users, senior citizens and medical experts respectively, on a regular basis. This created the need of first results at an early stage in the development phase in order to demonstrate the project's potential to the users, to establish feasibility and to gather valuable feedback

from the experts on applicability and usability. Therefore, early stage prototypes or "laboratory samples", as they were called, with reduced functionality have been developed. Section 4.2 offers minor insights into technical details to outline important steps in the development process. Johannes Oberzaucher's dissertation [Oberzaucher, 2011] offers a comprehensive description about the laboratory samples and their applications.

This thesis focuses on the third generation of prototypes and detailed information about these concerning technology, functionality and configuration is given in section 4.3. The first six subsections deal with the main components of the SHOE hardware: microprocessor (4.3.1), accelerometer (4.3.2), gyroscope (4.3.3), force sensitive resistors (4.3.4), bluetooth module (4.3.5) and operating circuitry (4.3.6). The components were then combined into an embedded system in the form of a printed circuit board (PCB), forming the basis for eSHOE. Schematics, layouts and photographs of the PCBs can be found in the beginning of section 4.3. Subsequently, the PCBs were integrated into orthopedic shoe insoles, which was achieved with the assistance of an orthopedic technician. The integration process is documented in subsection 4.3.7 Measurement parameters and sensor (-axes) or PCB orientations inside the insoles are documented in section 4.3.8.

All software-related topics are summarized in section 4.4. There is a strong focus on the firmware, which is running on the micro-controller and its basic features (subsection 4.4.1). Another defining part is the specially designed communication protocol (subsection 4.4.2), which provides crucial functions for interaction with the insoles. As first task of his work, Stefan Reich (who also contributed to chapter 5) wrote a simple software tool for controlling /issuing commands to the eSHOE system and for visualizing measurement data. Chapter 5 then deals with processing eSHOE raw sensor data into standard gait parameters in the course of a (clinical) pilot study.

4.1 Concept for mobile unobtrusive gait analysis

The name "eSHOE" is short for 'electronic shoe' and was derived from or composed, similar to other terms indicating the incorporation of electronics/ICT or technology in general into existing fields, such as eHealth (or e-health) and e-learning. In the context of this thesis, it, furthermore, signifies a device, or rather the whole process, of capturing motion data directly on the feet by means of electronic components and circuitry, built-into footwear. The idea for eSHOE derived from a combination of two things. The first being the vision of Wolfgang Zagler, head of the center for applied assistive technologies (AAT) at the University of Technology of Vienna, to develop an "intelligent" shoe for the detection and/or the prediction of falls. Falls are major health hazards among elderly people by contributing to severe secondary diseases and drastically increased mortality rates (see section 2.3). Therefore, a concept had been developed for a shoe, which is capable of detecting falls and, ideally, also the (increasing) risk of falling in elderly people's gait.

At this point the second influencing factor comes into play. The integration of biometric measurement systems into garments, and thereby creating so called wearable devices,
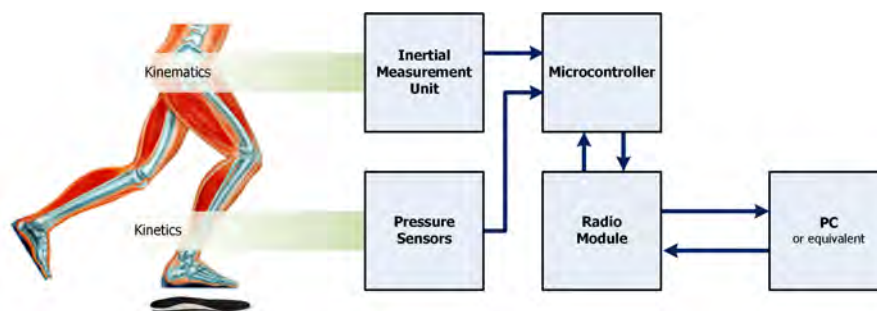
Figure 4.1: Concept for in-shoe/insole measurement of gait parameters.

became quite common over the last years [Bonato, 2005, Bonato, 2009, Patel et al., 2012]. So also the idea of integrating sensors fit for motion analysis into a shoe [Pappas et al., 2001, Morris and Paradiso, 2002] or onto a shoe [Schwesig et al., 2010, Barth et al., 2011] has been investigated and worked on. During his master's thesis, the author of this thesis dealt with the analysis of body segment movement by means of inertial measurement. In the course of the literature research a series of publications have been discovered about a so-called gait phase detection system (GPDS), which was developed by a group of researchers at the Swiss Federal Institute of Technology in Zurich (ETHZ). The group's GPDS consisted of a one-axis gyroscope, three force sensitive resistors and a microcontroller, all built-into a shoe insole [Pappas et al., 2001, Pappas et al., 2002, Pappas et al., 2004]. The project was conducted from 2001 to 2004, but then did not continue any further. Details about this device are presented in sub-subsection 3.2.4.

Reasons or causalities for fall incidents can often be found in the dysfunction of the ability to walk, which indicates a connection between the investigation of falls or fall risk and gait analysis. So, if one wants to understand falling, one must also learn about walking. Hence, the project idea was born to create an embedded sensor system, which is capable of gathering, processing and transmitting motion data. By that time (2006/07) it was already common practice in research to perform live measurements of movements of body parts with very small sensors, made up by microelectromechanical system (MEMS). Most popular and most used among those, accelerometers and gyroscopes. These two sensor types put together form a so-called inertial measurement unit (IMU). Such an IMU can be used for the detection of kinematic forces and movements. It also allows to determine (by applying certain calculations) the 3D orientation of any object they are attached to. Additionally FSRs can be applied for the measurement of kinetic forces in the form of plantar pressure. A microcontroller handles data collection, local data management and communication management. The integration of a radio module ensures remote control of the system and wireless data transmission, facilitating mobile and untethered measurement. It was envisioned to attach the system very closely to the human body or rather by being "worn" as a piece of garment (e.g. on the feet). At the same time it should be unobtrusive, in order to interfere as little as possible with the wearer. In that way it will be fit for the monitoring of recurring patterns in the sensors' raw data and, thereby, the

Figure 4.2: Conceptual schematic of the original idea for eSHOE.

detection of gait parameters. An extensive analysis of this data will then lead to finding indicators for an increased fall risk. Figure 4.1 shows a block diagram of the measurement system's most important functional blocks and their interconnections. The initial concept included the integration of the measurement and processing hardware into a pair of (ordinary) shoes, forming an instrumented shoe or "electronic shoe" (eSHOE), hence the name. Figure 4.2) shows a conceptual schematic of the eSHOE idea, with sensors directly below the insole and printed circuit boards inside the heel area of the shoe. In the course of the technical development it soon became clear that instrumenting a shoe or a pair of shoes comes with many disadvantages and restrictions from technical and practical point of view. There are of course certain (obvious) perks of considering a shoe for housing a measurement system, which is why it was chosen as starting point. A whole shoe provides **a lot of space** inside for storing all necessary electronic equipment, such as sensors, a microprocessor, a radio module, other components (which all have to be mounted onto a printed circuit board) and (ideally) a battery. Electronic equipment usually is very susceptible to (mostly environmental) influences or interferences/disturbances like humidity, heat, cold and mechanical stress. Inside a shoe electronic components are rather **well-protected against outside influences**.

But there are also a number of **limiting factors** for the in-shoe integration. Even though some of the following thoughts and considerations might seem trivial, they are of relevance when it comes to practicability.

Shoes are, and always have been, also an object of fashion and of purpose. So, people have shoes for different weather conditions, seasons, occasions and spare time activities which they wear regularly. If one has one pair for each season, one for running, one for hiking, that totals in six pairs of shoes. If one's activities or gait characteristics shall be measured/evaluated during one year, every single pair would have to instrumented with a measurement system. This would result in substantial financial effort, because one pair would be rather expensive, considering the built-in equipment. So it is not likely that a person with average income/salary would be willing to buy more than one pair of

instrumented shoes.

The integration of electronic components into a shoe requires **considerable effort and, thereby, results in substantial (manufacturing) costs**. The shoe practically has to be built around the embedded system, which introduces new and additional working steps.

The reflection of effort and costs in the market price and its effect on end-users directly is (only) one aspect. Considering the use of such a system in research context, which is the focus of this thesis, we are facing (similar) problems/challenges. In (clinical pilot) studies we have to provide (at least) one measurement system per shoe size, because the distribution of (shoe) sizes is not known beforehand and it should also not be made a limiting criterion, since it is not a legitimate ethical issue. When a reasonably large span of shoe sizes shall be covered, say from 37 to 44 (EU), eight pairs of shoes are necessary. That would be one complete set for clinical trials, but with no spares in case of failures.

Due to these practical disadvantages on the one hand and a limited budget on the other, the strategy was changed to integrate all hardware components into a pair of shoe insoles instead. Insoles provide just enough space to host all necessary components, they are also interchangeable among different pairs of shoes, cheaper to construct/manufacture (on a prototype scale) and easier to maintain. Miniaturization, especially of the MEMS components (accelerometer and gyroscope) was already advanced enough at that time, to allow the design and production of a PCB small enough to fit into an insole. It also was essential to develop a suitable environment of software for control and data management. Therefore, a framework of several software tools and a data base have been developed and set up.

4.2 Development of research prototypes (laboratory samples) for proof of concept

The first (and second) generation of prototypes served the purpose to establish feasibility of the idea and to gain a proof of concept, whether the measurement hardware can be successfully integrated into a pair of shoe insoles. Laboratory testing was conducted and the applicability for AAL purposes was evaluated.

The next step/second version of prototypes included a more sophisticated construction of the insole measurement system, with the involvement of an orthopedic technician, and the development of algorithms for semi-automated analysis of the measurement data. The accuracy (and validity) of these algorithms was evaluated in (purely technical) laboratory analyses with healthy subjects on a treadmill and an optical marker-based, four-camera motion analysis system as reference [David, 2012].

The first two generations of eSHOE were merely preliminary prototypes. But they were already fit for gait data collection and they also served the purpose to learn how such instrumented insoles could be designed best, focusing on questions concerning (insole)

material, sensor positioning, partitioning of the printed circuit boards in order to protect them from mechanical stress. In this course, testing with these archetypes also helped to reveal certain weaknesses.

4.2.1 Research prototype I

The "research prototype I" comprises the first general design of hardware, (microcontroller) firmware and a software tool for interaction between user and embedded system. In the design we followed the strategy of maintaining a modular structure, in order to keep the modules interchangeable and easier to maintain. Therefore, all components have been grouped in functional blocks, similar to fig. 4.1, which were then placed on three different printed circuit boards (PCBs).

There were two reasons for spreading the components onto (three) different PCBs instead of placing all on one big board. One was to define certain physical units, which can be maintained and exchanged if necessary. The other reason was to avoid mechanical stiffening of the insole via one single and, therefore, large(er) PCB, which would resulting two things. The person wearing the insole would most likely feel the stiff PCB inside the insole and it would probably affect the persons' gait. Another negative result would have been the increased mechanical stress, occurring when the insole is deformed during walking, which could damage the PCB and lead to malfunctions and failures. The resulting functional groups or modules are illustrated in fig. 4.3 via a block diagram and described in detail the following list:

1. **data processing unit** (or **main board**), including
   a) a microcontroller
   b) a voltage regulator
   c) a multiplexer
   d) operating circuitry

2. **inertial measurement unit** (**IMU**), consisting of
   a) a 3-axis accelerometer sensor
   b) a 2-axis gyroscope sensor
   c) a voltage regulator
   d) operating circuitry

3. OEM **radio module**, operating on the ZigBee® standard,
4. four **pressure sensors**

The first vision for the integration of the hardware into a shoe insole is presented in a schematic diagram in fig. 4.4.
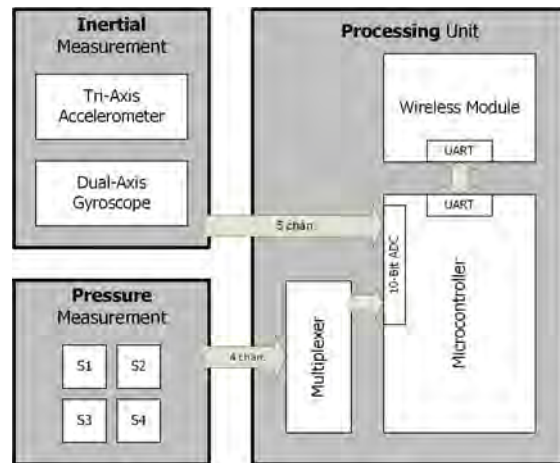
Figure 4.3: Block diagram of the functional units of the first prototype generation.
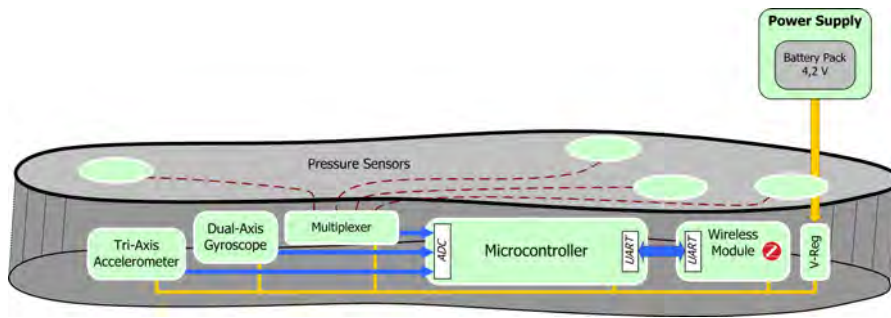
Figure 4.4: Schematic diagram of one instrumented insole with the included components. The insole's thickness is shown disproportionately in the picture for demonstration purposes.

It was necessary to manufacture specific PCBs for the data processing unit (main board) and for the IMU, based on self-developed schematics and layouts. For the ZigBee® radio module on the other hand it proved to be more efficient, concerning time and costs, to use an off-the-shelf product. Sensors for the first prototype generation are the ADXL330 accelerometer (Analog Devices, Norwood, Massachusetts, United States) with a minimum full scale range of ±3 *g* and a sensitivity of 300 *mV/g*. It can measure the static acceleration of gravity in tilt-sensing applications, as well as dynamic acceleration resulting from motion, shock, or vibration. Then there is the integrated dual-axis angular rate sensor (gyroscope) IDG-300 (Invensense, San José, California, United States). It has a full scale range of 500 °/s and a sensitivity of 2 *mV/°/s*. The force sensitive resistor (FSR) (Interlink Electronics, Camarillo, California, United States) have an average thickness of 0.5 *mm* and diameters of 15 *mm* and 27 *mm*, as there are two different types in use. Their force sensitivity ranges from 100 *g to* 10 *kg* while the pressure sensitivity range is 0.1 *kg/cm²* *to* 10 *kg/cm²*. The devices' rise time (mechanical response time) is

Characteristics	Accelerometer	Gyroscope	FSR
Type	ADXL330	IDG-300	
Manufacturer	Analog Devices	Invensense	Interlink
Output	Analog	Analog	Analog
Range	3 g	$\pm$ 500 $°/s$	100 g to 10 kg
Sensitivity	300 mV/g	2 $mV/°/s$	0.1 kg/cm^2 to 10 kg/cm^2
Resolution			
Interface	3-chan. analog	2-chan. analog	two-pin con.
Sampling Rate			
Power Consumption	0.32 mA	9.5 mA	
Dimensions	$4 \times 4 \times 1.45$ mm	$6 \times 6 \times 1.5$ mm	

Table 4.1: Main hardware components of research prototypes I and II.

$1 to 2$ ms and the stand-off resistance is > 1 $M\Omega$. The single part force repeatability is ± 2 % to ± 5 % (of established nominal resistance) and the part-to-part force repeatability is ± 15 % to ± 25 % (of established nominal resistance). The working principle is as follows: the sensor actually is a resistor, whose resistance is decreasing with an applied force e.g. mechanical pressure. More details on the sensors' specifications can be found in Table 4.1. The ZigBee® module was the ETRX2 (Telegesis Ltd., High Wycombe, United Kingdom). It features 37.75×20.45 mm in size, 250 $kBit/s$ over the air data rate, $+3$ dBm output power, an UART interface with DMA and a specific AT-command set.

An ATmega32 microprocessor with an 8-channel and a 10-bit analog-to-digital converter (ADC) forms the heart of the measurement system and samples data from the sensors with 200 Hz. Data is then transmitted to the ZigBee module via UART with a rate of 50 Hz, which is also the wireless data transmission rate. ZigBee offers a data rate of 250 $kbit/s$ with an actual data throughput (data rate - overhead) of 20 $kbit/s$. For the data transmission a fast and easy to implement protocol based on ASCII encoded characters was used.

The microcontroller acquires the sensor data with a rate of $200 samples per second$, which is more than 50 $times$ the frequency of walking at normal speed. After filtering and processing sensor information the resulting gait data are transmitted to a PC (wirelessly) with a rate of 50 Hz. So the values of angle, acceleration and pressure from both insoles are received at the PC 50 times per second. This sampling rate still is ideal for the analysis of walking because typical bandwidth of kinematics of normal gait is between 4 and 6 Hz [Winter, 1991]. Spectral power analysis from barefoot walking across a force plate has shown that 98 % of the spectral power is below 10 Hz and over 90 % below 5 Hz [Antonsson and Mann, 1985].

The basis for the early prototypes was an off-the-shelf shoe insole with no special characteristics, such as orthopedic support. The important feature was that it had to
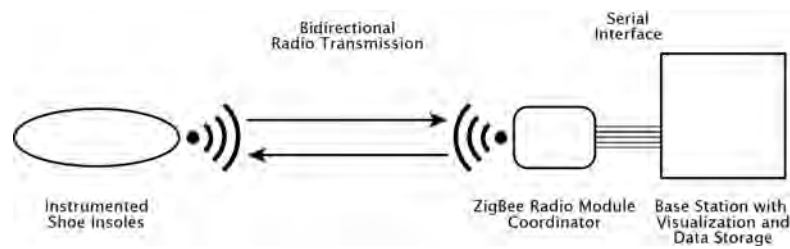
Figure 4.5: The basic concept for the eSHOE measurement setup. The instrumented shoe insoles communicate (via ZigBee) with a base station, which is responsible for data storage and visual representation. Since ZigBee is not commonly available as built-in device in notebooks or handheld devices, an external radio module must be used.

offer a certain level of mechanical stability, which is achieved by the insole being made of duroplastic material from underneath the arc of the foot to the heel. This stability is essential in order to protect the printed circuit boards from mechanical stress. The integration of all hardware modules into the insoles was performed manually, resulting in the very first set of hand-crafted instrumented insoles. Remote control of the embedded system, data storage and data visualization were handled by a specially designed LabView software, running on a PC. Photographic documentation of the results of these efforts are presented in the figures 4.6 and 4.7. Figure 4.6 shows a photograph with the bottom view of one eSHOE insole and the front view is shown in figure 4.7.

In the following a proof of concept had to be established, to assess the insoles' overall design principle, the accuracy and the mechanical stability. Furthermore, these tests were also supposed to help to identify possible weaknesses e.g. in the wireless data transmission, including the transmission protocol. Additionally to the lab trials, a small series of end-user trials was carried out. These were meant to evaluate the real-life applicability. The tests were carried out with five different test subjects, three young adults (25 to 35 years), and two older adults (60+). The test subjects were asked to perform nine different tasks:

1. sand still for a few seconds, to give full load to the pressure sensors;
2. walk straight with everyday-life speed, to gather data form ordinary walking, which is of primary interest;
3. walk straight with lower speed than everydaylife speed;
4. walk straight with higher speed than everyday-life speed;
5. walk straight, while counting backwards (aloud) at the same time – dual tasking I;
6. walk straight, with a metronome as pacemaker;
7. walk straight, while listing European city names (aloud) at the same time, dual tasking II;
8. perform the timed up and go test (TUG), which includes rising from a chair, walking straight ahead for three meters, performing a 180° turn, walking straight ahead (in direction of the chair) for three meters and sitting down again;
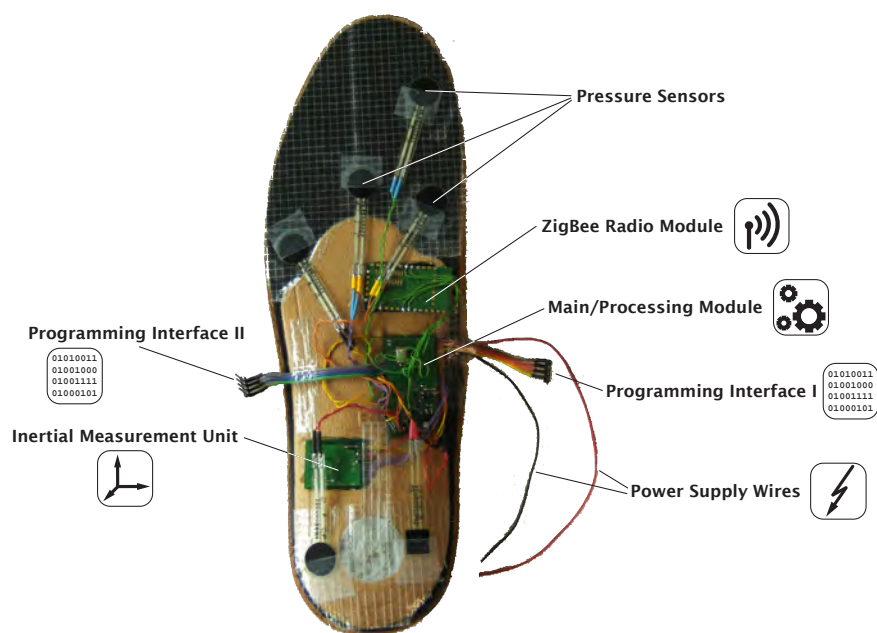
Figure 4.6: This figure shows a photograph of the bottom side of the very first eSHOE Prototype. All components (circuit boards, sensors, cables) are marked according to their function.

Figure 4.7: Side view of eSHOE Prototype I with all components already covered up with duct tape.

9. perform the chair rising test; getting up from and sitting down to a chair for five times.

The lab trials gave some indication about the basic functionality and the user trials showed that such a system is practically viable and gave a first impression about the usability. The (two pairs of hand-crafted) instrumented insoles met the requirements on mechanical stability, in order to last for this first series of trials. But clearly there was the need of improvement concerning placement and the insole carrier material. Apart from one task, the system delivered the expected data with such quality that exceeded all expectations. However, at some point, after several test cycles, the system's durability reached its limits, which becomes manifest for instance in the IMU ceasing to work

properly. This results from flaws in the hardware design in the face of the extreme loads, which were faced during the trials, e.g. concerning mechanical stress. The positioning of the printed circuit boards is also something which has to be optimized during the ongoing research in order to reduce mechanical stress. Unfortunately, the wireless connection via ZigBee was unstable, caused some data loss and proved to be inefficient for continuous data transmission. Therefore, it was clear that the radio transmission concept and the transmission protocol had to undergo major revisions in the future. A general difficulty was to measure walking at higher speeds (task 4). During this task even more transmission errors and system failures occurred compared to normal gait velocity.

4.2.2 Research prototype II

Experiences and results from laboratory trials and from the end user evaluation required re-design of certain hardware components and lead to the development of research prototype II. Since the measurement hardware proved to meet the (technical) requirements, no changes were made concerning the selection of sensors or processing electronics. But the integration of the hardware along with the workmanship had to be improved, both (also) reflecting in the overall mechanical stability. Therefore, one consequence was actively involving a professional orthopedic technician in the development process. This brought to light a few (more) weaknesses and new requirements concerning the hardware design. The new printed circuit boards should be integrated into the insoles in one (or more) additional working steps in the insoles' manufacturing process. Re-routing of the electrical conducting pathways, re-location of parts and connection pads were the main issues. All hardware components except the (battery) power supply could be integrated into the insole.

Due to the lessons learned from the first generation and the professional support, these prototypes represented a clear improvement. More extensive studies and analyses were possible. Including a thorough validation of the accuracy in a technical setting on a treadmill with healthy subject an optical marker-based, four-camera motion analysis system as reference. The validation efforts and results are presented in detail in a master thesis in 2010 from the university of applied sciences Technikum Wien by Veronika David [David, 2012]. Furthermore a PhD colleague, Johannes Oberzaucher, worked out and evaluated algorithms for the semi-automated analysis of geriatric assessments. His efforts are documented in his doctoral thesis "iAssessment - Aspekte eines instrumentieren Sturzrisikoassessments basierend auf einer extramuralen Gang- und Bewegungsanalyse - im Hinblick auf eine Anwendung im Bereich des Ambient Assisted Living" [Oberzaucher, 2011].

However, there were still several shortcomings with this second generation prototypes. The insoles were still relying/dependent on an external power supply, which made the whole system less unobtrusive and less usable as it had been intended. The only way to collect measurement data was to transmitted it over the air - via ZigBee$^®$ - to a PC. This proved to be (more and more) difficult/challenging due to several reasons. Wireless data transmission is always subject to data losses. ZigBee is an established
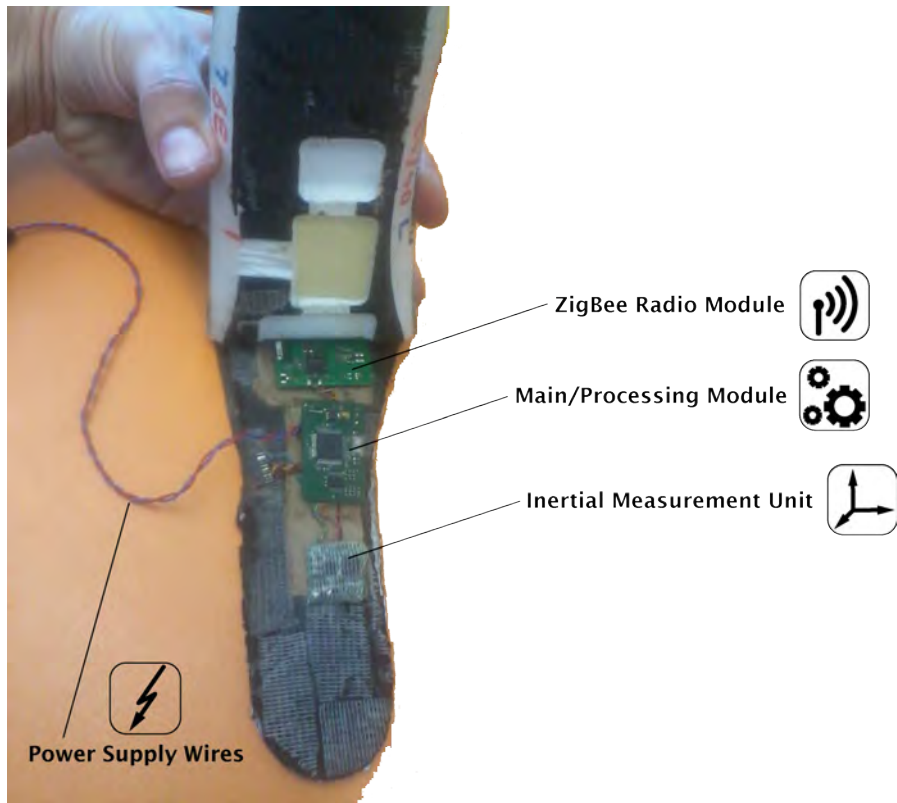
Figure 4.8: A photograph of one opened up insole of the eSHOE prototype II series. The three PCB modules as well as the power supply wires are visible.
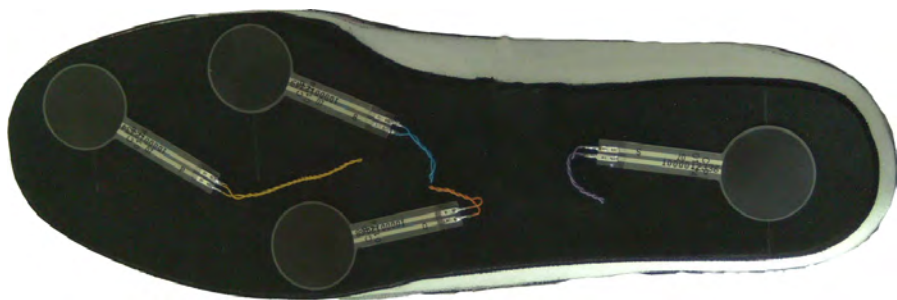
Figure 4.9: Bottom view of one (closed) eSHOE prototype II insole. The four pressure sensors are still visible, since they have not yet been covered up with duct tape.

Figure 4.10: This picture was taken during the manufacturing process of eSHOE prototype II. It shows (the hands of) an orthopedic technician, applying glue on the top half of an insole. This represents the last step in the manufacturing process.

standard but never managed to become more widespread than Bluetooth®. Therefore it almost always requires extra/external modules in order to be available for standard devices. Whereas Bluetooth became a standard module inside many end-devices, like mobile phones, smart phones, notebooks, tablet PCs, etc. A minor shortcoming ist the very simple and minimalistic communication protocol, which only allowed to start a measurement by opening a communication channel and stopping it by either closing the channel again or turning off the power.

4.3 Prototype stage III of the instrumented insoles - eSHOE

Several adjustments have been made for the third generation of eSHOE prototypes, following the experiences with the former versions. It became clear, that the ZigBee® radio standard was not sufficient for the intents and purposes of the project. Bluetooth was chosen as radio standard in its stead. Another manufacturer of pressure sensors (FSR) has been chosen. In the meantime new versions of the accelerometer and gyroscope became available. The addition of a local storage, in the form of a SD-card, represented an important supplement. The usage of a lithium-polymer battery also allowed incorporation of the power supply into the insole material, rather than left as an external element.

The main components of eSHOE prototype stage III are a PIC24 microcontroller from Microchip (Chandler, Arizona, USA), an ADXL346 3-axis accelerometer from Analog Devices (Cambridge, Massachusetts, USA), an ITG-3200 three-axis gyroscope from Invensense (San José, California, USA), four A401 force sensitive resistors from Tekscan (South Boston, Massachusetts, USA), a KC22.6 Bluetooth radio transmitter from KC wirefree (Tempe, Arizona, USA) and a microSD memory card. Figure 4.11, table 4.2 and the following subsections (4.3.1 to 4.3.6) contain more detailed information on the sensor and hardware characteristics. With these changes the third generation prototypes was finally fit for a field trial in the form of a clinical pilot study, as it was carried out in the course of this thesis (see chapter 5.1).

The microprocessor software provides several settings for the data acquisition (channel selection, sampling frequencies) as well as data handling (optional local data storage, Bluetooth data transmission to the PC). Obligatory data access from a PC is possible using a micro universal serial bus (USB) cable. Using the power supply feature of the USB-link the built-in battery will can be re-charged. For this thesis trials data was recorded (mostly) at 200 Hz and stored locally on the microSD card in order to prevent data loss through radio transmission. The integration of printed circuit boards into a pair of hand-crafted shoe insoles was again realized with the assistance of an orthopedic technician. All of the sensors, which are currently available on the market, meet the technical requirements for lower limb motion analysis, such as measurement range, sensitivity or sampling rate. The sensors have been selected primarily according to their price-performance ratio and to their degree of miniaturization. This was, of course, a key issue with respect to the necessity of integrating the PCB with the sensors on it into something as small and as thin as a shoe insole. Miniaturization of the hardware components also was a major issue. It was addressed by reducing the number of PCBs from three pieces to one. This became possible through manufacturing this one PCB as a multi-layer (four) board and, additionally, by attaching the components to both sides of the PCB (top and bottom) instead of only to one. This helped to save space and to reach a board with a total length of 50.7 mm and a width of 22.2 mm (with a resulting area of $\sim 10\ cm^2$). Figures 4.13 and 4.14 show image and layout of the PCB in its actual size, in top view.
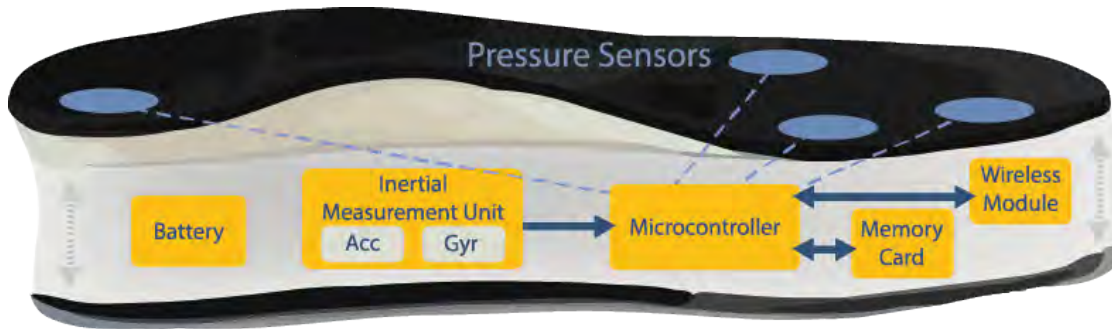
Figure 4.11: Schematic illustration of an instrumented eSHOE insole with its main functional units, all located onboard the PCB except the Li-Po battery. The PIC24 16-bit microcontroller, the IMU, formed by an ADXL-346 three-axis accelerometer (13 Bit, ±16 g) and an ITG-3200 three-axis gyroscope (16 Bit, ±2000 deg $/s$). Dimensions are distorted to provide better visibility.
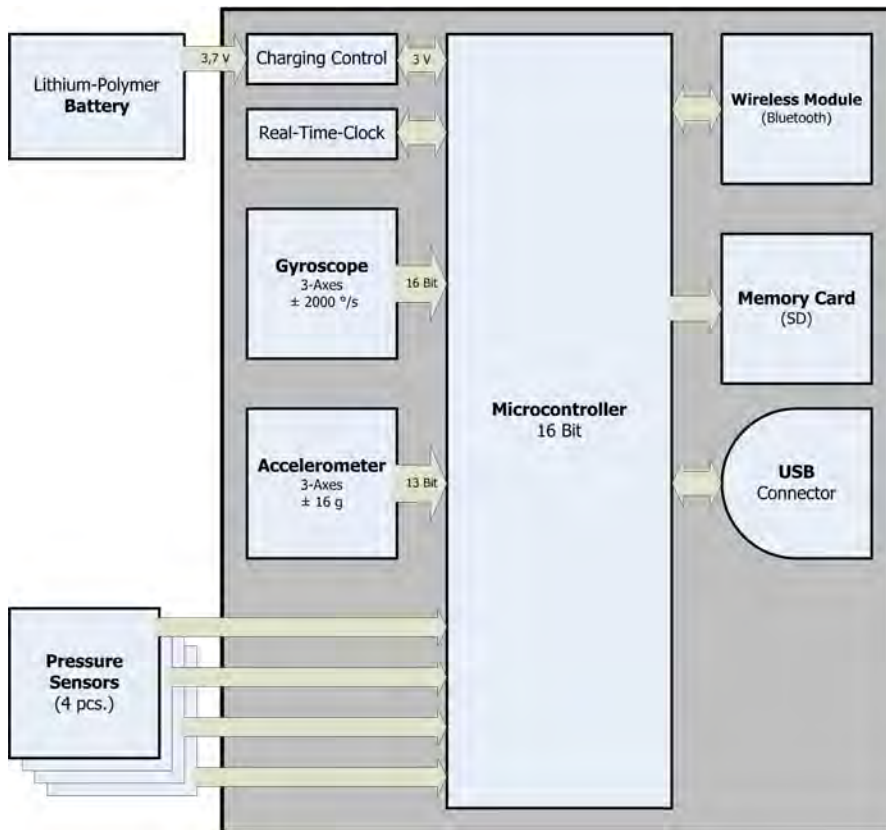
Figure 4.12: Block diagram of the embedded system on the printed circuit board, showing only the main components: battery, microcontroller/PIC, accelerometer, gyroscope and pressure sensors.

	Accelerometer	Gyroscope	FSR
Type	ADXL346	ITG-3200	A401
Manufacturer	Analog Devices	Invensense	Tekscan
Output	Digital	Digital	Analog
Range	$\pm16\ g$	$\pm2000°/s$	0 to $110N$
Sensitivity	$32\ mg/LSB$	$14.375\ LSBs/°/s$	$11\ g/LSB$
Resolution [Bit]	13	16	10 (PIC ADC)
Sensitivity Scale Factor	$256\ LSB/g$	$14.375\ LSBs/°/s$	
Zero Output Tolerance	$\pm0.05\ g = \pm0.5\ m/s^2$	$\pm40\ °/s$	
Sampling Rate	0.1 to 3200 Hz	400 kHz	-
Interface	SPI/I2C	I2C	ADC (PIC)
Power Consumption	140 μA	6.5 mA	-
Dimensions [mm]	$3 \times 3 \times 0.95$	$4 \times 4 \times 0.9$	$56.8 \times 31.8 \times 0.2$

Table 4.2: Main hardware components of research prototype III.

On the top half of the PCB the following components are located: (1) the real-time-clock circuit, (2) the memory card slot, (3) the Bluetooth radio module with (4) the associated antenna and (5) the programming interface. The bottom side contains (1) pads for the connection of the pressure sensors, (2) the charging regulator circuit, (3) the gyroscope and accelerometer sensors, (4) a USB connector and (5) the PIC micro-controller. Figures 4.15 and 4.16 show the PCB in top and bottom view, respectively. Each contains the PCB's schematic (on the left side) and a photograph of the board (on the right side). The above mentioned functional blocks are also indicated in the figures. The measurement system can be switched on and of via a small button, which is attached to one side of the PCB and can be reached from outside the sole. To retrieve the locally stored measurement data a USB (micro) cable has to be plugged into the dedicated connector. The same connection is used for recharging the battery.
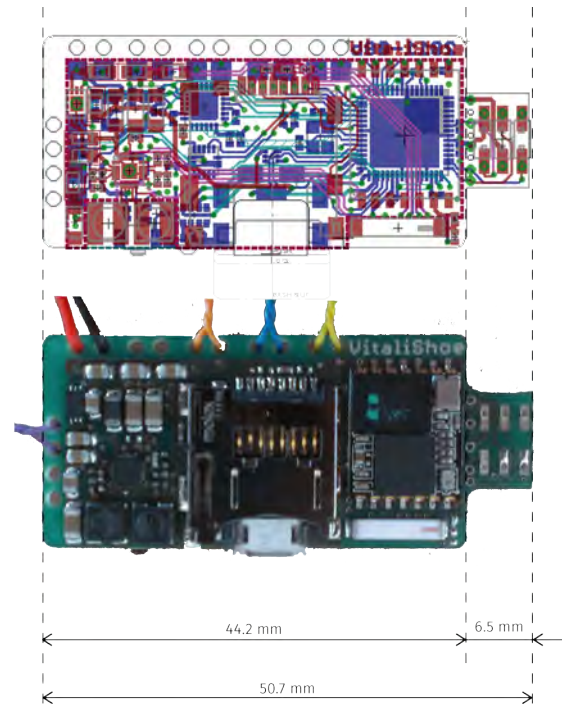
Figure 4.13: PCB schematic *in a ratio of 1:1* with the corresponding dimensions in millimeters.
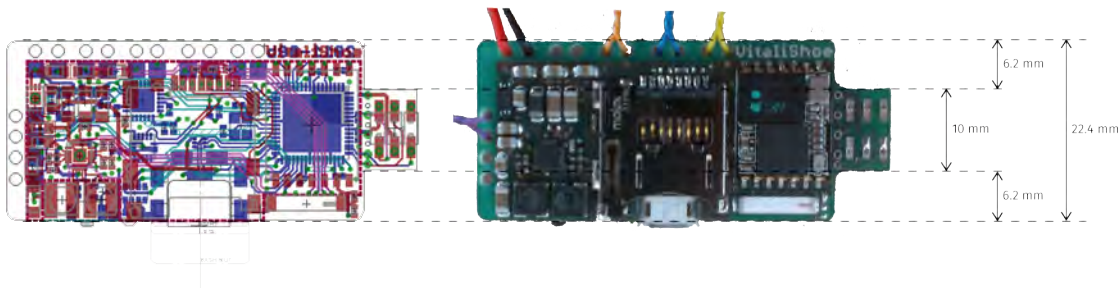
Figure 4.14: PCB schematic *in a ratio of 1:1* with the corresponding dimensions in millimeters.

4.3.1 Microcontroller PIC24 (PIC24FJ256GB206QFN)

The central processing unit (CPU) on the PCB is a PIC24FJ256GB206 flash microcontroller with a 16-bit modified Harvard architecture. It was used in the QFN package version with 64 pins (see fig. 4.17), 256 kilobytes program memory and 96 kilobytes of SRAM memory. Furthermore, it contains an on-chip USB transceiver, three I²C, three SPI and four UART modules, five 16-bit timers/counters with programmable prescalers, an up to 24-channel, 10-Bit analog-to-digital (A/D) converter. The controller supports several power management modes (incl. operation during sleep mode), up to 16 MIPS

65
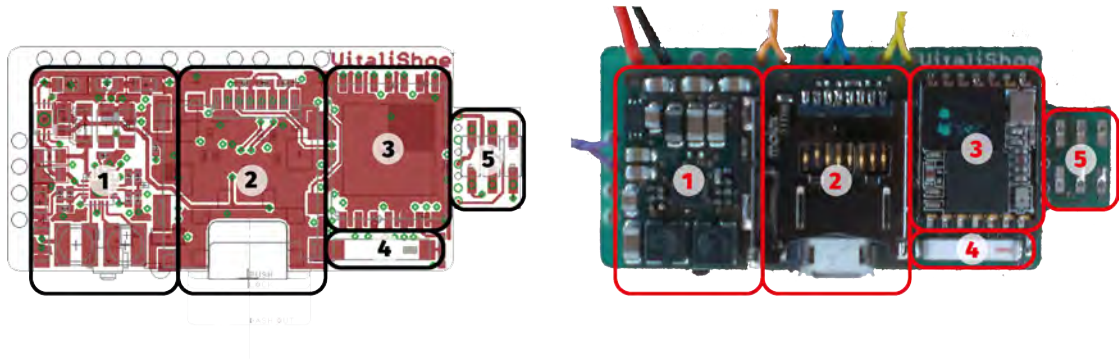
Figure 4.15: Top side of the eSHOE PCB, with (1) real-time-clock circuit, (2) micro SD card slot, (3) Bluetooth OEM module, (4) external ceramic antenna and (5) programming port.
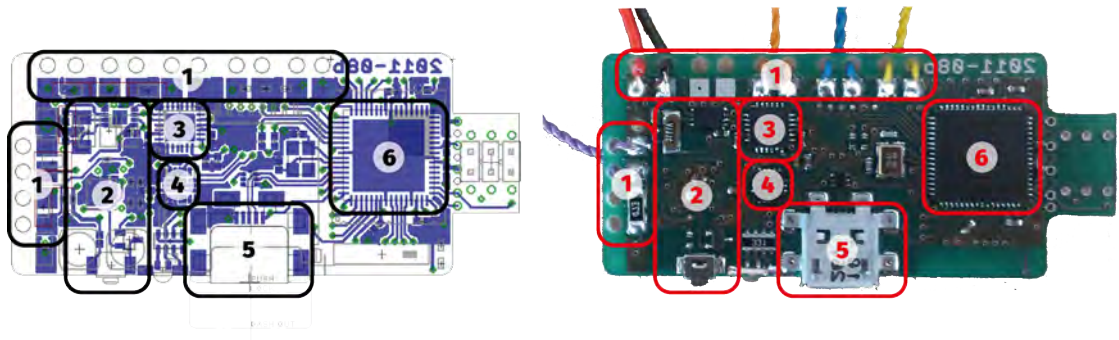
Figure 4.16: Bottom side of the eSHOE PCB, with (1) pressure sensor connectors, (2) charging regulator circuit including on/off push-button, (3) gyroscope, (4) accelerometer, (5) USB connector and (6) PIC microcontroller.

operations at 32 MHz. It is USB 2.0 on-the-go (OTG) compliant and provides low-speed (1.5 $Mbps$) and full-speed (12 $Mbps$) USB operation in host mode.

The microcontroller's tasks as eSHOE CPU were the following:

- Data Collection from the sensors,
- Data Conversion
  converting measurement into digital values (if not already provided by the sensors),
- Communication
  - processing date into a binary communication protocol and providing a set of commands to ensure controllability of the controller's firmware (see subsection 4.4.2),
  - handling the radio transmission via the Bluetooth module,
- Data Storage

- managing the data storage on the microSD memory card,
- managing the access to the (SD card) stored data via the USB port
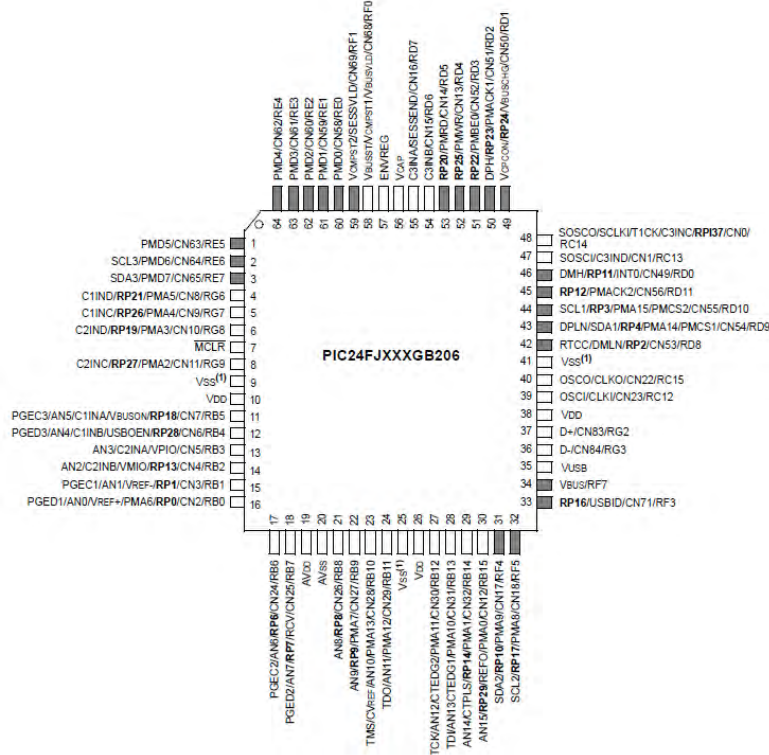
Figure 4.17: Pin Diagram (top view) of the PIC24FJ256GB206 microcontroller in its 64-Pin, QFN package. Shaded pins indicate pins that are tolerant to up to +5.5 V (note from the data sheet).

4.3.2 Accelerometer ADXL346

The ADXL346 accelerometer from Analog Devices (Norwood, Massachusetts, USA) is a small, thin ($3 \times 3 \times 0.95 \ mm$), ultralow power ($23 \ \mu A$ at $2.6 \ V$), 3-axis accelerometer with 13-bit resolution. The measurement range is selectable from $\pm 2 \ g$, $\pm 4 \ g$, $\pm 8 \ g$, or $\pm 16 \ g$. The ADXL346 is supplied in a 16-lead, plastic (LGA) package (see fig. 4.18). Digital output data is formatted as 16-bit twos complement and is accessible through either an SPI (3- or 4-wire) or I²C® digital interface. It is capable of measuring static as well as dynamic acceleration, allowing applications from tilt-sensing to the detection of motion or shock. A resolution of 4 mg/LSB even enables the determination of inclination changes of less than 1.0°.
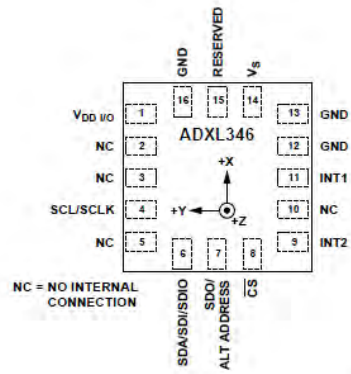
Figure 4.18: Pin Configuration (top view) of the ADXL346 accelerometer in its 16-pin LGA package.

4.3.3 Gyroscope ITG-3200

The ITG-3200 is a single-chip, digital-output, 3-axis MEMS gyroscope integrated circuit (optimized for gaming, 3D mice, and 3D remote control applications). It features three 16-bit analog-to-digital converters (ADCs) for digitizing the outputs ... with simultaneous sampling while requiring no external multiplexer, a user-selectable internal low-pass filter bandwidth, and a fast-mode I²C® (400 kHz) interface. The sensitivity is 14.375 $LSBs$ per °/sec and the full-scale range is $\pm2000°/sec$. Low operating current consumption (6.5 mA)combined with a supply voltage range of 2.1 V to 3.6 V for long battery life. The part comes in package size of $4 \times 4 \times 0.9$ mm (QFN) and features a robust 10,000 g shock tolerance.
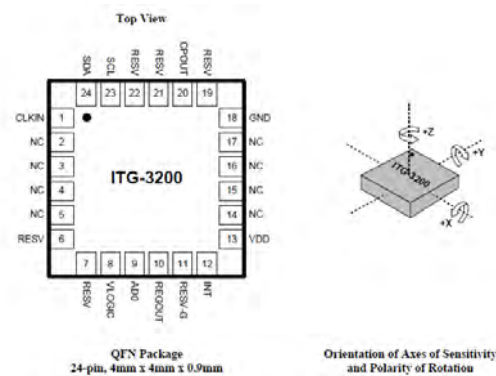
Figure 4.19: Pin Configuration (top view) of the ITG-3200 gyroscope in its 24-pin QFN package.

4.3.4 Force sensitive resistors (FSR) A401

Flexiforce A401 from Tekscan is a force sensitive resistor with a length of 56.9 *mm* and width of 31.8 *mm*. It is only 0.0203 *mm* thick and has a sensing area of 25.4 *mm* (diameter). The sensor is made of a polyester substrate with a measuring range of 0 *to* 111*N* and a response time of $< 5\mu s$.

Figure 4.20: Flexiforce A401 force sensitive resistor from Tekscan.

4.3.5 Bluetooth Module KC-22.6

The wireless module KC-22.6 from the KC wirefree corporation (Arizona, USA) is an off-the shelf OEM module with Bluetooth® v2.1 + EDR, class 2 radio, 128-bit encryption security, with a range up to 20 *meters* (line of sight). The KC22 contains an ARM7 microprocessor with (reprogrammable) embedded firmware for serial cable replacement using the Bluetooth Serial Port Profile (SPP). It provides an easy to use AT style command interface via UART and thereby also offers remote control capability, where AT commands can be issued remotely from any other Bluetooth device using SPP.
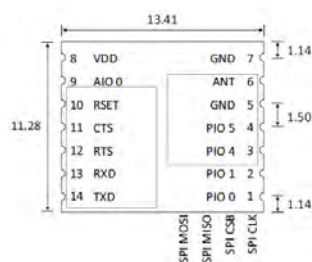
(a) Dimensions and pin configuration.   (b) Photo of KC-22.6 module.

Figure 4.21: The KC-22.6 bluetooth module from KC wirefree.

4.3.6 Operating circuitry

Furthermore a (USB) battery charger integrated circuit (IC), in combination with a battery gauge IC, regulate charging currents and ensure that charge, voltage and temperature of the single-celled Lithium-Polymer battery are kept within the requested limits. A real-time-clock (RTC) IC is used to generate time stamps in order to identify the measurement data, stored on the memory card. It is also equipped with an additional on-board serial EEPROM memory, which is used as a protected (non-volatile) storing space for the unique character strings, to identify each insole.

4.3.7 Insole integration

The orthopedic insoles, which form the basis of eSHOE, are made of ethylene-vinyl acetate (EVA) with a hardness of 40 Shore. The basic material (EVA) is shaped by hand via CNC milling. The milling machine is also used to carve out spaces for the printed circuit board and the battery. Figure 4.22 shows a quasi longitudinal section of an already prepared insole with the electronic components placed inside. After the
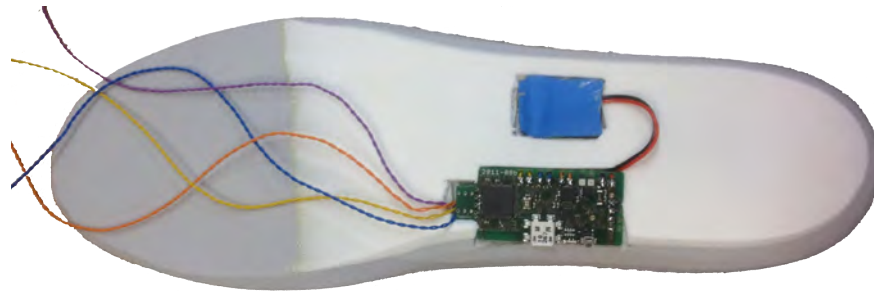
Figure 4.22: Quasi longitudinal section of one orthopedic insole. (1) the PCB (in bottom view) and (2) the Lithium-Polymer battery (covered in shrink tubing) are visible.

placement of the parts the insole is closed up with covering material of 1 mm in thickness. The wires for the pressure sensors are led outside through a hole in the cover. When the insoles are covered up, the edges are smoothed (once more), (see figure 4.23). In the next step, the bottom and the sides of the insole is coated with an elastic (light brown) textile material. After that, the force sensitive resistors are soldered to the wires (see fig. 4.24). Finally, gaffer tape is used to protect the FSRs and the free wires (see fig. 4.25). This concludes the eSHOE manufacturing process. An important notice is that, since the eSHOE measurement device is in fact a pair of shoe insoles and "ordinary" walking shoes only have a sewed-in insole, only a certain type of shoes are usable/compatible. Suitable types are shoes which have an additional (and removable) inner sole. Since shoe size generally varies among people, it was necessary to build a wide range of insoles, to avoid excluding any subjects, who are of interest and relevance to the study. Therefore eight pairs of insoles, ranging from 37 (EUR) / 7 (US) to 44/45 (EUR) / 12/13 (US), were crafted.

Figure 4.23: Smoothing of the insoles' edges after the cover up.
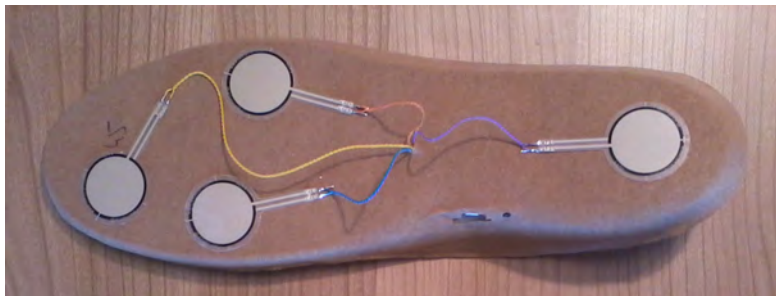
Figure 4.24: Next to last step of the insoles.

Figure 4.25: Final stage of the eSHOE insoles in the manufacturing process. FSR sensors and free wires are now covered with gaffer tape for (their) protection.

Figure 4.26: A pair of already integrated eSHOE insoles.

4.3.8 Measurement Configuration

Every sensor (unit) in our measurement system has its coordinate system/axes configuration (accelerometer in left insole, gyroscope in left insole, accelerometer in right insole, gyroscope in right insole). In order to avoid confusion, a global coordinate system (for both PCBs in one system) was defined and programmed into the micro-controller. This specific coordinate system is illustrated in fig. 4.27 and table 4.3 maps the technical and sensor-specific terms to the medical terms as well as the abbreviations, used throughout this thesis.
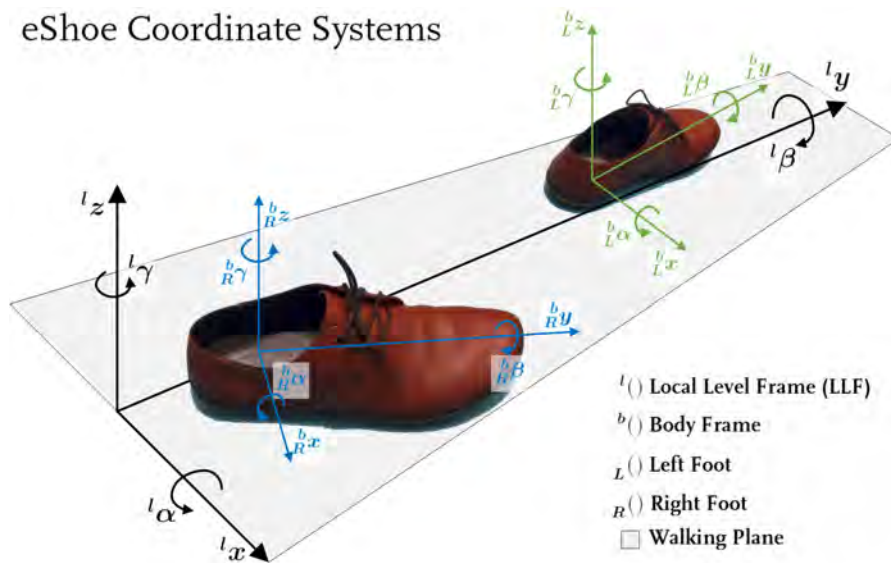
Figure 4.27: Coordinate systems of the eSHOE setup. Axis definitions for local level and body frames. Adopted from [Polasek, 2014, p. 61].

Sensor- and axes-specific terminology	Medical Terminology	Abbreviation
Tilt angle in sagittal plane	plantarflexion / dorsiflexion	ANGLE
Acceleration along transverse axis	medial / lateral	ACC-X
Acceleration along sagittal axis	anterior / posterior	ACC-Y
Acceleration along longitudinal axis	cranial / caudal	ACC-Z
Pressure under the heel	—	HEEL
Pressure under the metatarsal head V	—	META-V
Pressure under the metatarsal head I	—	META-I
Pressure under the big toe	—	TOE
Angular velocity around transverse axis	plantarflexion / dorsiflexion	GYRO-X
Angular velocity around sagittal axis	pronation / supination	GYRO-Y
Angular velocity around longitudinal axis	eversion / inversion	GYRO-Z

Table 4.3: List of abbreviations for the sensor- and axes-specific data fields. Adopted from [Reich, 2013].

Parameter	Direction	Side	Sign
Acceleration	medial	left	+
		right	-
	lateral	left	-
		right	+
	anterior	—	+
	posterior	—	-
	cranial	—	+
	caudal	—	-
Angular rate	Supination	left	+
		right	-
	Pronation	left	-
		right	+
	Lateral Rotation	left	+
		right	-
	Medial Rotation	left	-
		right	+

Table 4.4: Sensor-axes and corresponding directions in medical terminology.

4.4 Measurement Management and Software

Several software tools had to be developed in order to operate and (remote) control the eSHOE embedded system and to evaluate the measurement data. Therefore, a firmware was necessary to operate the micro-processor and to manage the workings of the sensors in combination with the Bluetooth module and the memory card. A (remote) control program (for the PC), including a graphical user interface (GUI), was developed for visual feedback on commands and the insoles' statuses as well as a visual representation of the transmitted data. For the management of study-related data a specific database has been implemented along with a connection to the GUI. Finally a tool for the (offline) evaluation of the measurement data was also implemented.
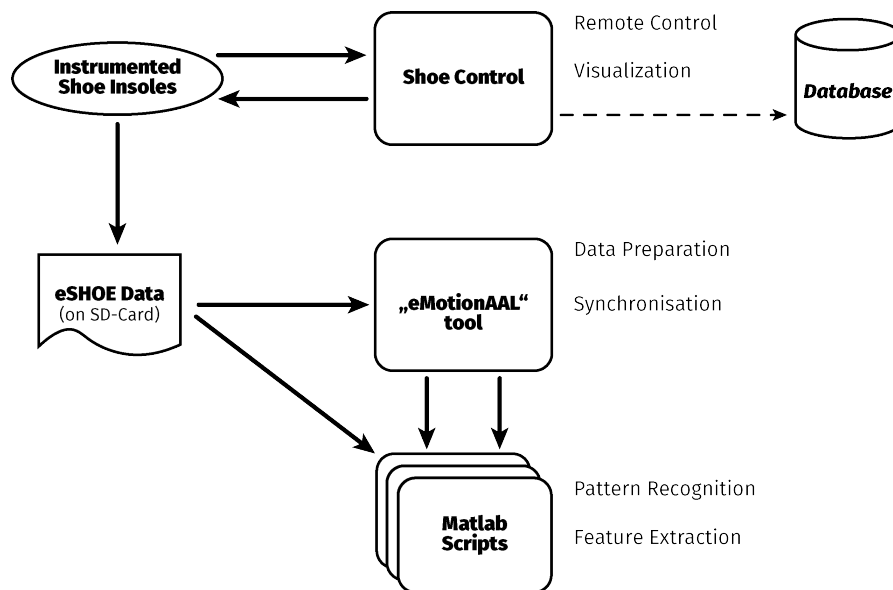
Figure 4.28: Block diagram of all software components.

4.4.1 Basic features of μC Software

The micro-processor's firmware contains a set of operational states and the attached light-emitting diode (LED) indicates to the user in which state the processor is currently in. Table 4.5 shows a list of all available/possible states and fig. 4.29 indicates the interconnection and dependencies of the states.

The microprocessor has to be programmed via an in-circuit debugger (ICD) from Microchip Technology, at least for the first time it is ever programmed. The eSHOE firmware comes with a bootloader, which makes it possible to program the PIC controller with a (source code) file from the SD card. After the device is turned on, it scans the SD card for firmware files and checks, if the version number of the stored file is higher than the one that is currently running. Is there a new(er) firmware file available, the micro-processor restarts and the new program is automatically flashed into the processor's memory.

LED color/status	PCB status
LED off	power off - no operation
LED orange	checking the firmware file on SDcard
LED red	PCB boot-up
LED white	PCB/μC ready / idle
LED blue	Bluetooth connection active
LED green	Measurement active/running
LED blinking (white/blue)	USB connection active

Table 4.5: Possible acknowledgements from the insoles to the different commands.

The eSHOE PCB, and with it the microcontroller and all electronic components, can be turned on, off and reset via a small push-button next to the LED (see fig. 4.16). The usual use case for the eSHOE PCB starts by turning it on via the on/off button. After pressing the button the LED turns red, indicating the starting/booting process. The LED turns orange instead of red, when a firmware file is detected on the SD card. It stays orange for a few seconds in case the file represents a new version of firmware and has to be flashed into the processors memory. After that the PCB turns itself off automatically. In case of an "ordinary start" the PIC enters the idle state, indicated by white LED light, where it is ready for operation and waiting for Bluetooth connection and in further consequence for input commands. As soon as the PCB is in idle state a Bluetooth connection (to a PC or equivalent) can be established. When an active Bluetooth link is established the LED turns blue. From this point on the PCB/embedded system/PIC is ready to receive and process the control commands. The communication protocol, including these commands, their structure and functions are described in detail in the following section (4.4.2). When the PCB receives the "start" command and, therefore, measurement data is recorded and/or transmitted, the LED turns green. The measured data can either be stored inside the shoe-insole on the SD memory card, wirelessly transmitted to a PC (or equivalent) or both, stored and transmitted at the same time. The sampling frequency can be switched between 50 Hz or 200 Hz. These options are defined in the start command and are also explained in more detail in the following subsection. If the locally stored data is to be accessed (via the PC), a (micro) USB cable has to be connected. This can be done during the idle state or also during the active Bluetooth link. In both cases the LED starts blinking in the currently active color.
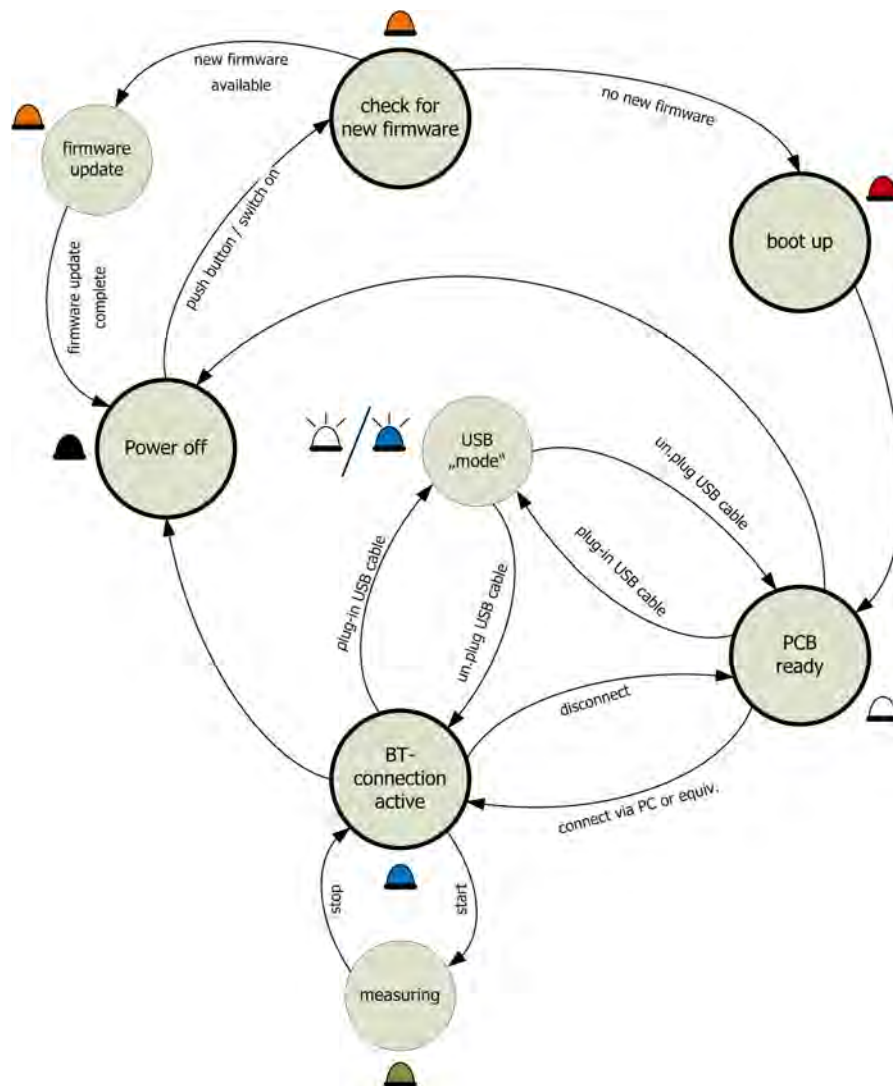
Figure 4.29: chart of the most important firmware states of the eSHOE insoles/PCBs.

4.4.2 Communication protocol of μC software

A binary communication protocol, consisting of a set of commands has been defined to regulate of the operation of the eSHOE hardware and to set or retrieve certain settings. As soon as the eSHOE PCB/embedded system is in idle mode with an active Bluetooth link the commands can be transmitted to it. The μC software can process incoming data and is also able to reply to certain commands in a pre-defined manner. In most cases this means sending a message of acknowledgment (to certain commands) but it also includes transmitting measurement data. Both sets of commmands, incoming and outgoing, are described later on in this subsection.

In many of the commands one byte is enough to encode necessary information. This applies especially to all control commands. But when it comes to measurement data, one byte is not enough. Because one byte can only represent values ranging from 0 to 255, or if also negative values have to be encoded, ranging from -128 to 127. Since all our sensors produce values which are above these numbers, two bytes had to be used to encode measurement data of one channel. These two bytes will henceforth be referred to as "most significant byte" (MSB) and "least significant byte" (LSB). Together they form a 16-Bit long number, which allows to encode values from 0 to $65,535$ or from $-32,768$ to $32,767$. The combination of these two eight-bit numbers is acheived by shifting the MSB eight bits to the left and then add the LSB with a mask that ensures using only the lower eight bits of the LSB. The value is calculated using the following pseudo-code: Vice-versa, a 16-bit number is divided into two 8-bit numbers (MSB & LSB) by using

---

1 16-bit value = (MSB « 8 | (255 & LSB))

---

the reverse operations. A section of (pseudo) code for copnverting a 16 bit number into MSB and LSB looks like this: By assigning the 16-bit variable "value" to the LSB the

---

1 value = 01010101 01011011
2 LSB = value
3 MSB = value » 8

---

last eight bits are transferred to the byte. The first eight bits are cut off and hence, the LSB is found. For the calculation of the MSB the variable "value" is shifted eight bits to the right. The last eight bits are cut off and the first eight bits are assigned to the MSB.

The eSHOE firmware uses the "little endian" format, which means that the least significant byte (LSB) is transferred first and the MSB is transferred last (or second).

Command Name	Description
Reset	Restarts the eSHOE insoles
Start	Starts a measurement in the defined operation mode
Stop	Stops the current measurement
Set Clock	Defines/sets the system time for the PCB/insole
Get Clock	Returns the time 'stored' in the RTC of the PCB/insole
Get Status	Returns the status (charge)of the battery
Get Version	Returns the version of the firmware current running on the PIC
Set Threshold	Sets the FSR thresholds for the Kalman filter
Calibrate	Calibrates the Kalman filter
Get Configuration	Returns the name (char.), which has been assigned to the PCB

Table 4.6: Control commands for the mobile gait analysis system eSHOE.

Byte Index	0	1	2	3 ...
Command Name	STX	TYP	LEN	PAYLOAD

Figure 4.30: Basic structure of all eSHOE firmware commands with the three-byte wide header - start index (STX), type (TYP) and length (LEN) bytes at the beginning followed by optional payload bytes.

Incoming commands - PC (or equivalent) to eSHOE

Table 4.6 contains a list and short description of all the commands the eSHOE hardware "understands". All commands follow the same basic structure and are segmented into bytes. At the beginning of each command there is a three-byte wide 'header'. It consists of a start index byte (STX), which indicates the beginning of a data package or command, followed by one byte defining the command type (TYP) and concluded by one byte containing the length of the command's payload. Each data package contains at least these three header bytes and is uniquely identifiable by the eight bit TYP code. There are also commands which have a specific payload including relevant information concerning the command. A graphical representation of the command structure can be found in fig. 4.30. Each byte can, of course, either be expressed in eight-digit binary code or in two-digit hexadecimal code. When it is necessary to mention the commands' configurations it will mostly be done in hexadecimal code. Table 4.7 lists all incoming commands (from PC to eSHOE), along with their first three bytes: start index (STX), type (TYP), length (LEN) and whether or not they contain payload. Descriptions of the payloads of these commands can be found in additional tables throughout the following paragraphs. First of all it was necessary to implement two commands to start and stop the measurement process. It was neither useful nor practical to have the hardware start measuring immediately after the power was turned on, especially concerning power consumption and data interpretation. Other than that it proved to be useful to adjust

Command Name	STX	Type	Length	Payload
Reset	0x55	0x01	0	No
Start	0x55	0x02	4	Yes*
Stop	0x55	0x03	0	No
Set Clock	0x55	0x04	0	Yes*
Get Clock	0x55	0x05	4	No
Set Configuration	0x55	0x06	33	Yes*
Get Status	0x55	0x07	4	No
Set Threshold	0x55	0x08	4	Yes*
Get Version	0x55	0x09	0	No
Calibrate	0x55	0x10	0	No
Get Configuration	0x55	0x16	0	No

Table 4.7: Syntax composition for incoming commands (from PC to eSHOE) to control measurements.

Payload Byte	Mode	Status	Hex-Code
1	Data transmission	on	0x00
		off	0x01
2	SD card storage	on	0x00
		off	0x01
3	Kalman filter type	off	0x00
		CEIT	0x01
		Madgwick	0x02
4	Sampling rate	50 Hz	0x00
		200 Hz	0x01

Table 4.8: Possible payload configurations for the start command. Its composition defines the operation mode of the PCB.

certain settings *before* starting a measurement. Possible settings for the measurements are (1) data transmission via Bluetooth (on/off), (2) data storage on SD card (on/off), (3) selection of filter algorithm for calculating the pitch angle (off/CEIT/Madgwick) and (4) sampling frequency (50/200 Hz). All possible configurations for the start command and their corresponding byte-codes (in hexadecimal) can be found in table 4.8. Hence, a start command for a measurement with data transmission turned on, no SD card storage, the CEIT Kalman filter and a sampling rate of 200 Hz is a seven byte long string containing "0x55 0x02 0x04 0x01 0x00 0x01 0x01" in hexadecimal code or "01010101 00000010 00000100 00000001 00000000 00000001 00000001" in binary code. The composition of this start command configuration is also illustrated in fig. 4.31. Most of the protocol's commands have a handshake character, meaning that they trigger a response command or a short acknowledge message by the micro-controller. Either to simply indicate the correct

Start Command

HEADER			PAYLOAD			
0	1	2	3	4	5	6
STX	TYP	LEN	Data Transmission	Data Storage	Pitch Angle Filter	Sample Rate
Start Index	Message Type	Message Length	0 == no transmission 1 == transmission active	0 == no SD card log 1 == SD card log active	0 == no pitch calculation 1 == CEIT filter 2 == Madgwick filter	0 == 50 Hz 1 == 200 Hz

0	1	2	3	4	5	6
0x55	0x02	0x04	0x01	0x00	0x01	0x01

0	1	2	3	4	5	6
01010101	00000010	00000100	00000001	00000000	00000001	00000001

Figure 4.31: Graphical representation of the structure of the start command with sample data encoded in hex and binary. It consists of the typical three-byte header, with start index, type and length bytes at the beginning, followed by four (as indicated in the length byte) payload bytes.

reception of a command or as an automatic response, containing inquired information (e.g. RTC status/time). The handshake principle is illustrated in fig. 4.32 by means of the start and stop commands and their respective acknowledgments. Especially for unidirectional commands (like start and stop) this handshake principle makes it easier to confirm whether the command was properly transmitted over the air and successfully received by the controller. The eSHOE PCB also contains a real-time-clock (RTC) chip. It is powered by a crystal and has to be synchronized from time to time. For that purpose two commands were implemented. One to poll the time from the RTC, namely the "get clock" command. And one to set the RTC to a date and time, set by the user, in the form of the "set clock" command. Get clock does not have a payload, since it only requests a response from the controller. Set clock on the other hand has to have a payload, in which information about the (current) date and time can be transmitted. Six (payload) bytes are used to transmit date and time in the format (1) year, (2) month, (3) day, (4) hour, (5) minute, (6) second. Table 4.9 contains a list-based description of the command, along with example data (hex coded).

Since a number of different subjects with different shoe sizes had to be provided with different sized insoles it was necessary to distinguish them (mainly concerning the management of Bluetooth devices) by some sort of name or identifier. Furthermore, the same PCB was used for left and right insoles, resulting in different orientations of

eSHOE Communication Protocol Handshake Process

PC   **eSHOE**

„Start"

`0x55 0x02 0x04 0x01 0x00 0x01 0x01`

start measurement

„Start-ACK"

`0x55 0x00 0x01 0x02`

„Stop"

`0x55 0x03 0x00`

stop measurement

„Stop-ACK"

`0x55 0x00 0x01 0x03`

PC   **eSHOE**
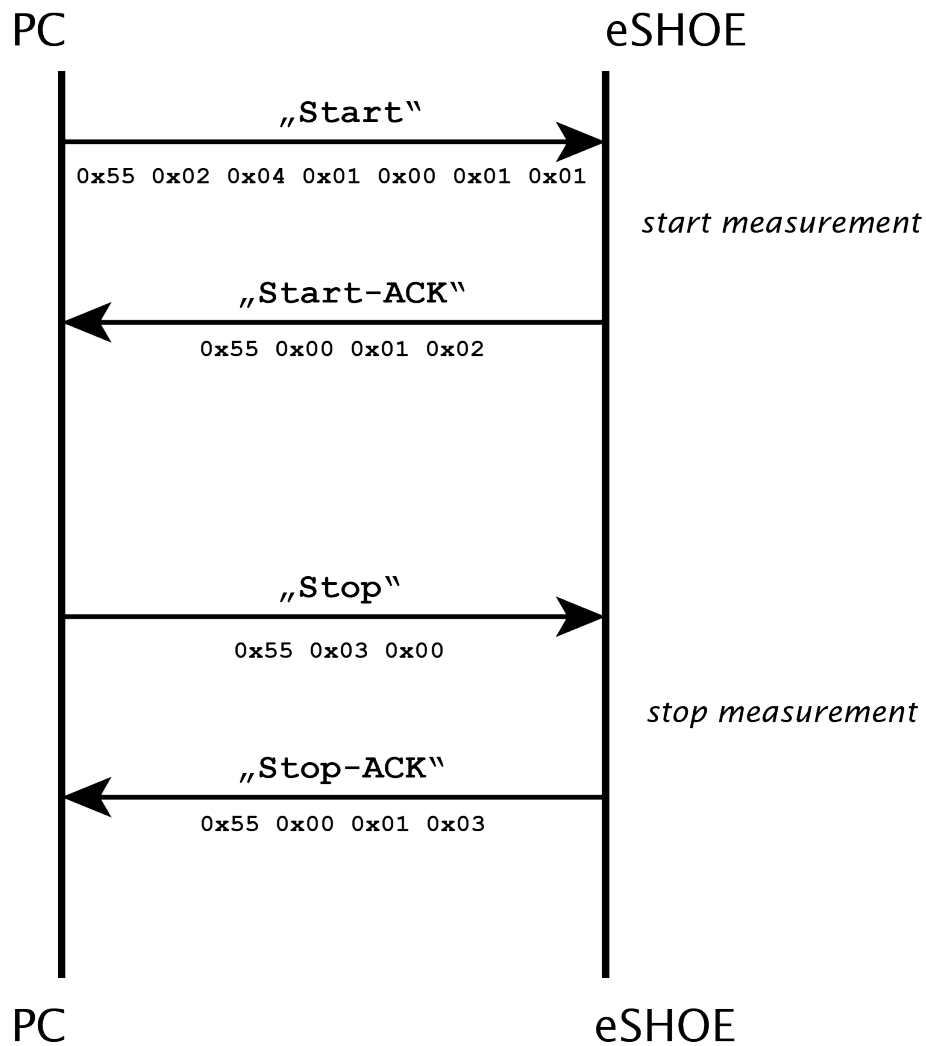
Figure 4.32: Handshake principle of the eSHOE communication protocol. The start command triggers, if received properly, a short "start ack" response, indicating the successful reception and the start of the measurement process. Similarly, the "stop ack" message signifies that the command was received and the measurement has been stopped.

Get Clock Handshake Process
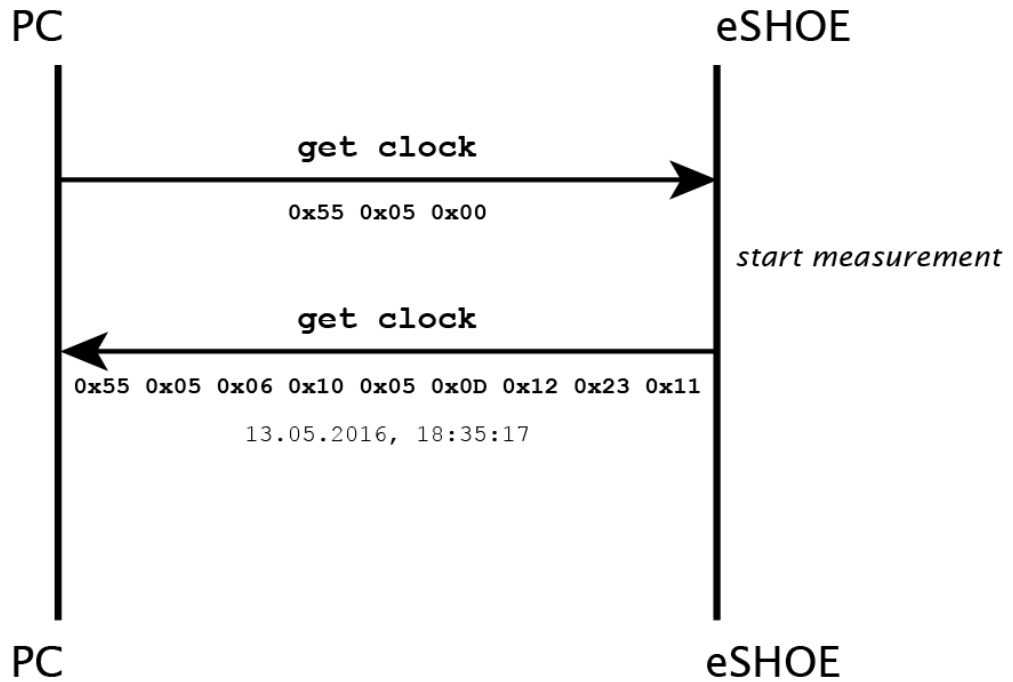
Figure 4.33: Handshake like process in case of the get clock query. Three byte string triggers a nine byte response by the micro-controller, containing year, month, day, hour, minute, second of the RTC's EEPROM memory.

Payload Byte	Field	Example (dec)	Example (hex)
1	Year	83	0x53
2	Month	1	0x01
3	Day	1	0x01
4	Hour	23	0x17
5	Minute	22	0x16
6	Second	17	0x11

Table 4.9: Syntax of the "Set Clock"-command.

the boards depending on the side they are integrated in. Therefore, a command and corresponding options to name each PCB and define their orientation were implemented. To name the eSHOE insoles and to define their axes configuration (left or right), the "set configuration" command is used. It contains 33 bytes of payload, where 32 bytes represent the name and one byte is used to distinguish between the left or right insole configuration. To name the insole "eSHOE 43 L", every letter (including spaces) must be translated into hexadecimal code, resulting in a ten byte long char array (in this particular case) containing "0x65 0x53 0x48 0x4F 0x45 0x20 0x34 0x33 0x20 0x4C". There is also a "get configuration" command, which causes the micro-controller to return the stored characters (respresenting the name and side). It is described in the next subsubsection.

The firmware of the eSHOE insoles provides functionalities to configure the implemented Kalman filter, which is responsible for the tilt angle calculation. For one, a threshold for the pressure data of every FSR-sensor can be set to a specific value, when the filter shall be triggered. Once this value is reached, the calculated tilt angle in sagittal plane is reset to the calibration value. For that purpose, the "set threshold"-command is used. The threshold needs to be set for all four FSR sensors, each consisting of two bytes (LSB & MSB). Hence, the payload is made up of eight bytes. The 'calibrate' command causes the processor to detect the current acceleration sensor values (hence, the current orientation) and store it as calibration value (see above). It is the only command though, that has no payload (0x55 0x10 0x00) and also only triggers an acknowledgment response (0x55 0x00 0x01 0x10) without a significant payload.

The user also has the possibility to inquire the status of the battery (current voltage and charge) by sending the 'get status' command. It is a short, three byte wide, command (0x55 0x07 0x00) which triggers a response with the required information in the payload.

In case one wants to know which version of the firmware is currently running on the micro-processor, the 'get version' command was implemented. Since it is also a simple request, it is only three bytes short (0x55 0x09 0x00).

Outgoing commands - eSHOE to PC (or equivalent)

There is also a number of messages the micro-controller generates, mostly in response to incoming commands. These messages can be divided into three groups, the acknowledgments (ACK), the get-responses and the measurement data. An overview of the *ACKs* can be found in table 4.10, get-responses in table 4.11 and the structure of the measurement data is explained separately.

Almost every command triggers a message of acknowledgment inside the micro-controller. In the least to provide feedback to the user whether the command was transmitted successfully. The ACKs have a very simple structure. They are four bytes long, with one byte of payload. In it the type of the ACK is encoded. Usually the payload corresponds to the type (TYP) of command. This implies that there is exactly one ACK for each command. The only exception is the start command, where there are five different ACKs (payloads: 0x02, 0x12, 0x22, 0x32, 0x42). The actual type of ACK depends on the start

Acknowledgments

HEADER			PAYLOAD
0	1	2	3
STX	**TYP**	**LEN**	**TYPE ID**
Start Index	Message Type	Message Length	0x00 == unknown command 0x02 == start 0x03 == stop 0x04 == set clock 0x06 == set config 0x08 == set threshold 0x10 == calibrate done 0x12 == start error - SD-card problem - ABORTED 0x22 == start warning - SD-card problem - TRANSMITTING 0x32 == start error - no SD-card & no transmission- ABORTED 0x42 == runtime warning - SD-card problem - data not properly saved

0	1	2	3
0x55	**0x00**	**0x01**	**0x12**

0	1	2	3
01010101	00000000	00000001	00010010

Figure 4.34: Structure of acknowledgment messages.

Acknowledgement	Byte-Code
Unknown command	0x00
Measurement started	0x02
Measurement stopped	0x03
Clock set	0x04
Configuration set	0x06
Threshold set	0x08
Insole calibrated	0x10
Start aborted due to SD-Card problems	0x12
Start successful, SD-Card problems, Data is transmitted.	0x22
Start aborted, SD-Card problems, Data is not transmitted.	0x32
Runtime Warning - SD-Card Problem, data not properly saved	0x42

Table 4.10: Possible acknowledgments from the insoles to the different commands.

Command Name	STX	Type	Length	Payload
Get Clock	0x55	0x05	6	Yes*
Get Status	0x55	0x07	4	Yes*
Get Version	0x55	0x09	1	Yes*
Get Configuration	0x55	0x16	33	Yes*

Table 4.11: The first three bytes of Status Responses (from PIC/the insoles).

command configuration (transmission of/off, SD on/off) and whether or not problems with the SD card occurred. For instance, if data transmission and SD card storage is selected but there is a problem with the SD card (or no card is inserted), this will still cause the measurement to start, but with a different ACK (0x55 0x00 0x01 0x22) than when the measurement started without problems (0x55 0x00 0x01 0x02). The second group is formed by the *get-command responses*. There are four get commands in the eSHOE communication protocol: "get clock", "get config", "get status" and "get version". Their structure and function was already explained in 3. These commands do not trigger an ACK-message, but they inquire specific information from the micro-controller. Therefore, the replies to those commands are more complex, and the payload that comes with them depend on the nature of command. Table 4.11 provides a list of the four responses, along with their header bytes. The get clock response is similar to the set clock command in structure and content (see tables 4.7 and 4.9). The only difference to set clock is the type (TYP) byte code, which is 0x05 instead of 0x04. Get status returns two values to the user: (1) the current voltage level of the battery and (2) the remaining charge of the battery, as calculated by the battery gauge circuit. During the development process there have been numerous revisions of the PIC/eSHOE firmware. In order to keep track which version of firmware is running on which PCB a command has been implemented to retrieve the version number of the currently running firmware.

Byte #	Field	Content	Ex. data (hex)	Ex. data (dec)
0	STX	Start index	0x55	85
1	TYP	Type	0x07	7
2	LEN	Length	0x04	4
3	P1	Voltage (LSB)	0x01	0x55
4	P2	Voltage (MSB)	0x17	0x55
5	P3	Charge (LSB)	0x16	0x55
6	P4	Charge (MSB)	0x11	0x55

Table 4.12: Composition of the get status response.

Byte #	Field	Content	Ex. data (hex)	Ex. data (dec)
0	STX	Start index	0x55	85
1	TYP	Type	0x07	9
2	LEN	Length	0x04	1
3	P1	Version	0x2A	42

Table 4.13: Composition of the get version response.

Byte #	Field	Content	Ex. data (hex)	Ex. data (dec)
0	STX	Start index	0x55	85
1	TYP	Type	0x16	22
2	LEN	Length	0x21	33
3 - 35	P1 - P32	Name	32 characters	
36	P33	Left/Right	0/1	

Table 4.14: Composition of the get version response.

The get version response is a four byte message, with one byte of payload that contains the version number (see table 4.13). The get configuration response is equal to the set configuration command, except the TYP byte, which contains 0x16 instead of 0x06 (4.14). Following the typical three byte header is a 33 byte long payload, containing a 32 byte character array and one byte at the very end, identifying whether it is a left or a right insole.

During measurement the micro-controller gathers raw data from the different sensors at 50 or 200 Hz (depending on the start command configuration) and transmits it in the form of a 27 byte long message, with 24 bytes of payload. These 24 bytes contain ten channels of raw data from all three sensor types, with two bytes per channel: three axes accelerometer, three axes gyroscope and four pressure sensors. Plus (the first) one channel for a counter variable and another for the tilt angle, which is already calculated inside the PIC. Measurement data from each channel is encoded in two bytes in little

Byte #	Field	Content	Unit	Conversion factor
0	STX	Start index		
1	TYP	Type		
2	LEN	Length		
3	P1	Counter (LSB)	1	
4	P2	Counter (MSB)	1	
5	P3	Angle (LSB)	deg	0.01
6	P4	Angle (MSB)	deg	
7	P5	Acc X (LSB)	g	0.004
8	P6	Acc X (MSB)	g	
9	P7	Acc Y (LSB)	g	
10	P8	Acc Y (MSB)	g	
11	P9	Acc Z (LSB)	g	
12	P10	Acc Z (MSB)	g	
13	P11	P. Heel (LSB)	1	
14	P12	P. Heel (MSB)	1	
15	P13	P. Meta V (LSB)	1	
16	P14	P. Meta V (MSB)	1	
17	P15	P. Meta I (LSB)	1	
18	P16	P. Meta I (MSB)	1	
19	P17	P. Toe (LSB)	1	
20	P18	P. Toe (MSB)	1	
21	P19	Gyro X (LSB)	deg/s	0.0696
22	P20	Gyro X (MSB)	deg/s	
23	P21	Gyro Y (LSB)	deg/s	
24	P22	Gyro Y (MSB)	deg/s	
25	P23	Gyro Z (LSB)	deg/s	
26	P24	Gyro Z (MSB)	deg/s	

Table 4.15: Composition of the data message.

endian format.

Finally, the sensor values have to be transformed into SI units by multiplying it with a conversion factor, pre-defined by the sensors' data sheets. Table 4.15 shows the data message, splitted into bytes in the order they are transmitted, along with their unit and corresponding conversion factor.
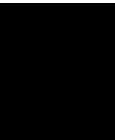
Detection of gait parameters in the eSHOE raw data

This chapter will elaborate on the detection of gait patterns and extraction of standard gait parameters from the eSHOE data, based on measurements conducted during a (clinical) pilot study. Work on the methods of this chapter were actively supported by Stefan Reich [Reich, 2013], who was a master student in the study program "healthcare and rehabilitation technology" at the University of Applied Sciences Technikum Wien (FHTW) at the time. His thesis was supervised by FH-Prof. Dr. Martin Reichel (from FHTW) and by the author of this thesis.

The first section of this chapter (5.1) is largely based on the study protocol, created for the study. Therefore, it deals with the pilot study's main issues: study design (5.1.1), study population (5.1.2) and ethical aspects (5.1.3).

Section 5.2 covers the first steps of the algorithm for gait parameter detection, namely the detection of gait cycle patterns in the eSHOE raw data. Starting from the method for segmenting the raw data into single cycles (5.2.1), moving on to finding/establishing standard patterns for all (relevant) sensor-axes (5.2.2) and concluding with how to find these patterns in other (e.g. patient) data (5.2.3).

The next stage in the gait parameter detection toolchain is the extraction of (two major) gait events from the gait cycle data. Detailed information about that process is presented in section 5.3. The extraction of two defining events in human gait, initial contact (5.3.1) and the last contact (5.3.2) of the foot with the ground is the main issue of that section. Based on the two key parameters (IC and LC), a variety of other gait parameters can be calculated. The methods for doing so are specified in section 5.4. Among them are stride time (5.4.1), stance phase and swing phase duration (5.4.2) and cadence (5.4.5).

Finally, the challenges and lessons learned from this pilot study are summarized in the (last) section (7.2) of this chapter.

5.1   Pilot study for the application of mobile gait analysis in order to support and supplement basic assessments and therapy progress monitoring in geriatrics

All necessary trials had to be conducted with three different subject groups. (1) a group of healthy senior citizens helped in the very first (pre-clinical) field test of the eSHOE (hardware and software) prototypes. This group will henceforth also be referred to as "REF". (2) continuous measurements during hospitalization to evaluate the feasibility of therapy progress monitoring with eSHOE was done with a group of hip fracture patients (from a local geriatric hospital in Vienna). When referring to the individuals of this group the identifier "PAT" will be used. (3) validation against an established clinical standard was done with two groups, patients from (2) and a group of healthy (young) adults, formed by employees of the geriatric hospital. For the healthy (young) adults "VAL" will be used substitutionally. An overview about the demographic and anthropometric characteristics of these three groups can be found in table 5.2.

Principal investigator of the study was *Prim. Dr. Katharina Pils*, head of the institute for physical medicine and rehabilitation at the Sophienspital Vienna.

The responsible ethics committee for the study was: *Ethikkommission der Stadt Wien, Magistratsabteilung 15 - Gesundheitsdienst der Stadt Wien.*
Thomas-Klestil-Platz 8, Town Town 1. Stock, CB 12. 103, 1030 Wien.
Telephone: 40 00, Fax: 40 00-99-877
E-Mail: ethikkommission@m15.magwien.gv.at

The following sections as well as all necessary documents have all been approved by the committee prior to the study. Table 5.1 shows a list of documents that had to be provided prior to the study. All of these documents, except the study protocol, were based on templates from the website of the forum of the Austrian ethics committees (`http://www.ethikkommissionen.at/`). This section and all subsections contained are excerpts from the study protocol and from the proposal for the local ethics committee. The informed consent form and case report form documents can be found in appendix C.

Document	Description
informed consent form for patients	Short description of the study and its goals,
informed consent form for healthy subjects	including a signature sheet
case report form (CRF)	Protocol sheet for the documentation of all relevant data from the subjects
Study protocol	Central document with detailed description of all aspects of the study (e.g. goals, ethical aspects, involved personnel, etc.)

Table 5.1: List of documents, relevant and necessary for the pilot study.

5.1.1 Study design

Study goals

The purpose of this study was to conduct measurements with the eSHOE system in a clinical setting for the first time. Furthermore, it should be tested whether it is possible to determine the progress of the rehabilitation process in patients after operative reconstruction of a proximal femur fracture. Therefore the pilot study pursued the following goals:

1. Conducting first measurements with the mobile motion measurement system eSHOE (as described in chapter 4) on patients after operative reconstruction of a proximal femur fracture. For that purpose certain standardized and clinically established assessments were carried out with the patients, while they were wearing eSHOE's instrumented insoles. Among these assessments were

   a) the timed "up and go" test (TUG),
   b) the ten meter walk test (10MWT),
   c) the six minute walk test (6MWT),
   d) stair climbing (StC),
   e) a four meter meter walk test (4MWT), for the purpose of validation with another gait analysis system.

   All of these assessments are standard features of the rehabilitation process at the study location. It will be analysed whether a basic analysis of the eSHOE data, collected from the 10MWT, allows the determination of quality and variance of the eSHOE data. For that purpose it has to be searched / we are searching for recurring patterns in the data, since walking is a cyclic process.

2. For the validation with another standard gait analysis system – GAITRite$^{®}$ – the 10MWT had to be downgraded to a test over only four meters. The spatial conditions of the room, where the GAITRite$^{®}$ system is kept, made this restriction necessary. The analysis and comparison of the data from both systems allow a comparison of the temporal measurement results.

3. Development of a surrogate parameter for the symmetry or asymmetry of the patients gait on the basis of the results from 1. Gait symmetry, according to medical knowledge (references!!), represents the quality of the sequence of movement while walking. Based on a series of measurements (per person) during the rehabilitation it is possible to deduce (infer) the extent of which a person has regained his/her ambulatory ability. In terms of temporal parameters of human gait asymmetry means a difference in the duration of the stance phase in the affected leg compared to the stance phase duration of the not-affected leg. The swing phases of both legs are affected accordingly. In order to make a statement about the progression of the gait parameters over time, it has to be established that it is possible to detect (relevant) changes in the eSHOE data from periodic measurements in a patient.

   - Changes over time in the gait symmetry can also be detected in the kinematic parameters of eSHOE.

- Patient gait data will be compared to a group of healthy individuals.

4. It hast to be evaluated whether the detectable changes in the eSHOE data are in conformity with the medical statements on the rehabilitation status.

   - The data of the control group makes up another target value. It is expected that the values of the movement data from the patient group will approximate the values of the control group over time. The course or the success of the rehabilitation progress can be estimated from a series of measurements in the patients.

5. Stair climbing will be examined for repeatable and reproducible patterns and also, if feasible, for changes related to the therapy / rehabilitation progress. Furthermore it will be analyzed if there is a dependency or correlation between the progress in symmetry and the progress in stair climbing parameters

6. The study also serves the purpose of generating (statistically recordable) hypotheses for a follow-up project.

7. Based on the results/insights from quality and distribution a concrete sample size estimate for a follow-up project shall be made possible.

Form of the study

The study design is that of a prospective study with exploratory evaluation. So, in essence, it is a mixture of feasibility and exploratory study. The goals were to introduce a new measurement tool (eSHOE) into everyday procedures in a clinical setting and thereby to evaluate this tool against an well-established system as a reference. A pilot study was necessary because there was little to none data available on the variance of the data delivered by eSHOE, especially concerning pathological gait data from patients. Therefore, it wasn't possible to determine the sample size beforehand with adequate accuracy in order to achieve statistically significant results. Another research goal of this study was the development of methods to calculate a surrogate parameter for gait symmetry.

Limitations (of the study)

The selected circle of elderly people with hip fracture who were involved in the study is still a very heterogeneous one, concerning their physical abilities. This means that the gathered data might exhibit a big variance. One possibility to meet this limitation is to view each test subject as a separate unit.

Study workflow

All subjects underwent/performed a set of geriatric assessment tests, while wearing a pair of eSHOE insoles. These tests were selected in close cooperation with physicians from the Sophienspital, a geriatric hospital in Vienna. For the senior citizens the test battery included a timed "up and go" test (TUG), a 10-meter walk test (10MWT), stair climbing

and a 6-minute walk test (6MWT). Each subject performed two to three repetitions of each test (on the same day), depending on its type. Data from the 10MWT test was utilized to collect standard gait data via the insoles' sensors of straight and level walking (as an example shows in fig. 5.2).

The first series of pre-clinical trials was conducted at the premises of the local senior citizen center of the municipality of Schwechat, Lower Austria. These tests served the purpose of properly testing of the eSHOE prototypes in real life and to gather the data necessary for the gait parameter detection algorithms.

5.1.2 Study population

Patients (PAT)

Inclusion Criteria:

- Patients, who are older than 60 years and who have been admitted to SMZ Sophienspital as an in-patient for remobilisation after a proximal low trauma fracture of the femur
- Operative stabilization not older than four weeks
- Singular fracture
- Cognition inconspicuous, corresponding to age with a mini mental state examination (MMSE) score of >= 27 and a clock test score of >= 7 [Folstein 1975]

Exclusion Criteria:

- Fracture unstable under load ("belastungsinstabil")
- Multiple fractures or periprosthetic fractures
- Patient does not wish to participate in the evaluation of the rehabilitation process via eSHOE
- Restriction of the ability to participate in rehabilitation on the basis of internistic or neurological accompanying diseases
- serious orthopedic problems in the lower extremities, e.g.: gonarthrosis, coxarthrosis, malalignment of the foot
- Amputations

Healthy subjects (CTRL, REF)

Inclusion Criteria:

- Persons, older than 60 years, who have agreed to participate in the study
- Cognition inconspicuous, corresponding to age: MMSE >= 27, clock test >= 7

Exclusion Criteria:

- Diseases of the musculoskeletal system, which affect walking/gait
- Neurological diseases, which affect walking/gait
- General gait pathologies
- Pain, which affects the sequence of movements during walking
- Medication, which affects walking/gait
- Serious orthopedic problems in the lower extremities, e.g.: gonarthrosis, coxarthrosis, malalignment of the foot
- Amputations

Number of subjects

20 subjects were included into the study, ten healthy subjects with unimpaired gait and ten patients after surgical treatment of a hip fracture (see chapter 2, section 2.3). The members of the control group with the healthy subjects ("CTRL") all were employees of the hospital at that time, who volunteered to participate in the study. Three physicians, who are specialised in physical medicine and rehabilitation, were responsible for medical supervision including the recruitment of the subjects for the patient group ("PAT").

Characteristics	REF	PAT	VAL
n	12	11	12
Gender (m / f)	6 / 6	0 / 11	1 / 11
Age (years)	73.2 ± 8.3	78.4 ± 7.7	40.78 ± 9.1
Height (cm)	168.5 ± 9.2	158.5 ± 2.8	168.0 ± 4.9
Weight (kg)	76.6 ± 15.1	56.9 ± 7.6	56.9 ± 7.6
BMI	26.8 ± 3.7	22.0 ± 3.5	23.7 ± 4.5

Table 5.2: Demographic and anthropometric characteristics of all subjects.

5.1.3 Ethical aspects

Patient information and informed consent forms

Informative material for patients and relatives were prepared as well as the necessary informed consent forms:

1. **Information for study groups (patients and healthy subjects)**
   In close cooperation with the responsible medical personnel of the SMZ Sophienspital we designed an informed consent form (ICF), which patients as well as healthy subjects had to sign. This ICF covers the following content:

   - Fundamental information about the study,
   - Possible sources of danger,
   - Handling of collected data (personal, medical, technical),
   - Exploitation rights, e.g.: pictures in publications,
   - Possibility to leave/quit/withdraw from the study at any time.

   Patients and healthy subjects were informed about the study and the above mentioned topics in an initial interview, prior to the start of the measurements. Measurements and data collections were only permitted after the informed consent form had been signed.

2. **Information for relatives**
   We also provided an information sheet, where the basic facts about the project eSHOE and the study itself have been recorded. Additionally the medical personnel and I offered the possibility for a one-to-one conversation in order to release fears and to silence scruples.

Potential problems and complications

- Not taking oportunity of leaving the study by the patient,
- Fear of intrusion on privacy,
- Mental overload.

Data security

Only the clinical investigators and their co-workers had access to sensitive data, where patients' names are mentioned (personal data). Furthermore, in order to verify the correctness of the study's records, representatives from national and international health authorities or from the responsible ethics committee can get access to this data. These persons are subject to a statutory obligation to maintain secrecy.

Data will be distributed for (strictly) scientific reasons only and in encrypted (indirectly individual-related) or non-personal (anonymized) form, guaranteeing that subjects' names will never be mentioned. The clinical investigators and their co-workers are subject to the regulations of the Austrian data privacy act (*Österreichisches Datenschutzgesetzes*

2000). In case one or more subjects choose to withdraw their consent the participation in the study ends immediately and no more data will be collected. For a period of time defined by law, due to legal requirements with regard to documentation (medical device directive), authorized personnel who are obliged to maintain confidentiality can get permission to inspect personal data for verification purposes.

Study cancellation

The study itself does not influence the treatment or further care of the patients. However, each subject can withdraw his or her willingness to participate at any time and without reason. Possible potential reasons for dropout of the study:

- insufficient or increased sensitivity of the sole of the foot and resulting insecurity, due to the new insole.
- increased fear of falling due to changes in the feeling of walking.
- stress or discomfort because of the participation of other persons in the personal therapy process.

Safety issues

The patients' personal safety was not in danger during this study, because the routinely carried out procedures had not been changed due to the study. One conceivable risk, resulting from wearing the eSHOE insoles is the following: a fall on the walk track, caused by stumbling due to limited sensitivity of the sole of the feet. That risk could be classified as "minimal", because eSHOE will be worn solely when patients are accompanied by a therapist or physician or both.

Therapy safety

The study doesn't change or influence the course and goals of the rehabilitation process. Patients still use their assigned walking aids, if needed. The measurements take place in the familiar premises and during the whole procedure a therapist or physician will be present. The following measures will be taken, in case something goes wrong:

- provide a seating accommodation.
- immediate removal of the eSHOE insoles.
- notification of a physician.

Data management

Data storage was conducted as follows. Personal data was stored on a personal computer in a .xls file, including an unique identification number. Data from the case report form (CRF), including assessment results, was stored in an xls-file on a second computer. There also the eSHOE measurement data was stored in the form of binary coded files.

For unambiguous assignment of the datasets to the test subjects only the identification number was used on this PC and never the names of the subjects.

5.2 Detection of gait cycle patterns

This section focuses on description of the methods for the detection of sensor- and axes-specific gait cycle patterns.

For the automated recognition of gait cycles it was necessary to determine standard patterns of sensor data that occurs during a gait cycle. The algorithm(s) manage to segment data sequences from straight (ahead) walking into single gait cycles and "learn", cycle by cycle, the pattern of an "ordinary" cycle. The data gathered by the eSHOE insoles during the 10MWT of the healthy elderly reference group (REF) are the basis for the extraction of an "ordinary" gait cycle pattern. Accuracy and reliability of the extracted gait cycle patterns were determined by manual comparison (count) of the amount of obtainable gait cycles from all measurements in the video data. Furthermore, the application of feature extraction allows the detection of distinct events within these patterns, e.g. "initial contact", "toeoff", "stride time" and "stance phase duration".

Subsequently, feature extraction algorithms were applied on these segmented cycles in order to detect basic gait events, like initial contact and toe-off. The initial contact (IC), which is the first contact of the foot with the ground, was best detectable from the pressure sensors underneath the heel and the accelerometer along the anterior-posterior axis. The toe-off (TO), representing the last contact of the foot with the floor, provided the most significant patterns in angular velocity data around the medial-lateral axis, the data from the pressure sensor beneath the big toe and foot's angle data in the sagittal plane. Using these two basic events (IC and TO) as trigger in all cycles, it was possible to determine the following standard gait parameters:

- stride time,
- stance phase duration,
- swing phase duration,
- step time,
- single support time,
- initial double support time,
- terminal double support time and
- cadence.

The main principle on which the analyses and algorithms are based is that sensors attached to the feet during (straight) walking are producing periodic signals.

The approach of this thesis was to use the cyclic principle of gait in order to automatically detect recurring patterns in the sensor data. Figure 5.2 shows a 15-second-long set with sample, data which was recorded during a walk of 18 steps in a straight line. It contains
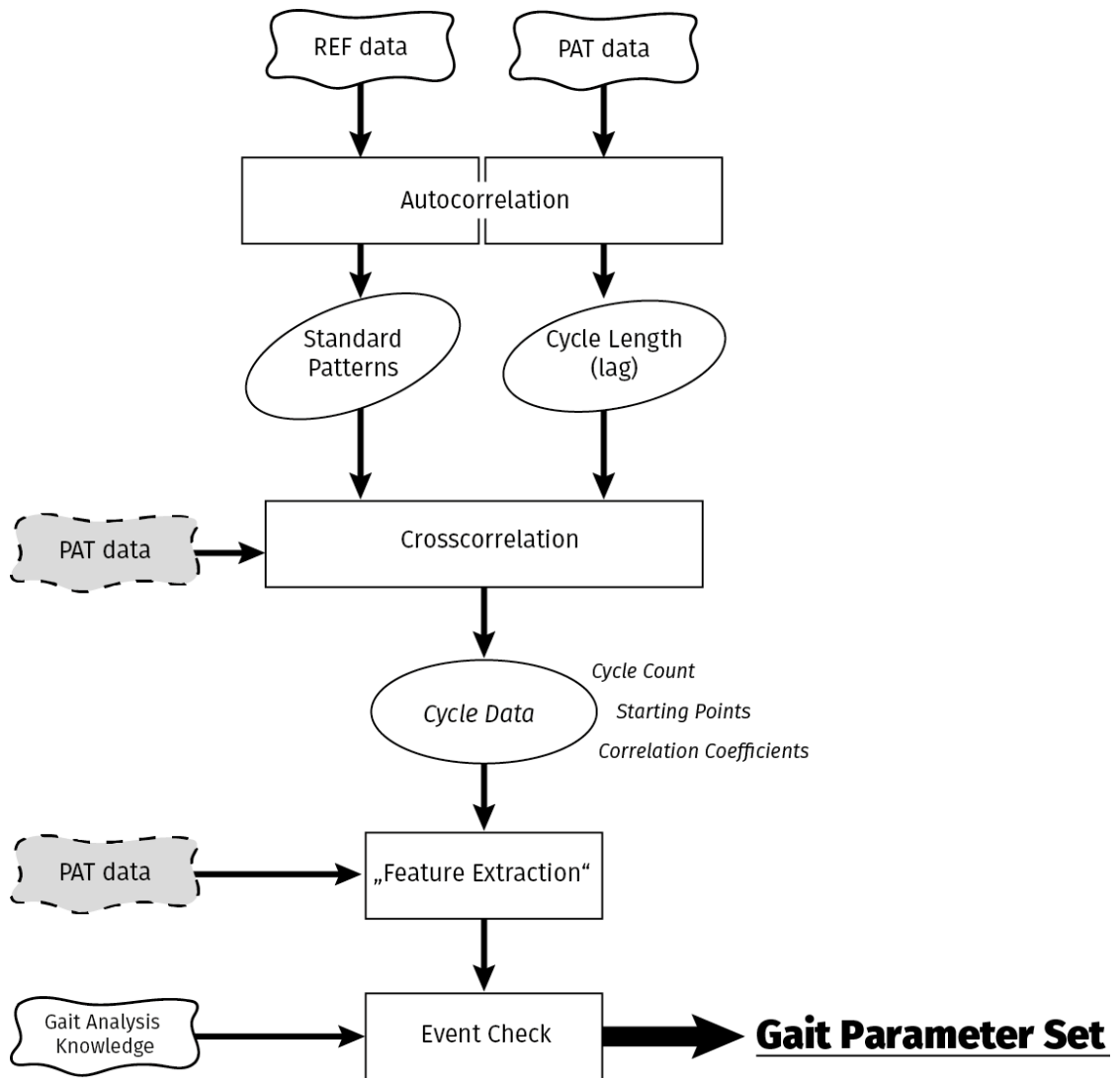
Figure 5.1: FLOWCHART - algorithm overview.

(raw) data from all sensors of one eSHOE insole. On the first glance periodic patterns can be identified in the data. All signals have nine periods, because 18 steps (of two feet) result in nine strides for each foot. Closer examination, however, shows that some sensors, more specifically, some sensor axes, provide better reproducible signal patterns than others. While walking straight ahead those axes from the motion sensors in walking direction, e.g. anterior/posterior acceleration (ACC-Y) and medial/lateral angular rate (GYRO-X) delivered the best signals. In the data from the pressure sensors, all four provide decent results, but heel and toe sensors stand out. In the beginning the data was analyzed visually and checked for periodic patterns and it was tried to identify well-known gait events in the data sets. Most significantly, "heel strike" or "initial contact" and "toe off" or "last contact". These two are also the defining events to separate the gait cycle into "stance phase" and "swing phase". A detailed description of gait analysis and its parameters was already given in chapter 3, subsection 2.2. Their automated detection is described in detail in the next section 5.3.

5.2.1 Gait cycle segmentation

The separation of the (basic) data into gait cycles can be achieved by (several) different pattern recognition methods. Autocorrelation has shown good applicability in studies also dealing with accelerometer data used for gait event identification [Moe-Nilssen and Helbostad, 2004, Tura et al., 2010]. Moe-Nilssen and Tura used autocorrelation for the determination of gait symmetry and regularity, based on signals from an accelerometer mounted on the subject's trunk.

Autocorrelation calculates the correlation of a signal with itself while the (copy of the) signal is shifted (sample by sample) to the right.

$$Ad(m) = \frac{1}{N - |m|} \sum_{i=1}^{N-|m|} x_i * x_{i+m}. \tag{5.1}$$

In equation 5.1 N represents the number of samples and m is the time lag expressed as the number of samples.

Figure 5.3 depicts a sample of autocorrelation data, calculated from (eSHOE) pitch angle data. The x-axis represents the time (segmented into samples, at a data rate of 200 Hz) and the y-axes represent (1) the angle in degrees and (2) the correlation (coefficient) between the signal with itself. The distance between the peaks in the autocorrelation function (ACF) is the so called time shift or time lag. The first peak exhibits an amplitude of 1, since that represents the moment, when the signal "overlaps" itself (perfectly) and, therefore, has a correlation of 1. By detecting the following two peaks, along with their distance (lag), gait characteristics like stride time and symmetry can be deduced. The distance on the x-axis between the very first and the second (highest) peak of the autocorrelation function in fig. 5.3, which is located at 334 samples or 1.67 seconds, represents the mean stride time duration.

Accelerometer
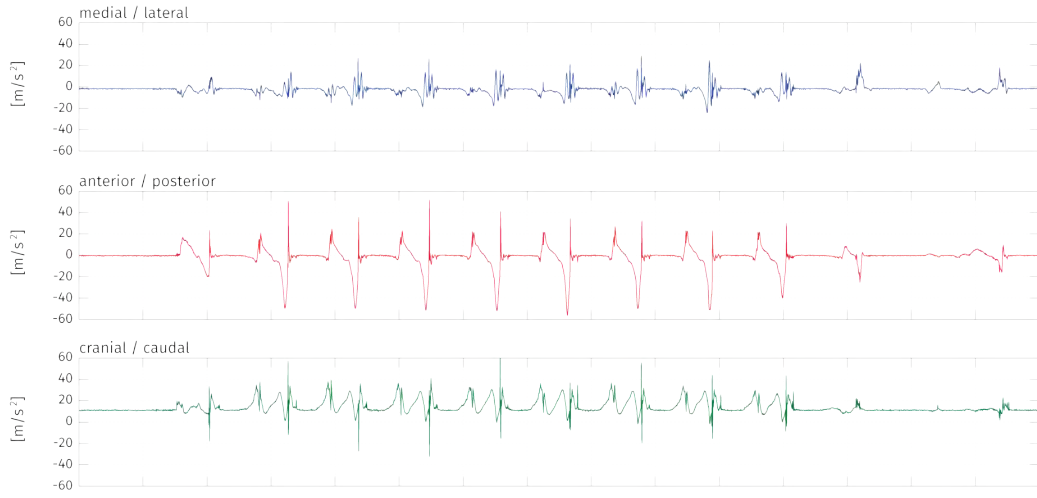
Gyroscope
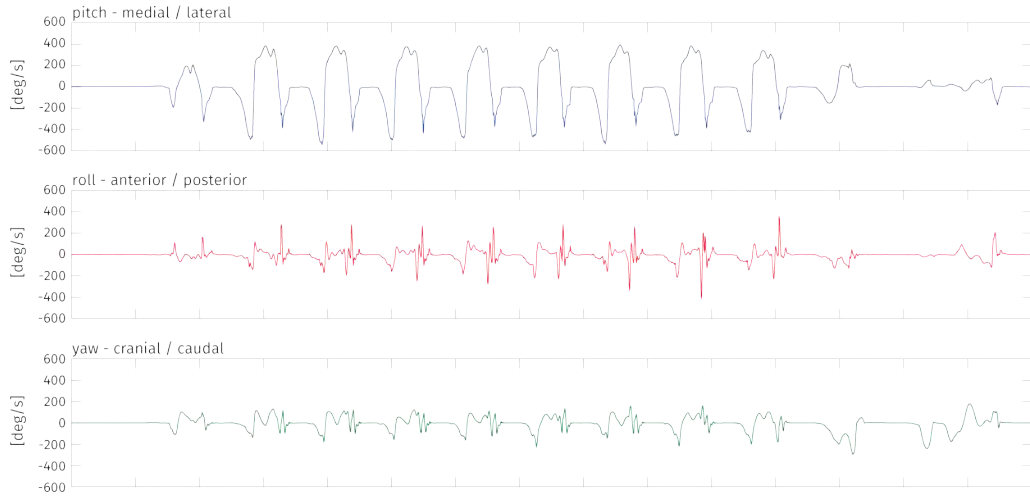
Force Sensitive Resistors / Pressure Sensors

Time [sec]

100
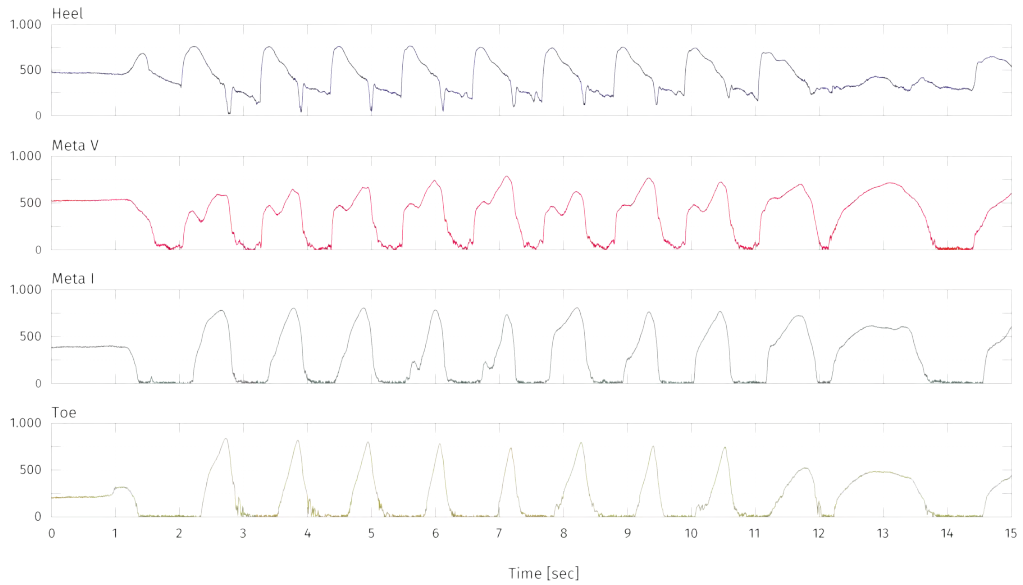
Figure 5.2: Sample data from one eSHOE insole. The data was collected over a period of 15 seconds and contains nine gait cycles.
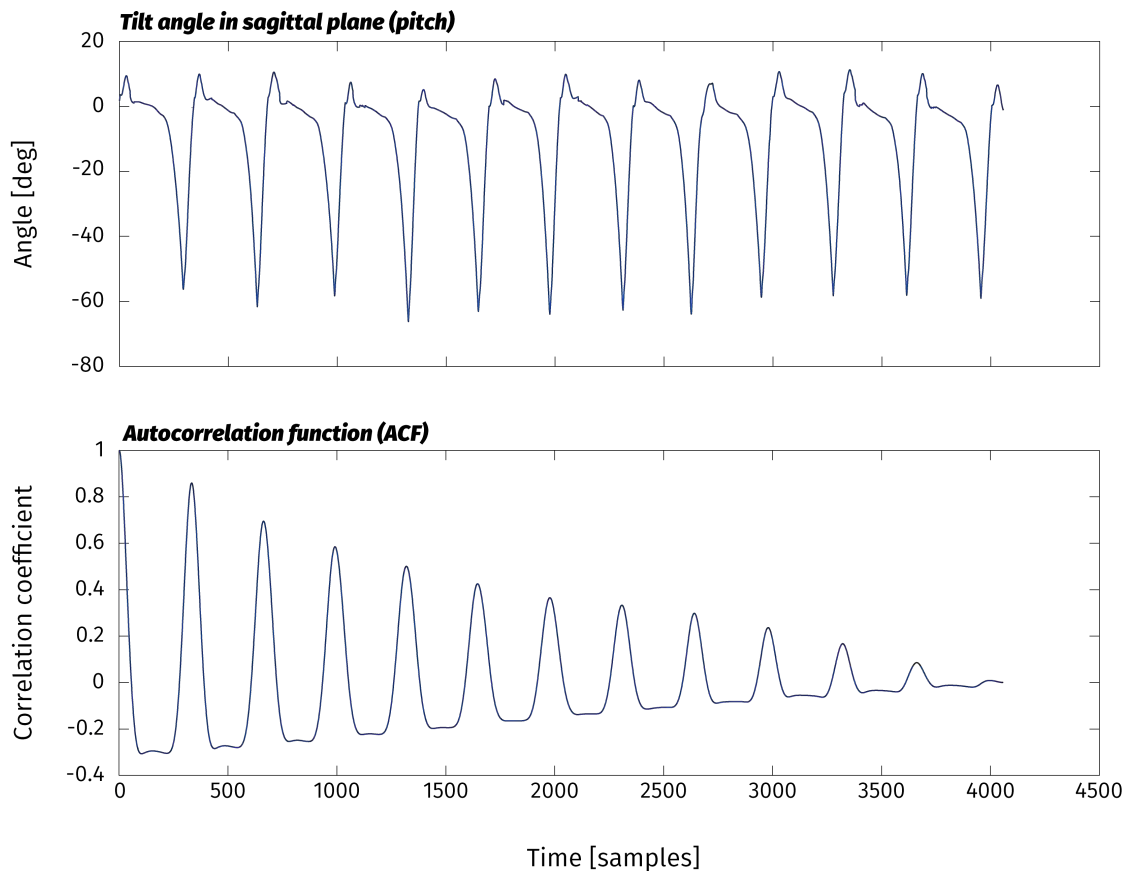
Figure 5.3: Illustration of the tilt angle (pitch) in sagittal plane (top) and the resulting the ACF; Correlation maximum (dash-dotted line) at a lag of 334 samples or 1.67 sec (bottom).

5.2.2 Generating standard patterns (pattern fitting)

Inter- and intra-subject gait variabilities are (major) issues affecting the detection of gait cycles. There are slight variations in everybody's gait, even during one and the same trial. The variations become more significant when different trials are considered. And they increase even further as soon as the trials are performed at different walking speeds. Variations between different subjects can be even bigger. All this means that the gait cycle duration, especially as it is approximated by the ACF's mean lag length, is not a static/fixed parameter. It is subject to fluctuations and, therefore, inaccurate. The algorithm, developed in the course of this thesis, takes these (above) considerations into account and tackles them as follows.

As described earlier, the autocorrelation function computes (a mean value for) the so called *lag (length)* parameter. In the case of (our) data, which was collected during straight ahead walking, this lag length represents the average duration of one gait cycle.

The time span defined by this parameter, is used to find the first (complete) gait cycle in a data sequence of straight ahead walking. This first cycle is then cut out and used as reference cycle. In the next step the algorithm checks, if there are more gait cycles left in the data sequence. In case there are, the next cycle is being cut out and the two cycles, reference and current, are compared. For this comparison the two signals are being put on top of each other and the correlation coefficient is calculated.

After that, the algorithm tries to maximize the correlation by adjusting the (length of the) current cycle. During these adjustments the signal is either compressed or expanded. Compressing the signal means using the segmented gait cycle with the defined lag-length and adding one data point of the original data to the end or beginning of the gait cycle. The current cycle now is one frame longer than the reference cycle. Then it is interpolated with the length of the reference cycle, hence, the signal is compressed. Similarly, during the expansion of the signal, the algorithm subtracts one data point at the end or beginning of the current cycle. The interpolation then expands the signal to the original lag-length.

The pattern fitting methods are applied until the maximum correlation is reached (maximum trials = 5). Once this is the case and the maximum correlation is higher than 0.7, the current cycle is added to the reference cycle and the average is calculated. These steps are repeated until the data sequence is out of cycles.

The algorithm is also described in the form of a flow chart in fig. 5.6. the process of the pattern fitting is illustrated in fig. 5.4 and 5.4 with sample data from the gyroscope (angular rate around the medial/lateral axis). As mentioned before, during expansion and compression, the correlation coefficient between the currently observed gait cycle and the reference cycle is computed. In order to be considered valid the correlation coefficient must reach the threshold of 0.7. As soon as a local maximum in the correlation is found, both cycles are being averaged (and a new reference cylce is generated). In that process, by "adding" more and more cycles to the reference, the algorithm creates a generic cycle pattern. The flowchart in fig. 5.6 depicts the general function of the algorithm.

5.2.3   Finding gait cycle patterns in PAT data

The resulting patterns from the preceding subsection, which were generated from the data or the reference group (REF), are used in this next step to identify gait cycles in the measurement data of a group of hip fracture patients. For this identification to work, cross-correlation between the patterns and patient data is performed. To compensate for differing walking velocities the patterns lengths are adjusted to the lag-length (result of autocorrelation) of the measurement (data) in focus via interpolation.

The (interpolated) pattern is then shifted over the whole data sequence, sample by sample, while the correlation coefficient between pattern and data sequence is calculated and stored. This process continues until the end of the data sequence is reached. The result is an array (cross-) correlation coefficients.
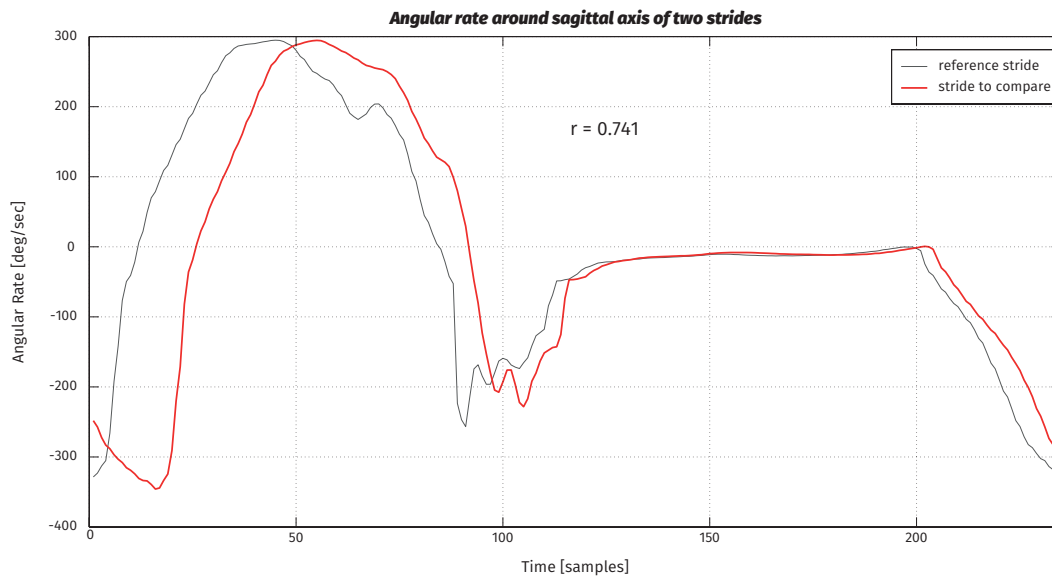
Figure 5.4: Illustration of two strides in angular velocity data around sagittal axis before further processing. Adopted from [Reich, 2013].
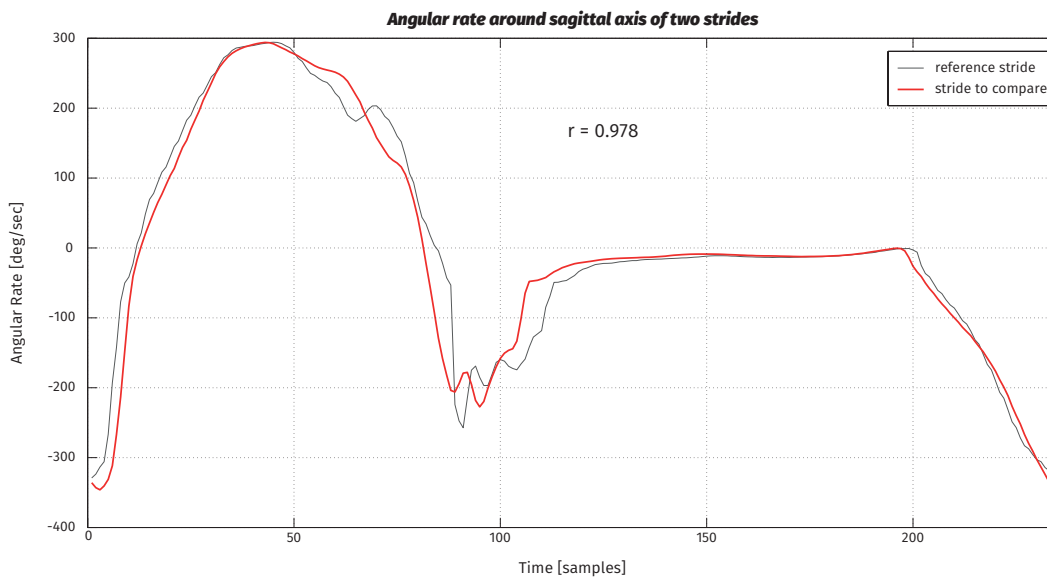
Figure 5.5: Illustration of two strides in angular velocity data around sagittal axis after further processing. The correlation R between the reference stride (blue) and the currently observed stride (red) is calculated and illustrated in the graph. Adopted from [Reich, 2013].
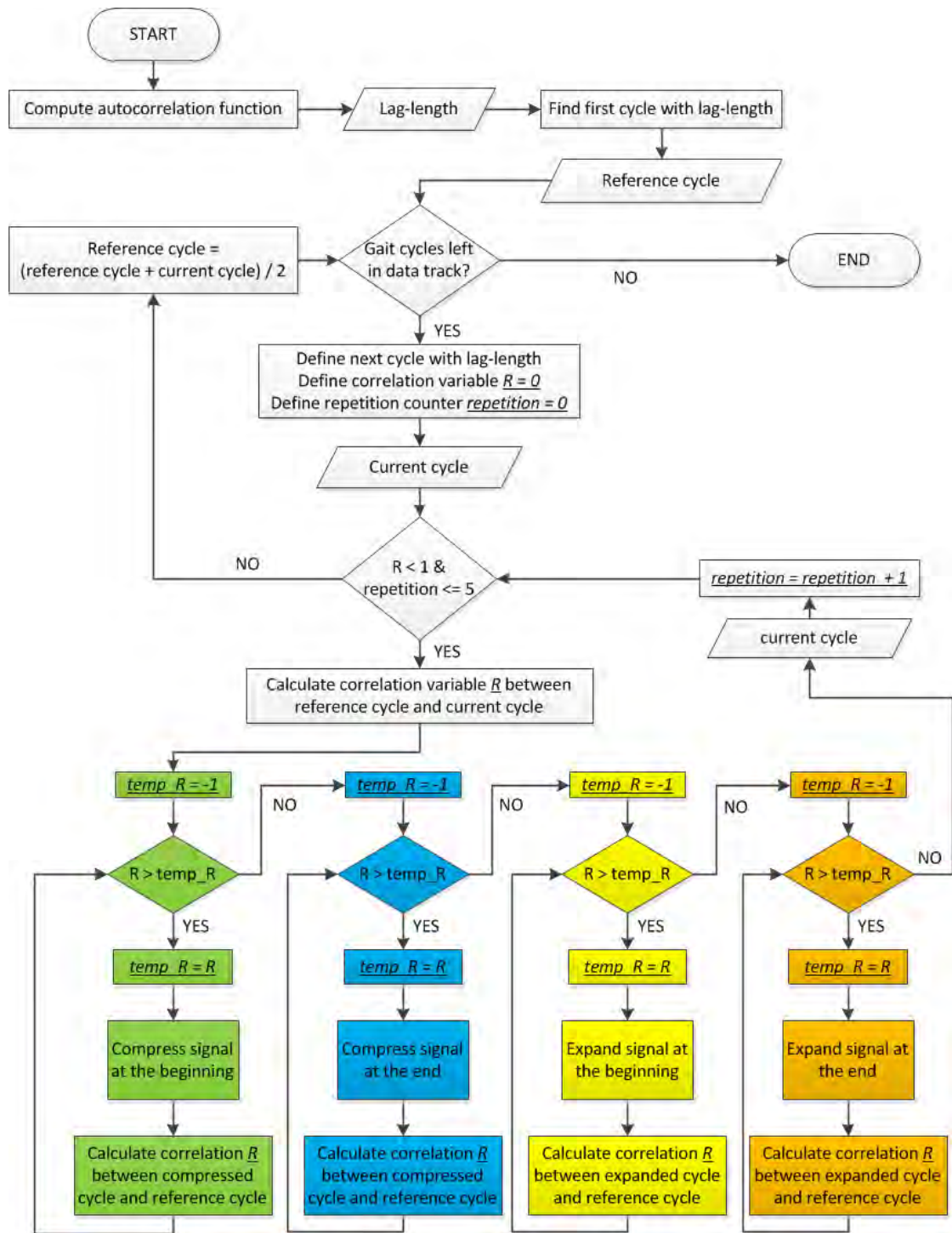
Figure 5.6: Methodology behind the learning process of the pattern recognition algorithm [Reich, 2013].
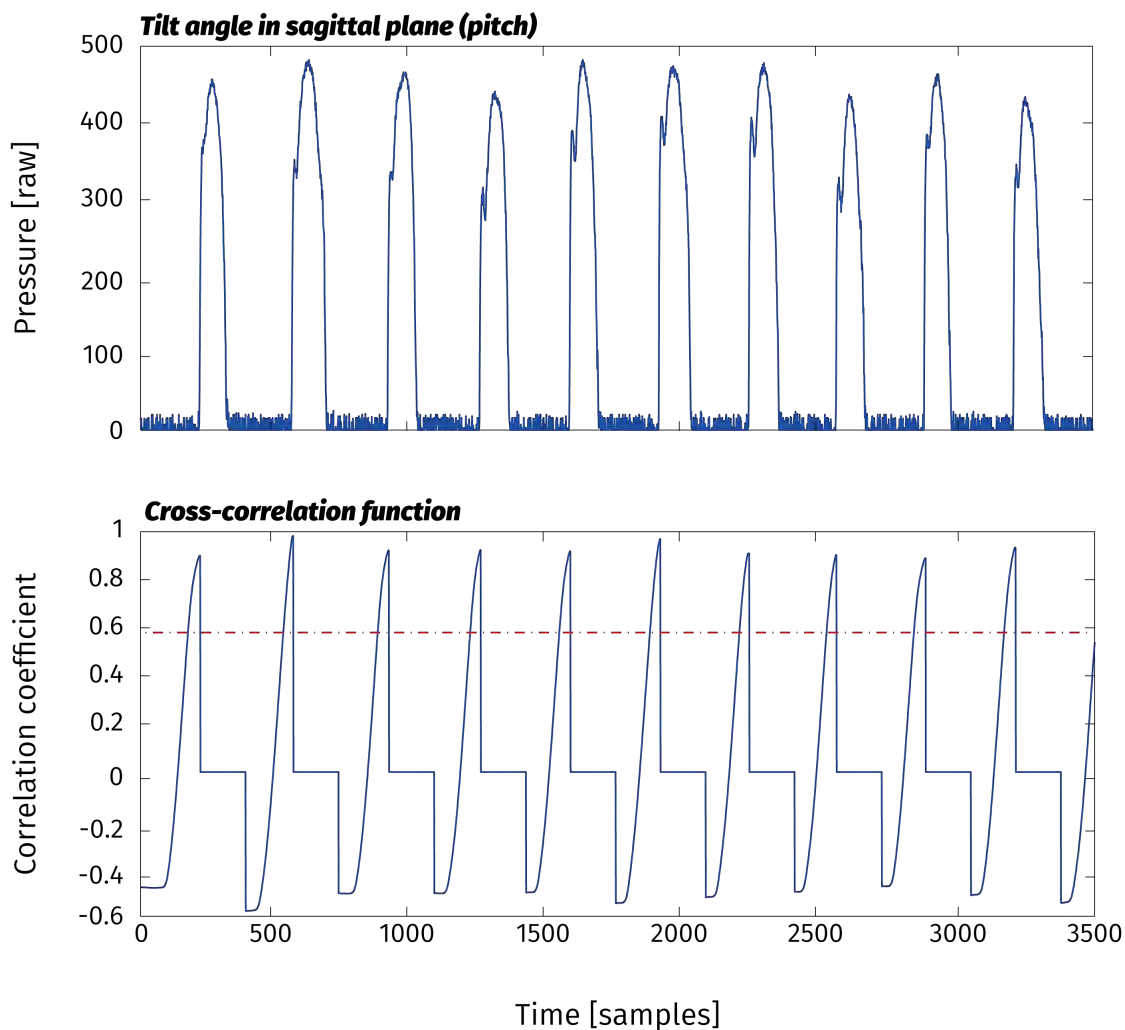
Figure 5.7: Illustration of the heel pressure (top) and the resulting the cross-correlation function. The minimum correlation threshold is indicated as dash-dotted line.

In a next step the algorithm checks the cross-correlation function for peaks of a specific height/amplitude. These peaks indicate the occurrence of the gait cycle pattern in the patient's data sequence. The time points when the peaks occur are stored and used for the segmentation into single gait cycles and they also play a role in the subsequent feature extraction (5.3).

As visual example, fig. 5.7 shows the cross-correlation function, which resulted from cross-correlating the heel pressure pattern with a heel pressure data sequence. In this graph eleven positive peaks can be identified (with the naked eye). Because they all exceed the pre-defined threshold (which is 0.5), eleven gait cycles could be found in this data sequence.

5.3 Extraction of basic gait events/features

As it was mentioned before (chapter 2, section 2.2), human gait has - when walking straight ahead at normal speed - a cyclic structure, with a certain chronology of specific events. These distinct events, which define human gait also appear in the eSHOE measurement data. Their extraction (from the segmented gait cycles) is the main focus of this section.

In her master thesis, Veronika David provided a proof of concept, that stable recognition of steps using heel sensor data is possible [David, 2012]. As distinct from this thesis, David only had one (healthy male) test subject, used ordinary walking shoes and the subject was walking on a treadmill. Two major differences: Due to regulations/specifications from the hospital (Sophienspital) our test subjects had to wear a pair of soft plastic clogs. Subjects were not walking on a treadmill, but on solid, tiled floor. Both conditions - soft plastic clogs and the treadmill - generate a certain dampening effect, which causes different conditions for feature extraction (e.g. the impact at initial contact is attenuated). Therefore, David's methods were not fully applicable to the data, resulting from this study, but her algorithms still formed a sound basis for further development. Her approach was extended and improved, e.g. through combining signals from different sensors (axes).

It proved to be a good basis, to build assumptions and conclusions from force sensitive resistor (FSR) data, since they have low(er) dimensionality (1D) and limited "action radius" (due to their size and functionality).

5.3.1 Initial contact (IC) / heel strike (HS)

Figure 5.8 shows a zoomed section of fig. 5.2, contains highlights of significant signal elements and illustrates the process of the first inspection. The focus is on pressure and accelerometer data and the identification of the initial contact. The graphs all show data from two and a half gait cycles. We now try to connect significant events occurring in both sensor types' data streams, rising edges, peaks, zero-crossings, etc. In this figure the two known event initial contact (IC) is highlighted via gray colored bars. Since this dataset contains three ICs there are three gray bars.

Detection via heel-pressure data

When a healthy subject walks a straight path at a normal speed (between 4 and 5 km/h), load is applied to the the pressure sensor beneath the heel, as soon as the subject's foot touches the ground. Load remains on the heel for a substantial part of the stance phase of the foot. After the initial contact load then "travels" a certain path along the sole of the foot. Starting from the heel, it continues on the lateral edge of the foot until it reaches the fifth metatarsal head. From there it crosses over to the medial edge of the sole, passing all five metatarsal heads, ending at the first head. After Meta I the next and last stop is the big toe, where the load finally subsides.
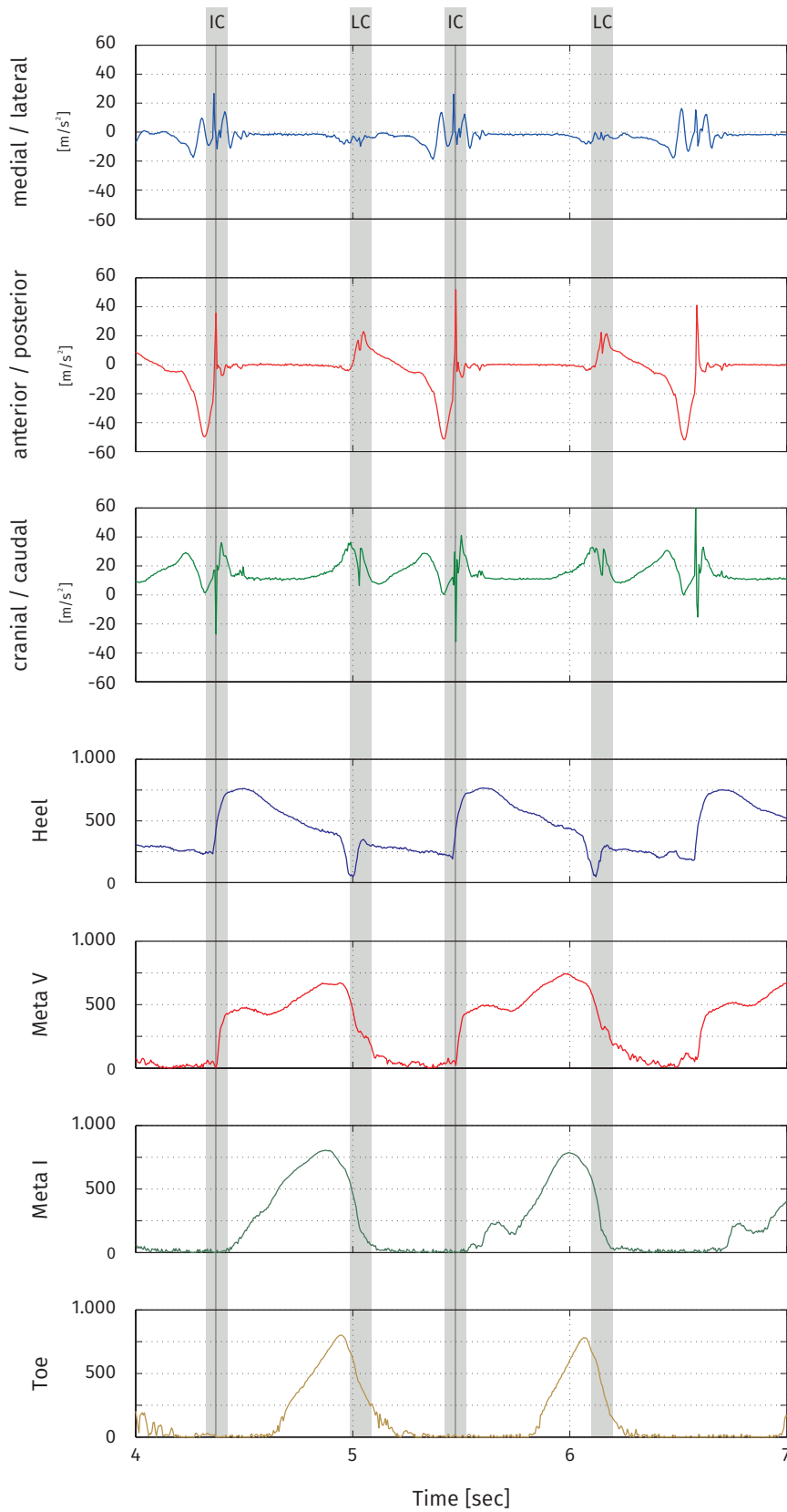
Figure 5.8: Zoomed-in eSHOE sample data.

107

This chronology can be well observed (three times in a row) in the dataset displayed in fig. 5.8. If measured at distinct points (on the sole of the foot) this process can also be pictured as a chronology of local loadings (with a distinct order). This knowledge in combination with the pressure data helps to identify certain gait events in other sensor data.

In order to detect the rising edge of the IC, the algorithm shifts a three sample wide window over the segmented gait cycle. Within this window three consecutive amplitude values are compared. A rising edge is detected, if the third value is larger than the second and the second is larger than the first. In order to avoid false positive detections, e.g. in the case of a noisy signal, the algorithms checks, if five samples later the amplitude still has a larger value (compared to the window). Are all these conditions fulfilled, an initial contact is successfully identified in the heel pressure data and the algorithm continues with the next segmented cycle.

Detection via sagittal acceleration data

Again, looking at fig. 5.8, at the same time as the rising edge occurs in the heel pressure data there are also distinct events in all three axes of the accelerometers. Within two samples (5 ms) spikes (of different amplitudes) occur on each sensor axis. These signal peaks are most pronounced in the anterior/posterior and the cranial/caudal axis. There is also a short spike in the medial/lateral axis, but it is surrounded by other signal artifacts,hence, less distinct and it occurs one sample (5 ms) before the other two peaks.

Fig. 5.9 provides a closer look on heel pressure (bottom) and anterior/posterior acceleration (top). There are now two cycles from both feet (left: blue, right: red) and black dash-dotted lines indicate the time point of the initial contacts. It becomes clear that at the same time as the heel pressure starts to rise there is a positive excitation in this (anterior/posterior) sensor axis, which represents the impact of the foot/heel on the floor. This event is preceded by a negative displacement of the signal, which concurs with the downward movement of the foot, immediately before the initial contact. Right after the positive peak there is a phase where the signal is at rest, which indicates the foot's resting state in the stance phase. Based on these conditions the second part of the algorithm for initial contact detection was developed.

To illustrate the conditions for initial contact detection in (anterior/posterior) acceleration data even better, fig. 5.10 shows data from one cycle of one foot, along with highlights for when the different conditions apply. The detection (algorithm) works as follows:

1. a three sample wide window is shifted over the sagittal acceleration data.
2. If there is a maximum in the middle of the window, a peak (the second peak) is detected.
   Again, like with the heel strike rising edge, such a excitation can also be the result of noise. To rule out this potential source of error, three more conditions have to be fulfilled to count a data point as initial contact.
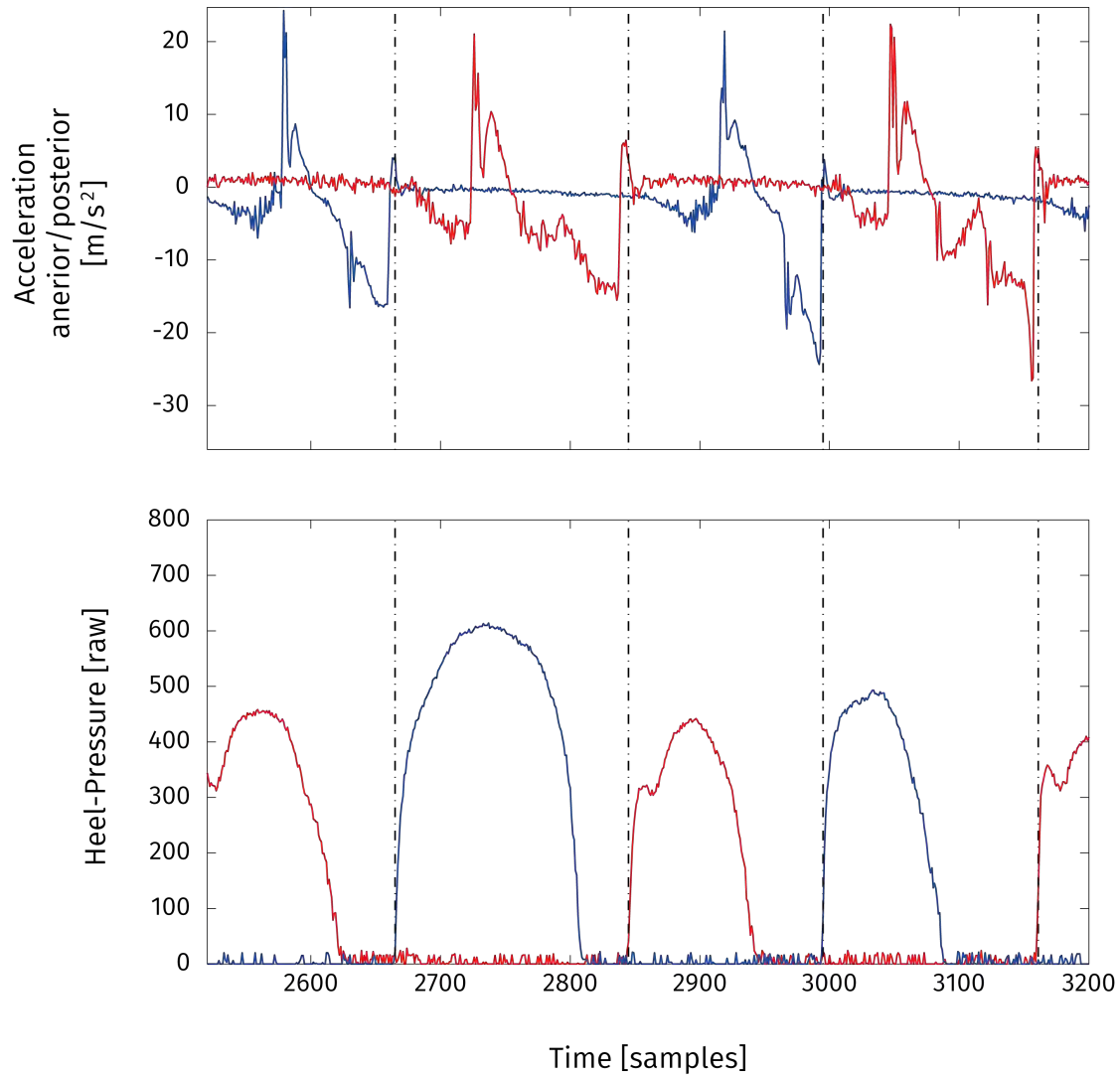
Figure 5.9: Sagittal acceleration data (top) and heel-pressure data (bottom) for left (blue) and right (red) foot during two strides; initial contact events marked as black dash-dotted lines. Adopted from [Reich, 2013].
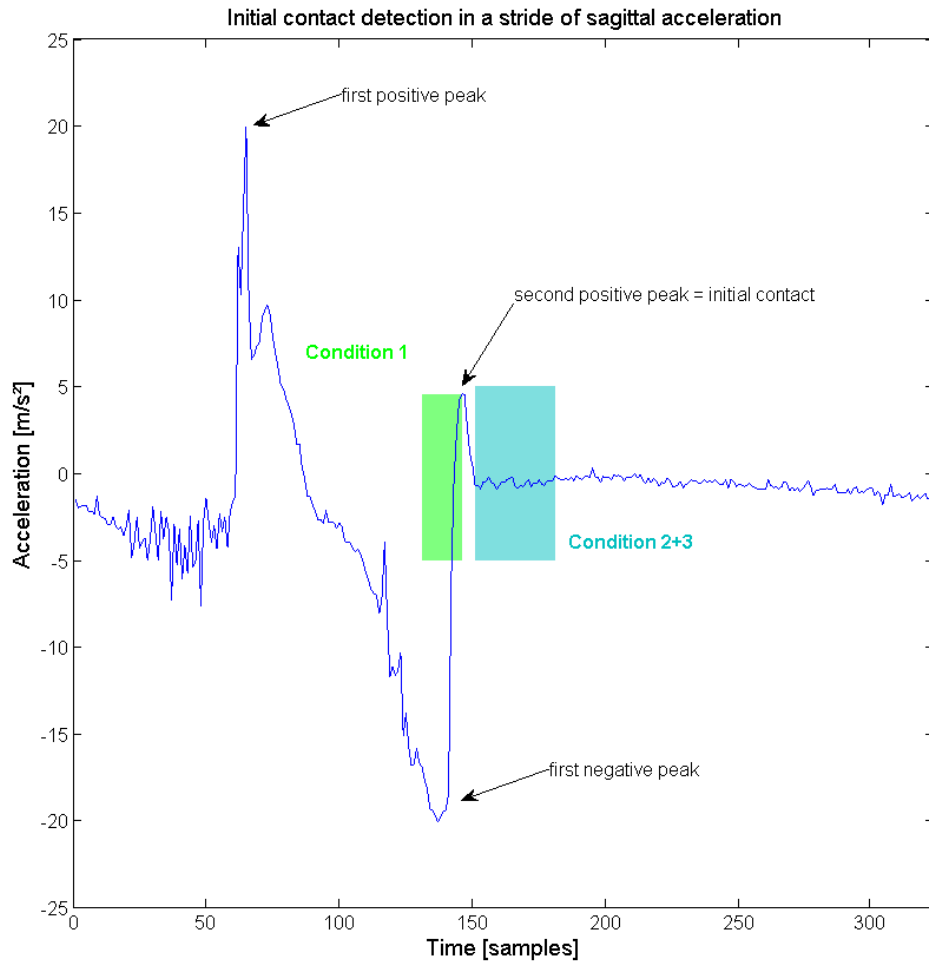
Figure 5.10: Illustration of the developed algorithm for initial contact detection in sagittal acceleration data. Adopted from [Reich, 2013].

a) **Condition 1**: In a time window of 15 frames, the amplitude of a data point before a peak must be lower than -5.
b) **Condition 2**: five samples after a peak, a window of 30 data points must have an amplitude lower than 5.
c) **Condition 3**: five samples after a peak, a window of 30 data points must have an amplitude higher than -5.

Finally, a routine was implemented, which checks for any deviances between the time points (for initial contact) delivered from heel pressure and from acceleration data. To produce a successfully detected initial contact, the rising edge of the heel-pressure and

the second positive peak of the sagittal acceleration have to occur within 10 samples (50 ms) of each other. Is that the case, the average (time) of both events is calculated and henceforth considered as the actual point of time the initial contact occurred. In case there is a larger difference (> 10 samples or > 50 ms) only the acceleration event is consulted as defining parameter. This is due to the fact that heel-pressure data more often showed lower quality (noise) than the sagittal acceleration data.

5.3.2 Last contact (LC) / toe-off (TO)

When looking at fig. 5.8, in toe pressure data the signal's elevation during the loading and unloading of the big toe can be observed. From the gait analysis theory it is known that after the push-off phase (where the pressure beneath the sole peaks for the last time) the foot leaves the ground. Therefore, the falling edge of the toe pressure was considered as possible trigger-event. But since the toe pressure has a rather long rising time (compared e.g. to the heel pressure) this signal was not suitable for the detection of the toe off event. Although, there are other (measurable) conditions of the feet, which could be consulted. For instance, it is also known that during the push-off phase the foot reaches its maximum plantar flexion and minimum inclination (relative to ground level). The inclination is something which is directly measurable through the eSHOE sensors. During the visual data inspection it was also discovered, that the zero-crossing of the angular velocity around the medial/lateral axis occurred at the same time as the inclination (pitch angle) minimum. Furthermore, synchronous to the above mentioned events, there are also falling edges in the metatarsal head data and there are minimal vibrations in the anterior/posterior as well as in the cranial/caudal acceleration.

Detection via tilt angle data

The "hypothesis" from above, that the tilt angle minimum represents the toe-off event can further be endorsed by the comparison of tilt angle, angular rate and toe pressure data. It can be observes that angle minimum and angular rate zero-crossing also coincide with the falling edge of toe pressure, as depicted in fig. 5.11. The assumption was confirmed by examination of eSHOE data and the corresponding synchronized video.
 Since angle data has very little noise and it was possible to extract the negative peaks simply with the built-in Matlab function "findpeaks". Its input parameters were adjusted to a minimum distance of 50 samples (or 250 ms at 200 Hz) and a minimum height (or amplitude) of 20 (degrees) was set.
It can be observed in fig. 5.11, that the signal's course includes a large negative displacement to ∼-60° followed by an increase in amplitude to ∼10°. Thereafter the signal settles to a period of rest at ∼0 °. These absolute values are strongly dependent on the subject, but the (relative) course always remains the same (as long as there are no severe injuries). By design, findpeaks is only capable of finding positive peaks. Therefore, it was not directly applicable, because it was the negative displacements that we were after. So the input signal had to be inverted.
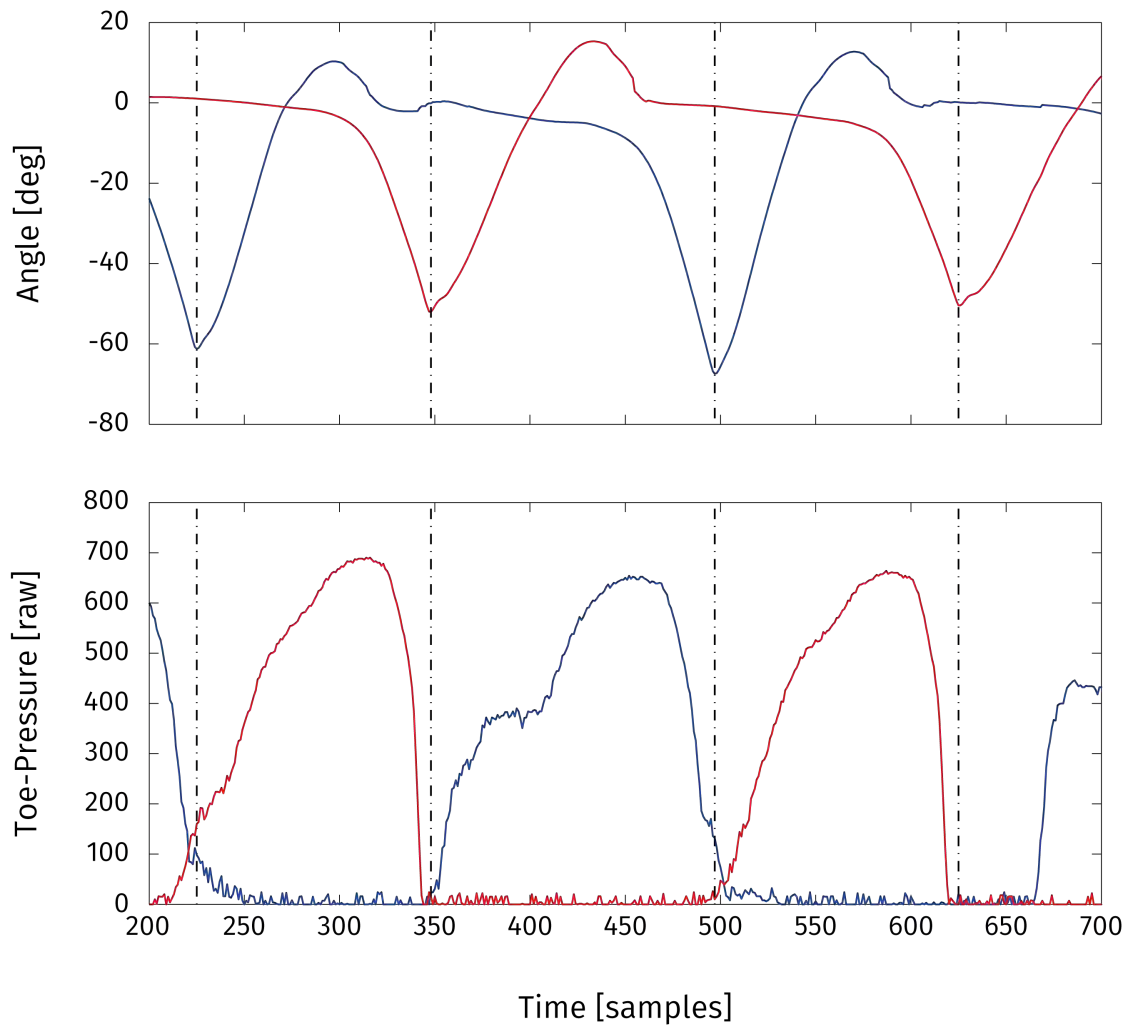
Figure 5.11: Last contact detection in two strides of tilt angle in sagittal plane (top) and the corresponding toe-pressure data (bottom); Data for left foot (blue) and right foot (red); Last contacts marked with black dash-dotted lines. Adopted from [Reich, 2013].

Detection via angular velocity data

Since the angle data provided very good reference points there was the assumption that angular velocity data might also hold viable information. In (normal) walking there is a lot of rotational movement (again, also indicated by the pitch angle) of the foot in the sagittal plane, which is detectable by gyroscopes. So angular velocity data around the medial/lateral axis was compared to pressure data an angle data, as shown in fig. 5.12. There it can be observed that at the time the toe-off events occur, according to the pitch angle and toe pressure, the angular velocity has a zero-crossing during a very steep signal edge.

Therefore, the following conditions were defined for automatic detection of this zero-crossing the following (algorithm):

1. **Condition 1**: The amplitude of the current sample must be lower than or equal to zero and the amplitude of the next sample must be higher than or equal to zero.
2. **Condition 2**: The amplitude of all five samples after the current data point must be higher than zero.
3. **Condition 3**: The amplitude of any of ten samples after the current sample must be higher than 20.
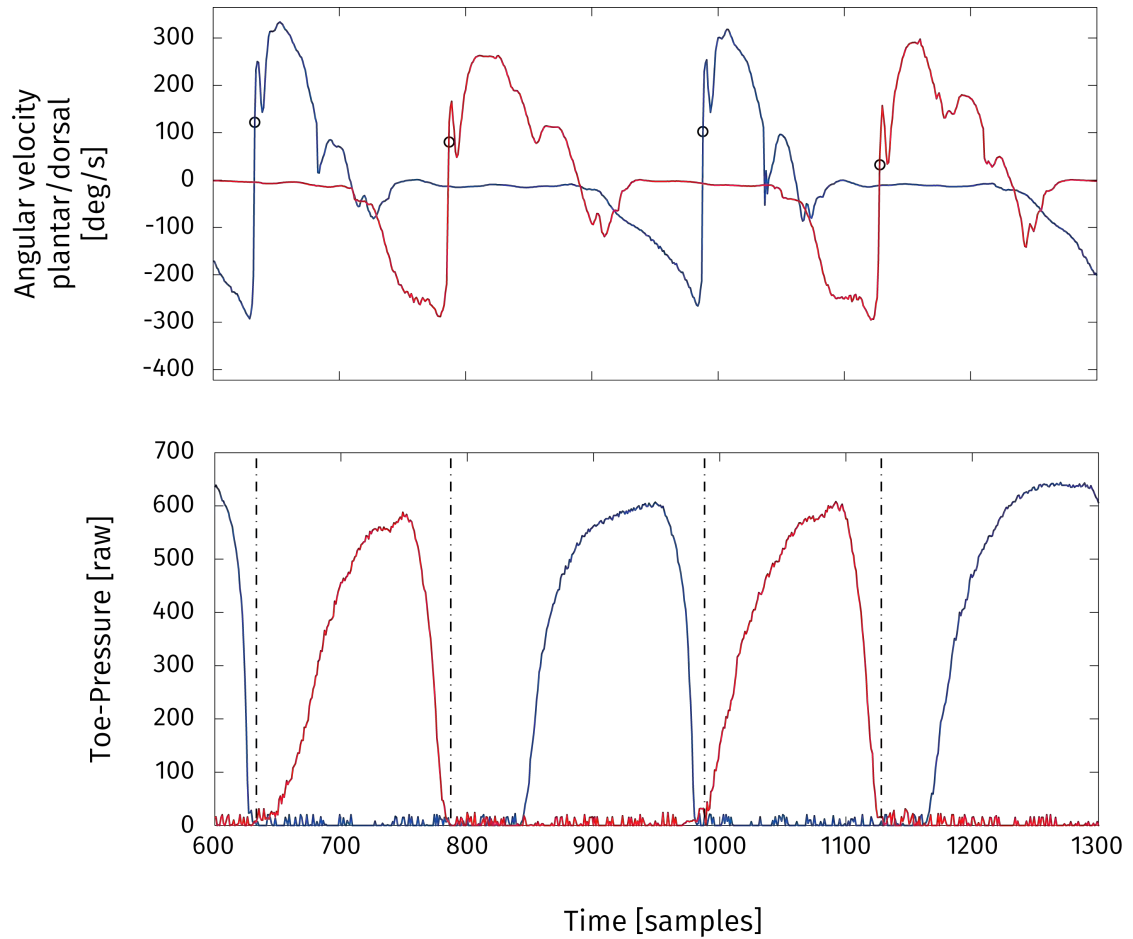
Figure 5.12: Last contact detection in two strides of angular velocity data around medial-lateral axis (top) and the corresponding toe-pressure data (bottom); Data for left foot (blue) and right foot (red); Last contacts marked with black circles (top) and dash-dotted lines (bottom). Adopted from [Reich, 2013].

5.4 Calculation of (indirect) gait parameters

There are, of course, more parameters of human gait than just initial contact (heel strike) and last contact (toe-off). For many/all of them these two events are the key to their definition. An overview was already given at the beginning of the thesis (chapter 3, section 2.2) in table 2.1 and fig. 2.4. However, all relevant parameters are described in detail in the following subsections. The analysis of these parameters (tracking over a longer period of time or comparison of different subjects) can help to make a statement about the quality of a person's gait or its development (after an injury).

As basis for further calculations, all detected IC and LCs events are stored into a matrix/vectors, where the data can easily be accessed by algorithms. Table 5.3 shows two vectors, one for the ICs and one for the LCs that are extracted and saved by the feature extraction algorithm.

Event #	IC occurrence [s]	LC occurrence [s]
1	0.30	0.95
2	1.40	2.00
3	2.45	3.20
4	3.60	4.00

Table 5.3: Sample vectors of initial and last contacts for one insole. Adopted from [Reich, 2013].

5.4.1 Stride Time (STR)

Stride Time (STR) is the time that elapses between two consecutive footfalls of the same foot. Since walking is a cyclic/periodic process, virtually any recurring gait event can be used as reference to calculate the stride or cycle time. For this study the initial contact was chosen, because it is the given convention to calculate stride time by it and the event is well-detectable within eSHOE data.

Based on the data presented before, namely vectors with the timepoints of the initial contact, stride time can be quite easily computed. The (time) difference between the single ICs is equal to the stride time. Within the algorithm a vector with ICs can simply by fed into a differentiation function and the stride times are returned. The sample results from this process, with input data from table 5.3 column two, can be seen in table 5.4.

Parameter #	Stride time [s]
1	1.10
2	1.05
3	1.15

Table 5.4: Calculation of the stride times from the arrays in table 5.3. Adopted from [Reich, 2013].

5.4.2 Stance phase and swing phase duration

Gait analysis experts state that one stride or one gait cycle is basically separated into two portions, the "stance phase" and the "swing phase" [Perry, 1992, Vaughan et al., 1992, Götz-Neumann, 2003].

Focusing on one leg, the stance phase is the weight bearing period of the gait cycle and the swing phase is the phase where the foot advances in walking direction. The stance phase is initiated by the same event the gait cycle itself is initiated, the first contact of the foot with the ground, the heel strike or initial contact. This weight bearing period of the gait cycle usually lasts for 60 to 65 % of the gait cycle. The stance phase ends as soon as the contact of the foot with the ground ceases, with the last contact (LC) or toe-off (TO). The time elapsed between IC and LC is being referred to as "stance phase duration", "stance time" or just "stance phase" (STA).

In case of healthy persons, the LC or TO is the moment when the big toe leaves the ground. With this event the swing phase begins, during which the foot is advancing in the walking direction. This phase takes 35 to 40 % of the gait cycle and is called "swing phase duration", "swing time" or just "swing phase" (SWI). It is concluded with the next initial contact of the same foot.

In this case now both columns (instead of just one) from table 5.3 are needed to generate stance phase as well as swing phase duration. Therefore, generally, stance time is calculated, according to equation 5.2, by subtracting IC(t) from LC(t) - of the same gait cycle - and swing time by subtracting LC(t) of the current gait cycle from IC(t+1) of the next gait cycle (equation 5.3).

$$Stance\ Phase(t)[s] = LC(t) - IC(t) \tag{5.2}$$

$$Swing\ Phase(t)[s] = IC(t+1) - LC(t) \tag{5.3}$$

This, of course, results in stance and swing time duration expressed in seconds. However, it is also customary to express both in percentage of a gait cycle. To achieve that, calculations according to the following equation are necessary.

Event #	stance time [s]	swing time [s]	stance [%]	swing [%]
1	0.65	0.45	59.1	40.9
2	0.60	0.45	57.1	42.9
3	0.75	0.40	65.2	34.8

Table 5.5: Results for stance and swing time, calculated from examples from table 5.3, expressed in time/seconds (columns 2 and 3) and in percent of gait cycle (columns 4 and 5). Adopted from [Reich, 2013].

Figure 5.13: initial contact (IC) extraction error. Visualization of extracted gait features in left insole data where one IC could not be extracted by the algorithm. Adopted from [Reich, 2013].

$$Stance\ Phase(t)[\%] = 100 * \frac{LC(t) - IC(t)}{Stride\ Time(t)} \tag{5.4}$$

$$Swing\ Phase(t)[\%] = 100 * \frac{IC(t+1) - LC(t)}{Stride\ Time(t)} \tag{5.5}$$

Applying equations 5.2 to 5.5 on data from table 5.3 result in stance and swing times presented in table 5.5.

There are cases when single gait events (IC or LC) cannot be successfully detected e.g. due to a higher noise level than usual. To give a tangible example fig. 5.13 illustrates such a scenario, where there are three strides (with three ICs and LCs). The algorithm successfully detects all LCs, but only the first and the last IC. Therefore one LC, namely the second, is missing and the third IC is considered to be the second. Such a case leads to an error in the subsequent stance and swing phase calculation. As counter measure, to avoid these kinds of errors as well as consequential errors, the algorithm contains two conditions. First the number of ICs and LCs are compared. Secondly, the chronological order is verified. Meaning that a sequence is considered valid if the events are occurring in an alternating fashion (e.g. IC, LC, IC, LC, ...). Only then the algorithm is able to calculate the corresponding subsequent parameters, such as stance phase and swing phase duration.

5.4.3 Double Support Time

Subsections 5.4.1 to 5.4.2 described parameters, where one leg/foot is in focus. However, there are also other characteristics which involve both feet. When focusing on both legs during a gait cycle there are a few more characteristics to be observed. During one stride (when walking at "normal" velocity) there are two periods (within the stance phase) when both feet are touching the ground at the same time. These are called Initial Double Support Time (IDS) and Terminal Double Support Time (TDS). Double Support describes the time span from heel contact of one footfall to toe-off of the opposite footfall. Therefore, when focussing on the right leg, Initial Double Support occurs from right heel contact of left toe-off and Terminal Double Support occurs from left heel strike to right toe-off (see fig. 2.4 as well as equations 5.6 and 5.7). Each double support phase lasts for $10 to 12$ % of the gait cycle.

$$IDS = LC_L - IC_R \tag{5.6}$$

$$TDS = LC_R - IC_L \tag{5.7}$$

$$IDS[\%] = 100 * \frac{LC_L - IC_R}{Stride\ Time} \tag{5.8}$$

$$TDS[\%] = 100 * \frac{LC_R - IC_L}{Stride\ Time} \tag{5.9}$$

5.4.4 Step Time

Step Time (STE) is the time elapsed from first contact of one foot to first contact of the opposite foot.

$$Step\ Time = IC_L - IC_R \tag{5.10}$$

5.4.5 Cadence

Cadence is defined as amount of steps per minute. The average cadence in grown-up individuals is 113 *steps per minute*. Women have a slightly larger cadence (117) than men (111) [Perry, 1992].

For the algorithm it is quite easy to compute cadence. The amount of steps equals the amount of initial contacts, which occur in the data of both insoles. The time span, during which these steps occur, is also calculated by using the time indices of first and last IC and subtracting the latter from the first.

5.5 Validation of spatio-temporal gait parameters

The validation measurements were performed in a separate room inside the hospital which is reserved for occupational therapy and GAITRite® evaluation (fig. 5.14). Due to hospital policy the subjects had to wear the eSHOE insoles inside a pair of plastic clogs. They were asked to walk over an eight-meter distance, including the six-meter walkway, at a comfortable speed for three trials. According to the measurement protocol data of both systems were gathered simultaneously and synchronized on the first initial contact of each walk. Due to the missing absolute time protocol of the eSHOE data, video recordings of the subjects' feet were used to support synchronization.

The version of GAITRite®, which was used in this study, is 4.6 m long with an active sensor area of 3.66 m in length and 0.61 m in width. This area contains 13, 824 pressure sensors, which are arranged in a grid pattern (288 × 48) with a spatial resolution of 0.0127 m (1.27 cm). The data from the sensors is sampled at a frequency of 60 Hz. The walkway is connected to a PC via the serial interface, where the spatial and temporal characteristics of gait are processed and stored by the GAITRite® software. One of the advantages of GAITRite® is that even gait with walking aids (e.g. including path and ground forces of a wheeled walker) can be analysed. GAITRite® proved to have good test-retest reliability [Menz et al., 2004, Bilney et al., 2003] as well as excellent agreement in comparison with the optical motion analysis system Vicon [Webster et al., 2005], which is the previously established standard. The measurement results have been analyzed primarily regarding their agreement. Methods used for these analyses can be found in the next subsection (5.5.1) and the corresponding results are located in section 6.2, subdivided into controls (subsection 6.2.1) and patients (subsection 6.2.1).

Other aspects of importance were eSHOE's "ability to distinguish" between healthy subjects and patients in terms of their gait parameters (in reference to GAITRite®). And also whether or not there is a detectable difference between the healthy leg and the affected leg among patients. Once again, methods are described within this section, group difference in 5.5.2 and leg difference in 5.5.3.

5.5.1 Analyses of agreement

Regarding agreement, scatterplots, histograms of the differences of both methods and the Bland-Altman analysis were used. Six gait parameters have been compared: stride time (STR), stance time (STA), swing time (SWI), step time (STE), initial double support time (IDS) and terminal double support time (TDS). Since the measurements were synchronized via video recordings, each stride could be compared separately.

The scatterplots and histograms are merely visual but effective methods for comparing measurement results of two devices. For the former the absolute results of GAITRite and eSHOE are plotted against each other, with GAIRite values on the x-axis and eSHOE values on the y-axis. Perfect agreement (which is practically impossible) would result in a straight line with a 45°slope. In practice, the result usually is a point cloud, scattered

Figure 5.14: The setup for the validation measurements inside the social medical center Sophienspital. The upper half shows one patient walking over the GAITRite® mat, while wearing a pair of eSHOE insoles. For synchronization of both systems a video of the patient's feet was recorded with a camera mounted onto a self-made cart. The lower half shows a schematic diagram of the measurement setup. The version of GAITRite® which was used in this study measured 460×61 *cm*, with an active sensor area of 366×61 *cm*. The part of the walkway without sensors is indicated by the shaded sections.

in proximity of the 45°reference line. The better the agreement, the smaller the deviation from the reference line.

In order to investigate the differences of the two systems further, the frequency distributions (for all parameters) have been visualized via histograms of the differences by applying equation 5.11 on each stride and grouping the results into certain intervals or "bins".

The Bland-Altman analysis finally allows also quantifiable results. Firstly, it comprises a plot of the differences between two methods on the y-axis (see equation 5.11) against their mean on the x-axis (see equation 5.12), which represents an approximation of the true value of a parameter. The plot further includes indicators (lines) for the mean difference ($\bar{d}$) and two times the standard deviation ($1.96 \times \sigma$), also called the "limits of agreement".

$$y(t) = GAITRite(t) - eSHOE(t) \tag{5.11}$$

$$x(t) = \frac{(GAITRite(t) - eSHOE(t))}{2} \tag{5.12}$$

Therefore, the resulting plot allows the investigation of a possible relationship between the measurement error and the true value. But it also enables the determination, whether or not 95 % of the differences are lying between the limits of agreements ($\bar{d} \pm 1.96 \times \sigma$). Due to the fact that two different measurement methods will practically never deliver identical results, the following two aspects can be investigated via Bland-Altman analysis: (1) how much one method is likely to differ from the other and (2) if the difference is insignificant - from a clinical point of view - both methods can be used interchangeably [Bland and Altman, 2010].

5.5.2 Differences between groups

The other aspect of interest was, whether the differences between healthy subjects and patients can be identified by GAITRite and eSHOE.

For that purpose, initially, all data have to be checked whether they are normally distributed or not. The outcome of these tests determine whether statistical tests of parametric or non-parametric nature have to be chosen for further analyses. For the determination of a normal distribution the Shapiro-Wilk test has been used [Shapiro and Wilk, 1965]. It provides a rather high *power* (also for smaller samples), compared to other tests. In case of a χ^2 distribution and with a sample size of only 20 it provides a power of 54 % in comparison to the D'Agostino test with a power of 29 %. [Seier, 2002]. By design the null hypothesis (H_0) of this test states that the analyzed sample exhibits a normal distribution and the alternative hypothesis (H_1) states that the sample has any other form of distribution. Since a proof of normally distributed data is needed, in this case H_0 is the desired statement.

Therefore, one has to take into account the *error of the second kind (type II error) β*. A type II error occurs, when the null hypothesis is not rejected, but is in fact false In order

Parameter	eSHOE		GAITRite	
	CTRL	PAT	CTRL	PAT
Stride Time	$2.49 \cdot 10^{-6}$	$2.40 \cdot 10^{-6}$	$1.22 \cdot 10^{-6}$	$1.90 \cdot 10^{-5}$
Stance Time	$5.45 \cdot 10^{-7}$	$1.27 \cdot 10^{-5}$	$6.96 \cdot 10^{-6}$	$6.65 \cdot 10^{-5}$
Swing Time	$1.70 \cdot 10^{-2}$	$1.72 \cdot 10^{-4}$	$2.08 \cdot 10^{-6}$	$6.54 \cdot 10^{-4}$
Step Time	$1.47 \cdot 10^{-5}$	$4.32 \cdot 10^{-4}$	$1.12 \cdot 10^{-6}$	$2.84 \cdot 10^{-5}$
Initial Double Support	$2.85 \cdot 10^{-5}$	$1.08 \cdot 10^{-3}$	$3.14 \cdot 10^{-5}$	$1.28 \cdot 10^{-4}$
Terminal Double Support	$3.89 \cdot 10^{-6}$	$2.66 \cdot 10^{-3}$	$2.52 \cdot 10^{-5}$	$3.90 \cdot 10^{-5}$

Table 5.6: Results from Shapiro-Wilk test (for normal distribution) from both groups: VAL and PAT, grouped in eSHOE and GAITRite data.

	> Median	< Median	Σ
Sample A	a	b	$a + b = N_A$
Sample B	c	d	$a + b = N_B$
Σ	$a + c$	$b + c$	N

Table 5.7: Fourfold table for the median test. It provides the necessary input variables for the subsequent calculation of the χ^2 test statistic (see equ. 5.13).

to (indirectly) minimize this error, the level of significance can be set to a "higher" level, such as $\alpha = 0.1$.

All parameters in both groups and from both measurement devices show p-values below the level of significance $\alpha = 0.1$ (see table 5.6). Hence, they are **not normally distributed**. This fact necessitates the usage of non-parametric tests when analyzing and/or comparing the results from the validation test series. The following three statistical tests, designed for independent samples, were used for the comparison of the VAL and PAT samples: (1) the median test, (2) the Mann-Whitney U-test and (3) the Kolmogoroff-Smirnov omnibus test (KSO) [Bortz and Lienert, 2008].

The H_0 of the **median test** states that the two samples are part of populations with identical medians. So, if the H_0 is valid, 50 % of all data (from both samples) have values lower than the joined median and 50 % have a higher value. In order to determine the number of data points above and below the (joined) median for both samples a fourfold table is created (5.7) and the χ^2 test statistic is calculated according to equation 5.13.

$$\chi^2 = \frac{N \cdot (a \cdot d - b \cdot c)^2}{(a + b) \cdot (c + d) \cdot (a + c) \cdot (b + d)} \tag{5.13}$$

The **Mann-Whitney U-test** is considered to be the non-parametric counterpart to the t-test for independent samples. The tests power is considerably higher than the median

Parameter	eSHOE		GAITRite	
	healthy leg	affected leg	healthy leg	affected leg
Stride Time	$4.06 \cdot 10^{-4}$	$1.25 \cdot 10^{-3}$	$1.52 \cdot 10^{-3}$	$5.24 \cdot 10^{-3}$
Stance Time	$1.30 \cdot 10^{-4}$	$9.06 \cdot 10^{-3}$	$1.47 \cdot 10^{-3}$	$1.68 \cdot 10^{-2}$
Swing Time	$1.02 \cdot 10^{-3}$	$2.61 \cdot 10^{-2}$	$5.35 \cdot 10^{-3}$	$9.43 \cdot 10^{-2}$
Step Time	$6.92 \cdot 10^{-2}$	$4.93 \cdot 10^{-4}$	$9.96 \cdot 10^{-4}$	$7.62 \cdot 10^{-4}$
Initial Double Support	$1.08 \cdot 10^{-1}$	$4.16 \cdot 10^{-4}$	$1.31 \cdot 10^{-2}$	$6.25 \cdot 10^{-3}$
Terminal Double Support	$5.79 \cdot 10^{-3}$	$4.53 \cdot 10^{-2}$	$3.01 \cdot 10^{-4}$	$3.76 \cdot 10^{-2}$

Table 5.8: Results from Shapiro-Wilk test (for normal distribution) in healthy and affected leg data among patients, grouped in eSHOE and GAITRite.

test. It uses the rank information, contained in the samples, to its full extent, rather than on a sole dichotomous basis (smaller/greater than the joined median).

Calculate the sum of all ranks for sample 1 (T_1) and sample 2 (T_2). The sum of $T_1 + T_2$ must be equal to the sum of all numbers from 1 to N. Applies to equation 5.14 and allowing a checkup with equation 5.15.

$$1 + 2 + 3 + ... + N = \frac{N \cdot (N + 1)}{2} \tag{5.14}$$

$$T_1 + T_2 = \frac{N \cdot (N + 1)}{2} \tag{5.15}$$

From the ranksums T_1 and T_2 the U-values can now be calculated, according to equations 5.16 and 5.17.

$$U_1 = N_1 \cdot N_2 + \frac{N_1 \cdot (N_1 + 1)}{2} - T_1 \tag{5.16}$$

$$U_2 = N_1 \cdot N_2 + \frac{N_2 \cdot (N_2 + 1)}{2} - T_2 \tag{5.17}$$

Again, a checkup is possible via equation 5.18.

$$U_1 + U_2 = N_1 \cdot N_2 \tag{5.18}$$

5.5.3 Differences between healthy and affected leg among patients

Another question to be answered was, whether there were any differences between the healthy and the affected leg in the patients' data. Also, as initial test, the legs were analyzed concerning their distribution. Again, using the Shapiro-Wilk test (see table 5.8).

All except one of the p-values (initial double support - eSHOE) were below the significance level of 0.1. Therefore, none - except one - of the samples are normally distributed and non-parametric tests have to be used. In difference to the data above, dealing with CTRL and PAT group differentiation, the samples of healthy and affected leg are dependent on each other. This fact requires different statistical tests such as (1) the **sign test** and (2) the **sign rank test** [Bortz and Lienert, 2008].

The results of both analyses are located in chapter 6, subsections 6.2.2 and 6.2.2.

5.6   Stride length estimation

Since the calculation of stride length (by means of accelerometer sensors) proved to be more challenging than the other gait parameters, the work on this topic was outsourced to a master student, Daniel Polasek, from the Zurich University of Applied Sciences (ZHAW). Due to the complexity of this topic this whole section dedicated to (Polasek's work on) stride length estimation, Instead of a only subsection like with the other gait parameters Daniel Polasek's thesis was (academically) supervised by Prof. Dr. Ruprecht Altenburger (from ZHAW), FH-Prof. Dr. Martin Reichel (from FHTW) as well as accompanied and supported (regarding content) by the author of this thesis.

In theory, the readings of an IMU can be (mathematically) integrated to determine the heading (also called attitude) and the traveled distance of the body it is fixed on. As long as it is known which way the accelerometer is facing, it is possible to integrate the sensor output twice to calculate its position in three dimensional space.

The practical application, however, of the determination of the location and trajectory of an IMU located inside a shoe insole proved to be more complex than the simple theoretical approach. Major challenges are measurement errors and sensor data drifts, inherent to state of the art IMUs. As found by [Polasek, 2014] the subject of inertial navigation (for pedestrian, or indoor navigation) provides strategies to cope with these problems.

Inertial Navigation Systems (INS) are used for the dead reckoning (DR) of a moving body [Noureldin et al., 2013]. Dead reckoning is autonomous and requires the knowledge of the initial location, speed and heading. Using the inertial sensors (gyroscope and accelerometer) all further movements can be traced. However, measurement errors cannot be avoided and they pose an error to the calculated position cubic to the measurement time.

5.6.1   Definitions

Stride length

A gait cycle can also be referred to as stride [Murray et al., 1964]. Colloquially, it is often called step, which is inadequate and wrong. A stride is defined by the actions of one leg. The duration of a stride equals the time interval between two subsequent ICs of
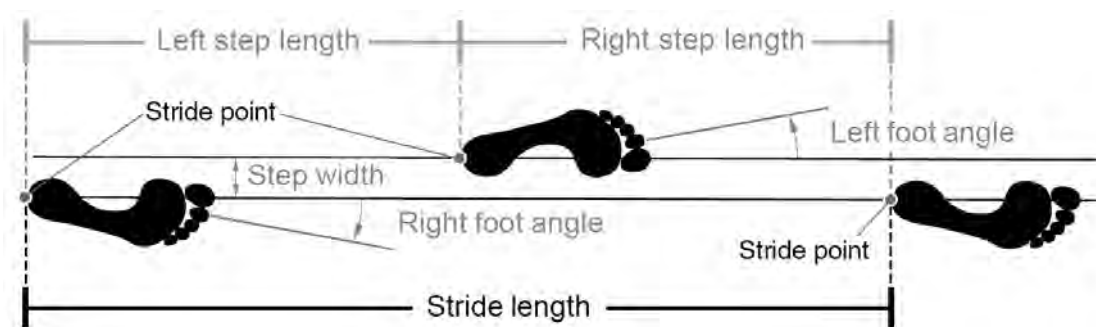
Figure 5.15: IC contact extraction error. "Illustration of extracted gait features from human gait in left insole data; one initial contact was not extracted by the feature extraction algorithm."

the same extremity. Namely from one IC right to the next IC right. A step on the other hand lasts from the IC right to the IC left (see also subsection 5.4.4). [Vaughan et al., 1992] describe the stride length as distance between two called stride points, where the posterior (rear) calcaneus (heel) touches the ground (see fig. 5.15). The Euclidian norm between two stride points is considered as the stride length.

Inertial navigation system

[Noureldin et al., 2013, pp. 2, 126] states that:

> An INS is an integration system consisting of a detector and an integrator. The detectors are inertial sensors which measure the rotation rate (gyroscope) and the specific forces from which acceleration (accelerometer) can be obtained. Starting from a known position and orientation, measurements are integrated once for gyroscopes and twice for accelerometers to provide orientation and position respectively.
>
> Inertial navigation systems are autonomous, which means they are self-contained and need no external references. Measurements of the acceleration are made in the inertial frame of reference and are then transformed in to the navigation frame. Measurements of the rotation is needed for the transformation from the inertial to the navigation frame and for the computation of the attitude.
>
> The positioning solutions obtained tend to drift with time due to the integrations performed, which can lead to unbounded accumulation of errors. Inertial navigation alone, especially with low cost sensors, is thus unsuitable for accurate positioning over an extended period of time.

An INS can be thought of as consisting three principal modules.

1. IMU – Accelerometer and gyroscope sensors
2. Pre-processing unit – signal filtering
3. Mechanization unit – attitude, velocity and position calculation algorithm

5.6.2   Methods

The main idea of stride length calculation from a foot-mounted IMU measurement is very straight forward on a first thought: As acceleration and rotation of the system is known, we determine the orientation of the foot at every time t and can double integrate the acceleration a of the foot in order to determine its position in *x, y, z*, given that we know the initial conditions. This can be formulated mathematically as

$$Stride\ Length = -norm_{xy}(K \cdot a_{LeftFoot} \cdot t_i\check{s}) + norm_{xy}(K \cdot a_{LeftFoot} \cdot t_{i+1}^2) \quad (5.19)$$

$$Sensitivity \ = \ \frac{9.81\ m/s^2}{256\ LSB/g} \ = \ 0.038\ \frac{m/s^2}{LSB} \quad (5.20)$$

$$Accuracy\ Estimation\ [\frac{m}{LSB}] \ = \ \iint_0^t\ Sensitivity \cdot dt \cdot dt \ = \ Sensitivity \cdot \frac{1}{2} \cdot t^2 \quad (5.21)$$

The equations 5.20 and 5.21 indicate that, when using the ADXL346 accelerometer, the distance can be estimated in steps of the size of 0.019 m = 1.9 cm ($\pm$ 0.95 cm). This uncertainty is due to the limited resolution of the sensor itself. It has to stated that this estimate is a best-case scenario, since it does not include any assumptions or considerations of possible error sources. Therefore, the inaccuracy can be expected to lie above the rounded $\pm$ 1 cm range. However, the method and algorithms developed by [Polasek, 2014] can be used independently of the underlying hardware (sensors) and can be applied to any further developed prototypes as well.

Possible errors and stabilization methods

In signal theory, error modeling is the mathematical approach to define errors within a signal. At first possible errors within a signal are classified and named. Based on these error definitions the mathematical formulation is stated. The more erroneous effects are removed from the true, specific force of the sensor the better are the measuring results. As will later be shown, good error estimations are bound to a good understanding of the system and a well-designed algorithm.

$$\tilde{f}^b = f^b + b_a + S_1 f^b + S_2 f^{b2} + N_a f^b + \varepsilon_a + \delta g \quad (5.22)$$

$$\tilde{\omega}_{ib}^b = \omega_{ib}^b + b_g + S_g\omega_{ib}^b + N_g\omega_{ib}^b + \varepsilon_g \tag{5.23}$$

Eight systematic and four random error effects influence the inertial sensor output.

The systematic errors:

1. **Systematic bias offset**
   All MEMS devices exhibit this kind of error. It is described as constant deviation from the expected output, when there is no input.
2. **Scale factor error**
   Deviation of the input-output gradient from unity.*
3. **Non-linearity** Non-linear deviation of the sensor's output from its input.*
4. **Scale factor sign asymmetry** Different scale factors for positive and negative inputs.*
5. **Dead zone**
   Measurement range outside of the sensor's range and, therefore, the input does not elicit any output.
6. **Quantization error**
   Typical error, inherent to all systems, generating digital output from analog input
7. **Non-orthogonality error**
   This error arises from slightly faulty manufacturing, resulting in misalignment of one of the sensor axes which are supposed to be orthogonal to each other.
8. **Misalignment error**
   deviation of the sensor frame from the body frame.

The random errors:

1. **Run-to-run bias offset**
   It is possible that the systematic bias offset changes every time the sensor is turned on. A known cause for bias offset is a change in temperature. Different temperature affects the the offset differently. Hence, the stochastic influence on the systematic bias offset.
2. **Bias drift**
   Bias offset can also change (over time) during the sensor is powered. This is due to the same reasons as before.
3. **Scale factor instability**
   Temperature variations can also cause random changes in the scale factor. In difference to bias offset and bias drift this error stays constant during a run (while the sensor is powered).
4. **White noise**
   Affecting all frequencies and uncorrelated, white noise can be caused by a wide variety of reasons, e.g. by power sources.

127

It has been shown that IMUs are subject to major measurement errors of different kinds. To cope with the uncertainty of the measurement results there are different approaches available to improve error loaded measurements.

A mathematically sophisticated approach is the Kalman Filter. It uses all information and inputs available and based on covariance matrices each available input is rated for its trustworthiness.

if the measurements are far away from the predicted behavior, the Kalman Filter cannot correct the error loaded measurements in the intended/engineered way.

[Noureldin et al., 2013] state that inertial navigation system (INS) are mainly influenced by accelerometer biases and gyro drifts. If accuracy is to be improved, stochastic errors have to be estimated and compensated in regular time intervals. Among others the zero velocity update (ZUPT) is suggested and was the method of choice in [Polasek, 2014].

Calibration

Several sophisticated calibration routines for *accelerometers* are described in [Noureldin et al., 2013]. For the pre-existing conditions (sensors and printed circuit boards (PCBs) already built-into a shoe insole) two were applicable:

1. 3D ellipsoid fitting [Zollinger, 2012] and
2. Six position static test [Noureldin et al., 2013].

3D ellipsoid fitting is used to calibrate an accelerometer for bias offset and scale factor sign asymmetry. In order to achieve that, the accelerometer has to be moved slowly in repeating turns in every direction so that the (imaginative) gravity vector describes the surface of a sphere. The sphere has a radius of 1 *g*, because of the specific force vector of the same length. Actual measurement results, however, show an ellipsoid rather than a sphere, due to certain measurement errors. By using fix radius and a corrected center point, this ellipsoid can be transformed into a sphere. These parameters represent bias offset and scale factor asymmetry and can the be used for sensor calibration.

For the **six position static test** the inertial system is mounted on a level surface with each sensitive axis pointing alternately up and down (two positions × three axes = six positions). Sensor readings from these positions are summed and differenced. Thereby, it is possible to extract estimates of the accelerometer bias and scale factor.

Usually, an expensive high precision turn-table is needed for the calibration of *gyroscopes*. Cheaper substitute methods, like using an LP turn-table, did not deliver satisfactory results. Rather than measuring the measurement error of the gyroscope these contraptions resulted in estimating the turning-irregularity error of the LP turn-table motor [Noureldin et al., 2013]. Therefore, the only possibility for a slight improvement is to perform **a static test for several minutes**. Since the gyro's sensitivity is not high enough to detect the earth's rotation, the inertial sensor bias can be assessed in that way.

	left			right		
$S_1 + N_a$	$\begin{bmatrix} 0.04 & 0 & 0 \\ 0 & 0.03 & 0.01 \\ 0 & 0 & 0.04 \end{bmatrix}$			$\begin{bmatrix} 0.02 & 0 & 0 \\ 0 & 0.03 & 0 \\ 0 & 0 & 0.04 \end{bmatrix}$		
b_a	$\begin{bmatrix} 0.12 \\ -0.06 \\ 1.01 \end{bmatrix}$			$\begin{bmatrix} -0.44 \\ 0.41 \\ 1.36 \end{bmatrix}$		

Table 5.9: Zero rate data for the eSHOE size 44/45. Raw, then calibrated against the bias offset. Adopted from [Polasek, 2014].

In order to assess the calibrations success/outcome, the distribution of the calibrated data has to be evaluated. Normally distributed data would be a desirable output.

Normal distribution can be verified via visual inspection. The simplest method is judging by the (distribution in the) histogram. Other fast and reliable tools are the Tukey-Anscombe plot (TAP) and the normal probability plot (NPP) [Montgomery and Runger, 2003]. In the Tukey-Anscombe plot (TAP) the residuals of the data are plotted against their expected values. Data should distribute normally around zero. The Tukey-Anscombe plot used here also include a trace representing the moving-average-filtered data (window size: 100 samples) and a linear trend line. They were added for better visual interpretability and for identification any dependency on the y-axis variable, respectively. The normal probability plot is a special case of the QQ plot (QQP) in which the quantile of the residuals is plotted against a perfect normal distribution. If the assessed data is normally distributed, the plot shows a skew "S"-form. For a better assessment of the linearity of the distribution a diagonal reference line has been included in the plots.

Numeric results from the ellipsoid fitting for eSHOE size 44/45 can be found in table 5.9 and a graphical representation of an exemplary result is shown in fig. 5.16.

Figures 5.17 and 5.18 contain the Tukey-Anscombe plots and normal probability plots of raw an calibrated data. Prior to the calibration the residuals in fig. 5.17a show clear deviations from zero (especially the moving average trace) which indicates (1) measurement errors and (2) translational movements of the hand (as the turning of the insoles was performed manually). The residuals in the Tukey-Anscombe plots represent the distance of the Euclidian norm of the accelerometer readings against the gravity vector g = 9.81 m/s^2. Additionally, the linear fit (red trace) exhibits a negative slope, reflecting the bias drift. After the calibration has been carried out the residuals are distributed normally around zero and the linear fit shows no more slope (fig. 5.17). Although, due to vibrations and translational movements, caused by the manual rotation of the insoles, some deviations still remain. The QQ plot in fig. 5.18a shows that the raw data clearly doesn't follow a normal distribution. There is no typical skewed S-shape, no linearity in the middle and the tails point in the wrong direction. Also the slope of the linear fit is rather low, indicating a wide distribution (leptokurtic). Again, calibrated data
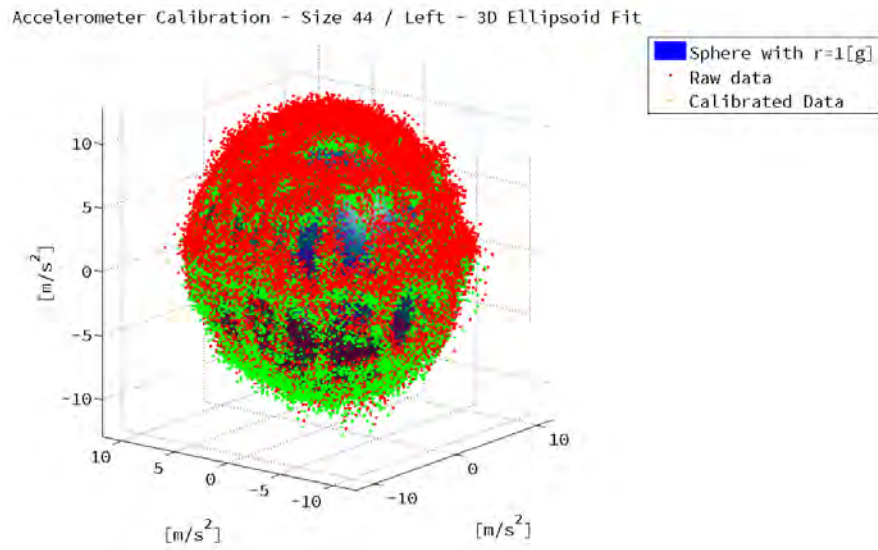
Figure 5.16: QQ Plot indicates a good normal distribution. Comparison with the uncalibrated data is unnecessary because the bias offset does not change the distribution but only shifts it. [Polasek, 2014]
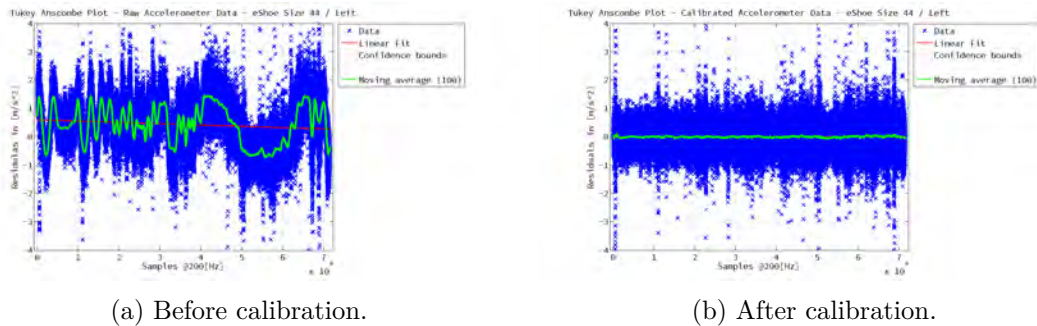
(a) Before calibration.

(b) After calibration.

Figure 5.17: Tukey-Anscombe plots of accelerometer data.
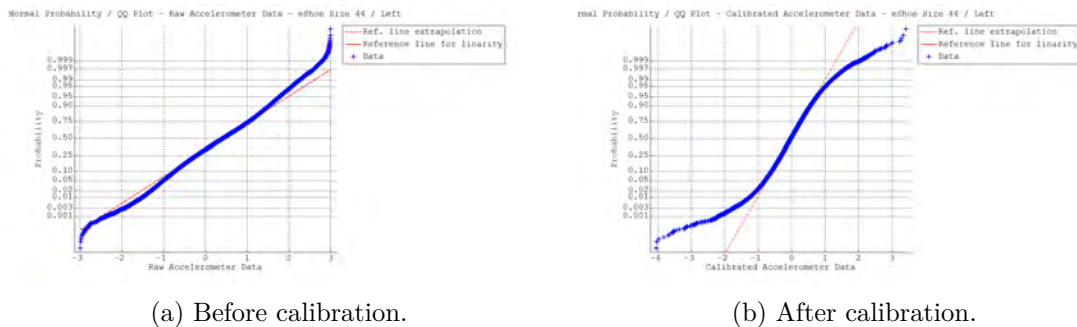
(a) Before calibration.

(b) After calibration.

Figure 5.18: QQ plots of accelerometer data.
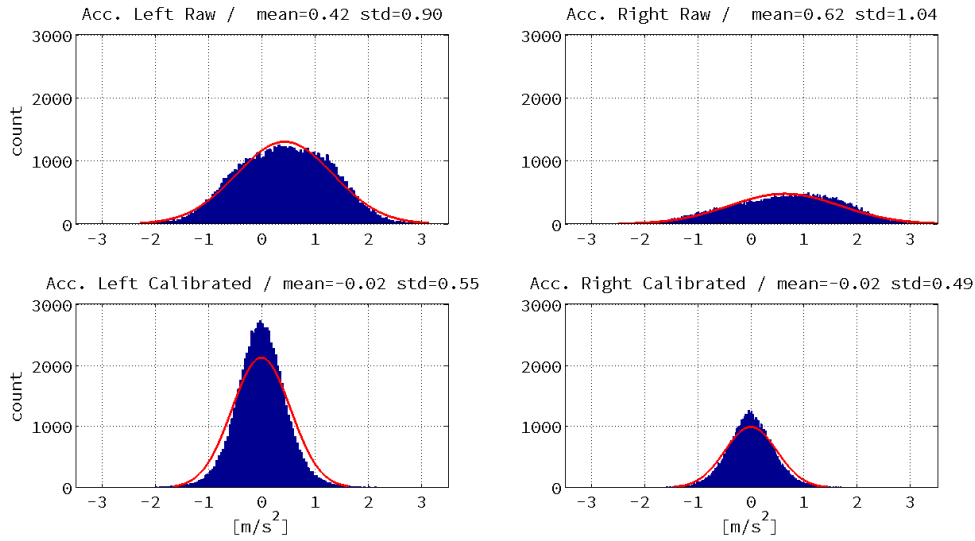
Figure 5.19: Histograms for the 3D ellipsoid fit data recording with both insoles of eSHOE size 44/45. Top row: results <u>before</u> calibration. Bottom row: results <u>after</u> calibration. [Polasek, 2014]

	left	right
Raw mean [deg/s]	0.42	0.62
Raw σ [deg/s]	0.90	1.04
Calibrated mean [deg/s]	-0.02	-0.02
Calibrated σ [deg/s]	0.55	0.49

Table 5.10: Changes in mean and σ through 3D ellipsoid calibration of the eSHOE insoles size 44/45 [Polasek, 2014].

(fig. 5.18b) exhibits all signs of normally distributed data.

The TAP and QQ plot (QQP) results are reinforced by the analysis of the histogram plots in fig. 5.19 and the numeric values in table 5.10.

After the calibration the data form a better normal distribution around zero. The form indicates a logistic distribution, which in this case can be seen as an even better result. Logistic distributions have steeper flanks and are thus narrower distributed around the expected mean value.

The measurements of the raw values are in accordance with the zero rate level specified of 0.5 m/s^2 in the ADXL346 data sheet, given in table 4.2 at the beginning of section 4.3. These levels were reduced to 0.02 m/s^2 after the calibration. The standard deviation (σ) remains quite high with ± 0.5 m/s^2.

	Left foot			Right foot		
	Gyro X	Gyro Y	Gyro Z	Gyro X	Gyro Y	Gyro Z
Raw mean [deg/s]	2.251	-2.672	0.195	1.315	1.964	0.406
Raw σ [deg/s]	0.074	0.093	0.117	0.075	1.159	0.239
Calibrated mean [deg/s]	0.000	0.000	0.000	0.000	0.000	0.000
Calibrated σ [deg/s]	0.074	0.093	0.117	0.075	1.159	0.239

Table 5.11: Zero rate data for the eSHOE size 44/45. Raw, then calibrated against the bias offset. Adopted from [Polasek, 2014].

During the stationary test of the gyroscope approximately 700,000 samples have been collected. The bias offset error is defined as the mean of these samples. Table 5.11 contains the numeric values for mean and standard deviation (σ) before and after calibration. After the subtraction of the bias offset, the mean is shifted to (almost) zero. The standard deviation (SD) remains the same and is close to the maximum resolution of the sensor of $0.0696 \deg/s$.

Fig. 5.20 and fig. 5.21 show the Tukey-Anscombe plot (TAP) and the QQ plot (QQP), where an almost ideal normal distribution can be observed. The similarity of the two TAPs in fig. 5.20 suggests that the gyroscope exhibits good measurement quality. The QQPs in fig. 5.21 even shows the quantization steps, indicating a very small distribution of the gyro data.

Unfortunately, it was not possible to determine or counteract the remaining error types: non-linearity, scale factor sign asymmetry, dead zone, non-orthogonality and misalignment. In order to investigate those errors special calibration tools are necessary, which are very expensive and, therefore, only available in specially outfitted laboratories for inertial sensor development.

Random stochastic errors, such as run-to-run bias offset, bias drift, scale factor instability and white noise have to be handled during data capturing and cannot be compensated through calibration measures. The stride length estimation algorithms contain routines to deal with run-to-run bias offset and bias drift.

If the known errors are not dealt with by some kind of error-handling mechanism trials showed a subsequent (mean) error in the distance estimation of 3965 %. This equals a wrongful distance estimation of 345 m when the true traveled distance was 8.7 m in $\sim 13\ s$ (see fig. 5.22).

Measurement setup

Walking in a straight line for a certain (pre-defined) distance was chosen as testing condition. In the whole experimental design two types of external references were used: a measurement tape (to determine a pre-defined length of the walking distance) and
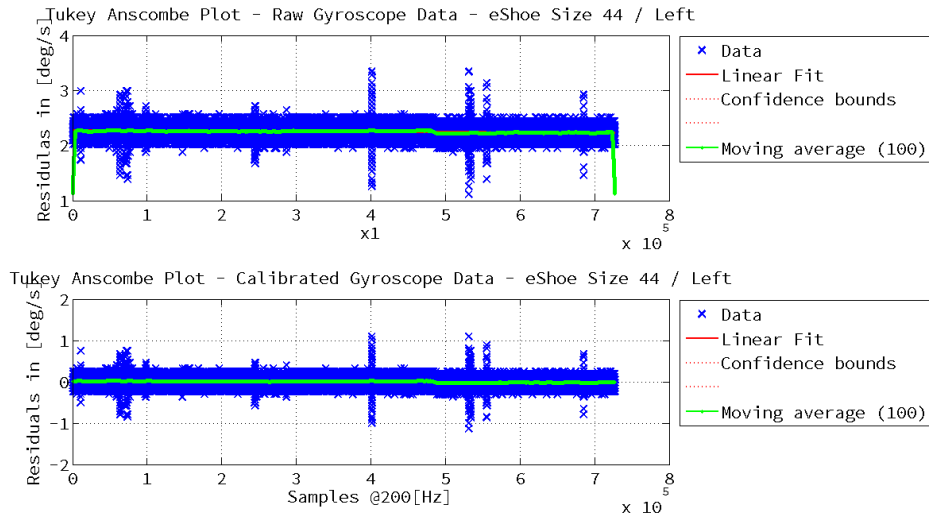
Figure 5.20: Tukey Anscombe Plot for the gyroscope calibration measurements. Above raw, below calibrated. It can be observed, that the bias offset subtraction simply shifts the distribution. The linear fit and confidence intervals are hidden beneath the moving average with windows size 100. The distribution of the data is good with some irregular data reading errors which do not influence the overall distribution. [Polasek, 2014]
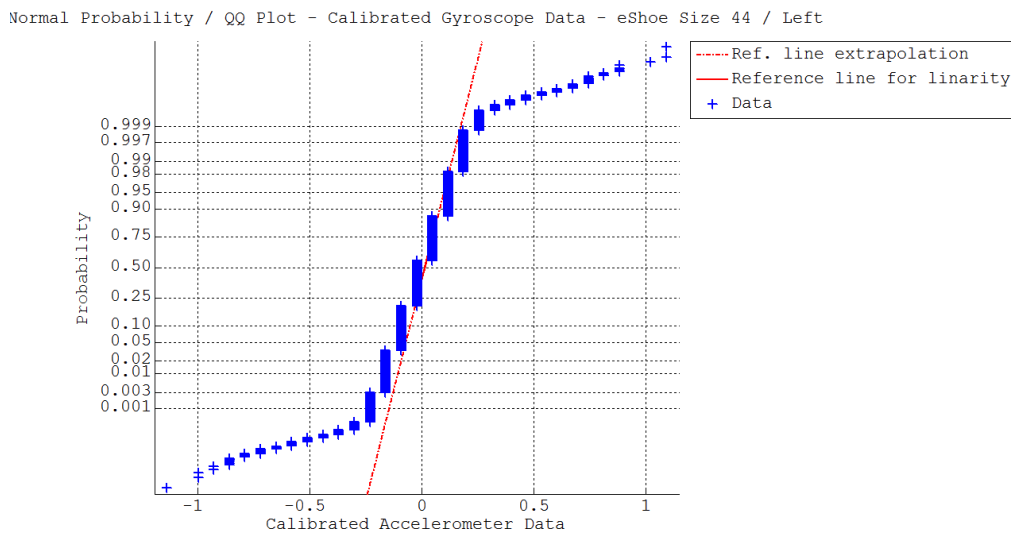
Figure 5.21: QQ Plot indicates a good normal distribution. Comparison with the uncalibrated data is unnecessary because the bias offset does not change the distribution but only shifts it. [Polasek, 2014]
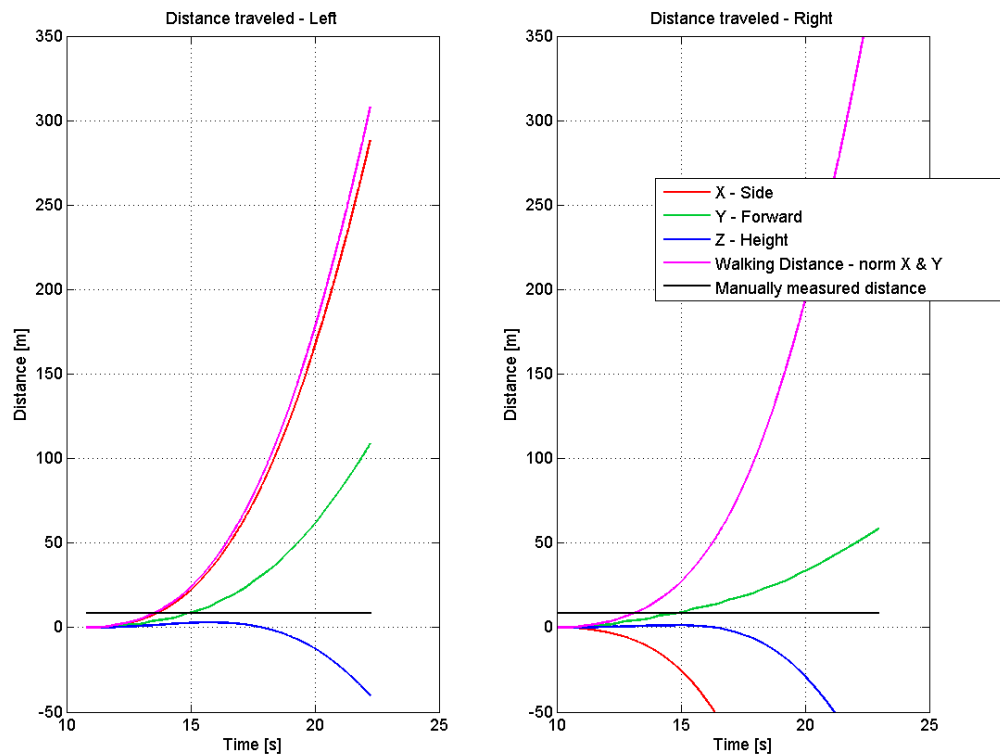
Figure 5.22: Results from distance estimation error test. The subject was walking in a straight line for 8.7 m and the test lasted $\sim 13\ s$. Two plots are displayed: the left foot on the left and the right foot on the right. The IMU data was calibrated, but no error correction was applied. The dataset has been validated with Vicon. [Polasek, 2014]

the motion capturing system Vicon. Polasek carried out indoor as well as outdoor measurements.

The outdoor setup involved a 50 m walking track. But these measurements were solely used for development, testing and fine tuning of the algorithm. 66 test runs have been recorded in this setup. The totally traveled distance is evaluated for these tests.

The indoor measurements contained a shorter walking distance of 8.7 m, due to spatial limitations of the room they were carried out in. But they allowed to use Vicon with a special camera setup as a reference system. 39 measurements were conducted and they were used for verification of the algorithms (distance) results. For this setup the accuracy of the stride length estimation is evaluated.

For the stride length estimation further influencing conditions were taken into account. The first and last strides in a straight walking task have significantly different characteristics, due to the necessity of acceleration at the beginning of walking and decelerating

Characteristics	
Age [years]	28
Gender	Male
Size [m]	1.85
Weight [kg]	100
Shoe size (EUR)	44/45

Table 5.12: Characteristics of Polasek's single test subject.
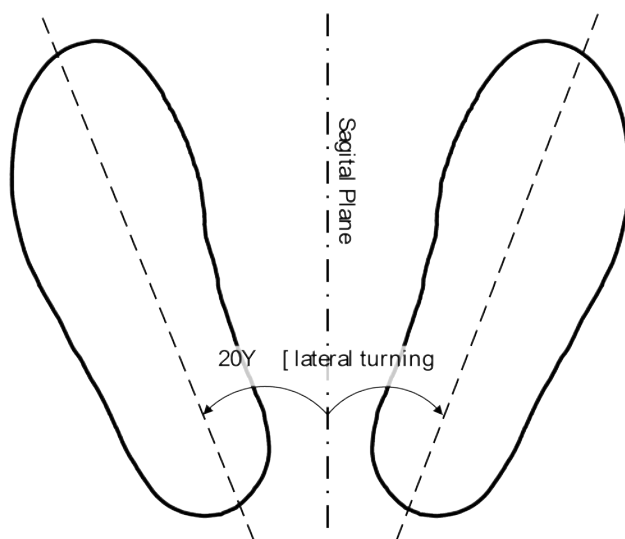
Figure 5.23: Outlines of shoes/feet, in order to define the initial conditions for the test setup. [Polasek, 2014]

at the end. Therefore, there will be different analyses, including/excluding two to four strides from a walk and the effect on the results will be observed.

The following conditions were in effect:

- Walking distance: 30 m (defined by measurement tape without specified precision class)
- Metronome with 100 bpm
- Straight walking trajectory
- Standing still at the beginning and the end of data recording (for ten to 60 s)
- eSHOE insoles were "warmed up" by placing them inside the subject's shoes 30 minutes prior to testing
- Subject has to assume a pre-defined initial stance, with a 20 deg lateral rotation of both feet (see fig. 5.23)

Application

Analysis of literature and state of the art showed much promise in stride-wise distance estimation approaches, where zero velocity updates (ZUPTs) are performed during the stance phase [Nilsson et al., 2010, Skog et al., 2010, Madgwick et al., 2011]. Therefore, and because the detection of ICs is easy to achieve in eSHOE data, a similar strategy was pursued.

Since the previously existing algorithm (from section 5.3) proved to be not entirely adequate, Polasek adjusted it to the needs of his stride length estimation purpose [Polasek, 2014, p. 74].

On the one hand, there is the problem that the very first and last strides cannot be properly detected because they are occurring (starting/ending) before the first and after the last IC. Furthermore, the algorithm turned out to be too sensitive, so that it detects false positive ICs in stationary phases due to measurement noise. To compensate, Polasek introduced a procedure to crop out phases with no movement from the measurement data. He also presented a way to define the first and last stride in a data set.

The following, so called, *"AutoCut"* algorithm has been implemented to identify sections of activity (movement) in a dataset:

1. Calculate the norm of the accelerometer and gyroscope measurements: acc_{norm} and $gyro_{norm}$.
2. Noise reduction and offset elimination through low-pass filtering: acc_{filt} and $gyro_{filt}$.
3. Calculate the threshold test statistics: T_{acc} and T_{gyro} from acc_{filt} and $gyro_{filt}$.
4. Acceptance or rejection of test statistics. In case of acceptance of T_{acc} and T_{gyro} it is assumed that movement has started: $AutoCut_{start}$.
5. Rejection of test statistic for the last time within a dataset indicates the end of movement: $AutoCut_{end}$.

For the detection of first and last stride another simple algorithm was developed:

1. Calculate average *stride length* from the IC events, found within the *AutoCut* sequence.
2. Locate the starting point of the first stride by "going back in time" one average stride length from the first found IC event. Resulting in a new event: *$AutoCut_{start}$ Extended*.
   a) *$AutoCut_{start}$ Extended* must occur before $AutoCut_{start}$. If not, then an IC event is missing.
   b) If an IC event is, in fact, missing, a new "artificial" IC event generated at the point in time of $AutoCut_{start} - mean(stride\ length)$.
3. Iterative repetition of this procedure from step 2 until
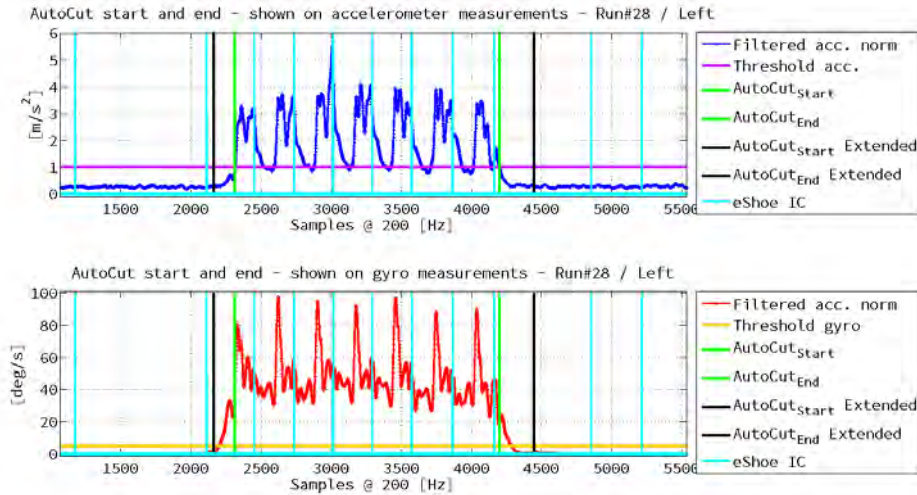
Figure 5.24: Graphical representation of the AutoCut results in the case of calibrated accelerometer data (above) and gyroscope data (below). Detected IC events (by the eSHOE algorithm) are displayed in vertical, cyan colored, lines. $AutoCut_{start}$ and $AutoCut_{end}$ are also indicated with two black vertical lines. Note that there are several false positive IC events in the dataset, but they are all outside of the relevant $AutoCut$ boundaries, where no foot movement occurs. [Polasek, 2014]

a) the newly found IC occurs before $AutoCut_{start}$ or
b) the newly found IC is the very first time sample in a dataset.

A similar procedure can applied to define the last stride in a dataset. Thereby, the last very stride is found by adding one average stride time to the last found IC event and verifying that this event occurs after the $AutoCut_{end}$. Results from the combination of both algorithms, eSHOE and $AutoCut$, merged into one vector, called $IC_{extended}$, can be seen in fig. 5.24. The events stored in $IC_{extended}$ can now be used to segment a continuous dataset into single strides. Now, further analysis and processing can be performed on these segmented, single strides, which improves data handling and visual representation significantly.

After segmentation and plotting of the sensor data from all strides of one dataset into one graph per sensor-axis, the identification of the ZUPT phase is rather simple. The example dataset from fig. 5.24 is presented in that way in fig. 5.25 (gyroscope and accelerometer data).
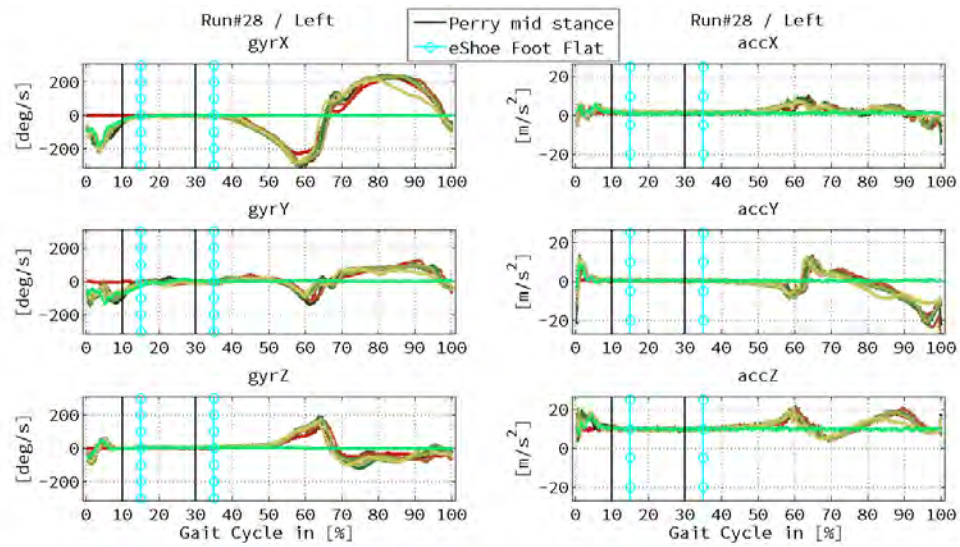
Figure 5.25: Segmented strides from the left foot of run 28 (fig. 5.24). Eight cycles each are plotted into six graphs, representing all axes from accelerometer and gyroscope. X-axes are scaled in percentage of gait cycle, 0 = initial contact (IC). The two vertical lines with circles (cyan) indicate the foot flat phase, as it was defined by [Perry, 1992]. The black vertical lines show an alternative foot flat phase, as the eSHOE data would suggest it, starting and ending 5 % earlier (shifted 5 % to the left). [Polasek, 2014]

Corresponding to what was mentioned about error handling in subsection 5.6.2, the following measures applied to the stride-wise data:

- leveling of the accelerometer data by
  transforming the accelerometer data to level ground. This is done by calculating pitch and roll angle (see equations 5.24 and 5.25) in the initial (resting) state of the foot and setting them to zero.
- Eliminate the run-to-run bias offset (in accelerometer and gyroscope data) by calculating the mean angular rate in all three axes (in the stationary phase) and subtracting the offset from each axis separately.
- Eliminating linear bias drift
  First, the mean of the bias offset during the ZUPT phase is considered. The last value of the stride is used to determine the slope. Then also this error can be subtracted from the current stride.

$$pitch = tan^{-1}\left(\frac{f_y}{\sqrt{f_x^2 + f_z^2}}\right) \tag{5.24}$$

Parameter	Reference	left foot	right foot
Complete distance [m]	8.72	7.77	8.09
Stride length [m]	-	1.11	1.08
Stride velocity [m/s]	-	0.7	0.6
Stride height [m]	-	0.1	0.095

Table 5.13: Calculated gait parameters for dataset run 28 from [Polasek, 2014].
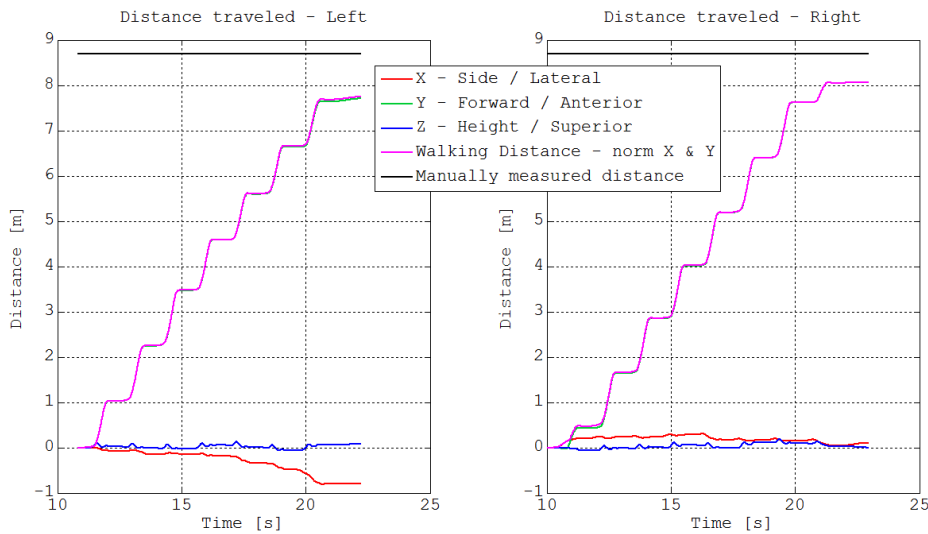
Figure 5.26: Results from distance estimation error test. The subject was walking in a straight line for 8.7 m and the test lasted ~ 13 s. Two plots are displayed: the left foot on the left and the right foot on the right. The IMU data was calibrated, but no error correction was applied. The dataset has been validated with Vicon. [Polasek, 2014]

$$roll = tan^{-1}\left(-\frac{f_x}{f_z}\right) \tag{5.25}$$

$f_{x,y,z}$ are accelerometer measurements in x-, y- and z-direction.

Finally, fig. 5.26 shows the end result of the distance estimation for test run 28, in the form of the calculated walking trajectory. The calculation for the complete distance is lower than the actual (manually measured) distance of 8.72 m. In difference to the simple approach in fig. 5.22 the single strides are clearly distinguishable. The distance errors in this data set are -0.95 m and -0.63 m for left and right foot (see table 5.13).

139
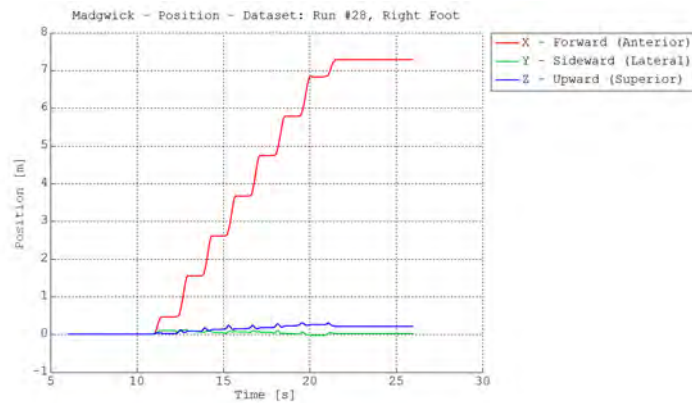
Figure 5.27: Final position mechanization of the IMU data with the Madgwick approach. Displayed in the Madgwick-defined coordinate system. [Polasek, 2014]

Comparison to Sota methods

Polasek also implemented the algorithms from Skog, Nilssen et al and Madgwick et al, which were available as open source, in order to compare their performance to the self-designed distance estimation method.

Madgwick appeared to work well with a selected few datasets, but in many others the detection of the stationary phase was not at all stable. He states that a dozen datasets were analyzed, which is not all of them, but enough to conclude that the Madgwick algorithm is not applicable to the given hardware configuration of eSHOE. The addition of a magnetometer (as it is already implemented in the further development of eSHOE) might deliver better results, since the Madgwick algorithm partly relies on this additional data. Polasek concludes further, that the implementation of a fixed value for the threshold (namely 0.05 g) is unsuitable. Therefore, the approach is highly susceptible for erroneous behavior in case of noise or unstable ZUPT phases. He also tried to adapt the threshold's value, but didn't succeed in improving the results.

When he applied the Madgwick algorithm to the test data of walking in a straight line for 8.72 m, the results were similarly disappointing (5.27). The algorithm delivered a total traveled distance of 7.30 m, which equals an error of -1.40 m or 16.14 %. He also divided the error by the amount of strides, resulting in -0.18 $m/stride$.

Unfortunately, the implementation of the algorithm by the Swedish group (Skog, Nilssen et al) was entirely unsuccessful. Occurring errors were so extreme, causing the design to fail completely. That was particularly disappointing, because this approach was, by far, the most promising. Polasek suspected the high gyroscope drift as main source of the problem. But he did not have enough time to analyze the problem thoroughly.

5.7 Therapy progress evaluation

The evaluation of the therapy progress measurements has been carried out in four major steps. (1) the measurements from all subjects have been grouped by measurement day (MD), gait parameter and affected or healthy leg, resulting in $12 \times 6 \times x$ data vectors (x equals the number of detected gait cycles for each leg at each measurement day). (2) each of these vectors has been checked for normal distribution, by means of the Shapiro-Wilk test, in order to determine which kind of statistical tests are to be used in the further analyses, parametric or non-parametric tests. (3) healthy and affected leg have been checked for statistical significant differences. (4) when there was a difference, the therapy progress has been analyzed for each leg (affected and healthy) separately. Where there was no difference the analysis was performed for both legs together.

5.7.1 Test method selection

Table 5.14 contains the results of the Shapiro-Wilk tests on the 10MWT data. In this table each column represent one of the six gait parameters and two rows contain data from one measurement day, split into affected leg and healthy leg per row. For instance, in the row marked "MD-2 A" the Shapiro-Wilk test results for the second measurement day of the affected leg can be found. With a few exceptions (concentrated on MD-5

	STR	STA	SWI	STE	IDS	TDS
MD-1 A	$8.72 \cdot 10^{-5}$	$5.81 \cdot 10^{-4}$	$2.06 \cdot 10^{-5}$	$9.50 \cdot 10^{-6}$	$3.54 \cdot 10^{-5}$	$1.35 \cdot 10^{-3}$
MD-1 H	$4.31 \cdot 10^{-5}$	$4.72 \cdot 10^{-4}$	$4.01 \cdot 10^{-8}$	$1.28 \cdot 10^{-4}$	$1.35 \cdot 10^{-3}$	$3.54 \cdot 10^{-5}$
MD-2 A	$1.40 \cdot 10^{-5}$	$4.04 \cdot 10^{-7}$	$8.49 \cdot 10^{-4}$	$1.30 \cdot 10^{-7}$	$5.66 \cdot 10^{-6}$	$8.05 \cdot 10^{-6}$
MD-2 H	$3.67 \cdot 10^{-5}$	$8.11 \cdot 10^{-7}$	$7.29 \cdot 10^{-12}$	$7.21 \cdot 10^{-5}$	$8.05 \cdot 10^{-6}$	$5.66 \cdot 10^{-6}$
MD-3 A	$3.00 \cdot 10^{-5}$	$8.44 \cdot 10^{-7}$	$5.65 \cdot 10^{-4}$	$8.69 \cdot 10^{-4}$	$1.32 \cdot 10^{-3}$	$4.18 \cdot 10^{-9}$
MD-3 H	$1.41 \cdot 10^{-5}$	$2.43 \cdot 10^{-7}$	$1.54 \cdot 10^{-12}$	$5.45 \cdot 10^{-7}$	$4.18 \cdot 10^{-9}$	$1.32 \cdot 10^{-3}$
MD-4 A	$1.84 \cdot 10^{-7}$	$9.75 \cdot 10^{-8}$	$1.54 \cdot 10^{-2}$	$7.78 \cdot 10^{-7}$	$7.05 \cdot 10^{-5}$	$1.10 \cdot 10^{-10}$
MD-4 H	$8.04 \cdot 10^{-8}$	$2.51 \cdot 10^{-6}$	$6.91 \cdot 10^{-8}$	$1.47 \cdot 10^{-6}$	$1.10 \cdot 10^{-10}$	$7.05 \cdot 10^{-5}$
MD-5 A	$1.29 \cdot 10^{-2}$	$4.49 \cdot 10^{-4}$	$1.79 \cdot 10^{-1}$	$4.12 \cdot 10^{-2}$	$6.14 \cdot 10^{-1}$	$1.66 \cdot 10^{-3}$
MD-5 H	$3.31 \cdot 10^{-2}$	$1.77 \cdot 10^{-1}$	$2.18 \cdot 10^{-1}$	$2.29 \cdot 10^{-1}$	$1.66 \cdot 10^{-3}$	$6.14 \cdot 10^{-1}$
MD-6 A	$2.45 \cdot 10^{-3}$	$3.45 \cdot 10^{-3}$	$2.01 \cdot 10^{-1}$	$1.85 \cdot 10^{-2}$	$3.88 \cdot 10^{-3}$	$2.83 \cdot 10^{-2}$
MD-6 H	$2.59 \cdot 10^{-4}$	$1.97 \cdot 10^{-4}$	$3.13 \cdot 10^{-1}$	$1.59 \cdot 10^{-3}$	$2.83 \cdot 10^{-2}$	$3.88 \cdot 10^{-3}$

Table 5.14: Shapiro-Wilk test exceedance probabilities for gait parameter results from all patients, segmented into measurement day (1 *to* 6) and affected (A) or healthy leg (H). Shaded cells indicate exceedance probabilities in favor of H_0 (suggesting normal distribution).

and MD-6) the results point out that the data are *not* normally distributed. Therefore, non-parametric tests have to be chosen for the further analyses. Since all subsequent analyses, the comparison of both legs and the progress evaluation, are dealing with *dependent samples*, the appropriate statistical tests are the sign test and the sign rank

test. The latter was chosen, due to its superior power compared to the former [Bortz and Lienert, 2008].

CHAPTER 6

Results

6.1 Pattern detection results and applicability

The algorithms described in sections 5.2, 5.3 and 5.4 produced a series of eleven patterns that occur during straight and level walking, one for each sensor axis. Figures 6.2 to 6.11 depict the (standard) signal patterns, which could be extracted from the measurement data. Each of the subplots represents the periodically reoccurring signal of one axis from the sensors during one gait cycle. Two things have to be noted concerning the appearance of those signals: (1) the patterns in figures 6.2 to 6.11 might seem to deviate from the original form shown in fig. 5.2. That is because the signal patterns in those figures are averaged over all the detected gait cycles. (2) Furthermore, these patterns do not all start at the "natural" beginning of a gait cycle (the first ground contact of the heel), since the autocorrelation algorithm only searches for reoccurring patterns and starts its search at the beginning of a data track, which is not automatically equal to the beginning of a gait cycle.

At the end it was also determined, how many of the (original) gait cycles the algorithm(s) were able to extract from the REF data. For that purpose, as a reference, the original total number of gait cycles was counted manually (in the data sequences) and subsequently compared to the number of cycles, delivered by the algorithm(s). 36 measurements have been conducted during the 10MWT trials. Reich decided to evaluate only 25 of those, since the other 11 were recorded at the lower sampling rate of 50 Hz. The data sets from the left insole contained a total of 216 gait cycles (which were manually counted). Data from the right insole was evaluated in the same way, but there were only 188 gait cycles, due to corrupted data files which made it impossible to be fed into the pattern extraction methods. Table 6.1 shows the absolute and normalized (in percentage from the total) numbers of gait cycles that were found by the algorithm(s) for each sensor axis. The top recognition rate in the *left* insole data was achieved for the pitch angle data (ANGLE), with 96.3 %, followed by the anterior/posterior acceleration (ACC-Y) with

Sensor	Extr. GCs		% of total	
	L	R	L	R
ANGLE	208	126	96.30*	67.02
ACC-X	53	33	24.54	17.55
ACC-Y	203	106	93.98*	56.38
ACC-Z	119	9	55.09	4.79
GYRO-X	203	176	93.98*	93.62*
GYRO-Y	86	30	39.81	15.96
GYRO-Z	130	127	60.19	67.55
P-HEEL	202	161	93.52*	85.64*
P-META-V	198	176	91.67	93.62*
P-META-I	199	172	92.13	91.49*
P-TOE	194	158	89.81	84.04

Table 6.1: Gait cycle detection results in absolute and relative numbers for left and right eSHOE insoles. For each side the four best results are indicated via *. Adopted from [Reich, 2013].

93.98 % and the angular velocity around the medial/lateral axis (GYRO-X) with 93.98 %. They are followed by the four pressure sensors, where data from underneath the heel (P-HEEL) shows the best result with 93.52 %, metatarsal head no. I (P-META-I) 92.13 %, metatarsal head no. V (P-META-V) 91.67 % and the big toe (P-TOE) with 89.81 %. Thereafter come the dynamic sensor data which is perpendicular to the walking direction, namely angular velocity around (GYRO-Z) and acceleration along the cranial/caudal axis (ACC-Z) with 60.19 % and 55.09 % respectively. Then there are angular velocity around the anterior/posterior axis (GYRO-Y) with 39.81 % and acceleration along the medial/lateral axis (ACC-X) with 24.14 %.

The best detection rate in the *right* insole data can be found in the angular velocity around the medial/lateral axis (GYRO-X) with 93.62 % ex aequo with pressure underneath the fifth metatarsal head (P-META-V). These are followed by the data from the remaining three pressure sensors, underneath the first metatarsal head (P-META-I), the heel (P-HEEL) and the big toe (P-TOE) with 91.49 %, 85.64 % and 84.04 %, respectively. Pitch angle data (ANGLE) and angular velocity around the cranial/caudal axis (GYRO-Z) are between 70 and 60 percent, with 67.55 % and 67.02 %.

Figures 6.1 to 6.11 show the results of the sensor- and axis-specific recurring patterns that could be extracted from the reference group (REF) data with to autocorrelation-based algorithm.
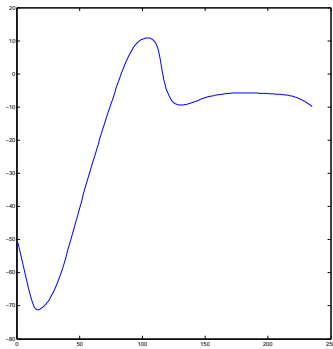
(a) Left foot
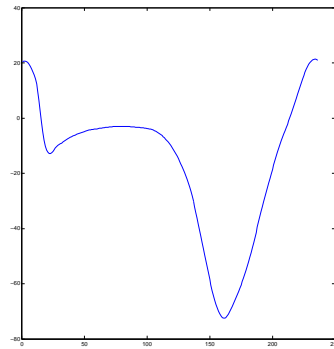
(b) Right foot

Figure 6.1: Pitch angle signal pattern during one gait cycle. 6.1a starts with a negative peak at -70 deg, which approximately resembles the point in time when the toe-off event takes place. Within the next 80 samples (0.4 s) the signal amplitude rises to a positive peak at 10 deg which is when the initial contact occurs. 20 samples later the signal settles at a level of slightly below 0 deg, where the foot is resting on the ground and this points to the conclusion that this is the stance phase (portion) of the gait cycle.
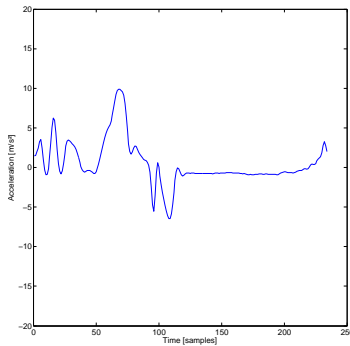
(a) Left foot
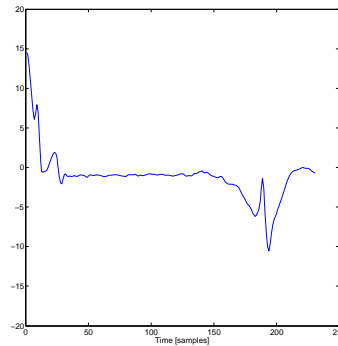
(b) Right foot

Figure 6.2: Medial/lateral acceleration (ACC-X) during one gait cycle. It shows minimal movement perpendicular to the walking direction. These movements are represented by three small negative peaks with amplitudes of -1 m/s^2 each and three small positive peaks with $3.5 m/s^2$, 6 m/s^2 and 3.5 m/s^2. The representativity of these patterns might be limited, due to the fact that only 53/24.5 % (L) and 33/17.6 % (R) cycles could be extracted.

145

(a) Left foot

(b) Right foot
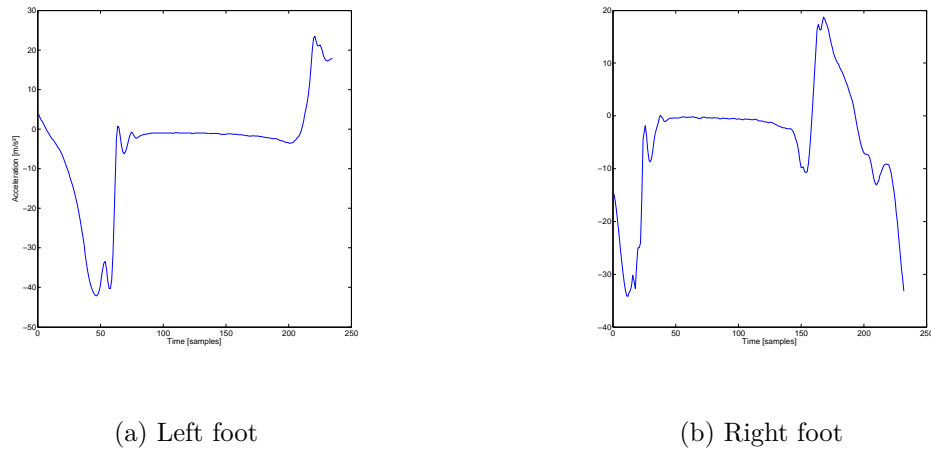
Figure 6.3: Anterior/posterior acceleration (ACC-Y) during one gait cycle. The left foot data starts approximately at the LC with 0 m/s^2. Lift-off of the foot is indicated by the strong negative displacement (-40 m/s^2 at 50 samples). During the swing phase no acceleration occurs, since it is a uniform motion (from ~ 100 to ~ 200 samples). Thereafter, the initial contact takes place, indicated by the rising edge (from 200 to 220 samples), reaching 23 m/s^2. Then the signal settles down again and, during the stance phase slowly changes to the negative displacement again. High reproducibility is suggested by the 203/93.9 % (L) and 106/56.4 % (R) detected cycles/detection rates.

(a) Left foot

(b) Right foot
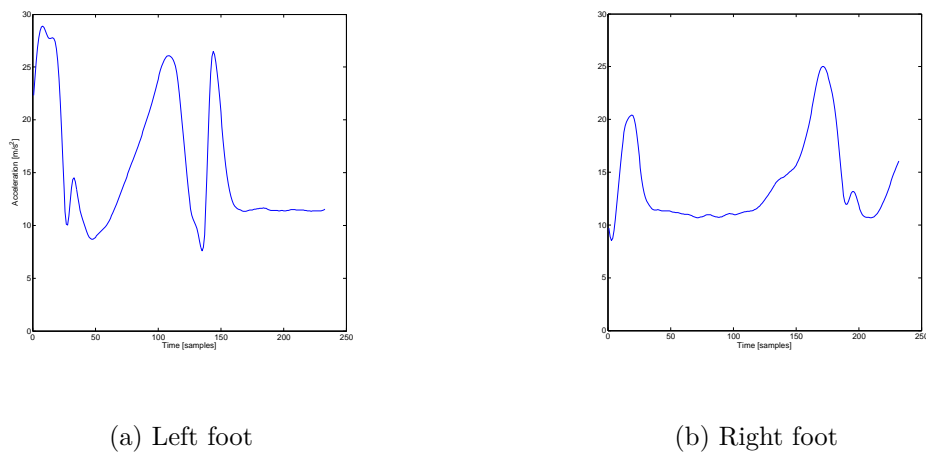
Figure 6.4: Cranial/caudal acceleration (ACC-Z) during one gait cycle. The pattern of the left foot shows a very unusual form, with characteristics atypical of a gait cycle, e.g. three consecutive positive peaks. Nevertheless, this pattern has a rather high detection rate of 55.1 %. Unfortunately, the pattern for the right foot data, containing two peaks which seem to match LC and IC, has a very low detection rate of 4.8 %.
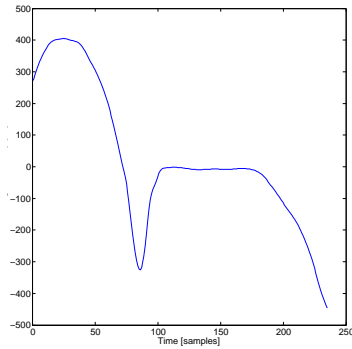
(a) Left foot
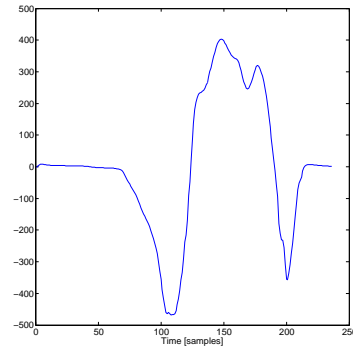
(b) Right foot

Figure 6.5: Angular rate around the medial/lateral axis (GYRO-X) during one gait cycle. The left foot pattern starts (in the middle of the swing phase) at $\sim 300 \deg / s$ and proceeds to its maximum of $\sim 400 \deg / s$ after 40 samples. As the foot is lowered to the ground the amplitude changes to negative displacement (with a local minimum of $\sim -300 \deg / s$ at 80 samples), followed by a quick rotation in the positive direction as the foot flat phase is reached, right after the IC. During the stance phase the signal remains at rest, as expected, before it starts to descend again during heel-off. The chronologically following LC event can be observed best in the right foot pattern, at the zero-crossing after the global minimum of $\sim -468 \deg / s$.
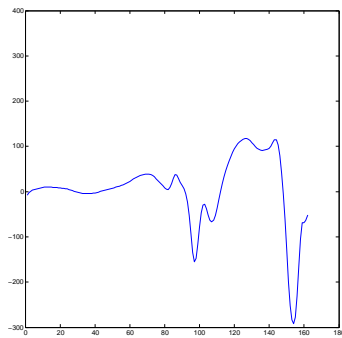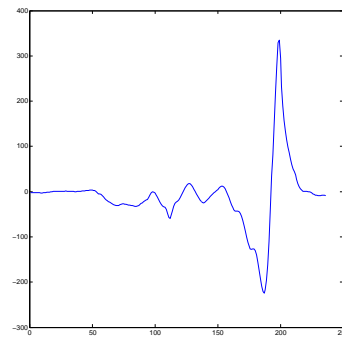
(a) Left foot

(b) Right foot

Figure 6.6: Angular rate around the anterior/posterior axis (GYRO-Y) during one gait cycle.

147
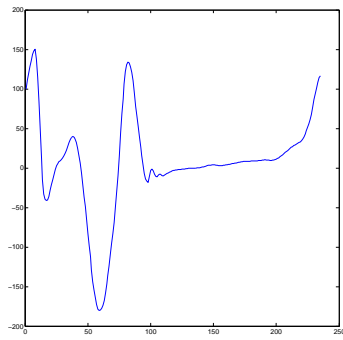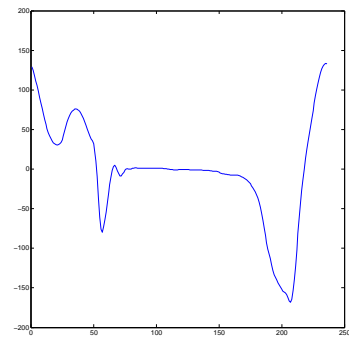
(a) Left foot

(b) Right foot

Figure 6.7: Angular rate around the cranial/caudal axis (GYRO-Z) during one gait cycle.
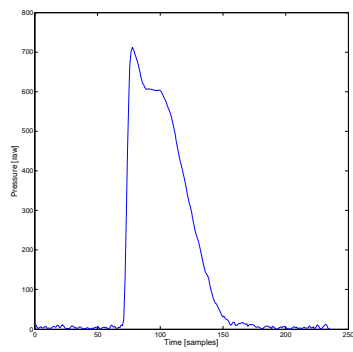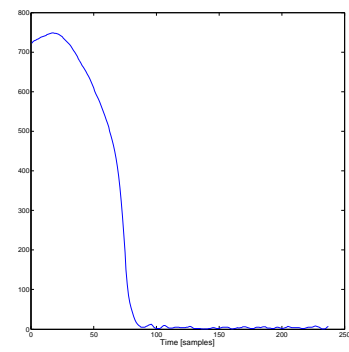
(a) Left foot

(b) Right foot

Figure 6.8: Pressure beneath the heel (P-HEEL) during one gait cycle.
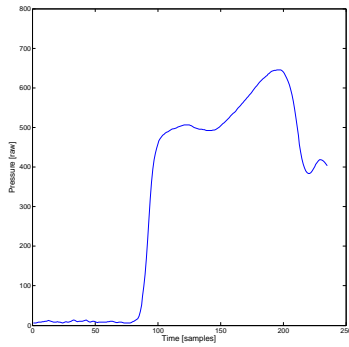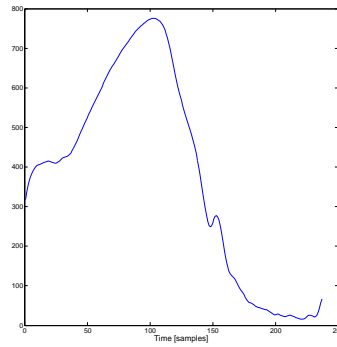
(a) Left foot

(b) Right foot

Figure 6.9: Pressure beneath the fifth metatarsal head (P-META-5) during one gait cycle.
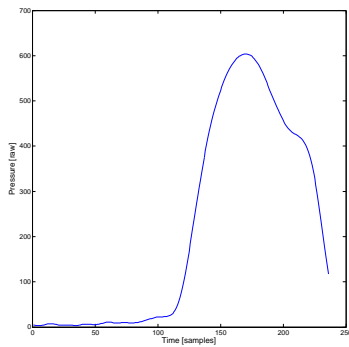
(a) Left foot
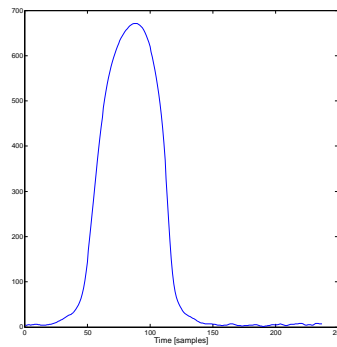
(b) Right foot

Figure 6.10: Pressure beneath the first metatarsal head (P-META-1) during one gait cycle.

(a) Left foot   (b) Right foot
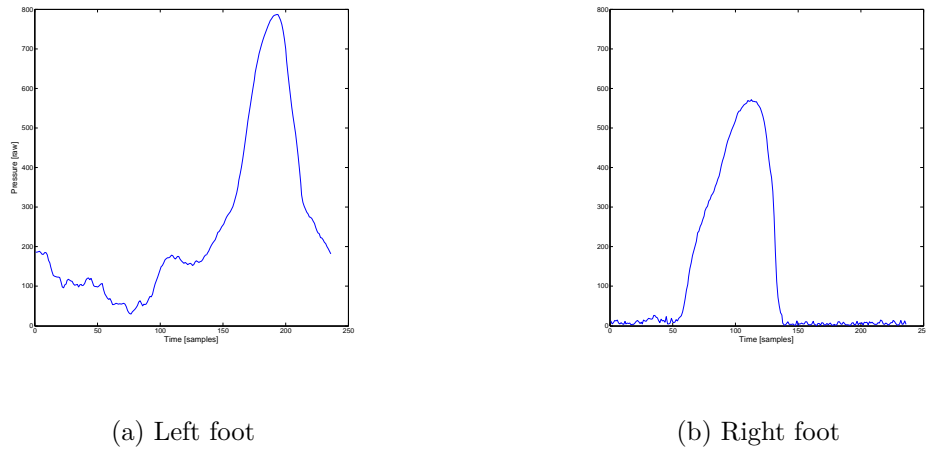
Figure 6.11: Pressure beneath the toe (P-TOE) during one gait cycle.

6.1.1 Pattern recognition accuracy

In order to determine feasibility and applicability of the pattern extraction approach, the patterns generated from the REF data were used to segment gait data from the PAT group's 10MWT into single gait cycles (via cross-correlation). The success ratio is defined by comparing the number of detected cycles, the algorithm produced with the number that were manually counted. The four patterns with the best results from above (table 6.1) were used to find and segment gait cycles in the PAT data.

For a cycle in the PAT data to be detected, the correlation-coefficient between the pattern and the current cycle had to be > 0.5. Since patterns for left and right foot are different, the data was analyzed separately for left and right insole data. Table 6.2 holds the results for the detection success rates.

6.1.2 Accuracy of IC and LC detection

Apart from the detection ratio of the gait cycles, the reliability of the gait event detection, namely IC and LC was of interest. Therefore, the number of extracted IC and LC events can (simply) be compared to the number of detected gait cycles. Naturally, every gait cycle "contains" one of each. Section 5.3 mentioned, that anterior/posterior acceleration (*ACC-Y*) and heel pressure (*P-HEEL*) data were used for the detection of the initial contact. Hence, the amount of cycles detectable in these two data sets are used as reference. Or rather the higher amount of those two, which is 665 *cycles* (*ACC-Y*) in the left insole data and 666 *cycles* (*P-HEEL*) in the right insole data (see table 6.2). The extraction of the last contact was done with the help of sagittal foot angle (*ANGLE*) and transverse angular rate (*GYRO-X*) data. Table 6.2 shows 650 and 647 counted *GYRO-X* cycles in left and right insole data, respectively.

Sensor	Manual		Automated		% of total	
	L	R	L	R	L	R
ANGLE	669	-	668	-	99.85	-
ACC-X	-	-	-	-	-	-
ACC-Y	665	-	623	-	93.68	-
ACC-Z	-	-	-	-	-	-
GYRO-X	671	671	650	647	96.87	96.42
GYRO-Y	-	-	-	-	-	-
GYRO-Z	-	-	-	-	-	-
P-HEEL	593	666	584	609	98.48	91.44
P-META-V	-	660	-	639	-	96.82
P-META-I	-	671	-	667	-	99.40
P-TOE	-	-	-	-	-	-

Table 6.2: Accuracy of the pattern recognition algorithm for left and right insole data. Adopted from [Reich, 2013].

	Detectable	Detected	% of total
IC left	665	653	98.20
IC right	666	645	96.85
LC left	650	638	98.15
LC right	647	641	99.07

Table 6.3: Accuracy of the IC detection algorithm in PAT-group data.

The two events in both insoles show (table 6.3) high detection rates of 98.2 % and 96.9 % for IC left and right, which makes a mean of **97.5 %** and 98.2 % for LCs left and 99.1 % for LCs right, making a mean of **98.6 %**.

6.2 Validation of eSHOE with state of the art gait analysis methods

The results from the validation measurements are, much like the methods in section xyz, grouped into the analysis of agreement and the comparison of healthy subject and patient data.

6.2.1 Analysis of agreement

Healthy subjects

CTRL Parameter	n	$\bar{d}$ [s]	σ [s]	Lower LoA [s]	Upper LoA [s]	inside LoA [%]
Stride Time	155	0.000	0.015	-0.030	0.029	94.8
Stance Time	155	-0.029	0.018	-0.065	0.007	95.5
Swing Time	155	0.029	0.018	-0.007	0.065	95.5
Step Time	190	0.000	0.032	-0.062	0.063	92.1
Initial DST	161	-0.028	0.023	-0.074	0.018	95.7
Terminal DST	161	-0.029	0.026	-0.080	0.021	95.0

Table 6.4: Numeric values from the Bland-Altman analysis for all six gait parameters of the control (CTRL) group, including number of detected gait cycles ("n"), mean difference ("Mean Diff"; $\bar{d}$), the standard deviation ("StD"; σ), the upper and lower limit of agreement ("upper LoA", "lower LoA"; $\bar{d} \pm 2\sigma$), the number and percentage of data points inside the limits of agreement ("inside LoA").

The subjects from the healthy control group produced 155 gait cycles, which were collected by eSHOE and GAITRite. The histograms all exhibit narrow distributions with short tails. A small bias is present in the Bland-Altman plots of all parameters. Accuracy (mean difference) and precision (standard deviation) are as follows 0 ± 0.015 s for STR, -0.029 ± 0.018 s for STA, 0.029 ± 0.018 s for SWI, 0 ± 0.032 s for STE, -0.028 ± 0.023 s for IDS, -0.029 ± 0.026 s for TDS. The mean differences from all parameters in the CTRL group range from -0.029 to 0.029 s, with three parameters exhibiting even 0 s. Four out of six parameters have more than 95 % of all data located within the limits of agreement in the Bland-Altman plots. The percentages of values inside the limits vary between 95.0 9% and 95.7 %. Stride time (94.8 %) and step time (92.1 %) have less than 95 % inside the limits. Five parameters present a SD lower than 0.025 s, resulting in their limits of agreement being closer together than $\bar{d} \pm 0.05$ s. Although step time's mean difference is 0 s, it has a SD of 0.032 s and its limits are 0.062 to 0.063 s.
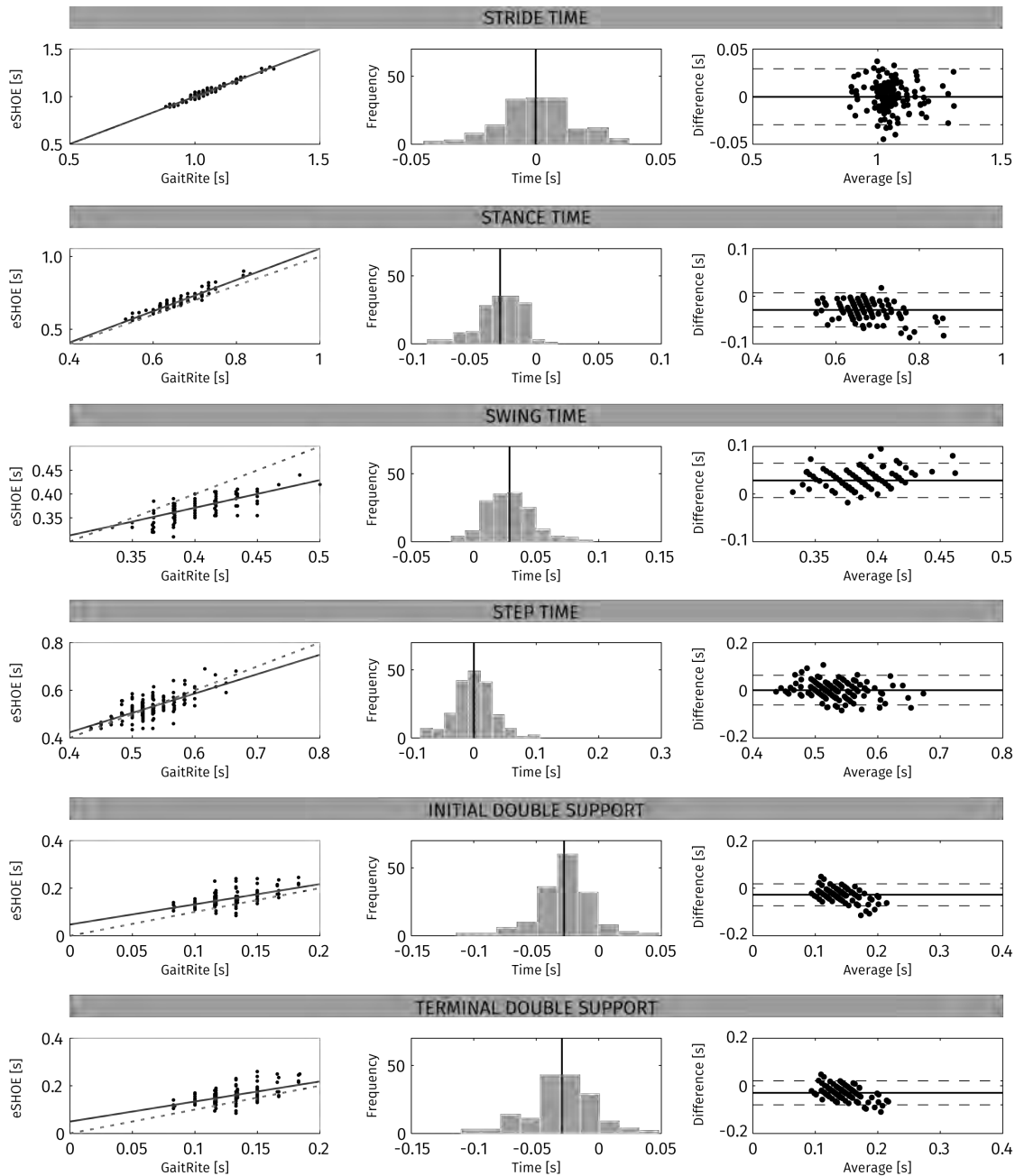
Figure 6.12: Analysis of agreement of control group data. Each row of graphs contains a scatterplot, a histogram and a Bland-Altman plot of one gait parameter. The scatterplots are made up of eSHOE values (y-axis) plotted against GAITRite values (x-axis), where each point represents one gait cycle. The plots also include a trend line (continuous) representing a least squares estimate from all data points and a 45°reference line (dashed) for the indication of perfect positive correlation. The histograms represent the distribution of the differences between GaitRite and eSHOE with the continuous line depicting the mean difference ($\bar{d}$). In the Bland-Altman plots the differences between GAITRite and eSHOE are displayed on the y-axis. The mean of the two methods, which represents an approximation of the true value, is plotted on the x-axis. The continuous line is the mean difference $\bar{d}$ and the two dashed lines stand for the lower ($\bar{d} - 2\sigma$) and the upper limit of agreement ($\bar{d} + 2\sigma$).

Patients

PAT Parameter	n	$\bar{d}$ [s]	σ [s]	Lower LoA [s]	Upper LoA [s]	inside LoA [%]
Stride Time	192	0.000	0.030	-0.059	0.059	94.8
Stance Time	191	-0.045	0.033	-0.109	0.020	93.7
Swing Time	190	0.045	0.030	-0.014	0.104	94.7
Step Time	216	0.004	0.062	-0.117	0.125	95.8
Initial DST	200	-0.045	0.033	-0.111	0.020	95.5
Terminal DST	199	-0.046	0.047	-0.139	0.047	96.0

Table 6.5: Numeric values from the Bland-Altman analysis for all six gait parameters of the patient (PAT) group. Details same as table 6.4.

In the patient group a total of 192 gait cycles were acquired. Accuracy and precision are 0 ± 0.03 s for STR, -0.045 ± 0.033 s for STA, 0.045 ± 0.030 s for SWI, 0.004 ± 0.062 s for STE, -0.045 ± 0.033 s for IDS, -0.046 ± 0.047 s for TDS. PATs mean differences from all parameters range from -0.046 to 0.045 s, one with 0 s. Three parameters exhibit more than 95 % of all data points inside the limits of agreement. Stride time (94.8%), stance time (93.7 %), swing time (94.7 %) are showing less than 95 % within the limits. The SDss from all except one parameter – step time – are less than 0.05 s. Therefore, the corresponding limits of agreement of those five parameters are narrower than $\bar{d} \pm 0.1$ s.
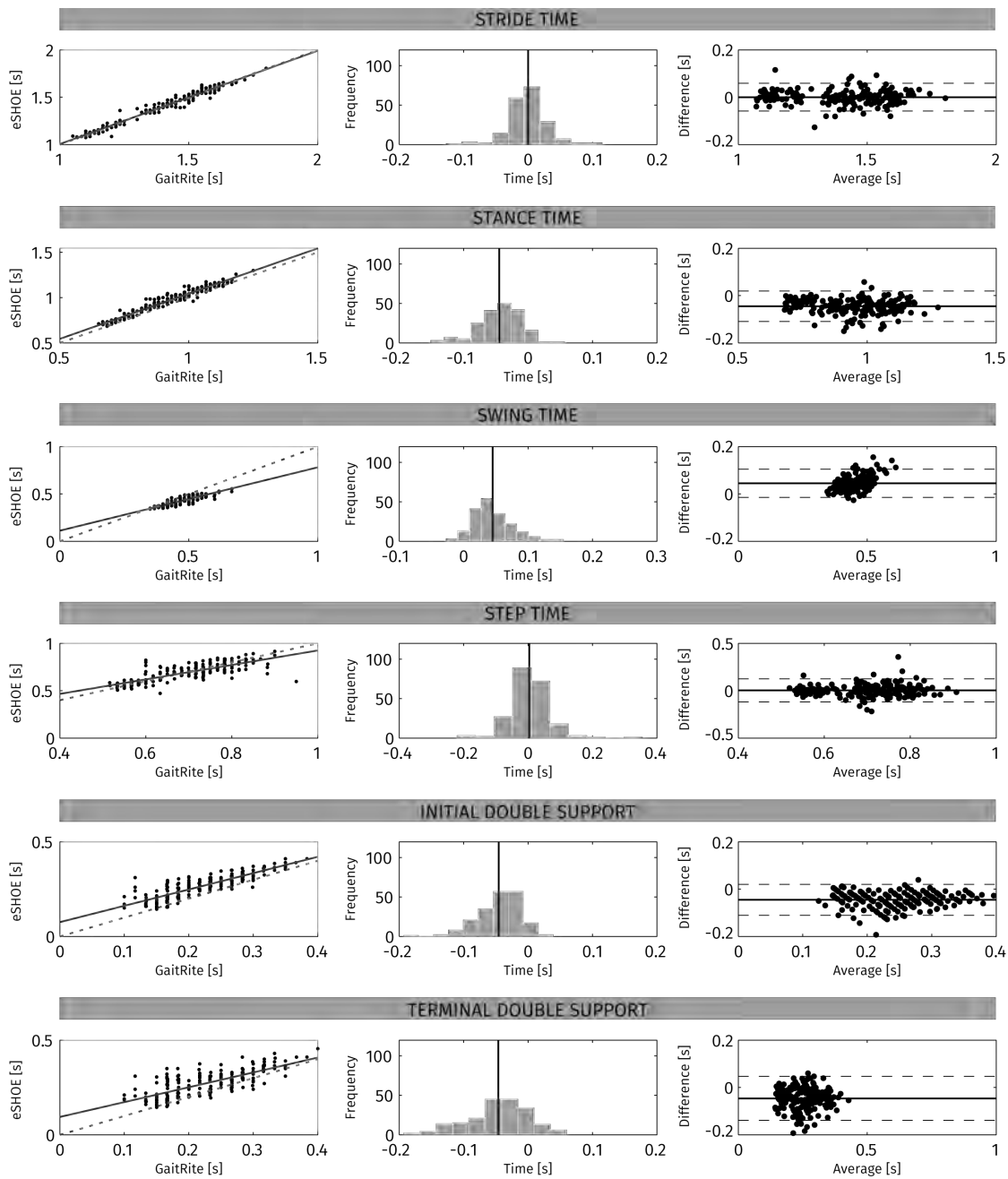
Figure 6.13: Analysis of agreement of patient group data. Details same as fig. 6.12.

6.2.2   Group differences

Results from the statistical analyses of the comparison of healthy subjects with patients and of healthy and affected leg in patients are presented within this subsection.

Differences between healthy subjects and patients

It was to be expected, that there is a certain difference in the gait parameters of healthy subjects and hip fracture patients. The unilateral injury inevitably leads to an asymmetric and, therefore, impaired gait. The visual analysis of both groups via box plots (fig. 6.14) gives a first, clear impression that there are differences between CRTL and PAT. The notched areas of none of the box plots are overlapping, which gives a first hint on significant differences.

When looking at the numeric values for all parameters from CTRL and PAT, as they are presented in tables 6.6 and 6.7 for eSHOE and GAITRite, the differences between median and mean also become obvious. In the eSHOE data there is an average difference

eSHOE	CTRL		PAT		Difference	
Parameter	Median	Mean	Median	Mean	Median	Mean
Stride Time	1.045	1.053	1.413	1.388	−0.368	−0.335
Stance Time	0.675	0.682	0.985	0.957	−0.310	−0.275
Swing Time	0.370	0.371	0.435	0.431	−0.065	−0.061
Step Time	0.525	0.528	0.700	0.691	−0.175	−0.164
Initial DST	0.150	0.155	0.270	0.264	−0.120	−0.109
Terminal DST	0.155	0.158	0.275	0.269	−0.120	−0.111

Table 6.6: Median, mean and SD of all six parameters, calculated from **eSHOE** data of both groups: CTRL and PAT.

in the medians and means of $-0.193\ s$ and $-0.176\ s$, respectively. These observations

GAITRite	CTRL		PAT		Difference	
Parameter	Median	Mean	Median	Mean	Median	Mean
Stride Time	1.050	1.053	1.408	1.388	−0.358	−0.335
Stance Time	0.650	0.653	0.933	0.912	−0.283	−0.259
Swing Time	0.400	0.399	0.483	0.476	−0.083	−0.077
Step Time	0.517	0.528	0.716	0.695	−0.199	−0.168
Initial DST	0.133	0.127	0.216	0.219	−0.083	−0.091
Terminal DST	0.133	0.129	0.217	0.223	−0.084	−0.094

Table 6.7: Median, mean and SD of all six parameters, calculated from **GAITRite** data of both groups: CTRL and PAT.
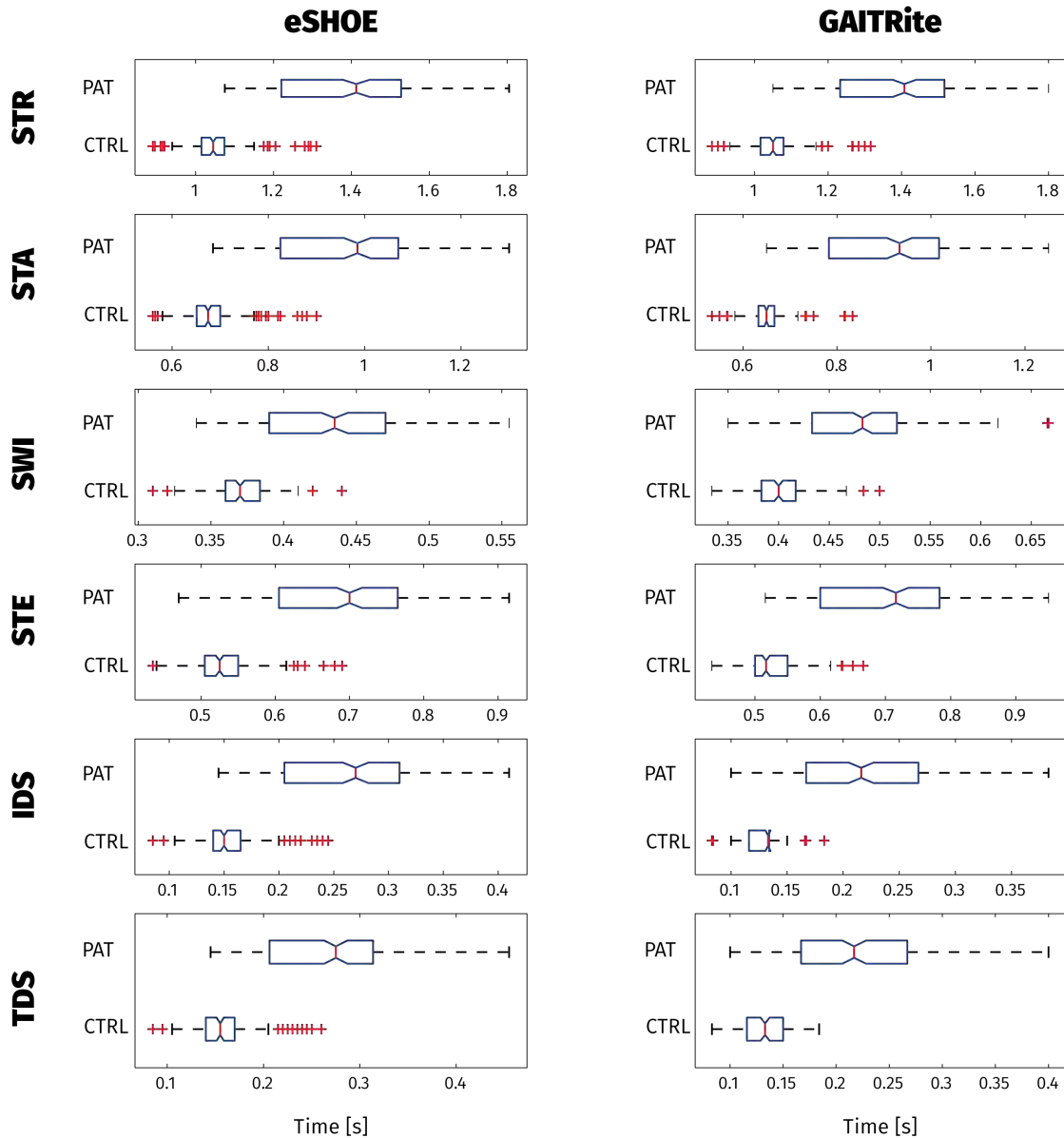
Figure 6.14: Visualization of the differences between CTRL and PAT data by means box plots. The left "column" contains the results from eSHOE data and the right column results from GAITRite data. Every "row" represents one of the six gait parameters: (1) Stride Time (STR), (2) Stance Time (STA), (3) Swing Time (SWI), (4) Step Time (STE), (5) initial double support time (IDS), (6) terminal double support time (TDS).

Parameter	eSHOE				GAITRite			
	Visual	χ^2	p (MWU)	p (KSO)	Visual	χ^2	p (MWU)	p (KSO)
STR	$\neq$	182.6	$4 \cdot 10^{-50}$	$3 \cdot 10^{-45}$	$\neq$	183.9	$3 \cdot 10^{-50}$	$3 \cdot 10^{-46}$
STA	$\neq$	182.6	$4 \cdot 10^{-50}$	$9 \cdot 10^{-47}$	$\neq$	199.8	$4 \cdot 10^{-50}$	$9 \cdot 10^{-46}$
SWI	$\neq$	121.2	$4 \cdot 10^{-32}$	$1 \cdot 10^{-28}$	$\neq$	138.6	$3 \cdot 10^{-34}$	$1 \cdot 10^{-30}$
STE	$\neq$	226.7	$3 \cdot 10^{-54}$	$8 \cdot 10^{-52}$	$\neq$	226.1	$6 \cdot 10^{-56}$	$8 \cdot 10^{-50}$
IDS	$\neq$	192.8	$4 \cdot 10^{-48}$	$4 \cdot 10^{-44}$	$\neq$	211.8	$7 \cdot 10^{-46}$	$4 \cdot 10^{-47}$
TDS	$\neq$	181.2	$7 \cdot 10^{-47}$	$6 \cdot 10^{-43}$	$\neq$	211.1	$3 \cdot 10^{-46}$	$6 \cdot 10^{-47}$

Table 6.8: Results from median-, Mann-Whitney U- and Kolmogoroff-Smirnov-test on eSHOE and GAITRite data for the comparison of both groups: CTRL and PAT.

have then been further evaluated by means of three statistical tests: (1) the median test, (2) the Mann-Whitney U-test (MWU) and (3) the Kologoroff-Smirnov-Omnibus Test (KSO). Results from all three statistical tests for eSHOE and GAITRite data - which were analyzed separately - are presented in table 6.8. The interpretation of the visual differences from the box plots in fig. 6.14 are located in the first and fifth column of table 6.8. The box plots of CTRL and PAT were considered to be equal ($\equiv$) when their notched areas overlapped and not equal ($\neq$) when they did not. For the statistical tests the level of significance was selected to be $\alpha = 0.1$. In the median test the critical value for the χ^2 test statistic which has to be exceeded (at a level of $\alpha = 0.1$) equals 1.64. For the remaining two tests table 6.8 already contains the corresponding p-values.

Whenever the result from a cell pointed to a decision in favor of the alternative hypothesis the cell is shaded. All χ^2 values are well above 2.71 and all p-values below the significance level. The average values for χ^2, p (MWU) and p (KSO) (over all parameters) are 181.2, $6.92 \cdot 10^{-33}$ and $6.92 \cdot 10^{-33}$ for eSHOE and 196.2, $5.55 \cdot 10^{-35}$ and $2.28 \cdot 10^{-31}$ for GAITRite.

Differences between healthy and affected leg in patients

It was suspected, that, within the patient data, there might be a detectable difference between the affected and the non-affected leg. To evaluate this hypothesis, a visual representation of the data as well as a statistical analysis has been performed. Figure 6.15 shows **box plots** of data from the non-affected leg, the affected leg and the controls as reference. Results from the statistical analyses in the form of **Sign Test** and **Sign Rank Test** (both non-parametric tests, chosen due to the non-normally distributed nature of the data) can be found in table 6.9. In this analysis, again, evidence is found that there is a clear difference between the data from the controls and the patient data, regarding both legs (independent of the presence of an injury). It also shows that there is a large variance in both legs of the patients, compared to the data from the controls. In the eSHOE data (left column of fig. 6.15) the medians appear to be different in stance time, swing time and initial double support time. GAITRite (right column of fig. 6.15), on the
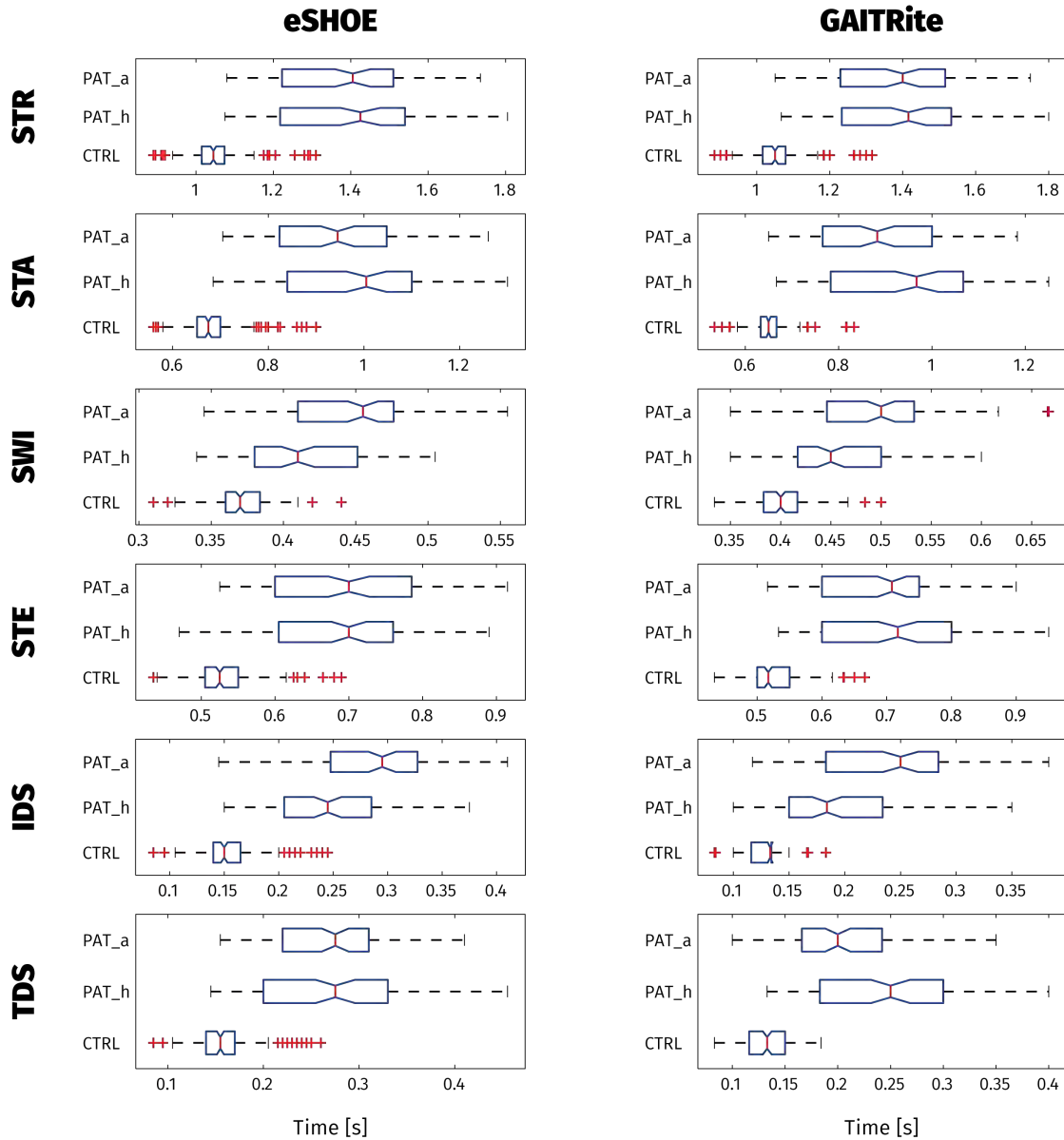
Figure 6.15: Visualization of the differences between CTRL, healthy and affected leg data from PAT by means box plots. The left "column" contains the results from eSHOE data and the right column results from GAITRite data. Every "row" represents one of the six gait parameters: (1) STR, (2) STA, (3) SWI, (4) STE, (5) IDS, (6) TDS.

Parameter	eSHOE			GAITRite		
	Visual	p (sign)	p (sign rank)	Visual	p (sign)	p (sign rank)
STR	$\equiv$	$2.98 \cdot 10^{-2}$	$5.08 \cdot 10^{-1}$	$\equiv$	$7.52 \cdot 10^{-1}$	$7.70 \cdot 10^{-1}$
STA	$\neq$	$3.75 \cdot 10^{-2}$	$7.91 \cdot 10^{-3}$	$\neq$	$6.11 \cdot 10^{-3}$	$7.00 \cdot 10^{-4}$
SWI	$\neq$	$2.97 \cdot 10^{-5}$	$8.13 \cdot 10^{-8}$	$\neq$	$1.88 \cdot 10^{-5}$	$7.50 \cdot 10^{-6}$
STE	$\equiv$	$9.87 \cdot 10^{-2}$	$1.45 \cdot 10^{-1}$	$\equiv$	$1.97 \cdot 10^{-2}$	$5.28 \cdot 10^{-2}$
IDS	$\neq$	$1.71 \cdot 10^{-5}$	$5.48 \cdot 10^{-9}$	$\neq$	$6.07 \cdot 10^{-8}$	$3.63 \cdot 10^{-10}$
TDS	$\equiv$	$3.15 \cdot 10^{-1}$	$8.68 \cdot 10^{-1}$	$\neq$	$1.15 \cdot 10^{-11}$	$8.90 \cdot 10^{-12}$

Table 6.9: Results from the comparison of healthy and affected leg by visual comparison, sign test and sign rank test. All three analyses have been performed on eSHOE and GAITRite data. A shaded background indicates the desired outcome or the statistical test decision in favor of the alternative hypothesis (H_1, claiming non-equality of the two samples.).

other hand, revealed differences in stance time, swing time, initial and terminal double support time.

Since the significance level was set to $\alpha = 0.1$ the resulting p-values have to be larger than this, in order to reject the null hypothesis (H_0), stating that both medians are equal.

The **Sign Test** rejects equal medians in the **eSHOE data** for four out of six parameters: stride time ($p = 0.030$), stance time ($p = 0.038$), swing time ($p = 0.00003$) and initial double support time ($p = 0.00002$) and doesn't reject it for the other two: step time ($p = 0.099$) and terminal double support time ($p = 0.315$).

The **Sign Rank Test's** results differ in one parameter from the Sign Test, namely stride time. Equal medians are rejected for three out of six parameters: stance time ($p = 0.008$), swing time ($p = 8.13 \cdot 10^{-8}$) and initial double support time ($p = 5.48 \cdot 10^{-9}$). The (null) hypothesis of equal medians cannot be rejected also for three parameters: stride time ($p = 0.508$), step time ($p = 0.145$) and terminal double support time ($p = 0.868$).

In the GAITRite data the sign test rejects equal medians four five out of six parameters: stance time ($p = 0.006$), swing time ($p = 0,00002$), step time ($p = 0.0197$), initial double support time ($p = 6.07 \cdot 10^{-8}$) and terminal double support time ($p = 1.15 \cdot 10^{-11}$). Only for stride time ($p = 0.752$) healthy and affected leg appear to have equal medians.

Again, sign rank results differ in one parameter from the sign test, namely step time. Rejection of the null hypothesis was confirmed in four out of six parameters: stance time ($p = 0.0007$), swing time ($p = 7.50 \cdot 10^{-6}$), initial double support time ($p = 3.63 \cdot 10^{-10}$) and terminal double support time ($p = 8.90 \cdot 10^{-12}$). It cannot be rejected for stride time ($p = 0.770$) and step time ($p = 0.053$). To summarize, in the **eSHOE data** two parameters, step time and terminal double support time show equality of medians in all three tests. Stride time ca also be considered equal, since (1) two out of three tests show

equality and (2) the stronger statistical test (the Sign Rank Test) points towards it. The **GAITRite data** shows equality in only two parameters, also stride time and step time. The latter is considered to be equal, because two of three tests point to it. Terminal double support time is, in contrast to the eSHOE results, (strongly) considered to be not equal.

6.3   Stride length estimation

The results from the stride length and distance estimation are structured according to the different sets of trials. There were:

1. outdoor measurements over 50 m (5000 cm) with the analysis of the total distance (6.3.1),
2. indoor measurements over 8.7 m (8700 cm) with, also, the estimation of the total distance (6.3.2) and
3. the estimation of the stride length (6.3.3).

In (1) the reference was the manually measured distance by measurement tape. For (2) and (3) the total distance was also pre-defined by measurement tape, but the verification of the distance and stride length estimation were performed via the VICON® optical motion capturing system.

Each of the categories has been evaluated three times, each with a different parameter set for the detection of the foot flat phase (FF) in the eSHOE data.

- A, the initial set, defining the FF or ZUPT phase to last from 15 to 35 % of the gait cycle, based on the data analysis in subsection 5.6.2.
- B, the optimized parameter-set (based on left eSHOE data), lasting from 10 to 33 %, which essentially reflects the original 10 to 30 % definition from [Perry, 1992].
- C, the optimized parameter-set (based on right eSHOE data), lasting from 9.5 to 17 %.

6.3.1 Total distance – 50 m (outdoor)

As mentioned in subsection 5.6.2, a total of 66 measurements were recorded. Two (number one and eight) had to be excluded from the evaluation, due to extreme outliers. The results of the 64 remaining test runs are presented in table 6.10 and fig. 6.16.

Parameter	Initial (set A)		Opt. I (set B) FF: 10-33%		Opt. II (set C) FF: 9.5-17%	
	L	R	L	R	L	R
Distance estimation [cm]	4610.1	4706.4	4677.0	4819.9	4698.3	4849.4
Estimation error [cm]	-389.9	-293.6	-323.0	-180.1	-301.7	-150.6
Estimation error σ [cm]	28.8	34.7	32.8	36.0	32.6	36.3
Normalized error [%]	-7.8	-5.9	-6.5	-3.6	-6.0	-3.0
Normalized σ [%]	0.6	0.7	0.7	0.7	0.7	0.7

Table 6.10: Three results (initial and after first and second optimization) for distance estimation, error and normalized error of the 50 m total distance estimation. Adopted from [Polasek, 2014].
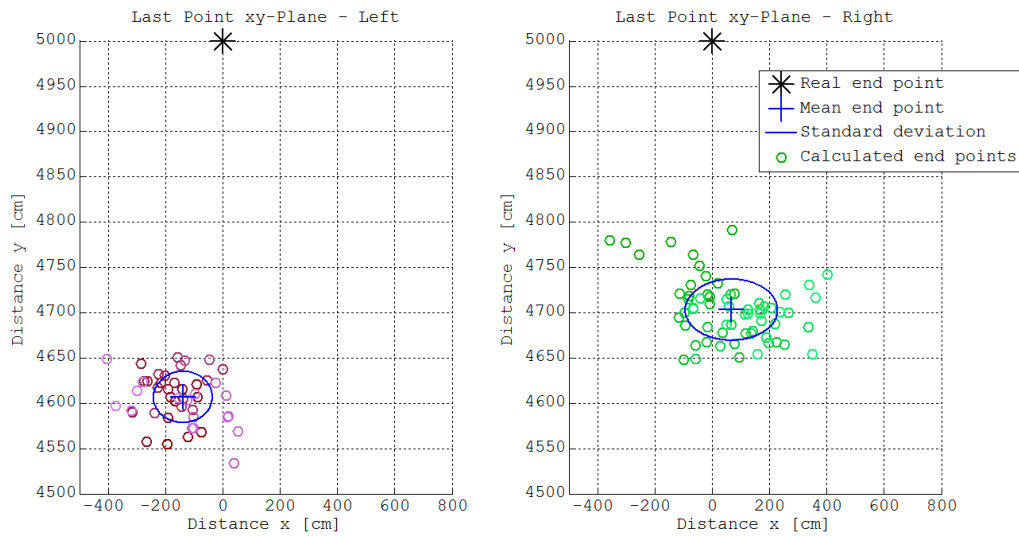
Figure 6.16: Manual measured complete distance versus the calculated end points in the walking plane, for the left and right foot. The mean and SD of the calculated end points is also indicated.

6.3.2 Total distance – 8.7 m (indoor)

The indoor trials have been evaluated two-fold, regarding the total distance and regarding the lengths of the single strides. In both cases estimations originating from eSHOE data were compared with measurement results from VICON. Table 6.11 shows the comparison of the total distance estimations from VICON and eSHOE, separately for left and right foot/shoe.

One obvious difference is that VICON was able to count more strides than eSHOE. This is due to the fact, that the eSHOE algorithms are not able to detect the very last strides in a walk, which are not "full-fledged" strides any more. When a person is asked to walk a certain distance, say from one marking on the floor to the next (as it was the task in these trials), then this person usually concludes this walk with a closed foot position at the second marking. This position is achieved (ideally) by more or less exactly reaching the marking with one foot and then setting the contralateral foot next to the ipsilateral one. Mostly, the contralateral foot does not perform a full physiological stride. It rather ends prematurely, somewhere in the middle of the swing phase. The eSHOE algorithm is not capable of detecting such "abnormal" strides as strides and, thereby, misses that stride completely. Therefore, three runs from the left foot and six runs from the right foot had to be excluded from the evaluation.

Parameter	Initial		Opt. I FF: 10-33%		Opt. II FF: 9.5-17%	
	L	R	L	R	L	R
Distance estimation [cm]	821.0	838.0	842.5	859,6	843.8	861.4
Estimation error [cm]	-49.0	-32.0	-27.5	-10.4	-26.2	-8.6
Estimation error σ [cm]	23.0	10.2	23.7	13.8	26.5	15.8
Normalized error [%]	-5.6	-3.7	-3.2	-1.2	-3.0	-1.0
Normalized σ [%]	2.6	1.2	2.7	1.6	3.0	1.8

Table 6.11: Total distance, distance estimation, error and normalized error of calculations in the x-y-walking-plane. [Polasek, 2014].

6.3.3 Stride length – indoor

For the evaluation of stride length also different strategies were applied. In general, stride length values from eSHOE and VICON were directly compared. The mean difference varied, depending from the inclusion or exclusion of the first and last few strides. Table 6.12 and table 6.12 show exemplary what happens to the mean difference, when all strides are included, and then when removing, the first, the last, the first and the last and the first and last two strides.

Cutting out the first and the last stride proved to be effective, in the sense that the SD could be reduced (significantly). After removing the first and last stride there was

Left foot	All	Cut first	Cut last	Cut first/last	Cut two first/last
Mean difference [cm]	-6.4	-7.6	-6.7	-8.0	-7.9
σ [cm]	9.2	8.1	7.1	4.5	3.9
Mean difference [%]	-4.4	-6.0	-4.4	-6.2	-6.1
σ [%]	12.5	10.8	8.6	3.5	3.0

Table 6.12: Total distance, distance estimation, error and normalized error of calculations in the x-y-walking-plane. [Polasek, 2014].

Right foot	All	Cut first	Cut last	Cut first/last	Cut two first/last
Mean difference [cm]	-4.7	-4.8	-5.2	-5.4	-5.5
σ [cm]	7.1	4.6	7.1	4.0	3.7
Mean difference [%]	-3.2	-3.6	-3.7	-3.1	-4.2
σ [%]	6.9	4.1	6.9	3.1	2.9

Table 6.13: Total distance, distance estimation, error and normalized error of calculations in the x-y-walking-plane. [Polasek, 2014].

	Initial		Opt. I FF: 10-33%		Opt. II FF: 9.5-17%	
Parameter	L	R	L	R	L	R
Mean difference [cm]	-8.0	-5.4	-4.6	-2.0	-3.6	-1.1
σ [cm]	4.5	4.0	5.2	4.6	4.8	4.2
Mean difference [%]	-6.2	-3.1	-3.5	-1.6	-2.7	-0.9
σ [%]	3.5	3.1	4.0	3.6	3.7	3.3

Table 6.14: Stride length error - eSHOE compared to VICON. [Polasek, 2014].

no more (significant) improvement. Therefore, this option (remove first and last stride) is used in all subsequent evaluations. Table 6.14 shows absolute and normalized mean difference for all three parameter sets and for left and right foot separately.

6.4 Monitoring of therapy progress based on eSHOE data gathered during multiple 10MWTs

As it was described in section 5.1 a series of measurements has been performed with each patient. During their stay at the hospital each subjects was tested multiple times. The actual number of measurements varied due to the different individual durations of the hospital stay.

The assessment by the help of which the therapy progress should be determined is the ten meter walk test (10MWT). For this test, the subject has to walk straight for a net length of ten meters at a comfortable walking speed. The gross length in this case was chosen to be 15 meters. This allowed for a 2.5 m "acceleration" and a 2.5 m "deceleration zone" at the beginning and at the end of the walking track.

After the application of the eSHOE gait analysis algorithms one measurement day's recording of one subject contains 6×2 vectors of data. Six gait parameters for each of the two legs. Vectors may differ in length from subject to subject and/or from measurement day to measurement day.

In the course of the pilot study a total of 576 vectors of data have been generated. 84 of these vectors or ($=$ 14 out of 50 datasets or measurement days) were excluded from the evaluation due to data corruption or extreme noise, which caused the algorithms to produce incorrect values. The affected datasets are all measurement days of F12 and F38, MD 1 and MD 2 of G57 and G68 and MD 1 of G82. Excluded datasets are also indicated as shaded cells in tables 6.17 and .

Before the actual evaluation of therapy progress, the results of a selection of reference measures are given. These will help to make a comparative connection between the clinically determined progress of the patients and the eSHOE gait parameter results. The following reference measures have been analyzed: (1) the progression of time needed to perform the 10MWT (see table 6.17 and fig. **??**), (2) the progression of walking speed (see table **??** and fig. **??**) and (3) the usage of walking aids of each subject during all measurements (table 6.18).

6.4.1 Test subjects' characteristics

Table 6.15 contains a list of patients' age (* at the point in time when they were admitted to the hospital), the body-mass index (BMI) and the diagnosis of the femur fracture, which includes: medial femoral neck fracture (MFNF), intertrochanteric femoral fracture (ITFF), subtrochanteric femoral fracture (STFF). Furthermore, the affected side or leg is indicated as well as the type of implant, which was used in the surgery after the fracture: total endoprosthesis (TEP), dynamic hip screw (DHS), proximal femur nail (PFN). The duration of the stay at the geriatric hospital (Sophienspital) of each patient varied and the actual number of days they did stay is documented in the column before the last. Lastly, the number of 10MWT measurements, which were carried out with each subject can be found in the last column. The mean age (by the time of admittance) of the

Subject ID	Age* [yrs.]	Diagnosis	Side	Implant	Stay [days]	Meas. #
G6	65	MFNF	left	TEP	21	4
F4	78	MFNF	right	TEP	31	5
F12	79	ITFF	right	DHS	22	5
G15	85	ITFF	left	DHS	16	3
G16	85	ITFF	left	PFN	20	4
F38	91	ITFF & STFF	right	DHS	20	4
G57	83	ITFF	right	DHS	30	6
G68	72	MFNF	left	BFNP	9	3
G82	79	MFNF	right	2 srews	14	4
G87	68	ITFF	right	PFN	16	5
G93	82	MFNF	left	BFNP	17	5
Mean	79		5 / 6		19.6	4
StD	8				6.5	1

Table 6.15: List of test subjects, including age, fracture type, affected side, type of implant, duration of stay in stationary geriatric care and number of conducted 10MWT eSHOE measurements.

patients, which were included in the study, was 79 ± 8 *yrs*, the youngest being 65 *yrs* and the oldest 91 *yrs*. Their BMI at that time was 24 ± 5 with a minimum of 15.3 and a maximum of 29.4. Five patients had the left leg affected and six had the injury on their right body half. Two subjects received a total endoprosthesis (TEP), four a dynamic hip screw (DHS), two a proximal femur nail (PFN), two a bipolar femoral neck prosthesis (BFNP) and one was treated with two screws. The average duration of the hospital stay was 19.6 ± 6.5 *days*, the shortest stay lasted for 9 *days* and the longest for 31 *days*. The total number of 10MWT measurements per subject ranged from 3 to 6 with a mean of 4 ± 1.

Subject ID	Age* [yrs.]	Height [m]	Weight [kg]	BMI	Leg length L	R
G6	65	1.58	38.2	15.3	84.5	84.7
F4	78	1.60	62.1	24.3	85.0	84.5
F12	79	1.58	60.0	24.0	87.0	88.0
G15	85	1.58	60.0	24.0	82.0	82.0
G16	85	1.61	57.9	22.3	93.0	93.5
F38	91	1.58	58.0	23.2	95.0	94.0
G57	83	1.58	53.0	21.2	84.0	85.0
G68	72	1.60	61.4	23.9	83.0	83.0
G82	79	1.61	57.4	22.1	79.0	78.5
G87	68	1.60	50.4	19.7	82.0	83.0
G93	82	1.51	67.0	29.4	84.0	84.0
Mean	79	1.59	56.90	24	85.45	85.62
StD	8	0.03	7.60	5	4.77	4.69

Table 6.16: List of patients, including basic anthropometric parameters: age, height, weight, body-mass index and leg length.

6.4.2 Reference measures and parameters

As an independent and external reference measure, the time it took the subjects to complete the 10MWT was taken with a stopwatch (table 6.17 and fig. 6.17). Since the walking distance was fixed and the time was taken, the walking velocity could also be calculated (table **??** and fig. **??**). By assigning numbers from 1 to 6 to each walking aid (in inverse weighting, 6 = no aid, 1 = most extensive aid) it was also possible to quantify the extent of each subject's mobility (see table xyz).

Duration of ten meter walk test

As documented in table 6.17, a certain progress in terms of walking speed, which resulted in shorter durations for the completion of the 10MWT, can be observed in all patients. The median of completion time from MD 1 to MD 5 progresses from 19.55 *to* 14.50 *s*. However, this reduction in completion time is not monotonous in nature. After a large drop from the first to the second measurement day of ~ 6 *s* (19.55 *to* 13.59 *s*) there is a slight increase of ~ 1.4 *to* 14.97 *s* on MD 3. On MD 4 the time continues to grow shorter by another ~ 0.6 *s*, reaching 14.35 *s*. Thereafter, it rises again, first by 0.15 *s* (to 14.50 *s*), then, on MD 6, to 18.99 *s*

The mean of completion time shows similar behavior. It starts at MD 1 with 24.89 *s* and progresses to 16.39 *s* and even 14.04 *s* (global minimum). But afterwards it exhibits a continuous increase from 14.22 *s* on MD 4 to 14.31 *s* and ending with 18.99 *s*.

Subject ID	MD 1	MD 2	MD 3	MD 4	MD 5	MD 6
G6	20.06	12.75	10.54	10.03	9.32	-
F4	38.29	21.24	16.15	15.09	14.52	-
F12	13.13	16.14	14.68	14.78	14.50	-
G15	52.97	19.52	16.49	-	-	-
G16	39.91	22.99	15.20	23.10	17.16	-
F38	11.44	11.08	10.12	12.36	-	-
G57	42.04	30.11	20.01	17.13	21.26	18.99
G68	10.88	10.37	9.83	-	-	-
G82	10.29	9.30	9.05	8.16	-	-
G87	19.55	13.59	17.39	12.98	12.82	-
G93	15.27	13.23	14.97	14.35	10.58	-
Median	19.55	13.59	14.97	14.35	14.50	18.99
Mean	24.89	16.39	14.04	14.22	14.31	18.99
StD	15.36	6.41	3.61	4.30	4.03	-

Table 6.17: List of all patients (rows) and measurement days (MD) (columns) with the corresponding 10MWT times (in seconds), averaged over three repetitions.

Walking aids / mobility

During their rehabilitation process patients receive walking aids, because they are not able to apply the full portion of body weight to their affected leg. Physicians together with physical therapists decide which walking aid is necessary and suitable throughout the rehabilitation process. The type of aid which is use may change over time when the patient's condition, mobility and performance improves. A generic order of necessary walking aids in a slow but continuously improving patient would be: (1) rollator (RL) (R), (2) roll mobile (RM), (3) two crutches (2C), (4) one crutch left (C-L) or one crutch right (C-R), (5) walking cane left (WC-L) or walking cane right (WC-R) and (6) no walking aid (none). The patients started out with three different walking aids 6×rollator (RL), 2×roll mobile (RM), 3×two crutches (2C). Approx. one week later, on MD 2, there were only 3×RL, 3×RM, still 3×2C, but already 2×WC. After another week, on MD 3 when still all patients were part of the study, there was only 1×RL left, which was replaced immediately after the measurement with 2C, 5×RM, 1×2C, 1×one crutch left (C-L), 2×WC and already 1×none. On MD 4 two subjects had progressed so far that they were discharged or moved on to another (more intense) rehabilitation facility. That left nine patients using 1×RM, 2×2C, 5×WC and 1×none. Only four subjects stayed until MD 5, one still using 2C and three WC.

In order to quantify the progress the subjects made related to the walking aids they used, each aid was assigned a number, from 1 to 6, following a self-defined (inverse) weighting scheme. There were six different walking aids in use, as was mentioned above. The walking aid which supported the subjects to the most extent was the rollator and the
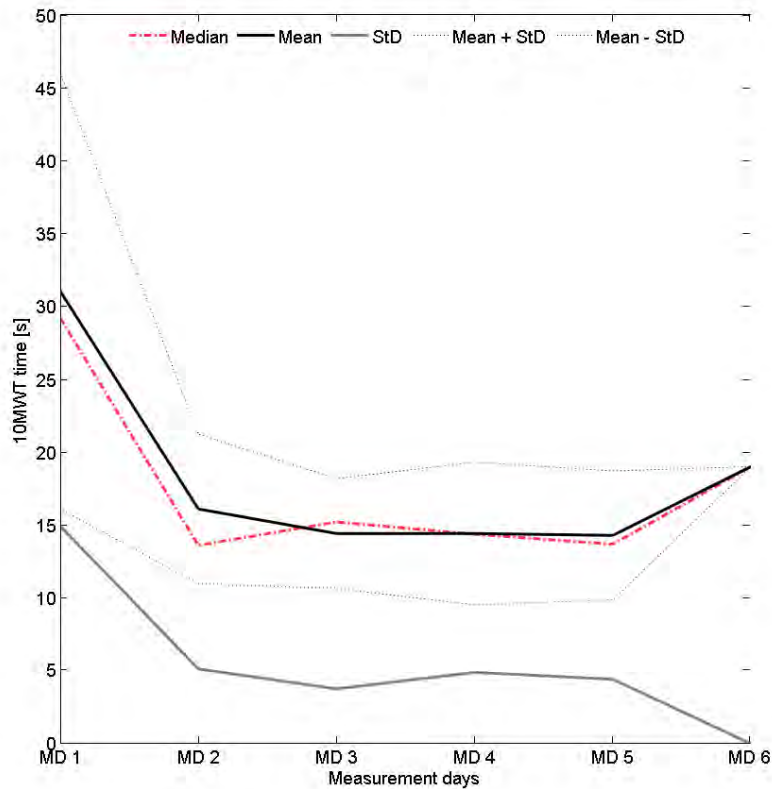
Figure 6.17: Progression of 10MWT times (y-axis) over measurement days (x-axis).

subject receives no support while using no aid. This means in turn, that the mobility can be considered best (6) when no walking aid is used and worst (1), when the rollator is in use. The scale in between is filled with numbers assigned to the rest of the walking aids, roll mobile (2), two crutches (3), one crutch (4), walking cane (5). The previous table (6.18) can then be transformed in a numeric one and a progression graph can be created (fig. 6.18).

Subject ID	MD 1	MD 2	MD 3	MD 4	MD 5	MD 6
G6	R*	RM	RM/WC-R	WC-R	-	-
F4	R	R	RM	WC-L	WC-L	-
F12	RM	2C	C-L	WC-L	WC-L	-
G15	R	RM	RM	-	-	-
G16	R	R	R/2C	2C	-	-
F38	RM	RM	RM	2C	-	-
G57	R	R	RM	RM	2C	WC
G68	2C	WC-R	WC-R	-	-	-
G82	2C	WC-L	none	none	-	-
G87	2C	2C	WC-L	WC-L	WC-L	-
G93	R	2C	2C	WC-R	-	-

Table 6.18: List of all patients (rows) and measurement days (MD) (columns) with the corresponding walking aids, which were used by each subject.

6.4.3   Progression of eSHOE gait parameters

Prior to the evaluation of the therapy progress by means of the gait parameters, detected by eSHOE, it has been determined whether or not there are any differences between the operated leg and the healthy leg. The outcome of this analysis affected the way in which the evaluation would proceed. Since the majority of all datasets (64 *out of* $72 = 89\%$) exhibited *no normal distribution* (see subsection 5.7.1), **non-parametric tests** were chosen for all further analyses.

Descriptive statistics for the evaluation of the therapy progress include the observation of the changes in each gait parameter's distribution (via the help of box plots) over the six measurement days. Furthermore, the courses of median, mean, standard deviation, interquartile range (IQR) and the total range have been documented in the form of tables and figures.
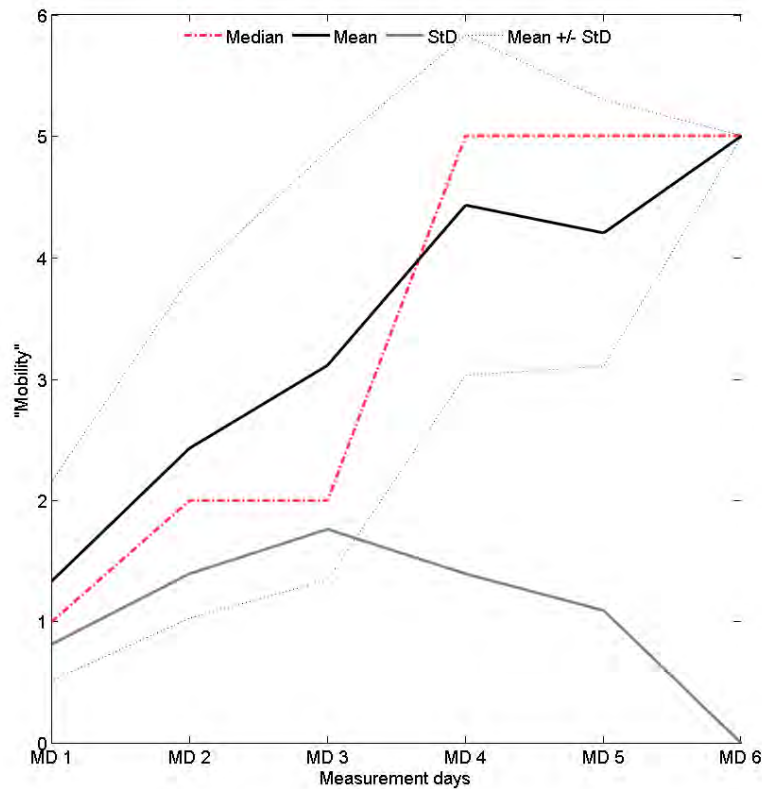
Figure 6.18: Progression of mobility by reference to the self-defined scale based on the used walking aids.

Differences between healthy and affected leg

Each parameter on each measurement day has been evaluated regarding statistical significant difference between healthy and affected leg, using *visual inspection of the distributions* (in the form of box plots) and the *sign rank test*. Table 6.19 contains the exceedance probabilities for all parameters and all measurement days. The statistical analysis (at the significance level of $\alpha = 0.1$) shows that there are no differences between the affected and the non-affected leg in stride time (STR) and in step time (STE). Stance time (STA), swing time (SWI), initial (IDS) and terminal double support time (TDS) on the other hand exhibit significant differences. This leads to a joint leg analysis of the rehabilitation progress for STR and STE. The other four gait parameters have to be inspected separately for each leg.

	STR	STA	SWI	STE	DS
MD 1	$8.21 \cdot 10^{-1}$	$1.24 \cdot 10^{-5}$	$2.43 \cdot 10^{-7}$	$2.57 \cdot 10^{-1}$	$2.49 \cdot 10^{-9}$
MD 2	$5.64 \cdot 10^{-1}$	$9.36 \cdot 10^{-21}$	$3.09 \cdot 10^{-27}$	$1.49 \cdot 10^{-1}$	$4.68 \cdot 10^{-28}$
MD 3	$4.44 \cdot 10^{-1}$	$2.37 \cdot 10^{-16}$	$8.62 \cdot 10^{-26}$	$7.81 \cdot 10^{-6}$	$9.78 \cdot 10^{-8}$
MD 4	$3.80 \cdot 10^{-1}$	$3.95 \cdot 10^{-9}$	$2.68 \cdot 10^{-10}$	$7.67 \cdot 10^{-1}$	$1.26 \cdot 10^{-9}$
MD 5	$8.35 \cdot 10^{-1}$	$3.59 \cdot 10^{-9}$	$3.29 \cdot 10^{-18}$	$1.20 \cdot 10^{-3}$	$1.66 \cdot 10^{-13}$
MD 6	$8.89 \cdot 10^{-1}$	$4.93 \cdot 10^{-2}$	$3.67 \cdot 10^{-2}$	$8.27 \cdot 10^{-1}$	$6.86 \cdot 10^{-3}$

Table 6.19: Sign rank test results for the comparison of healthy and affected leg.

Stride Time (STR)

The fluctuation range of Stride Time's median is 0.135 s (1.39 to 1.525 s) and 0.148 s from the mean (1.414 to 1.562 s). There is no clear tendency in any direction. The standard deviation (SD) is reduced from 0.677 s on MD 1 to 0.307 s on MD 2 ($\sim < 50$ %). By MD 3 it has reached almost one third of it's initial value, 0.236 s. Thereafter, on MD 4, there is another (slight) increase to 0.285 s and it finally continues to drop to 0.118 s on MD 5 and 0.111 s on MD 6. In total, the StD is reduced by 84 %. Interquartile range (IQR) and total range show courses similar to StD, with decreases of 67 % and 85 %.

(a) Box plot.

(b) Line plot.
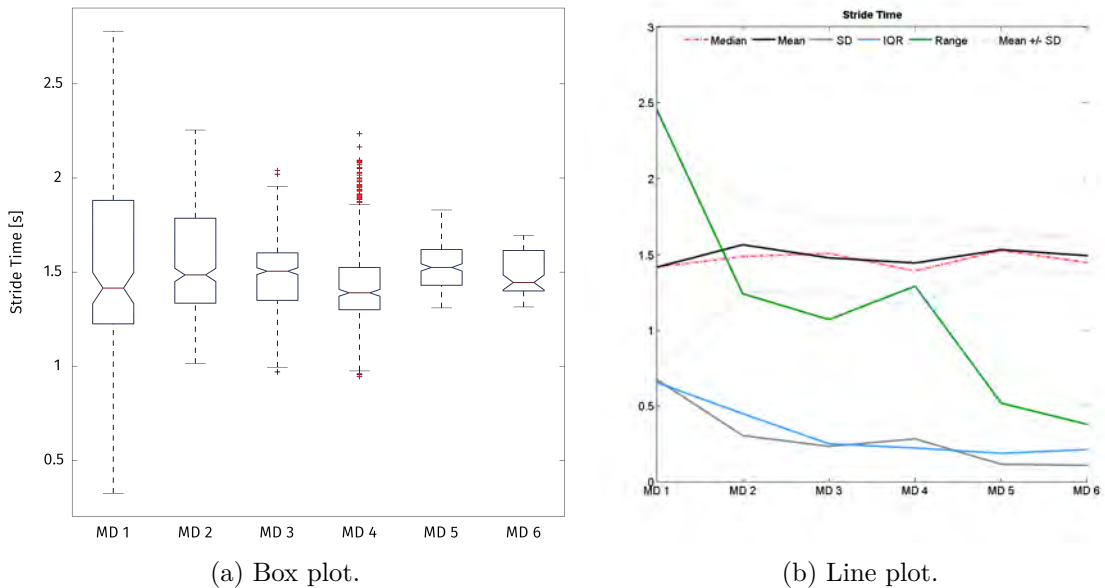
Figure 6.19: Progression of Stride Time (STR) over measurement days (x-axis).

STR	MD 1	MD 2	MD 3	MD 4	MD 5	MD 6
Median	1.415	1.485	1.505	1.390	1.525	1.445
Mean	1.414	1.562	1.476	1.442	1.530	1.490
StD	0.677	0.307	0.236	0.285	0.118	0.111
IQR	0.656	0.451	0.253	0.225	0.190	0.215
Min	0.325	1.015	0.970	0.945	1.310	1.315
Max	2.780	2.255	2.040	2.235	1.830	1.695
Range	2.455	1.240	1.070	1.290	0.520	0.380

Table 6.20: Numerical values for Stride Time progress.

Stance Time (STA)

Stance Time's median and mean on the affected leg vary by 0.117 s (from a minimum on MD 4 of 0.943 s to a maximum on MD 5 of 1.060 s) and 0.071 s (from 0.976 s on MD 4 to 1.048 s on MD 2). There is no continuous increase or decrease from MD 1 to MD 6. Standard deviation decreases continuously from 0.493 s to 0.089 s with the exception of MD 4 (82 % reduction). The IQR proceeds from 0.450 s to 0.178 s (61 % reduction) and the total range from 1.980 s to 0.275 s (86 % reduction).
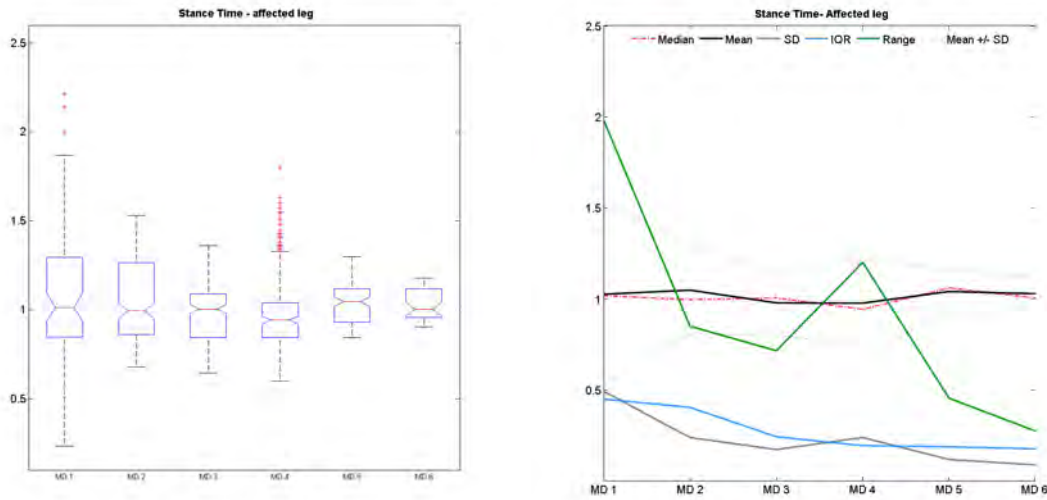
(a) Box plot.　　　　　　　　　　　　(b) Line plot.

Figure 6.20: Progression of Stance Time (STA) (affected leg).

On the healthy leg the STA' median and mean proceed from 1.020 s to 0.990 s (fluctuation of 0.110 s) and 1.117 s to 1.042 s (fluctuation of 0.113 s). Standard deviation starts out with 0.599 s and drops to 0.094, a reduction of 84 %. The IQR is even larger on the

STA-A	MD 1	MD 2	MD 3	MD 4	MD 5	MD 6
Median	1.018	0.995	1.005	0.943	1.060	1.005
Mean	1.025	1.048	0.978	0.976	1.040	1.028
StD	0.493	0.239	0.173	0.240	0.119	0.089
IQR	0.450	0.405	0.244	0.195	0.189	0.178
Min	0.235	0.680	0.645	0.600	0.845	0.905
Max	2.215	1.530	1.360	1.800	1.300	1.180
Range	1.980	0.850	0.715	1.200	0.455	0.275

Table 6.21: Numerical values for Stance Time progress [s] on the affected leg.

healthy leg on the first measurement day with $0.740\ s$ and settles on a similar amount as on the affected leg on MD 6, namely $0.186\ s$, representing a decrease of 75 %. The total range also has a larger initial value, $2.255\ s$, and is reduced to similarly small 0.280 (88 % reduction).
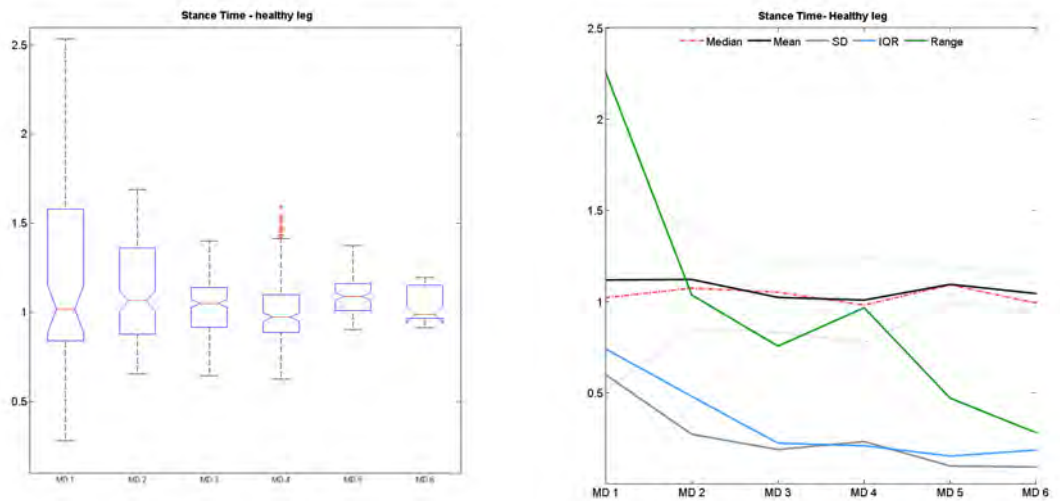
(a) Box plot.

(b) Line plot.

Figure 6.21: Progression of Stance Time (STA) (healthy leg) over measurement days (x-axis).

Both legs compared show differences between their means ($affected\ leg - healthy\ leg$) which are consistent over all six measurement days: $0.092, 0.072, 0.044, 0.031, 0.053, 0.015$. From MD 1 to MD 4 there is a constant reduction, on MD 5 it increases until it drops again on MD 6 below the level of MD 4. Generally, STA is always higher on the healthy leg but the difference grows smaller by 84 %.

STA-H	MD 1	MD 2	MD 3	MD 4	MD 5	MD 6
Median	1.020	1.073	1.050	0.980	1.090	0.990
Mean	1.117	1.120	1.022	1.007	1.093	1.042
StD	0.599	0.273	0.189	0.233	0.099	0.094
IQR	0.740	0.480	0.224	0.210	0.154	0.186
Min	0.280	0.655	0.645	0.625	0.905	0.915
Max	2.535	1.690	1.400	1.590	1.375	1.195
Range	2.255	1.035	0.755	0.965	0.470	0.280

Table 6.22: Numerical values for Stance Time progress on the healthy leg.

Swing Time (SWI)

Swing Time's mean and median on the affected leg exhibit no clear tendency in either direction during the six measurement days. They fluctuate between 0.410 s (min) and 0.518 s (max) and 0.410 s (min) and 0.518 s (max).

(a) Box plot. (b) Line plot.
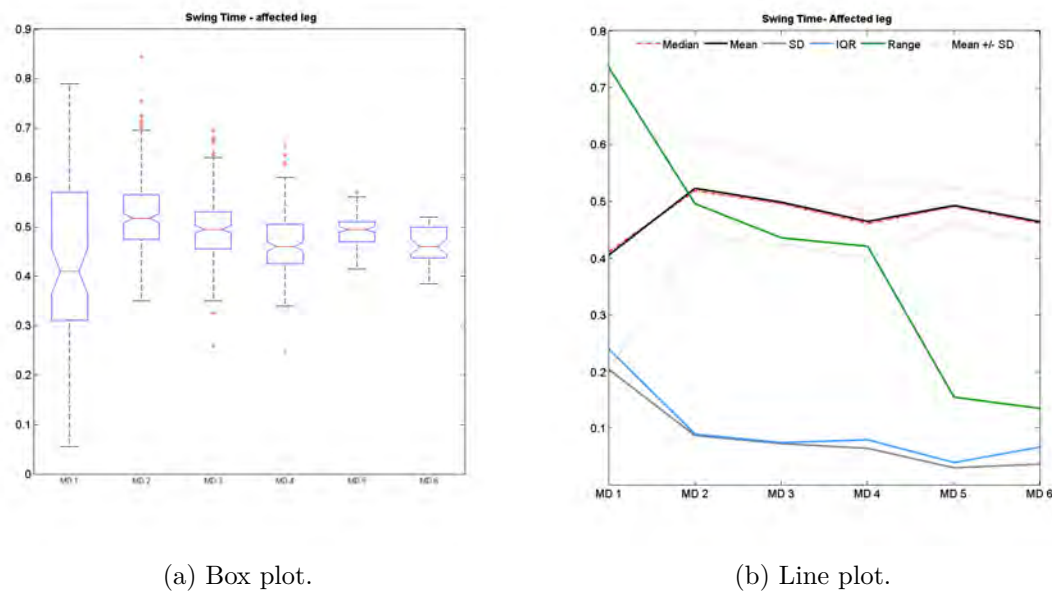
Figure 6.22: Progression of Swing Time (SWI) (affected leg).

Much like the affected leg, the healthy leg's SWI median and mean only vary by 0.108 s and 0.169 s. StD, IQR and range are constantly growing smaller, and end up reduced by 80 %, 82 % and 72 %.

The comparison of healthy and affected leg here also exhibit differences, although with minus-sign, which grow smaller during the stay. SWI means, affected leg minus healthy leg, progress from MD 1 to MD 6: $-0.119, -0.086, -0.043, -0.025, -0,054, -0.017$. Therefore,

SWI-A	MD 1	MD 2	MD 3	MD 4	MD 5	MD 6
Median	0.410	0.518	0.495	0.460	0.490	0.460
Mean	0.404	0.522	0.498	0.464	0.492	0.463
StD	0.204	0.088	0.073	0.065	0.031	0.037
IQR	0.240	0.090	0.075	0.080	0.040	0.068
Min	0.055	0.350	0.260	0.245	0.415	0.385
Max	0.790	0.845	0.695	0.665	0.570	0.520
Range	0.735	0.495	0.435	0.420	0.155	0.135

Table 6.23: Numerical values for Swing Time progress.

(a) Box plot.

(b) Line plot.
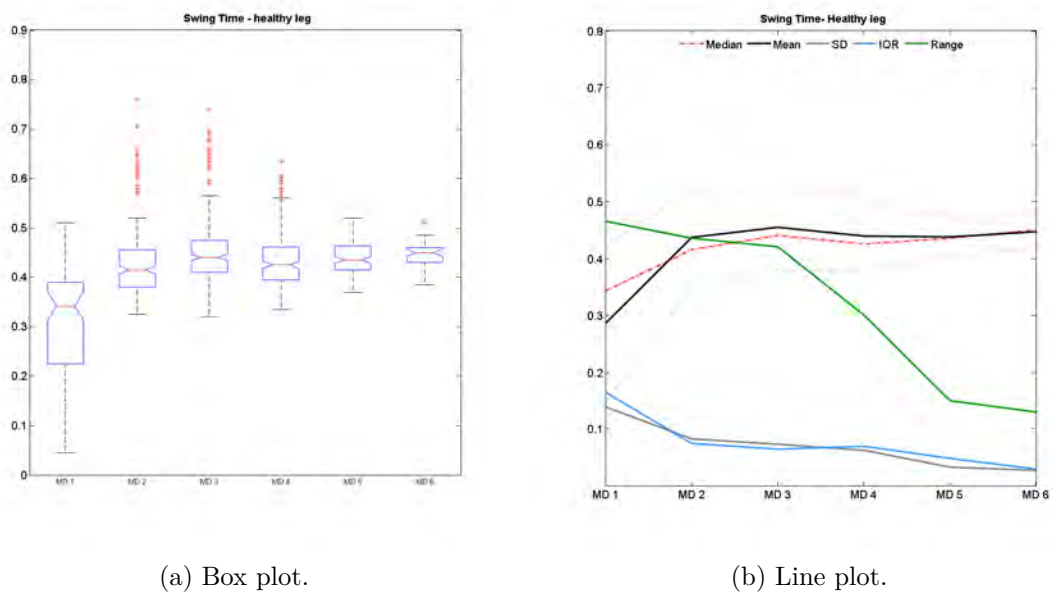
Figure 6.23: Progression of Swing Time (SWI) (healthy leg).

SWI on the healthy leg is always shorter and the difference is reduced by 86 % from first to last day.

SWI-H	MD 1	MD 2	MD 3	MD 4	MD 5	MD 6
Median	0.342	0.415	0.440	0.425	0.435	0.450
Mean	0.285	0.436	0.454	0.439	0.437	0.446
StD	0.139	0.083	0.074	0.063	0.033	0.028
IQR	0.165	0.075	0.065	0.070	0.049	0.030
Min	0.045	0.325	0.320	0.335	0.370	0.385
Max	0.510	0.760	0.740	0.635	0.520	0.515
Range	0.465	0.435	0.420	0.300	0.150	0.130

Table 6.24: Numerical values for Swing Time progress.

Step Time (STE)

Step Time' median and mean are fluctuating by 0.065 s (0.700 to 0.765 s) and 0.075 s (0.706 to 0.781 s). As in STR, the standard deviation (SD) drops during the first three measurement days(0.346, 0.161, 0.123), rises again on the fourth (0.149), but comes to a global minimum on the last MD (0.060). The IQR decreases continuously from MD 1 to MD 5 by almost two thirds (from 0.388 to 0.105 s) and on MD 6 there is a 5 % increase (to 0.115 s). Much like the StD, the total range reduces from MD 1 to MD 3 (from 1.325 to 0.645 s), rises the next day (0.75) and then continues to drop further (from 0.34 to 0.205 s). In total there are reductions in StD, IQR and range of 83 %, 72 % and 85 %.
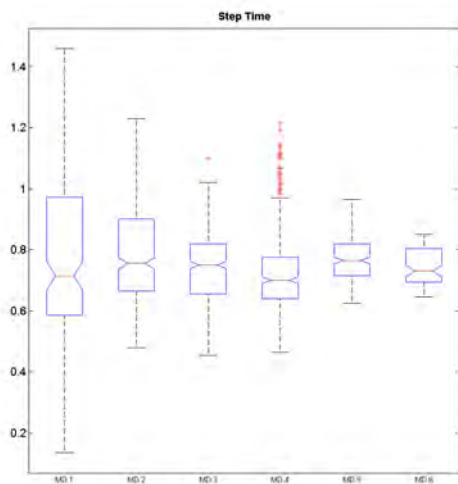
(a) Box plot.
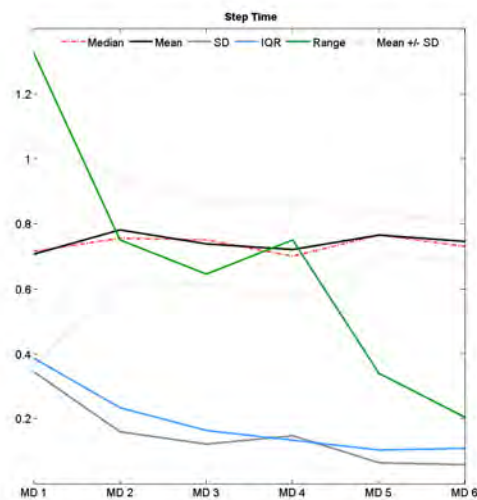
(b) Line plot.

Figure 6.24: Progression of Step Time (STE) over measurement days (x-axis).

177

STE	MD 1	MD 2	MD 3	MD 4	MD 5	MD 6
Median	0.715	0.755	0.750	0.700	0.765	0.730
Mean	0.706	0.781	0.738	0.721	0.765	0.745
StD	0.346	0.161	0.123	0.149	0.066	0.060
IQR	0.388	0.235	0.165	0.135	0.105	0.110
Min	0.135	0.480	0.455	0.465	0.625	0.645
Max	1.460	1.230	1.100	1.215	0.965	0.850
Range	1.325	0.750	0.645	0.750	0.340	0.205

Table 6.25: Numerical values for Step Time progress.

Double support time (DS)

Double support time on the affected leg does not experience noteworthy overall change. Median and mean start out on MD 1 at 0.335 s and 0.400 s. Both are decreasing until MD 3 to 0.285 s and 0.275 s. After that, however, $\bar{DS}-A$ and $\tilde{DS}-A$ continue to rise again until MD 5, reaching 0.320 s and 0.323 s. On the last day a final drop takes place, leaving median and mean at 0.290 s and 0.300 s. Standard deviation declines steadily with the exception of MD 4, where it rises by 0.001 s. IQR and total range are reduced continuously. On MD 6 StD, IQR and range experienced a reduction of 87 %, 77 % and 91 %.
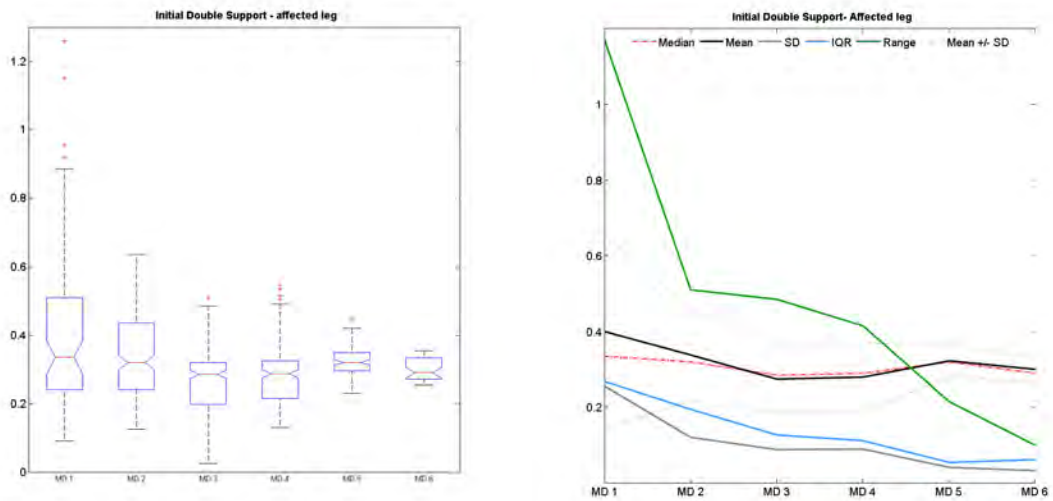
(a) Box plot.   (b) Line plot.

Figure 6.25: Progression of double support time (DS) (affected leg).

On the healthy leg the behavior of median and mean is a little more erratic.

DS-A	MD 1	MD 2	MD 3	MD 4	MD 5	MD 6
Median	0.335	0.320	0.285	0.290	0.320	0.290
Mean	0.400	0.338	0.275	0.280	0.323	0.300
StD	0.256	0.121	0.089	0.090	0.042	0.034
IQR	0.269	0.195	0.127	0.113	0.055	0.062
Min	0.090	0.125	0.025	0.130	0.230	0.255
Max	1.260	0.635	0.510	0.545	0.445	0.355
Range	1.170	0.510	0.485	0.415	0.215	0.100

Table 6.26: Numerical values for double support time-A progress.
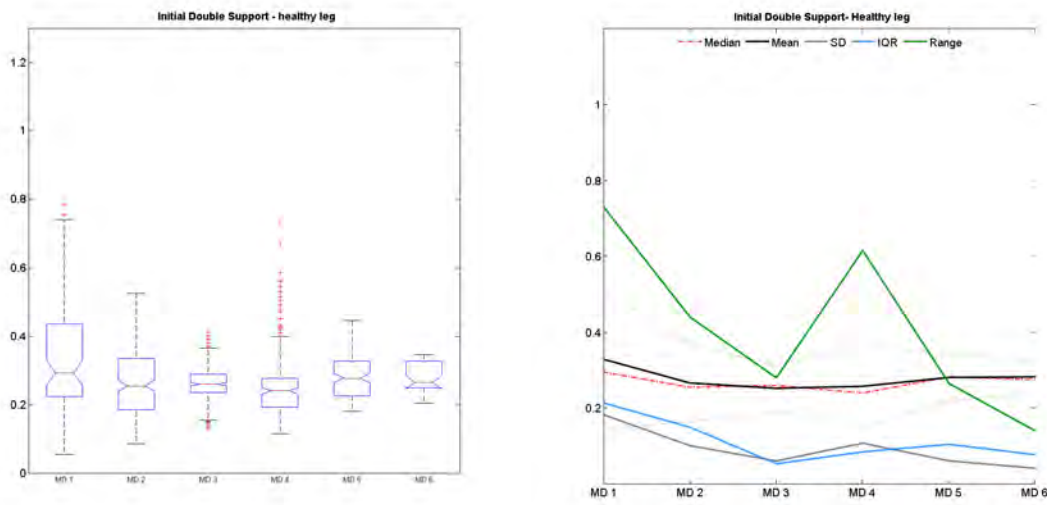
(a) Box plot.

(b) Line plot.

Figure 6.26: Progression of double support time (DS) (healthy leg).

DS-H	MD 1	MD 2	MD 3	MD 4	MD 5	MD 6
Median	0.295	0.255	0.260	0.240	0.283	0.275
Mean	0.329	0.266	0.252	0.258	0.281	0.282
StD	0.183	0.101	0.061	0.108	0.061	0.042
IQR	0.214	0.150	0.054	0.085	0.105	0.077
Min	0.055	0.085	0.130	0.115	0.180	0.205
Max	0.785	0.525	0.410	0.730	0.445	0.345
Range	0.730	0.440	0.280	0.615	0.265	0.140

Table 6.27: Numerical values for double support time-H progress.

CHAPTER 7

Discussion

7.1 Limitations of current gait analysis methods

In spite of all the achievements and insights that clinical gait analysis has provided, there are still issues regarding practicability, everyday relevance and costs. Gait analysis nowadays relies on two to three basic concepts: (a) motion analysis labs for extensive and quantitative evaluation, (b) visual observation from experts for a quick qualitative examination and, most recently, (c) wearable devices. Most stationary and - unfortunately also many - wearable motion analysis tools, which are currently available, are expensive to set up and maintain, require a lot of space and can also be cumbersome. Furthermore, instrumented gait analysis requires medical or technical professionals to operate the required materials. Therefore, their usage is limited to in-patient settings, such as hospitals and rehabilitation clinics.

Patients cannot benefit from such systems in their own homes and miss further documentation of the rehabilitation process after discharge from inpatient care. In a majority of cases measurements are still bound to a certain room in a hospital, rehabilitation clinic or equivalent. Two major consequences are that (1) the space in which the tested person can move - and with it the walking distance - is constrained. Walking of a rather short distance often reduces the quality of the measurement results and their everyday relevance, e.g. because walking always includes an acceleration and a deceleration phase, during which gait parameters do not reach their regular values [Oberg et al., 1993, Auvinet et al., 1999, Moe-Nilssen and Helbostad, 2004]. (2) The laboratory situation, in which a test person has to perform the analysis, always represents an "in the spotlight" sort of situation. Meaning the person is well aware of being observed, measured and evaluated, plus there are always other people in the same room with the subject, who are performing administrative tasks such as operating equipment. The relevance of the measurement results of such a small and biased **crop/cutout** for everyday life conditions is considered to be limited [Muro-de-la Herran et al., 2014]. There are studies which suggest, that

better insight might be provided, if patients (suffering from Parkinson's disease) were analyzed within their own homes and communities [Morris et al., 2001].

In the case of trauma surgery (e.g. ankle fractures) standard aftercare procedures, which are primarily based on radiographic controls, have not changed since they were established ([4] in [Braun et al., 2015a]). However, it has been shown that conventional clinical and radiographic controls have limited reliability [Augat2014] and also exhibit weak biomechanical correlation ([8,9] in [Braun et al., 2015a]). This reduces the actual feasibility and practicability to an unacceptable level.

7.2 Overall challenges (of gait pattern detection with eSHOE)

During the study and, thereby, during the numerous utilizations of eSHOE several obstacles were encountered and (partly) overcome. Most of them were technical shortcomings, resulting from trade-offs due to time or budget constraints. Overall, eSHOE's design and implementation was sufficient to cause no discomfort or danger to the wearers (most vulnerable of them, patients in the pilot study) and, at the same time, to provide usable measurement results.

Usability was definitely an issue. Although, since this was not the focus of this project, it was not the primary concern to make eSHOE perfectly usable for potential end-users. It was clear that, for the scope of this thesis that mostly technically savvy persons will operate the system. But, the prospect of commercialization has always been in mind as well. This meant that in the future the user group might shift from technical to non-technical personnel, such as physicians, therapists or even patients themselves.

Secondary aspects have been taken into account in order to ensure a smooth transition into a commercial product. Hardware and software were designed to be easy-to-use and thereby provide good accessibility, independent of the user's technical prowess. The measurement hardware was completely integrated into the everyday object of a shoe insole, so that there will be no stigmatization and analysis can be performed unobtrusively. Changes to the insoles general design were kept to an absolute minimum, to ensure no change in comfort to the user.

It has to be stated that, despite of all the precautionary measures, eSHOE is not yet entirely ready for usage at home and/or the operation by patients (or older adults) alone, unless they were properly instructed.

The main known obstacles for independent use by the target group (of older adults) are that the control components (the on/off-button, the LED, the micro-USB plug) have very small dimensions. The on/off push-button is only $1.7 \times 1.2\ mm$ wide, which makes it potentially difficult to handle for (older) persons who might suffer from limited fine motor skills. Although the LED is a tricolor one and has a rather wide viewing angle of 130°, its dimensions are also small $3.2 \times 1\ mm$ and its luminous intensity limited

280 *mcd*. These physical condition, in turn, limits the feedback to users with possibly reduced visual function. Additionally, a single LED can only convey so much information. It's three basic colors can be combined to a practical maximum of six (mixed) colors and blinking can be added the the static glowing, which would result in a total of 12 states. Even for an experienced user remembering 12 states and their interpretation by heart presents a challenge. Therefore, this concept's applicability for non-professional users is very poor. The handling and use of a micro-USB cable and the corresponding plug comes as natural to any tech-savvy person. Due to it's, also, small dimensions, the orientation-dependency and the certain amount of pressure needed in order to plug it in correctly, handling it can be challenging to people with little experience with consumer electronics and/or reduced fine motor skills.

Since these and some other challenges are well-known, thought concepts have already been developed to remedy some of the known shortcomings in the future. For instance, a button-less user-interaction strategy can be implemented (e.g. control via gestures/movements). Due to the small size of the built-in PCB there is little option for incorporating unser interface components (buttons, screens) of a larger size. But the motion sensing nature of the PCB can be utilized to implements basic controls in the form of dynamic movements (e.g. gestures) or static positions (e.g. upside down placement to turn off). Charging eSHOEs battery by means of a micro USB cable (with a wall power adapter) can be a tedious procedure. Micro USB has a rather tiny plug and the right orientation must be provided for the plug to fit into the socket. This can be difficult to manage for persons with limited fine motor skills (due to several reasons like advanced age, illness or disease). As an alternative (and also to meet current technical standards), the inductive standard "qi" can be used. In combination with gesture controls this would contribute to achieve a system design which is even more unobtrusive than the current prototypes. Because then there would be no openings (for sockets or buttons) in the insole and, from the outside, it would be completely indistinguishable from an ordinary orthopedic insole.

Limited space inside the insole, which can be utilized to integrate electronic components, also limits the dimensions of the battery, which can be integrated to power the embedded system. There is a linear relationship between a battery's volume and its capacity. Which means that the total energy capacity will always be limited to a certain amount. In theory, by generating power while walking, this can be compensated. An unsuccessful attempt has been made to implement an energy harvesting solution in combination with the eSHOE system in the course of a master's thesis [Haftner, 2015]. The necessary technology and the potential for producing energy through the occurring forces, momentums and displacements are there. But it wasn't feasible to produce voltages or currents of sufficient magnitude to charge or at least buffer the battery in any way with the available resources. With the right budget, increased know how and more focused development it is conceivable that an increase in battery life by means of energy harvesting is possible.

Another potential obstacle for usage by older persons is the fact that, for eSHOE to operate properly, a PC software application is necessary. This limits the accessibility to people who own are familiar with the operation of a PC or laptop. Additionally, the

available software (shoeCONTROL) was designed for research purposes and while it is possible to teach non-technical personnel (e.g therapists) to use the software, it is still not suitable for digital immigrants.

7.3 Feasibility of pattern detection and gait event extraction (algorithm accuracy)

The detection of recurring patterns in the sensor- and axes- specific data with reference patterns, generated by autocorrelation, proved to be very successful, according to table 6.1 in section 6.1. However, there were also several patterns with medium to bad results, such as ACC-X, the acceleration data along the medial/lateral axis, with only 25.54 % and 17.55 % detected cycles in left and right data, respectively. ACC-Z, acceleration data along the cranial/caudal axis, exhibited 55.1 % left and 4.8 % right. GYRO-Y, angular velocity data around the anterior/posterior axis with 39.8 % left and 15.9 % right. The most likely reasons for the low reproducibility of these patterns lies in the fact, that during straight walking there are large interpersonal variations. This conclusion is supported by the patterns of these axes themselves or rather their (low) amplitudes (fig. 6.2, 6.4) compared to those signals with more pronounced traces (fig. 6.3). The ACC-X patterns only range $\sim$ $from -10$ to 10 m/s^2 ($\Delta = 20$ m/s^2), ACC-Z $\sim$ $from$ 10 to 25 m/s^2 ($\Delta = 15$ m/s^2), whereas ACC-Y exhibits an amplitude range of $\sim$ $from -40$ to 20 m/s^2 ($\Delta = 60$ m/s^2). That means that ACC-X and ACC-Z have only 30 % and 25 % of ACC-Y's amplitude range. Additionally, these rather low amplitudes increase the susceptibility to noise. Angular velocities around the anterior/posterior (GYRO-Y) and the cranial/caudal (GYRO-Z) axes also exhibit considerably smaller amplitudes than angular velocity around the medial/lateral axis (GYRO-X). Figures 6.5, 6.6 and 6.7 show the representative patterns for GYRO-X to range from $\sim$ $from -400$ to 400 $ř/s$ ($\Delta = 800$ $ř/s$), whereas GYRO-Y and GYRO-Z have a ranges of $\sim$ $from -300$ to 100 $ř/s$ ($\Delta = 400$ $ř/s$) and $\sim$ $from -150$ to 150 $ř/s$ ($\Delta = 300$ $ř/s$). In relative terms (of GYRO-X) this means 50 % and 37.5 %.

Table 6.1 shows a distinct difference between the detection rate of ACC-Y left (93.9 %) and ACC-Y right (56.4 %). Reich reports in his master's thesis [Reich, 2013] of one possible explanation of this phenomenon. He states that "a bad reference cycle" is most likely the cause for the low detection rate in the right eSHOE data.

This is the result of the not entirely mature method for the creation of the reference cycle. Currently, the first detected complete gait cycle (in the reference data set) is automatically taken as reference cycle for the following cycles. If this cycle is of low quality, meaning that it is not entirely representative for the majority of the remaining cycles or, in other words, it does not represent the average pattern, the detection rate is bound to be limited.
A similar effect appears to be occurring in the pitch angle data, where in left foot data 96.3 % and in the right foot data 67 % could be extracted. In difference to before, the underlying reason as to why there was a bad first and/or reference cycle is known

and explained by Reich. It was a cascading effect, originating from another algorithm, responsible for calculating the pitch angle from the acceleration and gyroscope data. In the process of calculating the pitch angle, the naturally occurring drift has to be accounted for. Otherwise the error multiplies in the course of the calculation. The measure of choice for this algorithm was simply to force the angle signal to zero, whenever the heel pressure sensor is activated. This works well enough with "ordinary" walking shoes. But for the pilot study, due to hospital (hygiene) policy, patients had to wear clogs made of plastic. The soles of these clogs were rather soft, which, in some cases, had a dampening effect regarding the transmission of the force from the ground to the foot, or rather, the heel. This had the effect that the heel pressure threshold to reset the angle was not reached. So the drift was allowed to continue and accumulate over several cycles, which caused the main body of the recorded (pitch angle) cycles to look different from the reference cycle. Hence, the low detection rate.

Although there are still some issues that have to be worked out, the applied method showed good applicability and accuracy in the detection of recurring patterns with the help of a reference cycle. Especially the creation of a reference pattern is an issue which has to be dealt with in order to improve the detection rate and, thereby, the algorithm's stability.

For the gait cycle detection the algorithm takes the first cycle it finds in the data and uses it as a reference. All remaining gait cycles are processed and adapted (squeezed or stretched) to reach the best agreement (correlation) possible with this reference gait cycle. This carries the risk of a lower detection rate, should this first cycle be exceptional in its characteristics compared to the majority of other cycles. Mostly, this affects the duration of a cycle. In case the first detected cycle is shorter than the rest of the cycles, the algorithm squeezes all cycles to the size/length of the first cycle. Fortunately, the detection of gait cycles also works quite well, when using a less-than-perfect reference cycle. But this is still an issue which should be dealt with, when these algorithms are to be used further.

Based on the pattern detection algorithms, the gait feature extraction methods were implemented. The total number of the detectable gait features, IC/HS and LC/TO, was equal to the total number of gait cylces (presented in table 6.2) and was used as a benchmark for the IC and LC extraction success.

IC detection, based on P-HEEL and ACC-Y data, showed excellent results with 98.2 % and 96.9 % success rate for left and right eSHOE data. LC detection, based on GYRO-X and ANGLE data, delivered similar results with 98.2 % and 99.1 % in left and right insole data. These results can be reviewed in table 6.3.

These numbers lead to the conclusion, that the general detection of basic gait events is possible with acceptable error rates of 2.5 % and 1.4 % for IC and LC detection. Furthermore, it can be safely assumed that the error rates for all further derived gait parameters will be similarly small. Of course, this allows no insight into the accuracy of the detection of those events, yet. The accuracy is evaluated in the following section (7.4).

7.4   Accuracy of gait parameter detection via eSHOE - validated against GAITRite®

This prospective study of the analysis of agreement reveals the following findings. (1) eSHOE's results differ (in average) from GAITRite® by $-0.029\ s$ to $0.029\ s$ in healthy subjects and by $-0.046\ s$ to $0.045\ s$ in patients after hip fracture. (2) These differences are considered to be negligible by clinical experts, especially with regard to the advantages eSHOE provides. The direct comparison of the results from GAITRite® and eSHOE via scatterplots already indicates good agreement, especially in the data from healthy subjects. In the patient data the two methods also show sound agreement. The histograms of all parameters of both groups show distributions with no distinct kurtosis or skewness in either direction. Therefore, it was assumed that the distributions are (approximately) normal. In general PAT data did exhibit a higher variance. This can be observed in less dense data clouds in the scatterplots, in wider distributions in the histograms and it is also reflected in the limits of agreement of the Bland-Altman analysis, which are further apart than in the CTRL data. The most likely reason for the higher variance in PAT data lies in the fact that the patients' injuries cause increased irregularities in their walking patterns which, in turn, causes the gait cycle patterns to deviate from their standard shapes, making them harder to detect accurately. Therefore, the detection algorithms (work less efficient and) are prone to miss single gait events, e.g. due to a lower signal to noise ratio. This has to be accounted for in the further development of the algorithms.

The reason why patient data provided more detectable strides than data from the control group lies in the fact that elderly people in general and patients with an unilaterally affected leg, as it occurs in hip fractures, present a reduced walking speed and smaller stride lengths on their affected leg [Latham et al., 2008]. Stride length is directly related to walking speed and cadence [formula] and, in turn, walking speed to distance [equation]. So patients had to perform more strides, in order to cross the same distance as the healthy subjects who achieved larger stride lengths. The fact that Stance Time is shorter by the same exact amount as Swing Time is longer suggests that the algorithms for the detection of the condition(s) in the raw data, by which the toe-off event is identified, are too sensitive. Therefore, the toe-off is detected too early, extending the swing phase and reducing the stance phase. Step Time shows a rather high standard deviation (SD), $0.032\ s$ (CTRL) and $0.062\ s$ (PAT), compared to the other parameters. This might be due to the fact that it is the only one parameter, which is calculated by conditions depending on data from both insoles (or sensor printed circuit boards (PCBs)).

Since GAITRite® is one of the later gait analysis systems, it also had to be validated against an even older standard, namely optical motion capture with the Vicon® system. Results from Webster et al. [Webster et al., 2005] are given here in order to get a perspective of the amount of bias between eSHOE and GAITRite®. Webster et al. presented a comparison of GAITRite® with Vicon®, but unfortunately only analyzed two parameters, *stride length* and *step time*. In step time 81 % of their data did not differ by more than $0.02\ s$. In comparison, the mean difference (of step time) in the pilot study of

this thesis was $0 \pm 0.032\ s$ in the CTRLs and $0.004 \pm 0.062\ s$ in the PATs.

RehaWatch® and OpenGo® science are using very similar technology and measurement strategy as eSHOE, but with the difference that they focus, at least at the moment, on clinical or in-patient applications only. There is little evidence/data of those systems' accuracy or agreement with clinically established gait analysis systems. Schwesig et al [Schwesig et al., 2011] published results about test-retest reliability of RehaWatch and Braun et al [Braun et al., 2015b] published validation and reliability results of the OpenGo science system, but only for two gait parameters – *stance time* and *peak force*. In their study they used 12 healthy subjects and compared their system with a force plate. Their results showed a difference in stance time of $0.027 \pm 0.028\ s$, which is similar to the magnitude of the mean difference this thesis' study in the CTRLs in with $0.029\ s$ but with a smaller SD of $0.018\ s$.

Morris-Bamberg et al presented in their validation study from 2008 a comparison of the SIGS with the active optical motion capturing system "SELSPOT" [Bamberg et al., 2008]. A group of 15 people, subdivided into ten healthy subjects and five subjects with Parkinson's disease, performed a series of locomotor tasks, while "GaitShoe" and Selspot II collected data simultaneously. The mean differences between the two systems include heel-strike times: $-6.7 \pm 22.9\ ms$ ($-0.007 \pm 0.023\ s$) from 77 samples, toe-off times: $-2.9 \pm 16.9\ ms$ ($-0.003 \pm 0.017\ s$) from 75 samples. These results show incredibly high accuracy. However, mitigating factors are that the presented events are very basic and no actual gait parameters and a calculation of stance time, for instance, which involves both of the presented events may result in another value. Therefore, any changes to the accuracy/inaccuracy during further calculations are not accounted for. Considering the subject group consisting of 15 subjects there is also a rather low count of gait cycles (77/75). Additionally, some amount of uncertainty has to be assumed, since the results from the healthy part of the group and the Parkinson patients were mixed together.

The validation of the GPDS from Pappas et al in 2001 was carried out with three able-bodied subjects on a treadmill [Pappas et al., 2001]. These measurements revealed a certain time delay in the detection of the heel-strike and subsequent gait events, namely $40\ ms$ ($0.04\ s$) for heel-off, $35\ ms$ ($0.035\ s$) for swing, $70\ ms$ ($0.07\ s$) for heel-strike, and $70\ ms$ ($0.07\ s$) for stance. The results of the eSHOE validation showed differences in stance and swing time that are only half as big with $-0.029 \pm 0.018\ s$ for stance time and $0.029 \pm 0.018\ s$ for swing time. The comparison of these two results is not ideal, since (1) Pappas et al performed their measurements on a treadmill and (2) they only used three subjects (with 60 cycles), compared to 12 subjects and 155 cycles, which gives the possibility that the actual delays of the GPDS might be different. Additionally, no values for the standard deviation (σ) were given. Nevertheless, considering the available values, eSHOE proved to be twice as accurate, with only half of the time delay, in the CTRL group. Since Pappas et al only used healthy subjects, it makes little sense to compare the PAT difference from this study.

7.5 Stride length and distance estimation

Results showed that there are two major influence factors on the accuracy of then stride length estimation: (1) the time parameters of the ZUPT phase (beginning, ending and duration) and (2) the sensors' limited sensitivity which results in increased measurement errors.

For the ZUPT or FF phase three different parameter-sets, regarding beginning and ending of the phase, have been evaluated in detail. The third parameter-set (C), with the the ZUPT or FF phase lasting from 9.5 % *to* 17 % of the gait cycle, delivered the best results with a mean difference in stride length of -0.011 ± 0.042 m ($= -1.1 \pm 4.2$ cm). The standard deviation (SD) remained the same with all three sets and could not be reduced below ± 0.04 m ($= \pm 4$ cm).

As suggested by experts and literature [Oberg et al., 1993, Auvinet et al., 1999, Moe-Nilssen and Helbostad, 2004], the acceleration and deceleration phases of a straight ahead walk (involving the first and last few steps) have different characteristics than the "main portion" of steps in the middle of the track. This fact manifests as in a reduced SD, once the first and last strides are excluded from a dataset (see tables 6.12 and 6.13 in subsection 6.3.3.). These particular strides are performed (significantly) slower and have a reduced stride length. Apparently, the sensitivity of the IMU sensors is not high enough to record these slower movements properly, because they are lost in the quantization error.

On average the error of the proposed algorithm for parameter-set A amounts to -5.5 % with a SD of 2 %.

With the optimized parameter-sets B and C (and only option 4) an improved error and σ of -3.0 ± 2.2 % could be achieved. This results in an error of -3.9 ± 2.9 $cm/stride$ when applied to a stride length of 1.3 m.

Results for total distance estimation achieved with eSHOE and the algorithms from [Polasek, 2014] (parameter-set C, left and right data averaged) show higher absolute errors compared to the state of the art. On the 50 m outdoor track the relative error was -4.5 ± 0.7 % ($= -2.25 \pm 0.35$ m) and at the 8.7 m indoor track -2.0 ± 2.4 % ($= -0.174 \pm 0.2088$ m). [Sagawa, 2000] achieved an error of 5 % in total distance estimation on a 30 m walking track ($= 1,5$ $m = \pm 0.75$ m), using a 3D-accelerometer and 1D-gyro and implemented ZUPT-like strategy. [Foxlin2005] used a ZUPT principle and an extended Kalman filter in addition, resulted in an error of 0.3 % on 741 m ($= 2.22$ $m = \pm 1.11$ m).

There is a clear difference in the SDs for the complete distance estimation (2.2 %) and the stride length estimation (3.5 %). This can mean that measurement errors are less influential, the longer the measured distance.

An important conclusion, also in reference to the state of the art, is that the quality of the (stride) length estimation largely depends on the quality or rather sophistication

of the IMU. But very high quality IMUs are often of larger size and very expensive. Therefore, if the desired solution has to meet certain requirements concerning size, it comes down to the skills of an engineer required to manage errors and unreliability.

Reasons for the accuracy problem are argued to be a result of the inertial sensor hardware. Results do show, that the standard deviation cannot be influences much by optimization of the algorithm. From this analysis some suppositions can be formulated.

In the course of to work of [Polasek, 2014] it became clear stride length and distance estimation in general come with a number of limiting factors. For one the accelerometer data is intermixed with a lot of noise. Secondly, the gyroscopes sensitivity at slow movements (during walking) is too low. Environmental conditions influence the measurements' accuracy a great deal, among the most influential are temperature and pressure. Another technical factor is the sampling frequency. More successful related work (Swedish Open Shoe project) shows that even sampling rates of 820 Hz are not high enough to perform motion capturing with IMUs during walking. But still, an increase in the sampling rate from the current maximum of 200 Hz could only benefit the accuracy.

7.6   Therapy progress monitoring

The 10MWT time as an external reference measure shows that there is no unambiguous development in the the results over time. There is a clear reduction in time duration for median and mean of all subjects from day one to day two. But after that, until day four, the 10MWT time appears to be stagnating. There is even an increase on day six. It has to be stated at this point, that after day three the number of subjects who were still part of the study began to decline. While on the first three days all eleven subjects were still there, the number shrinks to nine on day four (-2), to seven on day five (-4) and to one (!) on day six (-10). The shrinking number of subjects is very likely distorting the results to some extent.

This is the first hint that this sample of patients does not present a textbook example of therapy progress which reflects also in the development of the gait parameters. The medians and means of Stride Time (STR), stance time (affected and healthy leg) and step time show very little change. Additionally, these changes do not exhibit any directional tendency, i.e. none of these parameters does seem to grow bigger or smaller. STR increases after the first day, then stagnates, then decreases, increases and decreases again. But these variations are never larger than 0.148 s. Stance Time (STA)-A stagnates for the first two transitions, then grows shorter, longer and again shorter. STA-H increases in the beginning from day one to day to, then decreases two times in a row (2-3, 3-4), increases (4-5) and finally decreases again (5-6). In the case of STA the variations are $< 0.117\ s$. Swing Time (SWI)-A shows the exact same behavior as STA-H, with fluctuations within 0.118 s. SWI-H increases along with SWI-A (1-2) and then continues to grow longer (2-3) until it drops (3-4), stagnates (4-5) and increases again (5-6). SWI-H variations are slightly higher with $< 0.169\ s$. The course of Step Time (STE) is equal to STA-H and variates within 0.075 s. Double support time-A shortens at the first transition, stagnates

for the following to, then increases again and stays there. On the healthy leg DS drops for two transitions, then rises for two and finally decreases again. DS's fluctuations on the affected leg are higher (0.125 s) than on the healthy leg (0.076 s).

It is almost impossible to derive any conclusion from the development of the median and mean values. The distribution parameters, standard deviation, interquartile range (IQR) and total range (TR) are drawing a different picture. All of them show at least a global reduction (from first to last measurement day) in all gait parameters. In fact, there is always a decrease in all of them from one day to the next with the exception of the transition from MD 3 to MD 4. This can most likely be explained by a high number of outliers on that day, which can be observed in the box plots of STR, STA-A, STE and DS-H. An inspection of the box plots, together with the development of the distribution parameters indicates a clear narrowing of the distributions of all gait parameters. In turn, this suggests a decreasing inter-personal gait variability, which can be interpreted as indirect proof that the therapy progress can be detected.

Reasons for the very broad distributions of the data are suspected to be the heterogeneous composition of the patient group, regarding fracture type, implant walking aids. The walking aids and their constant exchange (at random times) for less extensive ones during the stationary rehabilitation might also be a contributing factor to the scattering of the data. The selection and assignment of a specific walking aid to a patient is, of course, not at random but precisely coordinated with that persons mobility and individual needs. But there is no clear or time-coordinated change of the type of aid or a designated duration of usage. One aid device is exchanged for another, which provides just the right amount of support, at a point in time that is considered to be appropriate by the medical experts. It is only logical, that every aid device has a certain influence on its user's gait. From some of the individual datasets it can be concluded, that every time a change of walking aid occurs, there is a measurable effect in the data. Sometimes it shifts the whole distribution of one (or more) parameter(s). Thereby, creating some sort of cascading effect, where the first time with a new walking aid the progress of a parameter is reset to a "worse" value. But afterwards progress sets in again. In other cases it only effects the width of the distribution. For a confirmation of this effect larger and controlled studies are necessary.

Even though their absolute numbers are not large (≤ 120 ms), the statistical analysis showed significant differences between the healthy and the affected leg in stance, swing and double support time. These differences are all growing smaller during the monitored period of time and are all tending to zero. This effect is another indirect indicator for the successful progression of the therapy process.

During the pilot study there were no complications of any kind and patients as well as healthy subjects commented on the insoles being no disturbance, some even reported that they were quite comfortable.

Die Untersuchung einer größeren Gruppe an Testpersonen, bei denen eine noch feinkörnigere Gruppierung (nach genauer Frakturart und/oder Implantat), welche auch die gleichen

Gehhilfsmittel zur gleichen Zeit verwenden könnte hier Abhilfe schaffen. Im Fall einer weiterhin heterogenen Gruppe könnte evt. eine Gewichtung der Gangparameter (nach Frakturart, Implantat und Gehhilfsmittel) eingeführt werden. Gleichzeitig kann die Implementierung neuer Sensoren die Genauigkeit bei der Erkennung der Gangparameter verbessern und damit die Streuung mindern.

7.7   Limitations of eSHOE and the related pilot study

Due to the nature of a pilot study there was a rather low number of participants. Another limiting factor was that some datasets had to be excluded due to extreme noise in the raw data or very erratic patterns. A partial compensation for the small sample size was achieved by performing the analyses on gait cycle level.

Usually, clinical gait analysis is performed with the subjects walking barefoot. This was not possible in this study, since shoe insoles were used, which, by definition, need the subjects to wear shoes. Conditions were tried be standardized by having the subjects all use the same type of shoes. Therefore, the subjects might have experience (some) influence through wearing shoes and not walking barefoot, but at least it was the same kind of influence on all of the subjects. This leads to the interesting question, how different types of shoes, with different characteristics e.g. degree of stiffness, affect gait characteristics.

CHAPTER 8

Summary and future work

The step-by-step (based on each other) detection of standard gait parameters in raw motion (acceleration and angular velocity) data proved to be a useful approach. The identification and automated detection of recurring patterns in the motion data worked with a very good success rates. Therefore, at this level of the multilayer-approach, the branching out for the investigation of other activities with recurring patterns (e.g. ascending and descending stairs) is encouraged. Even the automated classification of different classes of activity is conceivable.

On the next tier, where the extraction of temporal and spatial parameters takes place, inaccuracies in the area of ~ 5 %, two-digit milliseconds or one-digit centimeters, are occurring. That presents a certain limitation, e.g. for clinical applications, no doubt. The comparison of results from healthy subjects and patients showed that this fundamental distinction is possible and statistically verifiable. With the prospect of eSHOE being a low-cost and highly mobile motion analysis system which provides the possibilities of location-independent and home-based long-term monitoring, the relevance of those inaccuracies is minor. eSHOE can be utilized for location-independent gait parameter monitoring, self-administered, home-based training, outdoor analysis, uncovering walking behavior on different surfaces [Menz et al., 2003, Zurales et al., 2016] and the investigation of the effects of different walking aids. An application in those new fields could lead to new understanding of e.g. stride-to-stride variability (fluctuations in gait cycle duration) in older persons with a history of falls [Hausdorff et al., 1997]. Furthermore, eSHOE enables measurements in everyday life and could thereby help to improve the long-term success of rehabilitation measures by gathering fluctuations in daily walking performance.

Despite the limited accuracy it is still conceivable, that in the future eSHOE could be integrated into clinical practice as a quick and easy support for the analysis of geriatric assessments by collecting standardized data. Compared to other, similar products or research projects, eSHOE stands out, because it's hardware is entirely integrated into a (pair of) shoe insole(s). Almost all related developments are focusing on applications in

193

the clinical or in-patient area. The basic idea behind eSHOE was to provide a system that can be used by patients independently in their own homes. This makes a certain lack of accuracy, compared to expensive and cumbersome stationary systems acceptable. Since all "competing" products are relying on more or less the same technology, they also have to make trade-offs regarding size, energy consumption and accuracy.
With a booming "quantified self" market, steadily growing numbers of older people in our society and thereby numbers of chronic conditions, the need for affordable long-term care supporting technologies will grow larger. And soon reasonably accurate, user-centered solutions will boon demanded.

Current research activities focus on the development of new applications for the support of therapy-progress monitoring. A masters thesis is underway, dealing with the implementation of a (live-) feedback system for partial weight bearing, based on the eSHOE insoles and a smartphone app [Bril et al., 2016]. Other research activities focus on the identification and development over time of gait symmetry, further development of automated assessment evaluation (such as the timed up and go test), detection of relevant parameters in stair ascending and descending. Ever-present underlying goals and technical issues such as further miniaturization of the measurement hardware and improvement of the usability are constantly being worked on.

The long-term goal is to expand eSHOE into a rehab@home system, including user interfaces for patients and medical experts [Jagos et al., 2015]. Patients will be able to perform a variety of assessments and training exercises while wearing eSHOE and getting adequate feedback about their performance and rehabilitation status. Meanwhile physicians or therapists can keep track about their patients' adherence and performance.

Subject-wise analysis of eSHOE vs. GAITRite validation
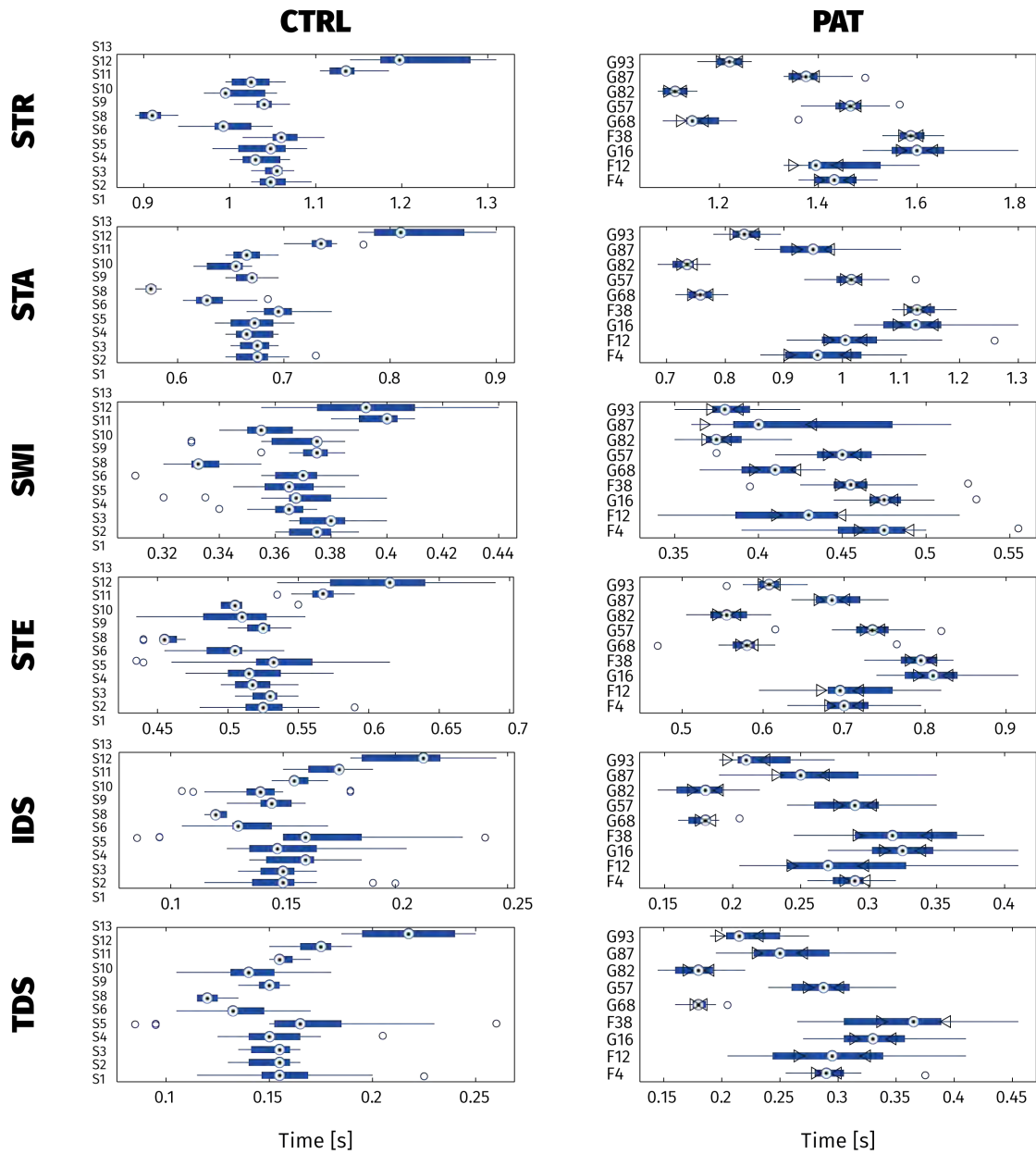
Figure A.1: Single-subject box plots of CTRL and PAT.

Subject-wise evaluation of therapy progress

B.1 Subject G6

65 year old female, with 1.58 *m* of height and body mass of 38.2 *kg* (BMI of 15.3). Leg length 0.845/0.847 *m* (L/R), thigh circumference of 0.35/0.34 *m* (L/R), shank circumference 0.28/0.27 *m* (L/R). Range of motion hip left: 50/0/85, right: 50/0/125; knee left: 50/0/125, right: 50/0/140; ankle left: 5/0/40, right 5/0/40. Heart rate of 96 *bpm*, blood pressure 130/70. She suffered from a medial femoral neck fracture (MFNF)

Subject ID	Age*	BMI	Diagnosis	Side	Implant	Stay	Measurements
G6	65	15.3	MFNF	left	TEP	21	4

Table B.1: Basic anthropometric parameters and injury-related characteristics of G6.

and received a hip total endo prosthesis (hip-TEP) two days after the fracture. Subject was admitted seven days post surgery and stayed at the hospital for 21 days. During her stay, four 10MWT measurements were conducted. Due to data corruption the very first measurement series was rendered useless and only three measurements could be evaluated.

G6	**MD 1**	**MD 2**	**MD 3**	**MD 4**	**MD 5**	**MD 6**
measurement dates	22.08.	28.08.	03.09.	03.09.	10.09.	-
Walking aid	R*	RM	RM	WCR	WCR	-
10MWT time [s]	20.06	12.75	10.54	10.03	9.32	-
Walking speed [km/h]	1.79	2.82	3.41	3.59	3.86	-

Table B.2: Therapy progress in terms of walking aids, 10MWT time and gait speed for subject G6.
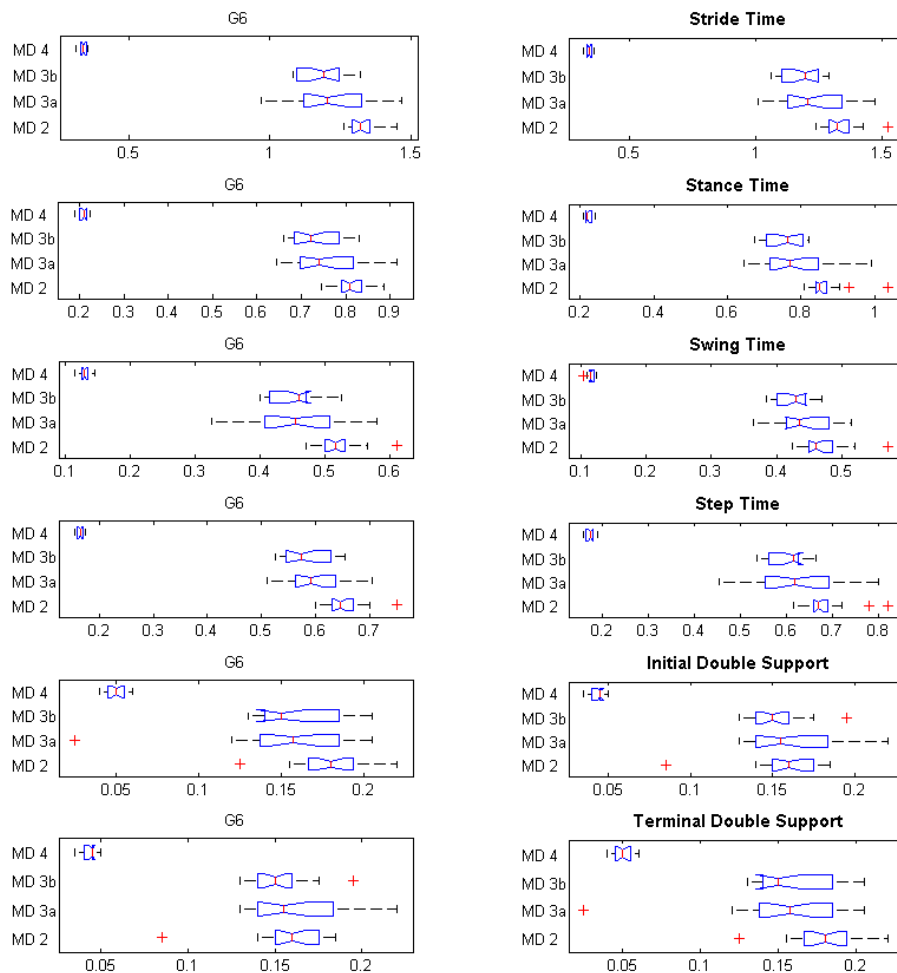
Figure B.1: Box plots for G6.

B.2 Subject F4

78 year old female, with 1.60 m of height and body mass of 62.1 kg (BMI of 24.3). Leg length 0.850/0.845 m (L/R), thigh circumference of 0.42/0.46 m (L/R), shank circumference 0.34/0.34 m (L/R). Range of motion hip left: 50/0/110, right: 50/0/50; knee left: 50/0/130, right: 50/0/110; ankle left: 10/0/30, right 5/0/30. Heart rate of 83 bpm, blood pressure 130/80. She suffered from a medial femoral neck fracture (MFNF) on her **right** leg and received a hip total endo prosthesis (hip-TEP) one day after the fracture. Subject was admitted 13 days post surgery and stayed at the hospital for 31

Subject ID	Age*	BMI	Diagnosis	Side	Implant	Stay	Measurements
F4	78	24.3	MFNF	right	TEP	31	5

Table B.3: Basic anthropometric parameters and injury-related characteristics of G6.

days. During her stay, five 10MWT measurements were conducted.

F4	MD 1	MD 2	MD 3	MD 4	MD 5	MD 6
measurement dates	22.08.	28.08.	03.09.	12.09.	19.09.	-
Walking aid	R	R	RM	WCL	WCL	-
10MWT time [s]	20.06	12.75	10.54	10.03	9.32	-
Walking speed [km/h]	1.79	2.82	3.41	3.59	3.86	-

Table B.4: Therapy progress in terms of walking aids, 10MWT time and gait speed for subject F4.
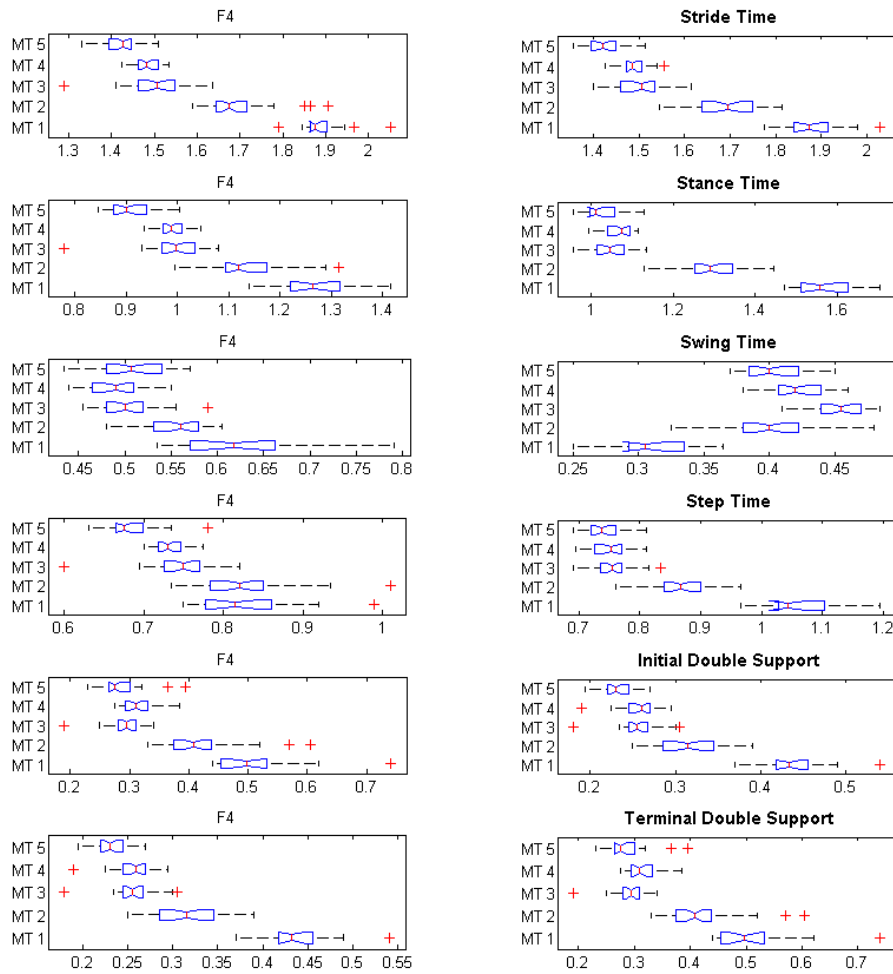
Figure B.2: Box plots for F4.

B.3 Subject F12

79 year old female, with 1.58 m of height and body mass of 60.0 kg (BMI of 24.0). Leg length 0.870/0.880 m (L/R), thigh circumference of 0.45/0.41 m (L/R), shank circumference 0.32/0.33 m (L/R). Range of motion hip left: 50/0/140, right: 50/0/60; knee left: 50/0/140, right: 50/0/90; ankle left: 10/0/40, right 10/0/40. Heart rate of 60 bpm, blood pressure 120/80. She suffered from a pertrochanteric fracture (PTF) which was treated with a dynamic hip screw two days after the injury. Admission into the geriatric hospital was seven days post surgery and subject stayed for 22 days. During her

Subject ID	Age*	BMI	Diagnosis	Side	Implant	Stay	Measurements
F12	79	24.0	PTF	right	DHS	22	5

Table B.5: Basic anthropometric parameters and injury-related characteristics of F12.

stay, five 10MWT measurements were conducted.

F12	MD 1	MD 2	MD 3	MD 4	MD 5	MD 6
measurement dates	03.09.	10.09.	12.09.	14.09.	19.09.	-
Walking aid	RM	2C	CL	WCL	WCL	-
10MWT time [s]	13.13	16.14	14.68	14.78	14.50	-
Walking speed [km/h]	2.74	2.23	2.45	2.44	2.48	-

Table B.6: Therapy progress in terms of walking aids, 10MWT time and gait speed for subject F12.
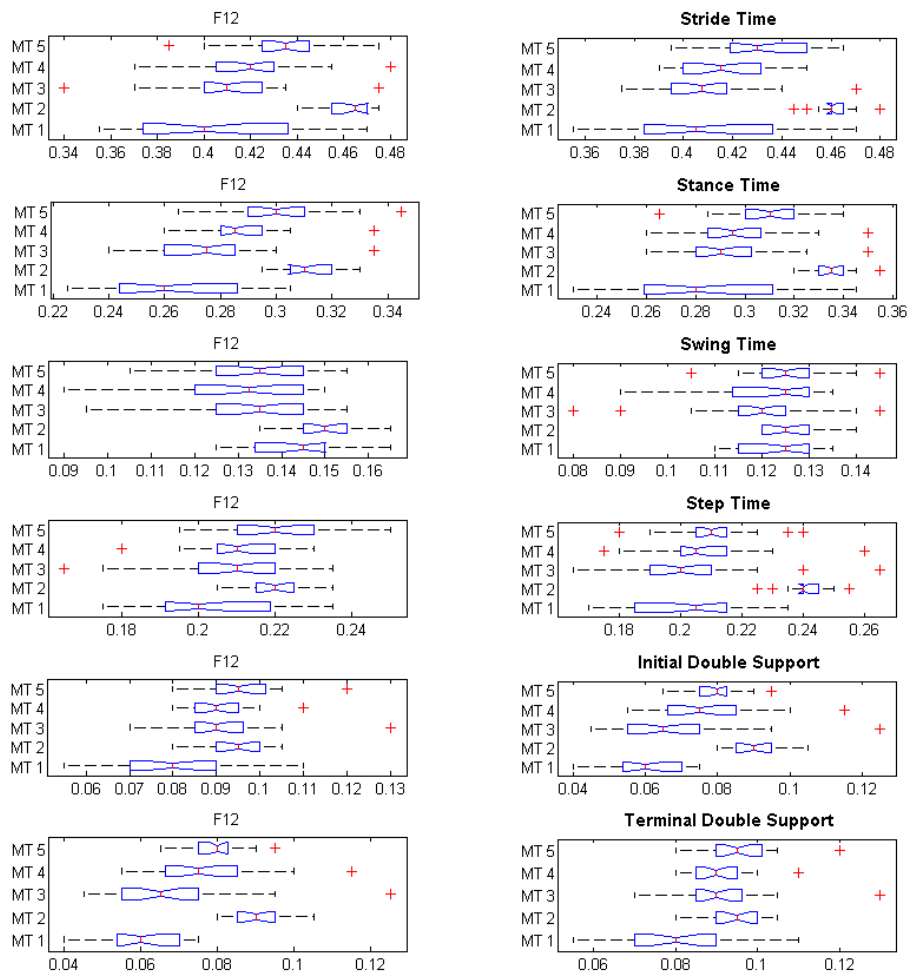
Figure B.3: Box plots for F12.

B.4 Subject G15

G15 was 85 years of age, when the measurements were conducted. She measures 1.58 m in height and weighs 60.0 kg (BMI of 24.0). Leg length 0.82/0.82 m (L/R), thigh circumference of 0.45/0.45 m (L/R), shank circumference 0.33/0.31 m (L/R). Range of motion hip left: 50/0/90, right: 50/0/65; knee left: 50/0/120, right: 50/0/135; ankle left: 5/0/35, right 5/0/35. Heart rate of 70 bpm, blood pressure 120/70. G15 suffered from a intertrochanteric femoral fracture (ITFF) which was treated with a dynamic hip screw (DHS) two days after the injury. Admission into the geriatric hospital was

Subject ID	Age*	BMI	Diagnosis	Side	Implant	Stay	Measurements
G15	85	24.0	PTF	left	DHS	16	3

Table B.7: Basic anthropometric parameters and injury-related characteristics of G15.

eleven days post surgery and subject stayed for 16 days. During her stay, three 10MWT measurements were conducted.

G15	**MD 1**	**MD 2**	**MD 3**	**MD 4**	**MD 5**	**MD 6**
Measurement dates	05.09.	12.09.	17.09.	-	-	-
Walking aid	R	RM	RM	-	-	-
10MWT time [s]	52.97	19.52	16.49	-	-	-
Walking speed [km/h]	0.68	1.84	2.18	-	-	-

Table B.8: Therapy progress in terms of walking aids, 10MWT time and gait speed for subject G15.
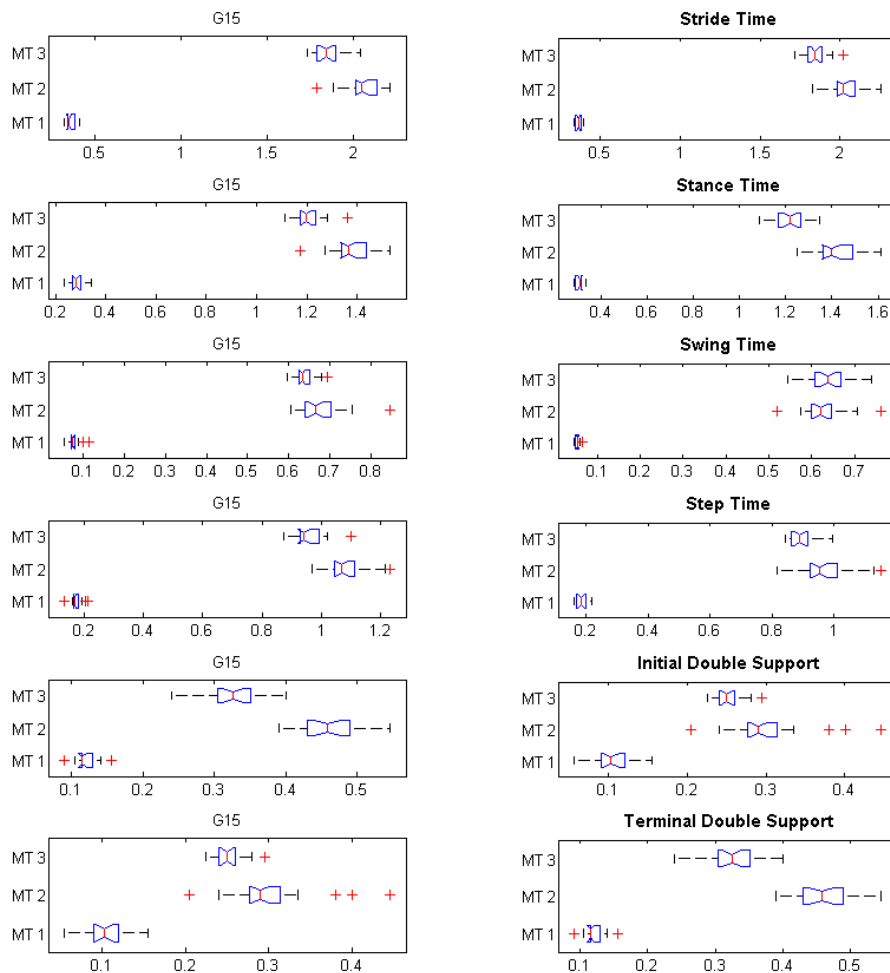
Figure B.4: Box plots for G15.

B.5 Subject G16

G16 was 85 years old at the time of admission. She measures 1.61 m in height and weighs 57.9 kg (BMI: 22.3). Leg length 0.930/0.935 m (L/R), thigh circumference of 0.41/0.36 m (L/R), shank circumference 0.32/0.29 m (L/R). Range of motion hip left: 0/0/20, right: 0/0/110; knee left: 0/0/80, right: 0/0/140; ankle left: 0/5/30, right 5/0/40. Heart rate of 73 bpm, blood pressure 130/70. This subject suffered from a intertrochanteric femoral fracture (ITFF) which was treated with a proximal femur nail (PFN) one day after the injury. She was admitted to the geratric hospital twelve days post surgery and stayed for

Subject ID	Age*	BMI	Diagnosis	Side	Implant	Stay	Measurements
G16	85	22.3	PTF	left	PFN	20	4

Table B.9: Basic anthropometric parameters and injury-related characteristics of G6.

20 days. During her stay she completed four 10MWT measurements.

G16	MD 1	MD 2	MD 3	MD 4	MD 5	MD 6
Measurement dates	07.09.	12.09.	14.09.	14.09.	21.09.	-
Walking aid	R	R	R	2C	2C	-
10MWT time [s]	39.91	22.99	15.20	23.10	17.16	-
Walking speed [km/h]	0.90	1.57	2.37	1.56	2.10	-

Table B.10: Therapy progress in terms of walking aids, 10MWT time and gait speed for subject G16.
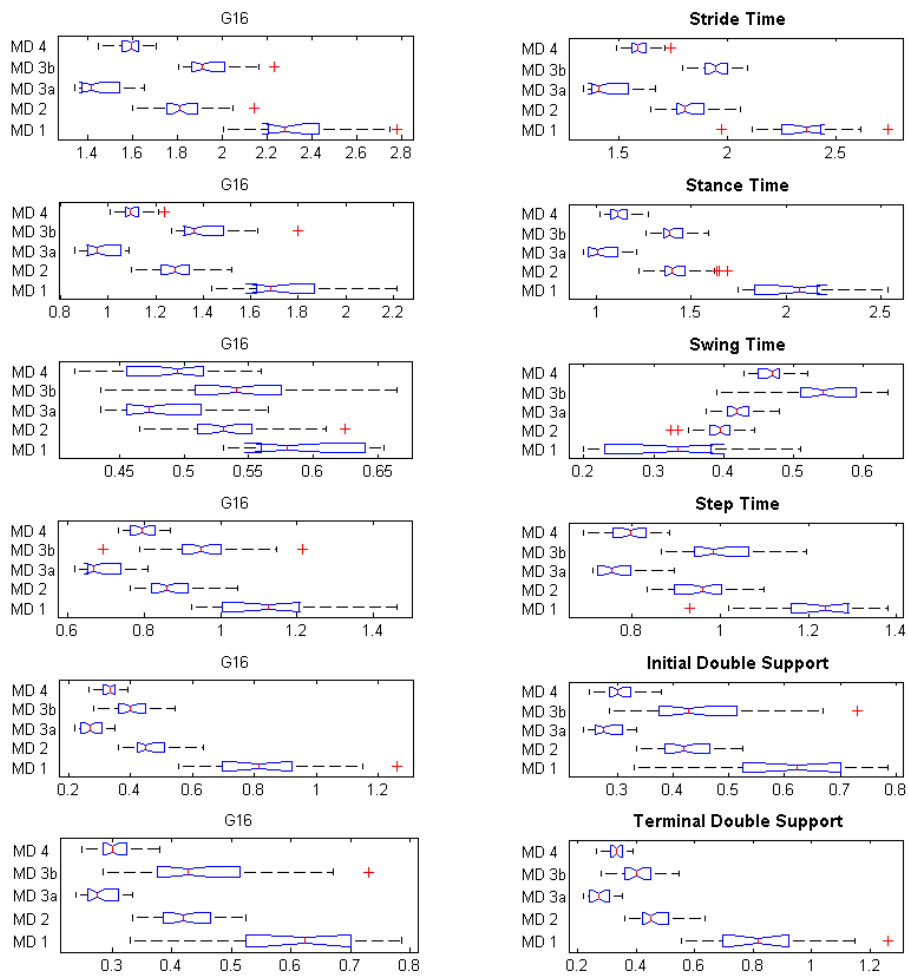
Figure B.5: Box plots for G16.

B.6 Subject F38

F38 is a 91 year old female, with 1.58 m of height and body mass of 58.0 kg (BMI of 23.2). Leg length 0.95/0.94 m (L/R), thigh circumference of 0.36/0.48 m (L/R), shank circumference 0.29/0.31 m (L/R). Range of motion hip left: 0/0/90, right: 0/0/40; knee left: 0/0/120, right: 0/0/60; ankle left: 0/0/30, right 0/0/30. Heart rate of 70 bpm, blood pressure 140/70. She suffered from a intertrochanteric femoral fracture (ITFF) and a subtrochanteric femoral fracture (STFF) on her **right** leg and received a dynamic hip screw (DHS) and Tukey-Anscombe plot (TAP) one day after the fractures. Subject

Subject ID	Age*	BMI	Diagnosis	Side	Implant	Stay	Measurements
F38	91	23.2	ITFF&STFF	right	DHS	20	4

Table B.11: Basic anthropometric parameters and injury-related characteristics of F38.

was admitted ten days after her surgery and stayed in acute geriatric care for 20 days. During her stay, four 10MWT measurements were conducted.

F38	**MD 1**	**MD 2**	**MD 3**	**MD 4**	**MD 5**	**MD 6**
Measurement dates	08.10.	12.10.	17.10.	22.10.	-	-
Walking aid	RM	RM	RM	2C	-	-
10MWT time [s]	11.44	11.08	10.12	12.36	-	-
Walking speed [km/h]	3.15	3.25	3.56	2.91	-	-

Table B.12: Therapy progress in terms of walking aids, 10MWT time and gait speed for subject F38.
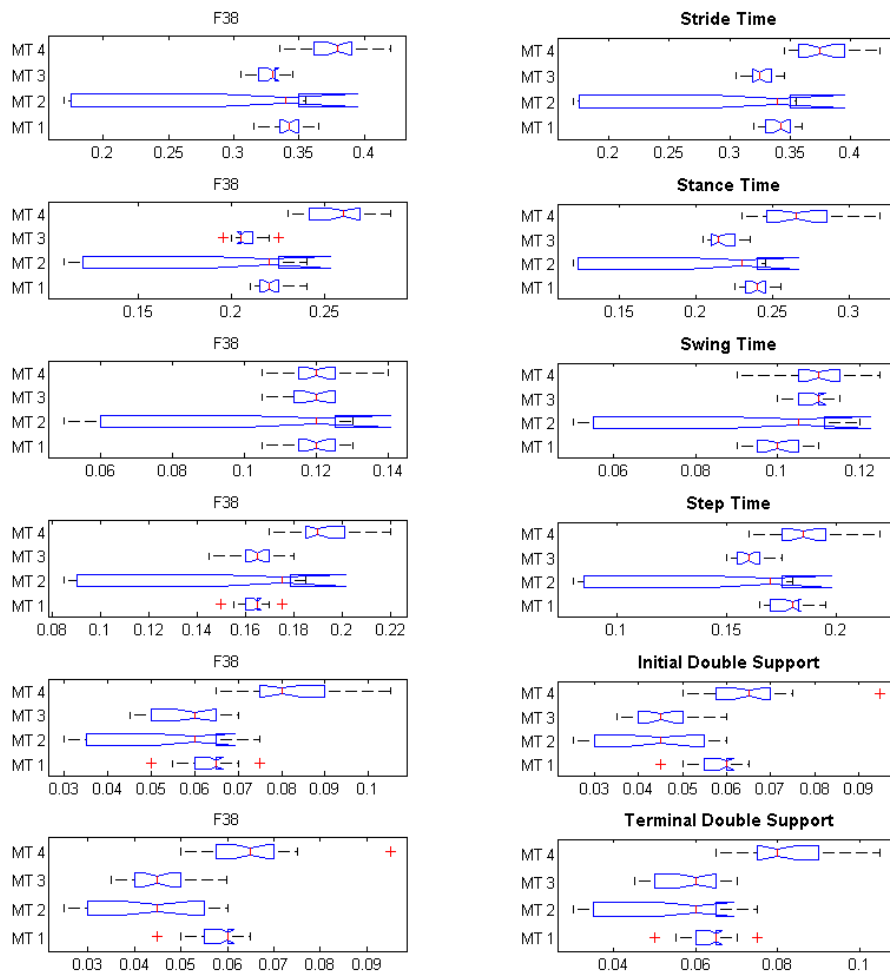
Figure B.6: Box plots for F38.

B.7 Subject G57

G57 is a 83 year old female, 1.58 *m* tall and weighs 53.0 *kg* (BMI of 21.2). Leg length of 0.84/0.85 *m* (L/R), thigh circumference of 0.39/0.42 *m* (L/R), shank circumference 0.35/0.37 *m* (L/R). Range of motion hip left: 0/5/120, right: 0/5/90; knee left: 0/0/90, right: 0/0/130; ankle left: 10/0/35, right 10/0/35. Heart rate of 85 *bpm*, blood pressure 155/80. She suffered from a intertrochanteric femoral fracture (ITFF) on her **right** leg and received a dynamic hip screw (DHS) and Tukey-Anscombe plot (TAP) one day after the fractures. Subject was admitted ten days after her surgery and stayed in acute

Subject ID	Age*	BMI	Diagnosis	Side	Implant	Stay	Measurements
G57	83	21.2	ITFF	right	DHS	30	6

Table B.13: Basic anthropometric parameters and injury-related characteristics of G57.

geriatric care for 30 days. During her stay six 10MWT measurements were conducted.

G57	**MD 1**	**MD 2**	**MD 3**	**MD 4**	**MD 5**	**MD 6**
Measurement dates	24.10.	30.10.	05.11.	09.11.	14.11.	21.11.
Walking aid	R	R	RM	RM	2C	WC
10MWT time [s]	42.04	30.11	20.01	17.13	21.26	18.99
Walking speed [km/h]	0.86	1.20	1.80	2.10	1.69	1.90

Table B.14: Therapy progress in terms of walking aids, 10MWT time and gait speed for subject G57.
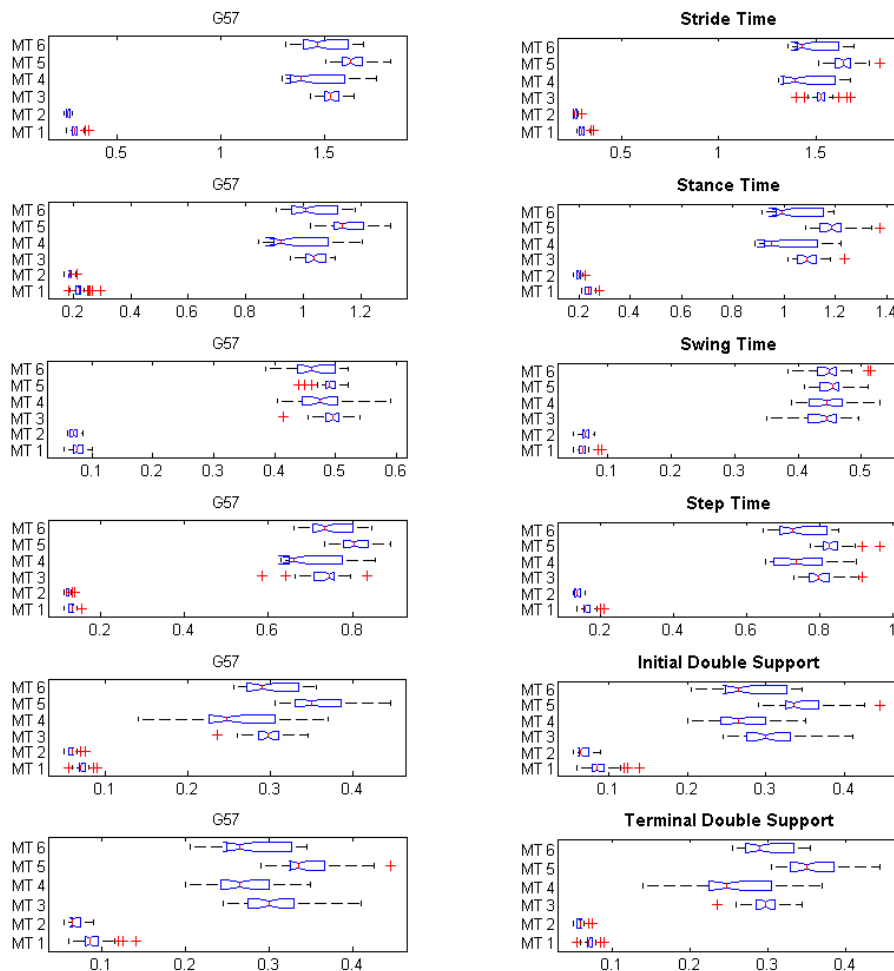
Figure B.7: Box plots for G57.

B.8   Subject G68

G68 is a 83 year old female, 1.58 *m* tall and weighs 53.0 *kg* (BMI of 21.2). Leg length of 0.84/0.85 *m* (L/R), thigh circumference of 0.39/0.42 *m* (L/R), shank circumference 0.35/0.37 *m* (L/R). Range of motion hip left: 0/5/120, right: 0/5/90; knee left: 0/0/90, right: 0/0/130; ankle left: 10/0/35, right 10/0/35. Heart rate of 85 *bpm*, blood pressure 155/80. She suffered from a medial femoral neck fracture (MFNF) on her **left** leg and received a bipolar femoral neck prosthesis (BFNP) one day after the fracture. Subject G68 was admitted 13 days after her surgery and stayed in acute geriatric care for nine

Subject ID	Age*	BMI	Diagnosis	Side	Implant	Stay	Measurements
G68	72	23.9	MFNF	left	BFNP	9	3

Table B.15: Basic anthropometric parameters and injury-related characteristics of G68.

days. During her stay three 10MWT measurements were conducted.

G68	MD 1	MD 2	MD 3	MD 4	MD 5	MD 6
Measurement dates	07.11.	09.11.	14.11.	-	-	-
Walking aid	2C	WCR	WCR	-	-	-
10MWT time [s]	10.88	10.37	9.83	-	-	-
Walking speed [km/h]	3.31	3.47	3.66	-	-	-

Table B.16: Therapy progress in terms of walking aids, 10MWT time and gait speed for subject G68.
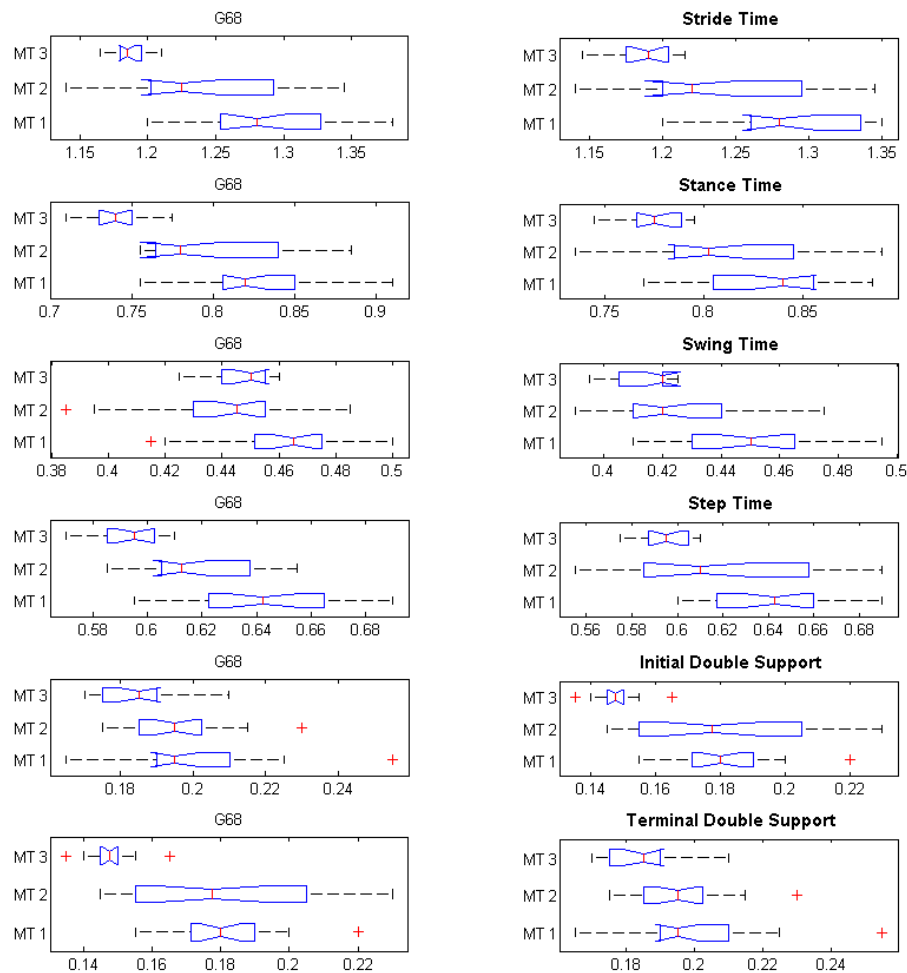
Figure B.8: Box plots for G68.

B.9 Subject G82

G82 is a 79 year old female, 1.61 m tall and weighs 57.4 kg (BMI of 22.1). Leg length of 0.79/0.785 m (L/R), thigh circumference of 0.46/0.465 m (L/R), shank circumference 0.3/0.3 m (L/R). Range of motion hip left: 0/0/130, right: 0/0/90; knee left: 0/0/140, right: 0/0/120; ankle left: 10/0/40, right 10/0/40. Heart rate of 66 bpm, blood pressure 140/80. She suffered from a medial femoral neck fracture (MFNF) on her **right** leg and was treated with two screws two days after the fracture. Subject G82 was admitted ten days after her surgery and stayed in acute geriatric care for 14 days. During her stay

Subject ID	Age*	BMI	Diagnosis	Side	Implant	Stay	Measurements
G82	79	22.1	MFNF	right	2 screws	14	4

Table B.17: Basic anthropometric parameters and injury-related characteristics of G82.

four 10MWT measurements were conducted.

G82	**MD 1**	**MD 2**	**MD 3**	**MD 4**	**MD 5**	**MD 6**
Measurement dates	26.11.	29.11.	03.12.	06.12.	-	-
Walking aid	2C	WCL	none	none	-	-
10MWT time [s]	10.29	9.30	9.05	8.16	-	-
Walking speed [km/h]	3.50	3.87	3.98	4.41	-	-

Table B.18: Therapy progress in terms of walking aids, 10MWT time and gait speed for subject G82.
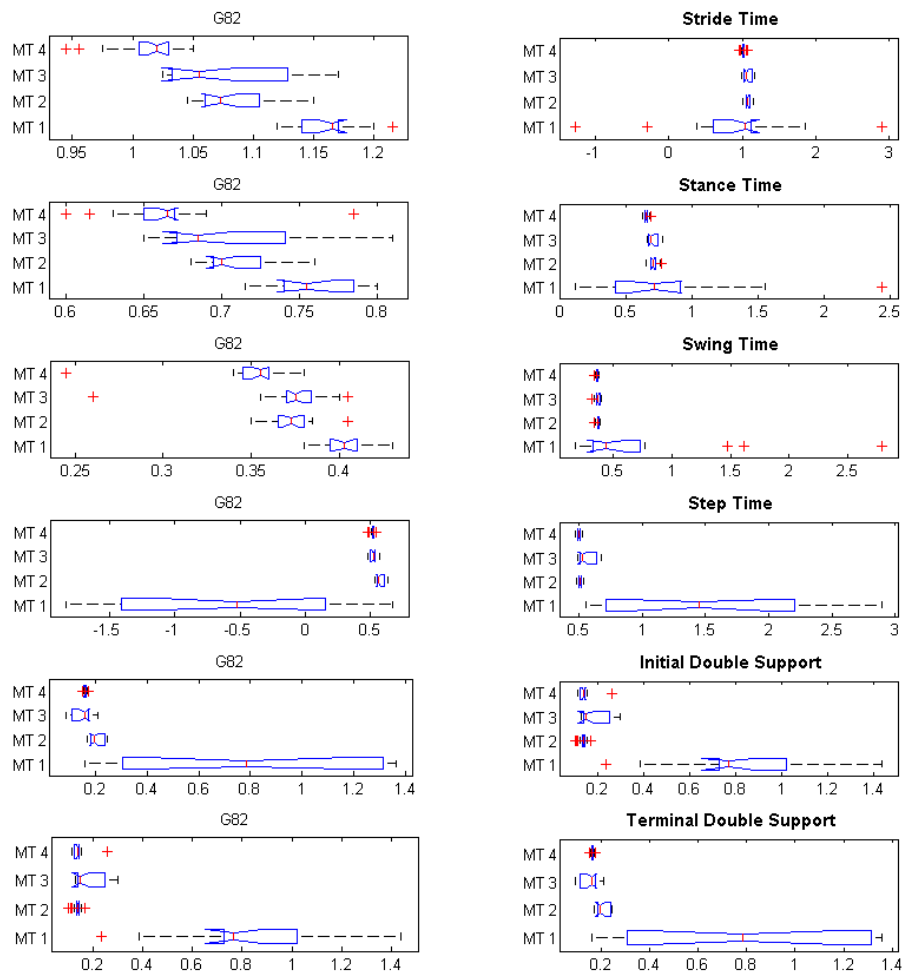
Figure B.9: Box plots for G82.

B.10 Subject G87

G87 is a 68 year old female, 1.60 m tall and weighs 50.4 kg (BMI of 19.7). Leg length of 0.83/0.83 m (L/R), thigh circumference of 0.45/0.45 m (L/R), shank circumference 0.33/0.34 m (L/R). Range of motion hip left: 50/0/140, right: 0/0/90; knee left: 50/0/140, right: 0/0/130; ankle left: 0/0/40, right 0/0/40. Heart rate of 79 bpm, blood pressure 125/70. She suffered from a intertrochanteric femoral fracture (ITFF) on her **right** leg and received a proximal femur nail (PFN) one day after the fracture. Subject G87 was admitted 16 days after her surgery and stayed in acute geriatric care for 16 days. During

Subject ID	Age*	BMI	Diagnosis	Side	Implant	Stay	Measurements
G87	68	19.7	ITFF	right	PFN	16	5

Table B.19: Basic anthropometric parameters and injury-related characteristics of G87.

her stay five 10MWT measurements were conducted.

G87	MD 1	MD 2	MD 3	MD 4	MD 5	MD 6
Measurement dates	29.11.	03.12.	06.12.	10.12.	13.12.	-
Walking aid	2C	2C	WCL	WCL	WCL	-
10MWT time [s]	19.55	13.59	17.39	12.98	12.82	-
Walking speed [km/h]	1.84	2.65	2.07	2.77	2.81	-

Table B.20: Therapy progress in terms of walking aids, 10MWT time and gait speed for subject G87.
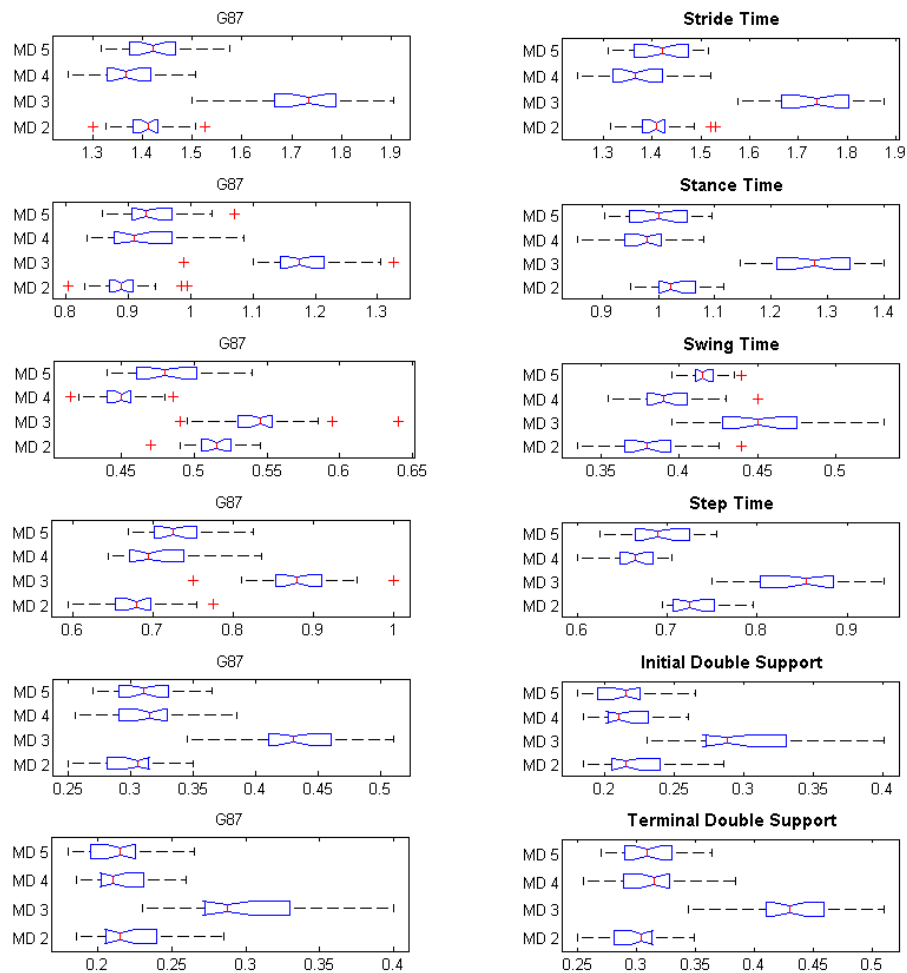
Figure B.10: Box plots for G87.

B.11 Subject G93

G93 is a 82 year old female, 1.52 m tall and weighs 67 kg (BMI of 29.4). Leg length of 0.84/0.84 m (L/R), thigh circumference of 0.52/0.50 m (L/R), shank circumference 0.32/0.33 m (L/R). Range of motion hip left: 0/0/90, right: 0/0/135; knee left: 0/0/140, right: 0/0/130; ankle left: 10/0/35, right 10/0/35. Heart rate of 69 bpm, blood pressure 140/80. She suffered from a medial femoral neck fracture (MFNF) on her **left** leg and received a bipolar femoral neck prosthesis (BFNP) one day after the fracture. Subject G93 was admitted 20 days after her surgery and stayed in acute geriatric care for 17

Subject ID	Age*	BMI	Diagnosis	Side	Implant	Stay	Measurements
G93	82	29.4	MFNF	left	BFNP	17	5

Table B.21: Basic anthropometric parameters and injury-related characteristics of G93.

days. During her stay five 10MWT measurements were conducted.

G93	**MD 1**	**MD 2**	**MD 3**	**MD 4**	**MD 5**	**MD 6**
Measurement dates	03.12.	06.12.	10.12.	13.12.	17.12.	-
Walking aid	R	2C	2C	WCR	WCR	-
10MWT time [s]	15.27	13.23	14.97	14.35	10.58	-
Walking speed [km/h]	2.36	2.72	2.40	2.51	3.40	-

Table B.22: Therapy progress in terms of walking aids, 10MWT time and gait speed for subject G93.
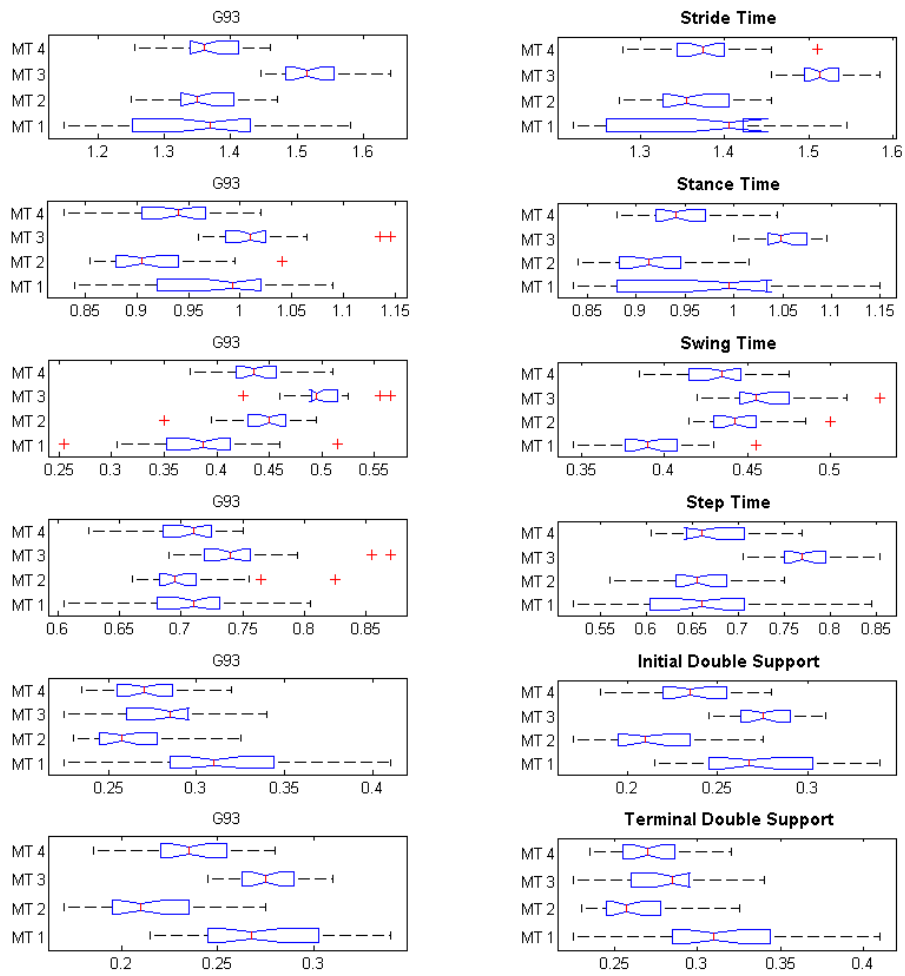
Figure B.11: Box plots for G93.

APPENDIX **C**

Documents for ethics committee

PatientInneninformation und **Einwilligungserklärung**
zur Teilnahme an der klinischen Prüfung

Pilotstudie zur Anwendung von Methoden der mobilen Ganganalyse als Unterstützung und Erweiterung von Basis-Assessments und Therapieverlaufskontrollen in der Geriatrie

Sehr geehrte Patientin, sehr geehrter Patient!

Wir laden Sie ein an der oben genannten klinischen Prüfung teilzunehmen. Die Aufklärung darüber erfolgt in einem ausführlichen ärztlichen Gespräch.

Ihre Teilnahme an dieser klinischen Prüfung erfolgt freiwillig. Sie können jederzeit ohne Angabe von Gründen aus der Studie ausscheiden. Die Ablehnung der Teilnahme oder ein vorzeitiges Ausscheiden aus dieser Studie hat keine nachteiligen Folgen für Ihre medizinische Betreuung.

Klinische Prüfungen sind notwendig, um verlässliche neue medizinische Forschungsergebnisse zu gewinnen. Unverzichtbare Voraussetzung für die Durchführung einer klinischen Prüfung ist jedoch, dass Sie Ihr Einverständnis zur Teilnahme an dieser klinischen Prüfung schriftlich erklären. Bitte lesen Sie den folgenden Text als Ergänzung zum Informationsgespräch mit Ihrer Ärztin sorgfältig durch und zögern Sie nicht Fragen zu stellen.

Eine **Pilotstudie** ist eine kleinere Untersuchung an der wenige PatientInnen teilnehmen. Mit den gewonnenen Erkenntnissen können spätere größere Studien besser geplant werden.

Das Ziel dieser Pilotstudie ist zu überprüfen, ob mit der Einlagesohle eSHOE das Gangbild im Therapieverlauf besser beurteilt werden kann und ob die gewonnen Erkenntnisse den Rehabilitationsverlauf nach Schenkelhalsbruch günstig beeinflussen.

Bitte unterschreiben Sie die Einwilligungserklärung nur

- wenn Sie Art und Ablauf der klinischen Studie vollständig verstanden haben,

- wenn Sie bereit sind, der Teilnahme zuzustimmen und

- wenn Sie sich über Ihre Rechte als Teilnehmer an dieser klinischen Studie im Klaren sind.

Zu dieser klinischen Prüfung, sowie zur Patienteninformation und Einwilligungserklärung wurde von der Ethikkommission der Stadt Wien eine positive Stellungnahme abgegeben.

1.   Was ist der Zweck der klinischen Studie?

Der Zweck dieser klinischen Studie ist, den Einsatz des eShoe zur Überprüfung des Gangbildes und der Gehsicherheit bei Gehtests und auf längeren Strecken zu testen. Das Gangbild wird zum Teil gleichzeitig mit der neuen Schuhsohle und dem Ganganalyseteppich überprüft. Beide Werte werden miteinander verglichen.

2.   Wie läuft die klinische Studie ab?

Diese klinische Studie mit der Einlagesohle eSHOE wird ausschließlich im SMZ-Sophienspital durchgeführt. Es werden keine zusätzlichen Untersuchungen oder Tests angewendet.

Nachdem Sie der Teilnahme an dieser Studie zugestimmt haben, stellt die Unterzeichnung dieses Dokuments den ersten Schritt dar. Im Zuge Ihres stationären Aufenthaltes im SMZ Sophienspital werden Sie im Rahmen der Physikalischen Therapie in regelmäßigen Abständen Tests zur Bestimmung Ihrer Gangsicherheit durchführen. Für vier dieser Tests bekommen Sie ein Paar zusätzlicher Einlagesohlen. Diese Einlagen werden in Ihre gewohnten Schuhe eingelegt. Die Sohlen sind mit Sensoren ausgestattet und nehmen, während Sie gehen, Informationen über Ihr Gangbild auf. Wenn sie die Einlagen das erste Mal verwenden, können Sie zur Eingewöhnung „Probegehen" und probieren, ob die Einlagen für Sie angenehm sind, Danach werden Sie gefragt ob Sie sich dadurch gestört oder in Ihrer Gangsicherheit negativ beeinflusst fühlen. Wenn das der Fall ist, werden die Einlagen wieder aus Ihren Schuhen herausgenommen und die Studie damit abgebrochen. Sollten Sie sich mit den instrumentierten Einlagesohlen genauso wohl fühlen wie immer, werden ab dem Zeitpunkt die vier folgenden Tests mit eSHOE durchgeführt:

1. „10-Meter Gehtest",

2. „Timed Up & Go Test",

3. "Sechs-Minuten Gehtest",

4. Stiegen steigen.

1. Zu Beginn wird ein Test durchgeführt, bei dem Sie, entlang einer markierten Strecke, 15 Meter geradeaus gehen. Innerhalb dieser 15 Meter langen Strecke befinden sich zwei weitere Markierungen, die 10 Meter voneinander entfernt sind. Es wird die Zeit gestoppt, die Sie zur Bewältigung der 10 Meter, innerhalb der 15 Meter Strecke, benötigen. Die 2,5 Meter vor und hinter der Strecke dienen als Bereiche zum Beschleunigen und Abbremsen. Wenn möglich, wird dieser Test drei Mal wiederholt.

2. Beim sogenannten „Timed Up & Go Test" (Abk. TUG) sitzen Sie zu Beginn auf einem Stuhl. Bei einem Startsignal, welches der Prüfer gibt, stehen Sie auf, gehen geradeaus bis zu einer 3 Meter entfernten Markierung, kehren dort um, gehen zurück zum Stuhl und setzen sich dort wieder hin. Es wird die Zeit gestoppt, die zwischen Aufstehen und Hinsetzen vergeht. Wenn möglich, wird der TUG ebenfalls drei Mal wiederholt.

3. Der Sechs-Minuten Gehtest ist eine Art Ausdauertest, bei dem Sie sechs Minuten am Stück gehen sollen. Und zwar gehen Sie zwischen den Markierungen der 15 Meter Strecke im Raum auf und ab. Während Sie gehen wird die Anzahl der Längen gezählt, die Sie innerhalb der sechs Minuten zurücklegen. Dieser Test wird erst knapp vor Ihrer geplanten Entlassung nach Hause durchgeführt.

4. Wenn Sie im Rahmen der Therapie Stiegen steigen, werden Sie auch dabei die Einlagesohlen tragen.

Die Anzahl der Messungen hängt von ihrem persönlichen Rehabilitationsverlauf ab und wird von der medizinischen Leitung individuell festgelegt.

Die regelmäßige Messung Ihrer Gangdaten während der Assessment Tests dient der Forschung, ob mit den Einlagesohlen die Erfassung Ihres Therapieerfolges möglich ist.

Bei den Tests wird zusätzlich ein Video von Ihnen beim Gehen aufgenommen. Ihr Gesicht wird auf dieser Aufnahme <u>nicht</u> zu sehen sein.

3.   Was ist der eSHOE?

Der eSHOE ist ein Medizinprodukt, welches sich in klinischer Erprobung befindet und noch nicht zugelassen ist.

Im Rahmen des Projektes eSHOE wird ein Monitoring- und Trainings-System entwickelt. Dieses hilft einerseits frühzeitig Probleme beim Gehen zu erkennen und andererseits durch spielerisches Training das Gleichgewichtsgefühl zu verbessern. Es soll langfristig zur Steigerung der körperlichen Aktivität anregen.

4.   Worin liegt der Nutzen einer Teilnahme an der klinischen Studie?

Durch Ihre Teilnahme erhalten Sie und Ihr, Ihre TherapeutIn mehr Informationen über Ihr Gangbild. Die gewonnenen Daten können in Ihr Rehabilitationsprogramm integriert werden.

Gleichzeitig unterstützen Sie uns bei der klinischen Testung eines mobilen Ganganalysesystems. Damit können wir in Zukunft das Gangbild nicht nur in einer „Laborsituation" sondern auch auf Stufen, im Freien und im Straßenverkehr überprüfen.

5.   Gibt es Risiken, Beschwerden und Begleiterscheinungen?

Da die Schuhsohle sich rein äußerlich von einer gängigen Schuhsohle nicht unterscheiden, nach außen mit Leder umkleidet ist, sind weder Risiken, Beschwerden oder Begleiterscheinungen zu erwarten. Sollte der Schuh mit der Sohle drücken oder Sie sich nicht wohlfühlen, können Sie die Untersuchung sofort unterbrechen. Sie ziehen den Schuh aus, die Sohle wird wieder herausgenommen und Sie können wie gewohnt weitergehen.

6.   Versicherung

Als Teilnehmer an dieser klinischen Prüfung besteht für Sie der gesetzlich vorgeschriebene verschuldensunabhängige Versicherungsschutz (Personenschadenversicherung gemäß § 47 Medizinproduktegesetz), der alle Schäden abdeckt, die an Ihrem Leben oder Ihrer Gesundheit durch die an Ihnen durchgeführten Maßnahmen der klinischen Prüfung verursacht werden können.

Die Versicherung wurde für Sie bei der Wiener Städtische Allgemeine Versicherung AG, Schottenring 30, 1010 Wien unter der Polizzennummer 08-U918234 abgeschlossen. Auf Wunsch können Sie in die Versicherungsunterlagen Einsicht nehmen.

Im Schadensfall können Sie sich direkt an den Versicherer wenden und Ihre Ansprüche selbständig geltend machen. Für den Versicherungsvertrag ist österreichisches Recht anwendbar, die Versicherungsansprüche sind in Österreich einklagbar.

Zur Unterstützung können Sie sich auch an die Patientenanwaltschaft oder Patienten-vertretung wenden.

Um den Versicherungsschutz nicht zu gefährden

- müssen Sie sich dem behandelnden Prüfarzt - oder der oben genannten Versicherungs-gesellschaft - eine Gesundheitsschädigung, die als Folge der klinischen Prüfung eingetreten sein könnte, unverzüglich mitteilen.

- müssen Sie alles Zumutbare tun, um Ursache, Hergang und Folgen des Versicherungs-falles aufzuklären und den entstandenen Schaden gering zu halten. Dazu gehört ggf. auch, dass Sie Ihre behandelnden Ärzte ermächtigen, vom Versicherer geforderte Auskünfte zu erteilen.

7.   Wann wird die klinische Studie vorzeitig beendet?

Die klinische Studie kann jederzeit vorzeitig beendet werden, sollten Sie sich mit der Sohle nicht wohlfühlen. Sollte sich Ihr Gangbild auf Grund von Schmerzen oder anderen Veränderungen verschlechtern, kann die Studie ebenfalls abgebrochen werden. .

8.   In welcher Weise werden die im Rahmen dieser klinischen Studie gesammelten Daten verwendet?

Im Rahmen des Spitalaufenthalts wird Ihr Gangbild und Ihre Mobilität in Rahmen von klinischen Tests beurteilt.

Für diese Pilotstudie tragen Sie während des Gehens die Einlagesohle eSHOE. Das hat keinen Einfluss auf die Spitalroutine oder die Zahl der Tests und Untersuchungen.

Die Ergebnisse werden, wenn es zu Ihrem Nutzen ist, dem Rehabilitationsteam zur Kenntnis gebracht.

Die erhobenen Daten werden anonymisiert ausgewertet und später publiziert.

Die Videoaufzeichnungen werden niemals veröffentlicht. Sie dienen nur zur Unterstützung der Datenauswertung.

Lediglich die Prüfärztinnen haben Zugang zu Ihren vertraulichen Daten. Weiters können Beauftragte von in- und ausländischen Gesundheitsbehörden, der zuständigen Ethikkommission, sowie – wenn zutreffend – des Auftraggebers der klinischen Prüfung Einsicht in diese Daten nehmen, um die Richtigkeit der Aufzeichnungen zu überprüfen. Diese Personen unterliegen einer gesetzlichen Verschwiegenheitspflicht.

In einer wissenschaftlichen Veröffentlichung der Untersuchungsergebnisse werden Sie nicht namentlich genannt.

Die Prüfärztinnen und ihre Mitarbeiter unterliegen im Umgang mit den Daten den Bestimmungen des österreichischen Datenschutzgesetzes 2000 in der jeweils geltenden Fassung.

Wenn Sie Ihre Einwilligung zurückziehen und damit Ihre Teilnahme vorzeitig beenden, werden keine neuen Daten mehr über Sie erhoben. Auf Grund gesetzlicher Dokumentationspflichten (Medizinproduktegesetz) kann jedoch weiterhin für einen gesetzlich festgelegten Zeitraum eine Einsichtnahme in Ihre personenbezogenen Daten zu Prüfzwecken durch autorisierte, zur Verschwiegenheit verpflichtete Personen erfolgen.

9. Entstehen für die Teilnehmer Kosten?

Durch Ihre Teilnahme an dieser klinischen Prüfung entstehen für Sie **keine** zusätzlichen Kosten.

10. Möglichkeit zur Diskussion weiterer Fragen

Für weitere Fragen steht Ihnen sehr gerne zur Verfügung:

Frau **Dr. Claudia Wassermann**: 01 52 103 - 3495

Frau **OA Dr. Christa Chhatwal**: 01 52 103 - 3477

11.   Einwilligungserklärung (Kopie für PatientIn)

Name des Patienten / der Patientin: ....

Geburtsdatum: ....   Identifikationsnummer (ID):................................

Ich erkläre mich bereit, an der klinischen Prüfung eSHOE teilzunehmen.

Ich bin von Frau **Dr. Wassermann** ausführlich und verständlich über den eSHOE, mögliche Belastungen und Risiken, sowie über Wesen, Bedeutung und Tragweite der klinischen Prüfung, die bestehende Versicherung sowie die sich für mich daraus ergebenden Anforderungen aufgeklärt worden. Ich habe darüber hinaus den Text dieser Patientenaufklärung und Einwilligungserklärung, die insgesamt 5 Seiten umfasst gelesen. Aufgetretene Fragen wurden mir vom Prüfarzt verständlich und genügend beantwortet. Ich hatte ausreichend Zeit, mich zu entscheiden. Ich habe zurzeit keine weiteren Fragen mehr.

Ich werde den ärztlichen Anordnungen, die für die Durchführung der klinischen Prüfung erforderlich sind, Folge leisten, behalte mir jedoch das Recht vor, meine freiwillige Mitwirkung jederzeit zu beenden, ohne dass mir daraus Nachteile für meine weitere medizinische Betreuung entstehen.

Ich bin zugleich damit einverstanden, dass meine im Rahmen dieser klinischen Prüfung ermittelten Daten gespeichert werden. Mir ist bekannt, dass zur Überprüfung der Richtigkeit der Datenaufzeichnung Beauftragte der zuständigen Behörden, der Ethikkommission und ggf. des Auftraggebers beim Prüfarzt Einblick in meine personenbezogenen Krankheitsdaten nehmen dürfen.

Beim Umgang mit den Daten werden die Bestimmungen des Datenschutzgesetzes 2000 beachtet.

Eine Kopie dieser Patienteninformation und Einwilligungserklärung habe ich erhalten. Das Original verbleibt beim Prüfarzt.

....
Datum und Unterschrift der Patientin, des Patienten

....
Datum, Name und Unterschrift der verantwortlichen Ärztin

12. Einwilligungserklärung (Kopie für Prüfarzt)

Name des Patienten/der Patientin:…………..

Geb.Datum: ....   Identifikationsnummer:................................

Ich erkläre mich bereit, an der klinischen Prüfung eSHOE teilzunehmen.

Ich bin von Frau **Dr. Wassermann** ausführlich und verständlich über den eSHOE, mögliche Belastungen und Risiken, sowie über Wesen, Bedeutung und Tragweite der klinischen Prüfung, die bestehende Versicherung sowie die sich für mich daraus ergebenden Anforderungen aufgeklärt worden. Ich habe darüber hinaus den Text dieser Patientenaufklärung und Einwilligungserklärung, die insgesamt 5 Seiten umfasst gelesen. Aufgetretene Fragen wurden mir vom Prüfarzt verständlich und genügend beantwortet. Ich hatte ausreichend Zeit, mich zu entscheiden. Ich habe zurzeit keine weiteren Fragen mehr.

Ich werde den ärztlichen Anordnungen, die für die Durchführung der klinischen Prüfung erforderlich sind, Folge leisten, behalte mir jedoch das Recht vor, meine freiwillige Mitwirkung jederzeit zu beenden, ohne dass mir daraus Nachteile für meine weitere medizinische Betreuung entstehen.

Ich bin zugleich damit einverstanden, dass meine im Rahmen dieser klinischen Prüfung ermittelten Daten gespeichert werden. Mir ist bekannt, dass zur Überprüfung der Richtigkeit der Datenaufzeichnung Beauftragte der zuständigen Behörden, der Ethikkommission und ggf. des Auftraggebers beim Prüfarzt Einblick in meine personenbezogenen Krankheitsdaten nehmen dürfen.

Beim Umgang mit den Daten werden die Bestimmungen des Datenschutzgesetzes 2000 beachtet.

Eine Kopie dieser Patienteninformation und Einwilligungserklärung habe ich erhalten. Das Original verbleibt beim Prüfarzt.

....
Datum und Unterschrift der Patientin, des Patienten

....
Datum, Name und Unterschrift der verantwortlichen Ärztin

Case-Report-Form

- Patienten -

eSHOE Pilotstudie – Seite 1

Version 22 || 06.09.2012	
Probanden ID:	
Untersucher:	
Datum:	

Anamnese bei Aufnahme

Datum der **Aufnahme**: Datum der **Entlassung**:

Geburtsdatum					
Geschlecht		□ weiblich		□ männlich	

Körper-größe	P:	Gewicht	P:	BMI	P:	Schuh-größe	normal
	M:		M:		M:		eSHOE-Größe

Beinlänge *Trochanter bis Boden, inkl. Schuhe*	li:	cm	re:	cm
Oberschenkelumfang I *10 cm prox. Patella*	li:	cm	re:	cm
Oberschenkelumfang II *20 cm prox. Patella*	li:	cm	re:	cm
Wadenumfang	li:	cm	re:	cm
ROM Hüfte S	li:		re:	
ROM Knie S	li:		re:	
ROM Sprunggelenk S	li:		re:	

Herzfrequenz	Schläge / Minute

Blutdruck	sys.:	mmHg	diast.:	mmHg

Hauptdiagnose	Betroffene Seite:	□ **links**	□ **rechts**

Frakturart		Zeitpunkt der Fraktur	
Implantat		Operationsdatum	
Stürze während des Aufenthalts		**Stürze** im letzten Jahr	

Vorerkrankungen und relevante Begleit-erkrankungen	
Medikation	

Mini Mental State		Uhrentest		Handkraft (dominante Hand)	L □
					R □

Schmerz (NRS)	Ruhe	Belastung	**Depression (DSI)**	

Verwendete Gehhilfsmittel

zum Zeitpunkt der **Aufnahme**	
zum Zeitpunkt der **Entlassung**	

Tinetti Test   ohne eSHOE

zum Zeitpunkt der **Aufnahme**	Balance	Gang	Gesamt
	Kommentar:		
zum Zeitpunkt der **Entlassung**	Balance	Gang	Gesamt
	Kommentar:		

Timed Up & Go Test   mit und ohne eSHOE

Messtag 1
zum Zeitpunkt der **Aufnahme**   Datum: Hilfsmittel:

ohne eSHOE		mit eSHOE		
Uhrzeit:	Kommentar:	Uhrzeit:	Kommentar:	V ☐
Benötigte Zeit:		Benötigte Zeit:		F ☐

Messtag 2
1. Tag nach der **Aufnahme**   Datum: Hilfsmittel: Sohlen (Gr.):   Clogs (Gr.):

ohne eSHOE		mit eSHOE		
Uhrzeit:	Kommentar:	Uhrzeit:	Kommentar:	V ☐
Benötigte Zeit:		Benötigte Zeit:		F ☐

Messtag 3
zum Zeitpunkt der **Entlassung**   Datum: Hilfsmittel: Sohlen (Gr.):   Clogs (Gr.):

ohne eSHOE		mit eSHOE		
Uhrzeit:	Kommentar:	Uhrzeit:	Kommentar:	V ☐
Benötigte Zeit:		Benötigte Zeit:		F ☐

10-Meter Gehtest   mit eSHOE

Messtag 1	Datum:	Hilfsmittel:	Sohlen (Gr.):
			Clogs (Gr.):

1. Durchgang	☐ möglich	☐ nicht möglich	
	Uhrzeit:	Kommentar:	V ☐
	Benötigte Zeit:		F ☐
2. Durchgang	☐ möglich	☐ nicht möglich	
	Uhrzeit:	Kommentar:	V ☐
	Benötigte Zeit:		F ☐
3. Durchgang	☐ möglich	☐ nicht möglich	
	Uhrzeit:	Kommentar:	V ☐
	Benötigte Zeit:		F ☐

Messtag 2	Datum:	Hilfsmittel:	Sohlen (Gr.):
			Clogs (Gr.):

1. Durchgang	☐ möglich	☐ nicht möglich	
	Uhrzeit:	Kommentar:	V ☐
	Benötigte Zeit:		F ☐
2. Durchgang	☐ möglich	☐ nicht möglich	
	Uhrzeit:	Kommentar:	V ☐
	Benötigte Zeit:		F ☐
3. Durchgang	☐ möglich	☐ nicht möglich	
	Uhrzeit:	Kommentar:	V ☐
	Benötigte Zeit:		F ☐

Messtag 3	Datum:	Hilfsmittel:	Sohlen (Gr.):
			Clogs (Gr.):

1. Durchgang	☐ möglich	☐ nicht möglich	
	Uhrzeit:	Kommentar:	V ☐
	Benötigte Zeit:		F ☐
2. Durchgang	☐ möglich	☐ nicht möglich	
	Uhrzeit:	Kommentar:	V ☐
	Benötigte Zeit:		F ☐
3. Durchgang	☐ möglich	☐ nicht möglich	
	Uhrzeit:	Kommentar:	V ☐
	Benötigte Zeit:		F ☐

Messtag 4		Datum:		Hilfsmittel:		Sohlen (Gr.):
						Clogs (Gr.):

1. Durchgang	□ möglich	□ nicht möglich
	Uhrzeit:	Kommentar: V □
	Benötigte Zeit:	F □

2. Durchgang	□ möglich	□ nicht möglich
	Uhrzeit:	Kommentar: V □
	Benötigte Zeit:	F □

3. Durchgang	□ möglich	□ nicht möglich
	Uhrzeit:	Kommentar: V □
	Benötigte Zeit:	F □

Messtag 5		Datum:		Hilfsmittel:		Sohlen (Gr.):
						Clogs (Gr.):

1. Durchgang	□ möglich	□ nicht möglich
	Uhrzeit:	Kommentar: V □
	Benötigte Zeit:	F □

2. Durchgang	□ möglich	□ nicht möglich
	Uhrzeit:	Kommentar: V □
	Benötigte Zeit:	F □

3. Durchgang	□ möglich	□ nicht möglich
	Uhrzeit:	Kommentar: V □
	Benötigte Zeit:	F □

Messtag 6		Datum:		Hilfsmittel:		Sohlen (Gr.):
						Clogs (Gr.):

1. Durchgang	□ möglich	□ nicht möglich
	Uhrzeit:	Kommentar: V □
	Benötigte Zeit:	F □

2. Durchgang	□ möglich	□ nicht möglich
	Uhrzeit:	Kommentar: V □
	Benötigte Zeit:	F □

3. Durchgang	□ möglich	□ nicht möglich
	Uhrzeit:	Kommentar: V □
	Benötigte Zeit:	F □

Case-Report-Form
- Patienten -

eSHOE Pilotstudie – Seite 5

Version 22 || 06.09.2012

Probanden ID:

Untersucher:

Datum:

Stufen steigen   mit eSHOE

Messtag 1

	Datum:	Hilfsmittel:	Sohlen (Gr.):	Handlauf:	□ ja
			Clogs (Gr.):		□ nein

Durchgang 1	□ möglich		□ nicht möglich	
Richtung:	Uhrzeit:	Kommentar:	L □ / R □	V □ / F □

Durchgang 2	□ möglich		□ nicht möglich	
Richtung:	Uhrzeit:	Kommentar:	L □ / R □	V □ / F □

Durchgang 3	□ möglich		□ nicht möglich	
Richtung:	Uhrzeit:	Kommentar:	L □ / R □	V □ / F □

Durchgang 4	□ möglich		□ nicht möglich	
Richtung:	Uhrzeit:	Kommentar:	L □ / R □	V □ / F □

Messtag 2

	Datum:	Hilfsmittel:	Sohlen (Gr.):	Handlauf:	□ ja
			Clogs (Gr.):		□ nein

Durchgang 1	□ möglich		□ nicht möglich	
Richtung:	Uhrzeit:	Kommentar:	L □ / R □	V □ / F □

Durchgang 2	□ möglich		□ nicht möglich	
Richtung:	Uhrzeit:	Kommentar:	L □ / R □	V □ / F □

Durchgang 3	□ möglich		□ nicht möglich	
Richtung:	Uhrzeit:	Kommentar:	L □ / R □	V □ / F □

Durchgang 4	□ möglich		□ nicht möglich	
Richtung:	Uhrzeit:	Kommentar:	L □ / R □	V □ / F □

Messtag 3

	Datum:	Hilfsmittel:	Sohlen (Gr.):	Handlauf:	□ ja
			Clogs (Gr.):		□ nein

Durchgang 1	□ möglich		□ nicht möglich	
Richtung:	Uhrzeit:	Kommentar:	L □ / R □	V □ / F □

Durchgang 2	□ möglich		□ nicht möglich	
Richtung:	Uhrzeit:	Kommentar:	L □ / R □	V □ / F □

Durchgang 3	□ möglich		□ nicht möglich	
Richtung:	Uhrzeit:	Kommentar:	L □ / R □	V □ / F □

Durchgang 4	□ möglich		□ nicht möglich	
Richtung:	Uhrzeit:	Kommentar:	L □ / R □	V □ / F □

6-Minute Walk Test   mit eSHOE

Abschlussassessment bei Entlassung	Datum:	Hilfsmittel:	Sohlen (Gr.):
			Clogs (Gr.):

□ möglich	□ nicht möglich

Uhrzeit:	Kommentar:	V □
Pausen:		F □
Distanz:		

4-Meter Gehtest   mit eSHOE und GAITRite

Validierung bei Entlassung	Datum:	Hilfsmittel:	Sohlen (Gr.):
			Clogs (Gr.):

1. Durchgang	□ möglich		□ nicht möglich	
	Uhrzeit:	Kommentar:		V □
	Benötigte Zeit:			F □
2. Durchgang	□ möglich		□ nicht möglich	
	Uhrzeit:	Kommentar:		V □
	Benötigte Zeit:			F □
3. Durchgang	□ möglich		□ nicht möglich	
	Uhrzeit:	Kommentar:		V □
	Benötigte Zeit:			F □

Sonstige Studienbezogene Informationen

Abbruch der Studie:	□ ja	□ nein
	Begründung:	
Unerwünschte Ereignisse:		
Sonstige Anmerkungen:		

ProbandInneninformation und **Einwilligungserklärung**
zur Teilnahme an der klinischen Prüfung

Pilotstudie zur Anwendung von Methoden der mobilen Ganganalyse als Unterstützung und Erweiterung von Basis-Assessments und Therapieverlaufskontrollen in der Geriatrie

Sehr geehrte Probandin, sehr geehrter Proband!

Wir laden Sie ein an der oben genannten klinischen Prüfung teilzunehmen. Die Aufklärung darüber erfolgt in einem ausführlichen Gespräch.

Ihre Teilnahme an dieser klinischen Prüfung erfolgt freiwillig. Sie können jederzeit ohne Angabe von Gründen aus der Studie ausscheiden. Die Ablehnung der Teilnahme oder ein vorzeitiges Ausscheiden aus dieser Studie hat keine nachteiligen Folgen für Ihre medizinische Betreuung.

Klinische Prüfungen sind notwendig, um verlässliche neue medizinische Forschungsergebnisse zu gewinnen. Unverzichtbare Voraussetzung für die Durchführung einer klinischen Prüfung ist jedoch, dass Sie Ihr Einverständnis zur Teilnahme an dieser klinischen Prüfung schriftlich erklären. Bitte lesen Sie den folgenden Text als Ergänzung zum Informationsgespräch mit Ihrem Arzt sorgfältig durch und zögern Sie nicht Fragen zu stellen.

Eine **Pilotstudie** ist eine kleinere Untersuchung an der wenige Probandnnen teilnehmen. Mit den gewonnenen Erkenntnissen können spätere größere Studien besser geplant werden.

Das Ziel dieser Pilotstudie ist zu überprüfen, ob mit der Einlagesohle eSHOE das Gangbild im Therapieverlauf besser beurteilt werden kann und ob die gewonnen Erkenntnisse den Rehabilitationsverlauf nach Schenkelhalsbruch günstig beeinflussen.

Bitte unterschreiben Sie die Einwilligungserklärung nur

- wenn Sie Art und Ablauf der klinischen Prüfung vollständig verstanden haben,

- wenn Sie bereit sind, der Teilnahme zuzustimmen und

- wenn Sie sich über Ihre Rechte als Teilnehmer an dieser klinischen Prüfung im Klaren sind.

Zu dieser klinischen Prüfung, sowie zur Probandeninformation und Einwilligungserklärung wurde von der zuständigen Ethikkommission eine befürwortende Stellungnahme abgegeben.

1. Was ist der Zweck der klinischen Studie?

Der Zweck dieser klinischen Studie ist, den Einsatz des eShoe zur Überprüfung des Gangbildes und der Gehsicherheit bei Gehtests und auf längeren Strecken zu testen. Das Gangbild wird zum Teil gleichzeitig mit der neuen Schuhsohle und dem Ganganalyseteppich überprüft. Beide Werte werden miteinander verglichen.

2. Wie läuft die klinische Studie ab?

Die Tests im Rahmen der klinischen Prüfung des eSHOE werden ausschließlich im Seniorenzentrum Schwechat durchgeführt.

Die Tests finden in einem eigens dafür vorbereiteten Raum im Seniorenzentrum Schwechat statt. Nach Ihrem Eintreffen und dem Feststellen Ihrer Schuhgröße, bekommen Sie ein passendes paar eSHOE Einlagesohlen in Ihre gewohnten Schuhe eingelegt. Sie können danach nach Belieben zur Eingewöhnung „Probegehen" und probieren, ob die Einlage für Sie angenehm ist. Wenn Sie sich einigermaßen eingewöhnt haben wird mit den Tests begonnen. Die Untersuchungen im Rahmen dieser Studie umfassen vier Tests, die auch „Assessments" genannt werden.

1. „10-Meter Gehtest",

2. „Timed Up & Go Test",

3. "Sechs-Minuten Gehtest",

4. Stiegen steigen.

1. Zu Beginn wird ein Test durchgeführt, bei dem Sie, entlang einer markierten Strecke, 15 Meter geradeaus gehen. Innerhalb dieser 15 Meter langen Strecke befinden sich zwei weitere Markierungen, die 10 Meter voneinander entfernt sind. Es wird die Zeit gestoppt, die Sie zur Bewältigung der 10 Meter, innerhalb der 15 Meter Strecke, benötigen. Die 2,5 Meter vor und hinter der Strecke dienen als Bereiche zum Beschleunigen und Abbremsen. Dieser Test wird drei Mal wiederholt.

2. Beim sogenannten „Timed Up & Go Test" (Abk. TUG) sitzen Sie zu Beginn auf einem Stuhl. Bei einem Startsignal, welches der Prüfer gibt, stehen Sie auf, gehen geradeaus bis zu einer 3 Meter entfernten Markierung, kehren dort um, gehen zurück zum Stuhl und setzen sich dort wieder hin. Es wird die Zeit gestoppt, die zwischen Aufstehen und Hinsetzen vergeht. Der TUG wird ebenfalls drei Mal wiederholt.

3. Der Sechs-Minuten Gehtest ist eine Art Ausdauertest, bei dem Sie sechs Minuten am Stück gehen sollen. Und zwar gehen Sie zwischen den Markierungen der 15 Meter Strecke im Raum auf und ab. Während Sie gehen wird die Anzahl der Längen gezählt, die Sie innerhalb der sechs Minuten zurücklegen.

4. Beim Stiegen steigen sind Sie aufgefordert auf einer Treppe im Seniorenzentrum Schwechat neun Stiegen nach oben zu steigen. Wenn möglich, wird auch dieser Test drei Mal wiederholt.

Bei den Tests wird zusätzlich ein Video von Ihnen beim Gehen aufgenommen. Ihr Gesicht wird auf dieser Aufnahme <u>nicht</u> zu sehen sein.

3.   Was ist der eSHOE?

Der eSHOE ist ein Medizinprodukt, welches sich in klinischer Erprobung befindet und noch nicht zugelassen ist.

Im Rahmen des Projektes eSHOE wird ein Monitoring- und Trainings-System entwickelt. Dieses hilft einerseits frühzeitig Probleme beim Gehen zu erkennen und andererseits durch spielerisches Training das Gleichgewichtsgefühl zu verbessern. Es soll langfristig zur Steigerung der körperlichen Aktivität anregen.

4.   Gibt es Risiken, Beschwerden und Begleiterscheinungen?

Da die Schuhsohle sich rein äußerlich von einer gängigen Schuhsohle nicht unterscheiden, nach außen mit Leder umkleidet ist, sind weder Risiken, Beschwerden oder Begleiterscheinungen zu erwarten. Sollte der Schuh mit der Sohle drücken oder Sie sich nicht wohlfühlen, können Sie die Untersuchung sofort unterbrechen. Sie ziehen den Schuh aus, die Sohle wird wieder herausgenommen und Sie können wie gewohnt weitergehen.

5.   Versicherung

Als Teilnehmer an dieser klinischen Prüfung besteht für Sie der gesetzlich vorgeschriebene verschuldensunabhängige Versicherungsschutz (Personenschadenversicherung gemäß § 47 Medizinproduktegesetz)*,* der alle Schäden abdeckt, die an Ihrem Leben oder Ihrer Gesundheit durch die an Ihnen durchgeführten Maßnahmen der klinischen Prüfung verursacht werden können.

Die Versicherung wurde für Sie bei der Wiener Städtische Allgemeine Versicherung AG, Schottenring 30, 1010 Wien unter der Polizzennummer 08-U918234 abgeschlossen. Auf Wunsch können Sie in die Versicherungsunterlagen Einsicht nehmen.

Im Schadensfall können Sie sich direkt an den Versicherer wenden und Ihre Ansprüche selbständig geltend machen. Für den Versicherungsvertrag ist österreichisches Recht anwendbar, die Versicherungsansprüche sind in Österreich einklagbar.

Zur Unterstützung können Sie sich auch an die Patientenanwaltschaft oder Patienten-vertretung wenden.

Um den Versicherungsschutz nicht zu gefährden

- müssen Sie dem Prüfer - oder der oben genannten Versicherungsgesellschaft - eine Gesundheitsschädigung, die als Folge der klinischen Prüfung eingetreten sein könnte, unverzüglich mitteilen.

- müssen Sie alles Zumutbare tun um Ursache, Hergang und Folgen des Versicherungs-falles aufzuklären und den entstandenen Schaden gering zu halten. Dazu gehört ggf. auch, dass Sie Ihre behandelnden Ärzte ermächtigen, vom Versicherer geforderte Auskünfte zu erteilen.

6.   Wann wird die klinische Prüfung vorzeitig beendet?

Die klinische Prüfung kann jederzeit vorzeitig beendet werden, sollten Sie sich mit der Sohle nicht wohlfühlen. Sollte sich Ihr Gangbild auf Grund von Schmerzen oder anderen Veränderungen verschlechtern, kann die Studie ebenfalls abgebrochen werden. .

7.   In welcher Weise werden die im Rahmen dieser klinischen Prüfung gesammelten Daten verwendet?

Die erhobenen Daten dienen einerseits zur Überprüfung des innovativen Ganganalysesystems andererseits als Vergleichgruppe gesunder Personen zur Beurteilung des Gangbildes von PatientInnen nach Schenkelhalsfraktur mittels eShoe. Die mittels der Sohle erfassten Parameter werden anonymisiert statistisch ausgewertet. Ihre Messergebnisse dienen als Kontrolldaten von gehgesunden Personen zur Bewertung des Schuhsohlenmessinstrumentes.

Die Videoaufzeichnungen werden niemals veröffentlicht. Sie dienen nur zur Unterstützung der Datenauswertung.

Lediglich die Prüfer haben Zugang zu Ihren vertraulichen Daten. Weiters können Beauftragte von in- und ausländischen Gesundheitsbehörden, der zuständigen Ethikkommission, sowie – wenn zutreffend – des Auftraggebers der klinischen Prüfung Einsicht in diese Daten nehmen, um die Richtigkeit der Aufzeichnungen zu überprüfen. Diese Personen unterliegen einer gesetzlichen Verschwiegenheitspflicht.

In einer wissenschaftlichen Veröffentlichung der Untersuchungsergebnisse werden Sie nicht namentlich genannt.

Die Prüfer und ihre Mitarbeiter unterliegen im Umgang mit den Daten den Bestimmungen des österreichischen Datenschutzgesetzes 2000 in der jeweils geltenden Fassung.

Wenn Sie Ihre Einwilligung zurückziehen und damit Ihre Teilnahme vorzeitig beenden, werden keine neuen Daten mehr über Sie erhoben. Auf Grund gesetzlicher Dokumentationspflichten (Medizinproduktegesetz) kann jedoch weiterhin für einen gesetzlich festgelegten Zeitraum eine Einsichtnahme in Ihre personenbezogenen Daten zu Prüfzwecken durch autorisierte, zur Verschwiegenheit verpflichtete Personen erfolgen.

8.   Entstehen für die Teilnehmer Kosten?

Durch Ihre Teilnahme an dieser klinischen Prüfung entstehen für Sie keine zusätzlichen Kosten.

9.   Möglichkeit zur Diskussion weiterer Fragen

Für weitere Fragen steht Ihnen sehr gerne zur Verfügung:

Herr **DI Harald Jagos**: 0664 854 43 97

10.   Einwilligungserklärung (Kopie für ProbandIn)

Name des Probanden / der Probandin: ....

Geburtsdatum: ....   Identifikationsnummer (ID):................................

Ich erkläre mich bereit, an der klinischen Prüfung eSHOE teilzunehmen.

Ich bin von Herrn **DI Harald Jagos** ausführlich und verständlich über den eSHOE, mögliche Belastungen und Risiken, sowie über Wesen, Bedeutung und Tragweite der klinischen Prüfung, die bestehende Versicherung sowie die sich für mich daraus ergebenden Anforderungen aufgeklärt worden. Ich habe darüber hinaus den Text dieser ProbandInnenaufklärung und Einwilligungserklärung, die insgesamt 5 Seiten umfasst gelesen. Aufgetretene Fragen wurden mir vom Prüfer verständlich und genügend beantwortet. Ich hatte ausreichend Zeit, mich zu entscheiden. Ich habe zurzeit keine weiteren Fragen mehr.

Ich werde den ärztlichen Anordnungen, die für die Durchführung der klinischen Prüfung erforderlich sind, Folge leisten, behalte mir jedoch das Recht vor, meine freiwillige Mitwirkung jederzeit zu beenden.

Ich bin zugleich damit einverstanden, dass meine im Rahmen dieser klinischen Prüfung ermittelten Daten gespeichert werden. Mir ist bekannt, dass zur Überprüfung der Richtigkeit der Datenaufzeichnung Beauftragte der zuständigen Behörden, der Ethikkommission und ggf. des Auftraggebers beim Prüfer Einblick in meine personenbezogenen Daten nehmen dürfen.

Beim Umgang mit den Daten werden die Bestimmungen des Datenschutzgesetzes 2000 beachtet.

Eine Kopie dieser ProbandInneninformation und Einwilligungserklärung habe ich erhalten. Das Original verbleibt beim Prüfer.

....
Datum und Unterschrift der Probandin, des Probandin

....
Datum und Unterschrift des Prüfers

10.   Einwilligungserklärung (Kopie für Prüfer)

Name des Probanden/der Probandin:………...

Geb.Datum: ....   Identifikationsnummer:................................

Ich erkläre mich bereit, an der klinischen Prüfung eSHOE teilzunehmen.

Ich bin von Herrn **DI Harald Jagos** ausführlich und verständlich über den eSHOE, mögliche Belastungen und Risiken, sowie über Wesen, Bedeutung und Tragweite der klinischen Prüfung, die bestehende Versicherung sowie die sich für mich daraus ergebenden Anforderungen aufgeklärt worden. Ich habe darüber hinaus den Text dieser ProbandInnenaufklärung und Einwilligungserklärung, die insgesamt 5 Seiten umfasst gelesen. Aufgetretene Fragen wurden mir vom Prüfer verständlich und genügend beantwortet. Ich hatte ausreichend Zeit, mich zu entscheiden. Ich habe zurzeit keine weiteren Fragen mehr.

Ich werde den ärztlichen Anordnungen, die für die Durchführung der klinischen Prüfung erforderlich sind, Folge leisten, behalte mir jedoch das Recht vor, meine freiwillige Mitwirkung jederzeit zu beenden.

Ich bin zugleich damit einverstanden, dass meine im Rahmen dieser klinischen Prüfung ermittelten Daten gespeichert werden. Mir ist bekannt, dass zur Überprüfung der Richtigkeit der Datenaufzeichnung Beauftragte der zuständigen Behörden, der Ethikkommission und ggf. des Auftraggebers beim Prüfer Einblick in meine personenbezogenen Daten nehmen dürfen.

Beim Umgang mit den Daten werden die Bestimmungen des Datenschutzgesetzes 2000 beachtet.

Eine Kopie dieser Probandeninformation und Einwilligungserklärung habe ich erhalten. Das Original verbleibt beim Prüfer.

....
Datum und Unterschrift der Probandin, des Probandin

....
Datum und Unterschrift des Prüfers

Case-Report-Form - Probanden -	Version 7 || 06.09.2012
	Probanden ID:
	Untersucher:
eSHOE Pilotstudie – Seite 1	Datum:

Grundlegende Daten

Geburtsdatum					
Geschlecht	□ weiblich			□ männlich	
Körper-größe	cm	Gewicht:	kg	BMI:	Schuhgröße

Vorgeschichte

Vorerkrankungen und relevante Begleit-erkrankungen	
Medikation	
Verwendung von (Geh-) Hilfsmitteln	□ ja □ nein Wenn „ja", welche(s):

Studienbezogene Daten

Verwendetes Schuhwerk	
Unerwünschte Ereignisse	
Sonstige Anmerkungen	
Abbruch der Studie	□ ja □ nein Wenn ja, Begründung?

Timed Up & Go Test   mit und ohne eSHOE

Messtag 1
zum Zeitpunkt der **Aufnahme**   Datum: Hilfsmittel:

ohne eSHOE		mit eSHOE	
Uhrzeit:	Kommentar:	Uhrzeit:	Kommentar: V □
Benötigte Zeit:		Benötigte Zeit:	F □

Messtag 2
1. Tag nach der **Aufnahme**   Datum: Hilfsmittel:

ohne eSHOE		mit eSHOE	
Uhrzeit:	Kommentar:	Uhrzeit:	Kommentar: V □
Benötigte Zeit:		Benötigte Zeit:	F □

Messtag 3
zum Zeitpunkt der **Entlassung**   Datum: Hilfsmittel:

ohne eSHOE		mit eSHOE	
Uhrzeit:	Kommentar:	Uhrzeit:	Kommentar: V □
Benötigte Zeit:		Benötigte Zeit:	F □

10-Meter Gehtest   mit eSHOE

Messtag 1   Datum: Hilfsmittel:

1. Durchgang	□ möglich	□ nicht möglich	
	Uhrzeit:	Kommentar:	V □
	Benötigte Zeit:		F □
2. Durchgang	□ möglich	□ nicht möglich	
	Uhrzeit:	Kommentar:	V □
	Benötigte Zeit:		F □
3. Durchgang	□ möglich	□ nicht möglich	
	Uhrzeit:	Kommentar:	V □
	Benötigte Zeit:		F □

Messtag 2   Datum: Hilfsmittel:

1. Durchgang	□ möglich	□ nicht möglich	
	Uhrzeit:	Kommentar:	V □
	Benötigte Zeit:		F □
2. Durchgang	□ möglich	□ nicht möglich	
	Uhrzeit:	Kommentar:	V □
	Benötigte Zeit:		F □
3. Durchgang	□ möglich	□ nicht möglich	
	Uhrzeit:	Kommentar:	V □
	Benötigte Zeit:		F □

Messtag 3   Datum: Hilfsmittel:

1. Durchgang	□ möglich	□ nicht möglich	
	Uhrzeit:	Kommentar:	V □
	Benötigte Zeit:		F □
2. Durchgang	□ möglich	□ nicht möglich	
	Uhrzeit:	Kommentar:	V □
	Benötigte Zeit:		F □
3. Durchgang	□ möglich	□ nicht möglich	
	Uhrzeit:	Kommentar:	V □
	Benötigte Zeit:		F □

Stufen steigen   mit eSHOE

Messtag 1	Datum:		Hilfsmittel:		Handlauf:	□ ja □ nein
Durchgang 1 Richtung:	□ möglich			□ nicht möglich		
	Uhrzeit:	Kommentar:	L □ R □			V □ F □
Durchgang 2 Richtung:	□ möglich			□ nicht möglich		
	Uhrzeit:	Kommentar:	L □ R □			V □ F □
Durchgang 3 Richtung:	□ möglich			□ nicht möglich		
	Uhrzeit:	Kommentar:	L □ R □			V □ F □
Durchgang 4 Richtung:	□ möglich			□ nicht möglich		
	Uhrzeit:	Kommentar:	L □ R □			V □ F □

Messtag 2	Datum:	Hilfsmittel:	Handlauf:	□ ja □ nein
Durchgang 1 Richtung:	□ möglich		□ nicht möglich	
	Uhrzeit:	Kommentar:	L □ R □	V □ F □
Durchgang 2 Richtung:	□ möglich		□ nicht möglich	
	Uhrzeit:	Kommentar:	L □ R □	V □ F □
Durchgang 3 Richtung:	□ möglich		□ nicht möglich	
	Uhrzeit:	Kommentar:	L □ R □	V □ F □
Durchgang 4 Richtung:	□ möglich		□ nicht möglich	
	Uhrzeit:	Kommentar:	L □ R □	V □ F □

Messtag 3	Datum:	Hilfsmittel:	Handlauf:	□ ja □ nein
Durchgang 1 Richtung:	□ möglich		□ nicht möglich	
	Uhrzeit:	Kommentar:	L □ R □	V □ F □
Durchgang 2 Richtung:	□ möglich		□ nicht möglich	
	Uhrzeit:	Kommentar:	L □ R □	V □ F □
Durchgang 3 Richtung:	□ möglich		□ nicht möglich	
	Uhrzeit:	Kommentar:	L □ R □	V □ F □
Durchgang 4 Richtung:	□ möglich		□ nicht möglich	
	Uhrzeit:	Kommentar:	L □ R □	V □ F □

6-Minute Walk Test   mit eSHOE

Durchgang 1	□ möglich		□ nicht möglich	
	Uhrzeit:	Kommentar:		V □
	Distanz:			F □
	Pausen:			
Durchgang 2	□ möglich		□ nicht möglich	
	Uhrzeit:	Kommentar:		V □
	Distanz:			F □
	Pausen:			

Curriculum Vitae - Harald Jagos

Harald Jagoš

⌂ Anton-Sattler-Gasse 91/1/18
1220 Vienna
Austria

☎ +43 660 685 06 15

✉ harald.jagos@gmx.at

PERSONAL INFORMATION

Date of birth	01.01.1983
Nationality	Austria
Civil status	Unmarried

PROFESSIONAL EXPERIENCE

10/2016 - ongoing

SIMCharacters GmbH
R&D / Project management

Cooperation in development, documentation and certification of medical simulators, as well as on the creation of applications for funding of innovation projects.

01/2016 - 09/2016

Looking for work.

09/2014 - 12/2015

Medical University of Vienna, Center for Medical Physics and Biomedical Engineering.
Researcher

Coordination of the nationally funded R&D projects MISTRAAL, dealing with rehabilitation support for stroke patients.

09/2014 - ongoing

University of Applied Sciences FH Campus Wien,
Master´s degree program "Health Assisting Engineering".
Part time teaching

Teaching practical contents from the field of wearable technologies in the study course "quality of life and aids".

04/2014 - 08/2014	**No engagement,** Transitional phase of MISTRAAL.
	Gratuitous coordination of the R&D project MISTRAAL
	Caused by the suprising bankruptcy of CEIT a period without engagement occurred during MISTRAAL, during which the proceedings within the project were continued.
06/2006 - 03/2014	**Central European Institute of Technology (CEIT),** Institute of Rehabilitation and Assisted Living Technologies.
	Researcher
	Research and development of novel technical aid devices for elderly anddisabled people. (Co-) editing of proposals for the acquisition of national und international funding.

EDUCATION

10/2005 - 01/2017 **(presumably)**	**Vienna University of Technology,** *Faculty of Informatics.*
	*PhD	Dr. techn.*
	Development, validation and clincal evaluation of a mobile gait analysis system (eSHOE).
09/2001 - 06/2005	**University of Applied Sciences Technikum Wien,** Master´s degree program *"Elektronik".*
	*MSc	Dipl.-Ing.(FH)*
	Specialization: biomedical engineering, telecommunication technology. Master's thesis: "Measurement of the inclination of leg segments for patients requiring functional electrical stimulation".

LANGUAGES

German	Native language.
English	Business fluent.
French	Basics.

COMPUTING SKILLS

Operating systems	Windows, MacOS.
Office	MS Word, MS Excel, MS Powerpoint, MS Visio, LaTeX.
Programming languages & software tools	Matlab, Eagle, Creo, C, C#, Java, HTML.
Design	Adobe Illustrator, Adobe InDesign, Adobe Photoshop.

OTHER QUALIFICATIONS

Driving license A, B

Trainings

2009 Exercise instructor in Ultimate Frisbee.

2005 Certified instructor in Nine-pin Bowling.

2003 Exercise instructor in Nine-pin Bowling.

Recent
seminars & workshops

Medical University of Vienna - 2015/16
- Clinical studies according to medical device directive.
- Good clinical practice.
- Data visualization tools.
- "The other side" - experiential workshop in the wheelchair.

FH Campus Wien - 2015
- Basic module for tertiary principles of teaching.

ACTIVITIES

Sports

Martial arts Taiji Quan.

Outdoor Running, cycling, hiking, Ultimate Frisbee.

Volunteer work

raltec Research group for assistive technologies.
Board member (auditor).
www.raltec.at

ISOB **I**nternational **S**ociety **o**f **B**iotelemetry.
Board member (treasurer).
www.biotelemetry.org

Memberships

GAMMA Society for the analysis of human motor function and its clinical application.
www.g-a-m-m-a.org

CETA **C**henJiaGou-**E**urope **T**aijiquan **A**ssociation.
www.taichi-pushhand.com

Glossary

digital immigrant Antonym of "digital native". Meaning a person who did not grow up using technology, but was only confronted with it at a later age. 182

initial contact First contact of the foot with the ground. Sometimes also referred to as "heel strike" (in the case of a healthy gait pattern). 8, 25, 36, 104, 111, 113, 115, 136, 148

Intertrochanteric femoral fracture Intertrochanteric femoral fracture is the medical term for a fracture of the femur in the area between greater trochanter and lesser trochanter. 9, 162, 202, 203, 206, 212

Kolmogoroff-Smirnov-Omnibus Test ... non-parametric statistical test evaluates the null hypothesis, that two samples belong to populations with distributions of the same shape 155

last contact Last contact of the foot with the ground. Sometimes also referred to as "toe-off" (in the case of a healthy gait pattern). 8, 25, 36, 109, 111, 148

Mann-Whitney U-Test This non-parametric statistical test evaluates the null hypothesis, that two samples belong to populations with the same median and distributions of the same shape. 155

Medial femoral neck fracture The medial femoral neck fracture is the most common fracture of the femur. These are fractures of the femoral neck either near or directly at the femoral head. Contrary to the lateral femoral neck fracture it is located within the joint capsule (intracapsular). 9, 162, 209, 212

Subtrochanteric femoral fracture Subtrochanteric femoral fracture is the medical term for a fracture of the femur below the *linea intertrochanterica*, the imaginary line running between greater trochanter and lesser trochanter. 9, 162, 203

University of Applied Sciences Technikum Wien The University of Applied Sciences Technikum Wien (FHTW; German: Fachhochschule Technikum Wien) is located in the city of Vienna (Höchstädtplatz 6, 1200 Wien). It is one of the largest University of Applied Sciences in Austria. 87

Zurich University of Applied Sciences The Zurich University of Applied Sciences (ZHAW; German: Zürcher Hochschule für Angewandte Wissenschaften) is located in the city of Winterthur (Gertrudstraße 15, 8401 Winterthur). It is one of the largest University of Applied Sciences in Switzerland. 121

Acronyms

10MWT ten meter walk test. 89, 139, 141, 162, 163, 165–167, 187, 197–199, 201, 203, 204, 206, 209, 210, 212, 213

2C two crutches. 166, 167

4MWT four meter meter walk test. 89

6MWT six minute walk test. 89

ACF autocorrelation function. 98, 99

BFNP bipolar femoral neck prosthesis. 13, 163, 209, 212

C-L one crutch left. 166

C-R one crutch right. 166

CRF case report form. 88, 89, 94

DHS dynamic hip screw. 12, 162, 163, 202, 203, 206

DoF degrees of freedom. 26

DR dead reckoning. 122

ECG electrocardiography. 27

EMG electromyography. 21, 22, 27

ETHZ Swiss Federal Institute of Technology in Zurich. 18, 27, 49

FES functional electrical stimulation. 27, 28, 33, 34

FF foot flat phase. 158–161, 186

FHTW University of Applied Sciences Technikum Wien. 87, 121, *Glossary:* University of Applied Sciences Technikum Wien

FSR force sensitive resistor. 28, 29, 31, 32, 35, 36, 40, 49, 53, 54, 59, 104

GPDS gait phase detection system. 18, 27–35, 49, 185

HS heel strike. 8, 36, 104, 111, 183

IC integrated circuit. 67

IC initial contact. 8, 25, 31, 36, 87, 104, 111, 113–116, 122, 134–136, 144, 145, 148, 149, 183, *Glossary:* initial contact

ICF informed consent form. 88, 89, 92

IDS initial double support time. 175–178

IMU inertial measurement unit. 24–26, 38, 40, 49, 52, 56, 60, 121–123, 132, 137, 186, 187

INS inertial navigation system. 125

IQR interquartile range. xiii, 169, 188

ITFF intertrochanteric femoral fracture. 9, 162, 163, 202, 203, 205, 206, 212, *Glossary:* Intertrochanteric femoral fracture

KSO Kologoroff-Smirnov-Omnibus Test. 155, *Glossary:* Kolmogoroff-Smirnov-Omnibus Test

LC last contact. 8, 25, 36, 87, 109, 111, 113, 114, 144, 145, 148, 149, 183, *Glossary:* last contact

LED light-emitting diode. 19, 72, 73, 180, 181

MEMS microelectromechanical system. 36, 42, 49, 124

MFNF medial femoral neck fracture. 9, 162, 163, 209, 212, *Glossary:* Medial femoral neck fracture

MIT Massachusetts Institute of Technology. 18

MWU Mann-Whitney U-test. 155, *Glossary:* Mann-Whitney U-Test

NPP normal probability plot. 126, 127

OWD One-Way Delay. *Glossary:* One-Way Delay

252

PCB printed circuit board. 2, 35, 36, 39, 40, 48, 51, 52, 58, 60, 62–64, 68, 69, 72–74, 77, 78, 126, 184

PFN proximal femur nail. 12, 13, 162, 163, 203, 212

PVDF polyvinlylidine fluoride. 35, 36

QQP QQ plot. 126, 128, 129

REF reference group. 142

RL rollator. 166

RM roll mobile. 166, 167

SD standard deviation. xiii, 118, 128, 129, 150, 153, 155, 159, 160, 170, 175, 184–187

SIGS shoe-integrated gait sensor system. 18, 34, 36–38, 185

STA Stance Time. 113, 170–173, 187, 188

StC stair climbing. 89

STE Step Time. 175, 176, 188

STFF subtrochanteric femoral fracture. 9, 162, 163, 203, 205, *Glossary:* Subtrochanteric femoral fracture

STR Stride Time. 8, 111, 170, 171, 175, 187, 188

SWI Swing Time. 113, 173–175, 187

TAP Tukey-Anscombe plot. 126–129, 206

TEP total endoprosthesis. 12, 162, 163

TO toe-off. 8, 36, 109, 111, 113, 183

TR total range. xiii

TUG timed "up and go" test. 89

USB universal serial bus. 25, 60, 63, 64, 67, 73, 180, 181

WC-L walking cane left. 166

WC-R walking cane right. 166

ZHAW Zurich University of Applied Sciences. 121, *Glossary:* Zurich University of Applied Sciences

ZUPT zero velocity update. 125, 133, 135, 136, 138, 158, 186

Bibliography

[Aminian et al., 1999] Aminian, K., Robert, P., Buchser, E. E., Rutschmann, B., Hayoz, D., and Depairon, M. (1999). Physical activity monitoring based on accelerometry: validation and comparison with video observation. *Medical & Biological Engineering & Computing*, 37(3):304–308.

[Andriacchi and Alexander, 2000] Andriacchi, T. P. and Alexander, E. J. (2000). Studies of human locomotion: past, present and future. *Journal of biomechanics*, 33(10):1217–24.

[Antonsson and Mann, 1985] Antonsson, E. K. and Mann, R. W. (1985). The frequency content of gait. *Journal of Biomechanics*, 18(1):39 – 47.

[Auvinet et al., 1999] Auvinet, B., Chaleil, D., and E, B. (1999). Accelerometric gait analysis for use in hospital outpatients. *Revue du rhumatism (English ed.)*, 66(7–9):389–97.

[Baláš et al., 2014] Baláš, J., Panáčková, M., Jandová, S., Martin, A. J., Strejcová, B., Vomáčko, L., Charousek, J., Cochrane, D. J., Hamlin, M., and Draper, N. (2014). The effect of climbing ability and slope inclination on vertical foot loading using a novel force sensor instrumentation system. *Journal of human kinetics*, 44:75—81.

[Bamberg et al., 2008] Bamberg, S. J. M., Benbasat, A. Y., Scarborough, D. M., Krebs, D. E., and Paradiso, J. A. (2008). Gait analysis using a shoe-integrated wireless sensor system. *IEEE Transactions on Information Technology in Biomedicine*, 12(4):413–423.

[Barth et al., 2011] Barth, J., Klucken, J., Kugler, P., Kammerer, T., Steidl, R., Winkler, J., Hornegger, J., and Eskofier, B. (2011). Biometric and mobile gait analysis for early diagnosis and therapy monitoring in parkinson's disease. In *2011 Annual International Conference of the IEEE Engineering in Medicine and Biology Society*, pages 868–871.

[Barth et al., 2015] Barth, J., Oberndorfer, C., Pasluosta, C., Schülein, S., Gassner, H., Reinfelder, S., Kugler, P., Schuldhaus, D., Winkler, J., Klucken, J., and Eskofier, B. M. (2015). Stride segmentation during free walk movements using multi-dimensional subsequence dynamic time warping on inertial sensor data. *Sensors*, 15(3):6419.

[Barth et al., 2012] Barth, J., Sünkel, M., Bergner, K., Schickhuber, G., Winkler, J., Klucken, J., and Eskofier, B. (2012). Combined analysis of sensor data from hand and gait motor function improves automatic recognition of parkinson's disease. In *2012 Annual International Conference of the IEEE Engineering in Medicine and Biology Society*, pages 5122–5125.

[Benbasat et al., 2003] Benbasat, A. Y., Morris, S. J., and Paradiso, J. A. (2003). A wireless modular sensor architecture and its application in on-shoe gait analysis. In *Sensors, 2003. Proceedings of IEEE*, volume 2, pages 1086–1091 Vol.2.

[Bilney et al., 2003] Bilney, B., Morris, M., and Webster, K. (2003). Concurrent related validity of the GAITRite walkway system for quantification of the spatial and temporal parameters of gait. *Gait & posture*, 17(1):68–74.

[Bland and Altman, 2010] Bland, J. M. and Altman, D. G. (2010). Statistical methods for assessing agreement between two methods of clinical measurement. *International Journal of Nursing Studies*, 47(8):931–936.

[Bonato, 2005] Bonato, P. (2005). Advances in wearable technology and applications in physical medicine and rehabilitation. *Journal of NeuroEngineering and Rehabilitation*, 2(1):1–4.

[Bonato, 2009] Bonato, P. (2009). Advances in wearable technology for rehabilitation. *Studies in health technology and informatics*, 145:145–59.

[Bortz and Lienert, 2008] Bortz, J. and Lienert, G. A. (2008). *Kurzgefasste Statistik für die klinische Forschung*. Springer-Lehrbuch. Springer Medizin Verlag Heidelberg, 3rd edition.

[Bovi et al., 2011] Bovi, G., Rabuffetti, M., Mazzoleni, P., and Ferrarin, M. (2011). A multiple-task gait analysis approach: Kinematic, kinetic and {EMG} reference data for healthy young and adult subjects. *Gait & Posture*, 33(1):6 – 13.

[Braun et al., 2015a] Braun, B. J., Bushuven, E., Hell, R., Veith, N. T., Buschbaum, J., Holstein, J. H., and Pohlemann, T. (2015a). A novel tool for continuous fracture aftercare - clinical feasibility and first results of a new telemetric gait analysis insole. *Injury*.

[Braun et al., 2015b] Braun, B. J., Veith, N. T., Hell, R., Döbele, S., Roland, M., Rollmann, M., Holstein, J., and Pohlemann, T. (2015b). Validation and reliability testing of a new, fully integrated gait analysis insole. *Journal of foot and ankle research*, 8:54.

[Bril et al., 2016] Bril, A. T., David, V., Scherer, M., Jagos, H., Kafka, P., and Sabo, A. (2016). Development of a wearable live-feedback system to support partial weight-bearing while recovering from lower extremity injuries. *Procedia Engineering*, 147:157 – 162. The Engineering of {SPORT} 11.

256

[Burden et al., 2003] Burden, A., Trew, M., and Baltzopoulos, V. (2003). Normalisation of gait emgs: A re-examination. *Journal of Electromyography and Kinesiology*, 13(6):519–532. cited By 104.

[Canales, 2002] Canales, J. (2002). Photogenic venus: The "cinematographic turn" and its alternatives in nineteenth century france. *Isis*, 93(4):585–613.

[David, 2012] David, V. (2012). Development of validation methods for the mobile gait and motion pattern analysis system vitalishoe. Master's thesis, University of Applied Sciences Technikum Wien, Institute for Biomedical Engineering, Healthcare and Rehabilitation Technology, Höchstädtplatz 6, 1200 Wien.

[Dimai et al., 2011] Dimai, H. P., Svedbom, A., Fahrleitner-Pammer, A., Pieber, T., Resch, H., Zwettler, E., Chandran, M., and Borgström, F. (2011). Epidemiology of hip fractures in austria: evidence for a change in the secular trend. *Osteoporosis International*, 22(2):685–692.

[Donath et al., 2016a] Donath, L., Faude, O., Lichtenstein, E., Nüesch, C., and Mündermann, A. (2016a). Validity and reliability of a portable gait analysis system for measuring spatiotemporal gait characteristics: comparison to an instrumented treadmill. *Journal of NeuroEngineering and Rehabilitation*, 13(1):1–9.

[Donath et al., 2016b] Donath, L., Faude, O., Lichtenstein, E., Pagenstert, G., Nüesch, C., and Mündermann, A. (2016b). Mobile inertial sensor based gait analysis: Validity and reliability of spatiotemporal gait characteristics in healthy seniors. *Gait & Posture*, 49:371 – 374.

[Feier et al., 2006] Feier, C., Kauert, R., Liedecke, W., Lingner, M., and Weber, P. (2006). Patient shoe inertial sensor attachment system has holder on u shaped stirrup held round heel by tensioned straps.

[Götz-Neumann, 2003] Götz-Neumann, K. (2003). *Gehen verstehen: Ganganalyse in der Physiotherapie. [Understanding gait: gait analysis in physiotherapy].* Thieme, Stuttgart(GER), 2nd edition.

[Greene et al., 2010] Greene, B. R., McGrath, D., O'Neill, R., O'Donovan, K. J., Burns, A., and Caulfield, B. (2010). An adaptive gyroscope-based algorithm for temporal gait analysis. *Medical & Biological Engineering & Computing*, 48(12):1251–1260.

[Haftner, 2015] Haftner, T. (2015). Energy harvesting and power management for the mobile gait analysis system eshoe. Master's thesis, University of Applied Sciences Technikum Wien, Institute for Biomedical Engineering, Healthcare and Rehabilitation Technology, Höchstädtplatz 6, 1200 Wien.

[Hansen et al., 2002] Hansen, A. H., Childress, D. S., and Meier, M. R. (2002). A simple method for determination of gait events. *Journal of Biomechanics*, 35(1):135 – 138.

257

[Hausdorff et al., 1997] Hausdorff, J. M., Edelberg, H. K., Gudkowicz, M. E., Singh, M. A. F., and Wei, J. Y. (1997). The relationship between gait changes and falls. *Journal of the American Geriatrics Society*, 45(11):1406–1406.

[Hausdorff et al., 1995] Hausdorff, J. M., Ladin, Z., and Wei, J. Y. (1995). Footswitch system for measurement of the temporal parameters of gait. *Journal of Biomechanics*, 28(3):347 – 351.

[Hegewald, 1999] Hegewald, G. (1999). *Ganganalytische Bestimmung und Bewertung der Druckverteilung unterm Fuß und von Gelenkwinkelverläufen – eine Methode für Diagnose und Therapie im medizinischen Alltag und für die Qualitätssicherung in der rehabilitationstechnischen Versorgung.* PhD thesis, Humboldt Universität zu Berlin, Institut für Rehabilitationswissenschaften.

[Jagos et al., 2015] Jagos, H., David, V., Haller, M., Kotzian, S., Hofmann, M., Schlossarek, S., Eichholzer, K., Winkler, M., Frohner, M., Reichel, M., Mayr, W., and Rafolt, D. (2015). A framework for (tele-) monitoring of the rehabilitation progress in stroke patients. *Applied Clinical Informatics*, 06:757–768.

[Kidder et al., 1996] Kidder, S. M., Abuzzahab, F. S., Harris, G. F., and Johnson, J. E. (1996). A system for the analysis of foot and ankle kinematics during gait. *IEEE transactions on rehabilitation engineering : a publication of the IEEE Engineering in Medicine and Biology Society*, 4(1):25–32.

[Kirtley, 2006] Kirtley, C. (2006). *Clinical Gait Analysis: Theory and Practice.* Elsevier.

[Klucken et al., 2011] Klucken, J., Barth, J., Maertens, K., Eskofier, B., Kugler, P., Steidl, R., Hornegger, J., and Winkler, J. (2011). Mobile biosensor-based gait analysis: a diagnostic and therapeutic tool in parkinson's disease. *Der Nervenarzt*, 82(12):1604–11.

[Kugler et al., 2012] Kugler, P., Schlarb, H., Blinn, J., Picard, A., and Eskofier, B. (2012). A wireless trigger for synchronization of wearable sensors to external systems during recording of human gait. *Conference proceedings : ... Annual International Conference of the IEEE Engineering in Medicine and Biology Society. IEEE Engineering in Medicine and Biology Society. Annual Conference*, 2012:4537–40.

[Latham et al., 2008] Latham, N. K., Mehta, V., Nguyen, A. M., Jette, A. M., Olarsch, S., Papanicolaou, D., and Chandler, J. (2008). Performance-based or self-report measures of physical function: which should be used in clinical trials of hip fracture patients? *Archives of physical medicine and rehabilitation*, 89(11):2146–55.

[Madgwick et al., 2011] Madgwick, S. O. H., Harrison, A. J. L., and Vaidyanathan, R. (2011). Estimation of imu and marg orientation using a gradient descent algorithm. In *2011 IEEE International Conference on Rehabilitation Robotics*, pages 1–7.

[Marey, 1882] Marey, t.-J. (1882). Le fusil photographique. [the photographic gun]. *La nature: revue des sciences et de leurs applications aux arts et à l'industrie.*, pages 326–330.

[Mariani et al., 2010] Mariani, B., Hoskovec, C., Rochat, S., Büla, C., Penders, J., and Aminian, K. (2010). 3D gait assessment in young and elderly subjects using foot-worn inertial sensors. *Journal of biomechanics*, 43(15):2999–3006.

[Mattar et al., 2015] Mattar, R., Diab, J., Wehbe, S., Merhej, C., and Abu-Faraj, Z. O. (2015). Normative plantar pressure distribution in asymptomatic adult subjects: A pilot study. In *2015 International Conference on Advances in Biomedical Engineering (ICABME)*, pages 222–225.

[Mayagoitia et al., 2002] Mayagoitia, R. E., Nene, A. V., and Veltink, P. H. (2002). Accelerometer and rate gyroscope measurement of kinematics: an inexpensive alternative to optical motion analysis systems. *Journal of Biomechanics*, 35(4):537 – 542.

[Menz et al., 2004] Menz, H. B., Latt, M. D., Tiedemann, A., Mun San Kwan, M., and Lord, S. R. (2004). Reliability of the gaitrite walkway system for the quantification of temporo-spatial parameters of gait in young and older people. *Gait & posture*, 20(1):20–5.

[Menz et al., 2003] Menz, H. B., Lord, S. R., and Fitzpatrick, R. C. (2003). Age-related differences in walking stability. *Age and Ageing*, 32(2):137–142.

[Moe-Nilssen and Helbostad, 2004] Moe-Nilssen, R. and Helbostad, J. L. (2004). Estimation of gait cycle characteristics by trunk accelerometry. *Journal of Biomechanics*, 37(1):121–126.

[Montgomery and Runger, 2003] Montgomery, D. C. and Runger, G. C. (2003). *Applied Statistics and Probability for Engineers*. John Wiley & Sons, Inc., 3rd edition.

[Morris et al., 2001] Morris, M. E., Huxham, F., McGinley, J., Dodd, K., and Iansek, R. (2001). The biomechanics and motor control of gait in parkinson disease. *Clinical Biomechanics*, 16(6):459 – 470.

[Morris and Paradiso, 2002] Morris, S. and Paradiso, J. (2002). Shoe-integrated sensor system for wireless gait analysis and real-time feedback. *Proceedings of the Second Joint 24th Annual Conference and the Annual Fall Meeting of the Biomedical Engineering Society] [Engineering in Medicine and Biology*, 3:2468–2469.

[Muro-de-la Herran et al., 2014] Muro-de-la Herran, A., Garcia-Zapirain, B., and Mendez-Zorrilla, A. (2014). Gait analysis methods: An overview of wearable and non-wearable systems, highlighting clinical applications. *Sensors (Basel)*, 14(2):3362–94.

[Murray et al., 1964] Murray, M. P., Drought, A. B., and Kory, R. C. (1964). Walking patterns of normal men. *The Journal of Bone & Joint Surgery*, 46(2):335–360.

[Muybridge, 1899] Muybridge, E. (1899). *Animals in motion: an electro-photographic investigation of consecutive phases of animal progressive movements*. Chapman & Hall, London (UK).

[Muybridge, 1907] Muybridge, E. (1907). *The human figure in motion: an electro-photographic investigation of consecutive phases of muscular actions.* Chapman & Hall, London (UK).

[Muybridge, 1957] Muybridge, E. (1957). *Animals in motion: an electro-photographic investigation of consecutive phases of animal progressive movements.* Dover Publications, New York (NY).

[Nilsson et al., 2010] Nilsson, J. O., Skog, I., and Händel, P. (2010). Performance characterisation of foot-mounted zupt-aided inss and other related systems. In *Indoor Positioning and Indoor Navigation (IPIN), 2010 International Conference on*, pages 1–7.

[Noureldin et al., 2013] Noureldin, A., Karamat, T. B., and Georgy, J. (2013). *Fundamentals of Inertial Navigation, Satellite-based Positioning and their Integration.* Springer, 1st edition.

[Oberg et al., 1993] Oberg, T., Karsznia, A., and Oberg, K. (1993). Basic gait parameters: reference data for normal subjects, 10-79 years of age. *Journal of rehabilitation research and development*, 30(2):210–23.

[Oberzaucher, 2011] Oberzaucher, J. (2011). *iAssessment - Aspekte eines instrumentieren Sturzrisikoassessments basierend auf einer extramuralen Gang- und Bewegungsanalyse - im Hinblick auf eine Anwendung im Bereich des Ambient Assisted Living.* PhD thesis, Vienna University of Technology.

[Pappas et al., 2002] Pappas, I. P. I., Keller, T., and Mangold, S. (2002). A reliable, gyroscope based gait phase detection sensor embedded in a shoe insole. In *Sensors, 2002. Proceedings of IEEE*, volume 2, pages 1085–1088 vol.2.

[Pappas et al., 2004] Pappas, I. P. I., Keller, T., Mangold, S., Popovic, M. R., Dietz, V., and Morari, M. (2004). A reliable gyroscope-based gait-phase detection sensor embedded in a shoe insole. *IEEE Sensors Journal*, 4(2):268–274.

[Pappas et al., 2001] Pappas, I. P. I., Popovic, M. R., Keller, T., Dietz, V., and Morari, M. (2001). A reliable gait phase detection system. *IEEE Transactions on Neural Systems and Rehabilitation Engineering*, 9(2):113–125.

[Paradiso et al., 1999] Paradiso, J., Hu, E., and Hsiao, K.-y. (1999). The CyberShoe: a wireless multisensor interface for a dancer's feet. *Proceedings of International Dance and Technology*, 99:57–60.

[Paradiso et al., 2004] Paradiso, J. A., Morris, S. J., Benbasat, A. Y., and Asmussen, E. (2004). Interactive therapy with instrumented footwear. In *CHI '04 Extended Abstracts on Human Factors in Computing Systems*, CHI EA '04, pages 1341–1343, New York, NY, USA. ACM.

[Patel et al., 2012] Patel, S., Park, H., Bonato, P., Chan, L., and Rodgers, M. (2012). A review of wearable sensors and systems with application in rehabilitation. *Journal of neuroengineering and rehabilitation*, 9:21.

[Perry, 1992] Perry, J. (1992). *Gait analysis: normal and pathological function.* Slack incorporated, Thorofare(NJ), 1st edition.

[Pinter et al., 2013] Pinter, G., Likar, R., Schippinger, W., Janig, H., Kada, O., and Cernic, K. (2013). *Geriatrische Notfallversorgung.* Springer-Verlag Wien, 1st edition.

[Polasek, 2014] Polasek, D. (2014). Foot-mounted imu sensor – data processing for gait analysis parameter extraction. Master's thesis, Zurich University of Applied Sciences, School of Engineering, Institute for Mechatronic Systems, Gertrudstraße 15, 8401 Winterthur.

[Reich, 2013] Reich, S. (2013). Development of a software package to gather, analyze and store gait data with the mobile motion analysis system eshoe. Master's thesis, University of Applied Sciences Technikum Wien, Institute for Biomedical Engineering, Healthcare and Rehabilitation Technology, Höchstädtplatz 6, 1200 Wien.

[Sagawa, 2000] Sagawa, K. (2000). Non-restricted measurement of walking distance Horizontal distance Estimation of swing phase. pages 1847–1852.

[Schwesig et al., 2010] Schwesig, R., Kauert, R., Wust, S., Becker, S., and Leuchte, S. (2010). [Reliability of the novel gait analysis system RehaWatch]. *Biomedizinische Technik. Biomedical engineering*, 55(2):109–15.

[Schwesig et al., 2011] Schwesig, R., Leuchte, S., Fischer, D., Ullmann, R., and Kluttig, A. (2011). Inertial sensor based reference gait data for healthy subjects. *Gait & posture*, 33(4):673–8.

[Seier, 2002] Seier, E. (2002). Comparison of tests for univariate normality. *Interstat*, 1:1–17.

[Shapiro and Wilk, 1965] Shapiro, S. S. and Wilk, M. B. (1965). An analysis of variance test for normality (complete samples). *Biometrika*, 52(3/4):591–611.

[Skog et al., 2010] Skog, I., Nilsson, J. O., and Händel, P. (2010). Evaluation of zero-velocity detectors for foot-mounted inertial navigation systems. In *Indoor Positioning and Indoor Navigation (IPIN), 2010 International Conference on*, pages 1–6.

[Stillman et al., 1882] Stillman, J. D. B., Muybridge, E., and Stanford, L. (1882). *The horse in motion : as shown by instantaneous photography : with a study on animal mechanics founded on anatomy and the revelations of the camera : in which is demonstrated the theory of quadrupedal locomotion / by J.D.B. Stillman ; executed and published under the auspices of Leland Stanford ; [photographs by Eadweard Muybridge].* Boston: J.R. Osgood,. http://www.biodiversitylibrary.org/bibliography/20651.

[Stirling et al., 2005] Stirling, R., Fyfe, K., and Lachapelle, G. (2005). Evaluation of a New Method of Heading Estimation for Pedestrian Dead Reckoning Using Shoe Mounted Sensors. *The Journal of Navigation*, 58(01):31–45.

[Sudarsky, 1990] Sudarsky, L. (1990). Gait disorders in the elderly. *New England Journal of Medicine*, 322(20):1441–1446. PMID: 2184358.

[Tura et al., 2010] Tura, A., Raggi, M., Rocchi, L., Cutti, A. G., and Chiari, L. (2010). Gait symmetry and regularity in transfemoral amputees assessed by trunk accelerations. *Journal of neuroengineering and rehabilitation*, 7:4.

[Vaughan et al., 1992] Vaughan, C., Davis, B., and O'Connor, J. (1992). *Dynamics of human gait.* Kiboho Publishers, Cape Town(RSA), 2nd edition.

[Webster et al., 2005] Webster, K. E., Wittwer, J. E., and Feller, J. A. (2005). Validity of the GAITRite® walkway system for the measurement of averaged and individual step parameters of gait. *Gait and Posture*, 22(4):317–321.

[Windolf et al., 2008] Windolf, M., Götzen, N., and Morlock, M. (2008). Systematic accuracy and precision analysis of video motion capturing systems–exemplified on the vicon-460 system. *Journal of biomechanics*, 41(12):2776–80.

[Winter, 1991] Winter, D. (1991). *The Biomechanics and Motor Control of Human Gait: Normal, Elderly and Pathological.* University of Waterloo Press.

[Yun et al., 2007] Yun, X., Bachmann, E. R., Moore, H., and Calusdian, J. (2007). Self-contained position tracking of human movement using small inertial/magnetic sensor modules. In *Proceedings 2007 IEEE International Conference on Robotics and Automation*, pages 2526–2533.

[Zijlstra et al., 2008] Zijlstra, A., Goosen, J. H. M., Verheyen, C. C. P. M., and Zijlstra, W. (2008). A body-fixed-sensor based analysis of compensatory trunk movements during unconstrained walking. *Gait and Posture*, 27(1):164–167.

[Zollinger, 2012] Zollinger, S. (2012). Human motion tracking using inertial and magnetic sensors with quaternion-based extended kalman filter for orientation determination and a human body model incorporating anatomical constraints. Master's thesis, University of Applied Sciences Rapperswil, Institute for Communication Systems.

[Zurales et al., 2016] Zurales, K., DeMott, T., Kim, H., Allet, L., Ashton-Miller, J., and Richardson, J. (2016). Gait efficiency on an uneven surface is associated with falls and injury in older subjects with a spectrum of lower limb neuromuscular function: A prospective study. *American Journal of Physical Medicine and Rehabilitation*, 95:83–90.